Impacts of Meteorology-Driven Seed Dispersal on Plant Migration: Implications for Future Vegetation Structure under Changing Climates

by

Eunjee Lee

B.S. in Chemical Engineering, Seoul National University, 2002
M.S. in Chemistry, The Ohio State University, 2005

Submitted to the Department of Earth, Atmospheric and Planetary Sciences
in partial fulfillment of the requirements for the degree of

Doctor of Science in Atmospheric Science
at the
MASSACHUSETTS INSTITUTE OF TECHNOLOGY

September 2011

Signature of the Author: _____

Department of Earth, Atmospheric, and Planetary Sciences
Aug 17, 2011

Certified by: _____

Ronald Prinn
TEPCO Professor of Atmospheric Chemistry
Thesis Supervisor

Accepted by: _____

Maria Zuber
Head, Department of Earth, Atmospheric, and Planetary Sciences

Impacts of Meteorology-Driven Seed Dispersal on Plant Migration: Implications for Future Vegetation Structure under Changing Climates

By

Eunjee Lee

Abstract

As the impacts among land cover change, future climates and ecosystems are expected to be substantial (e.g., Feddema et al., 2005), there are growing needs for improving the capability of simulating the dynamics of vegetation structure across the global landscape as accurately as possible. In order to serve these needs, Dynamic Global Vegetation Models (DGVMs) are used to describe the current status of vegetation structure and biogeography as well as estimate their future dynamics, either with prescribed climates or coupled to climate models. Yet, current DGVMs generally assume ubiquitous availability of seeds and do not generally consider seed dispersal mechanisms and plant migration processes, which may influence the impacts of vegetation structural changes on the climate system (i.e., change in albedo, runoff, and terrestrial carbon sequestration capacity). For the first time, this study incorporates time-varying wind-driven seed dispersion (i.e., the SEED configuration) as a dynamic constraint to the migration of natural vegetation in the Community Land Model (CLM)-DGVM.

Compared to estimates of satellite-derived tree cover, simulations by this model configuration shows significantly improved representation of boreal forests in Western Siberia and temperate forests in Eastern Europe. The prevailing wind pattern, along with the existing vegetation structure in nearby grid cells, alters the competition dynamics of the trees in these regions by filtering unrealistic plant functional types through adjustment of establishment rates.

The SEED configuration was applied to project future vegetation structures under two climate mitigation scenarios (No-policy vs. 450ppm CO_2 stabilization) for the 21st century. The simulation results indicate that regional changes of vegetation structure under changing climates are expected to be significant. In the high latitudes, regions such as Alaska and Siberia are expected to experience substantial shifts of forestry structure, characterized by expansion of needle-leaf boreal forest and shrinkage of C3 grass Arctic. In the mid-latitudes, temperate trees are likely to expand in South America, South Africa, and East Asia at the expense of C3 grass during the latter part of the 21st century. In the

Tropics, the most notable degree of change is in the composition of tropical trees and C4 grasses in the Amazon and in Africa.

The vulnerability assessment suggested by this study shows that vegetation structures in Alaska, Greenland, Central America, southern part of South America, East Africa and East Asia are susceptible to changing climates, regardless of the two climate mitigation scenarios. Regions such as Greenland, Tibet, South Asia and Northern Australia, however, may substantially alleviate their risks of rapid change in vegetation structure, given a robust greenhouse gas stabilization target.

The impacts of future vegetation change on radiation budget cannot be neglected. The results of this study suggest that depending upon the climate mitigation scenarios, vegetation change may enhance or mitigate the anticipated warming trend of the 21st century. Proliferation of boreal forests in the high latitudes to amplify the warming trend (i.e., a positive feedback to climate) if no mitigation policy is implemented. In contrast, under the 450ppm scenario, changes in vegetation structure may reduce the rate of warming, which is a negative feedback to climate. A series of hydrologic processes including interception of rainfall by forest canopy, evapotranspiration, and runoff are also influenced by modifications in vegetation structure. The magnitude of the runoff response by the vegetation change is not projected to exceed the direct response of hydrology to climate change (i.e., changes in precipitation); however, the spatial pattern of changes in runoff associated with vegetation changes indicates that vegetation change may in some regions offset or lessen increases in runoff due to enhanced precipitation under climate warming. Reduction of terrestrial productivity and a conservative estimate of vegetation carbon storage (-8PgC/yr and 24PgC, respectively under the no policy scenario) in the 21st century may be due to ignoring the CO_2 fertilization effect and partially applying the new SEED configuration to project future vegetation structures.

The SEED configuration developed in this study may serve to more comprehensively represent future vegetation structure across the global landscape and therefore may provide a tool to better assess the impacts of natural vegetation dynamics on the climate system. This model configuration may also provide outputs that can be used to assess the impacts of climate change on the goods and services that ecosystems provide to society.

CONTENTS

Acknowledgements

I would like to thank my thesis advisor, Prof. Ronald G. Prinn for his support and advice. He has trusted me all time, even when I had hard times with this research project. I hope that I will be an advisor like him, who trusts and supports the students. My sincere thanks also go to Dr. C. Adam Schlosser, who supported me and helped me so much to complete this research project. I would like to thank my thesis committee members, Dr. Mick Follows, Prof. A. David McGuire, Prof. Jerry Melillo, and Prof. Elfatih Eltahir for their advice and help.

Many thanks to Dr. Ho-jeong Shin, Dr. Eun-gul Lee, and Dr. Xiang Gao who provided advice and assistance for this research. I would like to thank Dr. Kyung-min Nam, Prof. Ben Felzer, David Kicklighter, and Prinn group members.

I would like to thank Boston Onnuri Church members, MIT/Kendall prayer meeting members, my friends Hyojung Kim, Elise Olson, Kyungwon Seo, Esther Youngju Lee, Woojung Kim, Eun Cho, Jeonggu Lee, Mi-yeon Han for their prayers and support for me. I also thank my voice teacher, Soyoung Park, my violin teacher Jungwon Kim, who taught me to love music, and my personal trainer Shue-Fen Tung, who taught me the pleasure of a workout. Many thanks go to Jooeun Lim Choi, Melissa Bender, Dr. Kanghyun Ji and Dr. Giyeon Kim, Jongmi Lee, Minsub Shim, Dr. Yong-sang Choi, Prof. In-Yeong Yeo, Dr. Shin-Chan Han, Melissa Fox, and Fannie Barnes.

I send my love to my parents in Korea, my sister Eunhwa Lee, my cousin Younghye, my uncle and aunt Dr. DongEun Lee and Younghee Lee, my aunt Ok-sun Pak, and family members in Korea and in the United States. I praise my God for teaching me stewardship of the nature that He created, and for allowing me to experience His lead throughout my life.

Chapter 1

Introduction

1.1 Introduction

One third of the total global land area is covered by forests. As forests generate oxygen and provide homes and foods for humans and animals, about 80% of the terrestrial biodiversity relies upon forests. Currently, humans utilize about 30% of world's forests for wood production and non-wood goods (United Nations International Year of Forests, http://www.un.org/en/events/iyof2011/index.shtml).

Not only humans, but also environment stresses affect forest structure, or more generally the natural vegetation structure that includes all types of forests and grasslands. For example, under changing climates over the past 1,000 years, the evidence shows the northward movement of spruce trees in Canada (e.g., MacDonald et al., 1993). For the last century, studies also show shifts in tree line northward in northern high latitudes and upward in elevation as forests expand into treeline taiga and tundra (Kullman, 2002; Moiseev and Shiyatov, 2003; Esper and Schweingruber, 2004; Lloyd, 2005; Devi et al., 2008).

1.1.1 Vegetation dynamics and ecosystem structure and function

Given the evidence for tree line shifts, it is crucial to understand the mechanisms of the response of vegetation to changing climates. In addition, as climate change draws more attention from the decision makers, the demands for modeling the impacts of climate change on the ecosystems are growing. The capability of simulating future vegetation structure becomes more important because both directly and indirectly, responses of influences ecosystem function and structure (e.g., Feddema et al., 2005; Bonan, 2008).

Vegetation influences climate in several ways. As vegetation structure changes, the terrestrial surface albedo is modified, altering the radiation budget because forests and grasslands have different reflectivities of incident solar radiation (i.e, vegetation-albedo feedback). Change in albedo and radiation budget can also cause further change in vegetation as temperature and moisture conditions change. Vegetation change in the Arctic, for example, could accelerate summer warming (Chapin et al., 2005).

Indirectly, changes in vegetation structure also impact the water cycle. Expansion or shrinkage of forests/grasslands affects the rate of interception of rainfall by the canopy.

In addition, the rate of transpiration depends on stomatal conductance. As both temperature and atmospheric CO_2 concentration are elevated under the anticipated climate change scenarios, the sign of the change in transpiration is uncertain as stomata tend to open more widely in response to greater moisture availability, but tend to close under higher atmospheric CO_2 concentration (Betts et al., 2007). The amount of water storage at the soil column may also vary as shifts of vegetation structure occur above ground. Consequently, change in vegetation structure may alter the runoff. Another link that is recently suggested by Swann and coauthors (2010) is between the altered hydrologic cycle due to vegetation and the radiative budget, showing that the enhanced transpiration due to expansion of deciduous forests may cause radiative imbalance at the top of the atmosphere.

Terrestrial carbon dynamics are also linked to changes in vegetation structure. Reduced Net Primary Production (NPP) may result in the loss of trees and grasses for the vegetation. As new types of plants proliferate at the expense of previously existing types, the transition affects NPP and vegetation carbon storage to affect terrestrial carbon dynamics. Studies have discussed the relationship between the vegetation structure and the terrestrial carbon cycle (e.g., Cox et al, 2000; Gerten et al., 2005), but the magnitude of the feedbacks to the climate system is highly uncertain (Arneth et al., 2010). This is because vegetation changes may simultaneously result in both positive and negative feedbacks to the climate system. For example, Betts (2000) suggested that expansion of boreal forests in tundra may have cooling effects on the atmosphere associated with increased vegetation carbon storage that are offset by warming effects associated with decreased albedo. More realistic representations of vegetation structure can thus lead to better estimates of NPP, terrestrial vegetation and soil carbon storage, and land-atmosphere carbon exchanges.

Figure 1.1 illustrates the relationship between the vegetation structure and the ecosystem properties that may undergo the impacts due to the change in the terrestrial biogeography under changing climates. In addition to the close relationship between vegetation structures and ecosystem dynamics, estimates of future land cover change have implications for land management policy (e.g., forest management (Canadell and Raupach, 2008)) and climate policy.

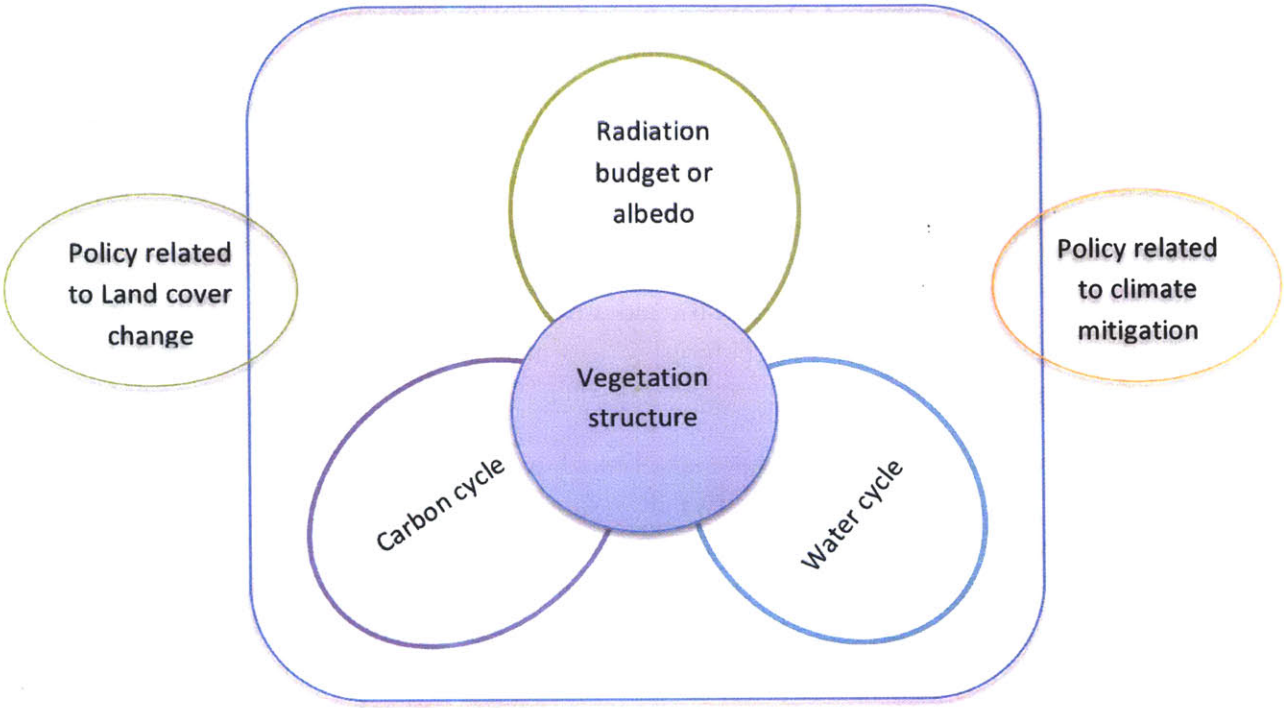

Figure 1.1: Vegetation structure and its related areas of interest

1.1.2 Dynamic Global Vegetation Models (DGVMs)

In order to serve the need for realistic representation of vegetation structure and dynamics, Dynamic Global Vegetation Models (DGVMs) are used to describe the response of vegetation structure and biogeography to climate change. DGVMs are mechanistic and rule-based models that simulate "vegetation development and dynamics through space and time" (IPCC, 2007, in Appendix I: Glossary) either driven by prescribed climate or coupled to the earth system models. The models also allow the exploration of the impacts of vegetation structure ecosystem dynamics and feedbacks to the climate system.

Several DGVMs are currently used in studies that explore how vegetation structural responses influence feedbacks to climate and ecosystem dynamics. The Integrated Biosphere Simulator (IBIS) is a DGVM that was developed at University of Wisconsin (Foley et al., 1996; Kucharik et al, 2000). The Top-down Representation of Interactive Foliage and Flora Including Dynamics (TRIFFID) model was developed in the Met Office, U.K. (Cox, 2001), and is embedded in the Hadley Center General Circulation Model (GCM) (e.g., Huntingford et al., 2008). The HYBRID (Friend et al., 1995), the Sheffield-DGVM or SDGVM (Woodward et al., 1995; Woodward and Lomas, 2004), and the ORCHIDEE (Krinner et al., 2005) are other DGVMs that have been developed. The Lund-Potsdam-Jena (LPJ) model is a very widely used DGVM (Sitch et al., 2003). The model was also incorporated into the Community Land Model (CLM-DGVM) (e.g., Bonan and Levis, 2006). The dynamics of these five DGVMs (LPJ, HYLAND, SDGVM, TRIFFID, and ORCHIDEE) have been compared by Sitch et al. (2008). In this study, I used the CLM-DGVM, which adopts the essence of the vegetation dynamics from the LPJ model. The processes of the slow vegetation dynamics of the CLM-DGVM are further described in Chapter 2.

The CLM-DGVM simulates the dynamic changes of natural vegetation either driven by prescribed climate or coupled to a climate model (e.g., Bonan and Levis, 2006). Studies show that estimates of change in future vegetation structure under different Special Report Emission Scenarios (SRES) either with prescribed climates or coupled to climate models (e.g., Fischilin et al., 2007; Sitch et al., 2008).

1.1.3 What is missing in the current DGVMs?

Current DGVMs assume ubiquitous availability of seeds and do not generally consider seed dispersal mechanisms and plant migration processes. Ignoring plant migration processes has the potential to unrealistically estimate fast forest expansion in response to future climate, and may lead to misleading estimates of carbon sequestration capacity (Neilson et al., 2005) and unrealistic representation of net radiation and hydrologic changes associated with terrestrial vegetation change.

Plant migration processes may cause a time lag in response of tree distribution to climate. Davis (1989) argued that the response of tree distribution to climate may be delayed because of inadequate seed dispersal or competition from the resident plants, including existing trees and herbaceous plants. Also some natural dispersal agents such as animals may be less abundant or even missing so that the seed dispersal may become less effective in the current environment. Another factor that may cause a delay in vegetation response to climate change is the reduction in tree population because of logging. It is challenging to estimate how vegetation structural changes influences the climate system

because many trees may not respond rapidly due to the insufficient seeds, which could cause some tree species to become extinct. The climate cooling during the Younger Dryas (12,800 ~ 11,500 BP) did not cause a delayed response of trees because they were killed due to the sudden drop of temperature, as the fossil records show; however the warming after the Younger Dryas caused a delayed expansion of trees (Davis, 1989, Iversen, 1954).

On the other hand, the Reid's paradox (Clark et al., 1998) is the debate over the unusually rapid migration after the last glacial period. Long-distance dispersal is a mechanism that could explain this rapid migration. The chance of the long-distance dispersal is rare, but possible as very small proportion of seeds can be transported long distances. Nathan et al. (2002) showed that there are two modes in seed dispersal mechanism by wind. One mode is short distance dispersal that applies to most seeds, and the other mode is long-distance dispersal that allows some seeds to travel much longer distance when they are uplifted by turbulence and influenced by the winds above the forest canopy structure.

The migration process depends upon environmental suppression and dispersal capacity of a population of seeds (Sauer, 1988). Environmental suppression is implicitly included in the climatic rules of survival and establishment of plants in the current generation of DGVMs; however, the dispersal capacity of a population of seeds has not been adequately represented. Therefore, representations of seed dispersal mechanisms for each plant type and the probability of long-dispersal in DGVMs has the potential to improve the simulation of vegetation structural responses to climate change. It is crucial to represent seed dispersal mechanisms to constrain plant migration processes in DGVMs to better estimate the influence of vegetation structural changes on the climate system.

1.1.4 Previous studies that addressed plant migration processes

Previous modeling studies have used descriptive scenarios to represent different plant migration rates. For example, Solomon and Kirilenko (1997) applied an assumption that invasion of trees to new territory does not occur until atmospheric CO_2 concentration is doubled. Using the IBIS model, Higgins and Harte (2006) evaluated alternative maximum and minimum migration scenarios, neighbor-only migration, and grass-only migration. They demonstrated that plant migration influences land surface processes through changes in carbon storage, evapotranspiration, and solar radiation that is absorbed by land. Another modeling study by van Minnen and colleagues (2000) used the IMAGE2 model (Alcamo et al. 1998) and evaluated the effects of three scenarios of unlimited migration, gradual migration, no-migration. These studies, however, do not

represent the dynamics of plant migration involving wind-driven seed dispersal using meteorological data and altered establishment rates.

1.2 Motivation, research task and goals of this thesis

Given the importance of seed dispersal mechanisms to plant migration, development of a tool that incorporates a more comprehensive treatment of plant migration using meteorological data can provide an explicit representation of plant migration process, thus improving the understanding of the impacts of change in future vegetation structure to natural ecosystems. The tool developed in this study incorporates a time-varying, wind-driven seed dispersal mechanism as a dynamic constraint to the plant migration process of natural vegetation (hereafter, the tool is called the "SEED configuration").

Using the SEED configuration, a set of questions addressed below is to be answered:

1. What are the mechanisms by wind-driven seed dispersal to plant migration process and the competition dynamics?
2. Does the SEED configuration provide a better representation of vegetation structure?
3. What does the future vegetation structure look like under different climate mitigation scenarios using the SEED configuration?
4. What are the impacts of change in future vegetation structure to the ecosystems in the 21st century?
5. Would climate mitigation policies impact the local and migratory response of the natural ecosystems, and if so, how?

In the following chapters, the questions above will be investigated and answered. Details of model development and calibration efforts are described in Chapter 2. Evaluation of the SEED configuration, driven by contemporary climate, is presented in Chapter 3, followed by an application to project future vegetation distributions (Chapter 4) and subsequent changes in the ecosystem (Chapter 5). Conclusion and summary are in Chapter 6.

Chapter 2

Development of the SEED configuration

2.1 Introduction

This chapter describes the modeling tool used for this study, the Community Land Model (hereafter called CLM). The CLM, which was developed at the National Center for Atmospheric Research (NCAR), has been continuously updated. When this research project started, the most updated version, CLM 3.5, was available to the public; therefore, it was selected, modified and used for this study. The most updated version is the CLM 4, but its description of biogeography, which our study heavily focuses on, remains as same as the CLM 3.5. More information about the CLM can be found at http://www.cgd.ucar.edu/tss/clm/.

Overviews of the CLM and the CLM-DGVM are briefly discussed in the following sections (2.2 and 2.3). Section 2.4 illustrates the development of the MIT-CLM-SEED, which is an improved tool to simulate time-varying wind-driven seed dispersion as a dynamic constraint to the migration process of natural vegetation. This tool allows more in-depth research on the degree of impact of wind-driven seed dispersal to plant migration via seed availability, as well as answering the question if dispersion of seeds is a significant limiting factor in shaping global and regional biogeography of natural vegetation. In addition, Section 2.5 addresses the issue of calibration in simulating realistic vegetation carbon fluxes while generating a reasonable vegetation distribution map.

2.2 Overview of the CLM model

The CLM is a process-based model that simulates biogeophysics, biogeochemistry and biogeography of land processes including water cycle, radiation, plant physiology, and vegetation dynamics. Details of this model can be found elsewhere (Levis et al., 2004; Oleson et al., 2007). In this study, we used version 3.5, which was released to the public in 2007.

Previous studies explored various areas in land processes including climate statistics (Dickenson et al., 2006), global plant biogeography and Net Primary Production (Bonan and Levis, 2006), and the hydrological cycle (Hack et al., 2006; Lawrence et al., 2007). Lawrence et al. (2007) investigated hydrologic parameters on partitioning

evapotranspiration for both offline and online simulations, and also impacts of DGVM on evapotranspiration and runoff, especially for the western United States and the Amazon.

The CLM model can be run offline or online coupled to an atmospheric model (e.g., Bonan and Levis, 2006). To force the model, information on at least five atmospheric variables (atmospheric temperature, winds, humidity, precipitation, and incoming solar radiation) is required (Table 2.1).

Table 2.1 Input variables required for the simulations using the CLM

Variable	Description	Unit	Required/Optional
tbot	Atmospheric air temperature	K	Required
qbot	Specific humidity	kg/kg	Required
fsds	Total incident solar radiation	W/m^2	Required
wind	Wind; sqrt of $(u^2 + v^2)$	m/s	Required
prectmms	Total precipitation	mm/s	Required
psrf	Surface pressure	Pa	Optional
flds	Incoming longwave radiation	W/m^2	Optional

For this study the spatial resolution of 2 ° x 2.5 ° (approximately 220 km x 180 km, varying on latitudes) is used. The time step for biogeophysics and biogeochemistry is 20 minutes. Slow processes in vegetation dynamics are updated annually (see Section 2.3 for details). Since this model development effort focuses on slow processes of vegetation dynamics, which illustrates the biogeography of natural vegetation, further details of the CLM-DGVM are in the following section.

2.3. Biogeography in the CLM-DGVM

The CLM-DGVM heavily adopts the features from the Lund-Potsdam-Jena (LPJ) DGVM. In the form of the Land System Model (LSM), which is a predecessor to the CLM (Bonan et al., 2003), it was evaluated against observations. Bonan and Levis (2006) used this model in identifying biases of the land model (CLM3) and the atmospheric model (CAM3), simulating cases both offline and online.

Ten default Plant Functional Types (PFTs) are defined: two tropical forests, three temperate forests, two boreal forests, and three grasses. Shrubs are not defined in the CLM-DGVM, which may cause potential errors in evaluating vegetation distribution patterns and biogeochemical and hydrological variables. Recently, a study by Zeng (2010) evaluated a revised model that considers boreal and temperate shrub PFTs; however they have not been officially introduced into the currently available version of the CLM.

Table 2.2: Ten PFT types defined in the CLM-DGVM

CLM PFT number	Abbreviation	Description
1	NET temperate	Needleleaf Evergreen Tree - temperate
2*	NET boreal	Needleleaf Evergreen Tree – boreal
4	BET tropical	Broadleaf Evergreen Tree – tropical
5	BET temperate	Broadleaf Evergreen Tree - temperate
6	BDT tropical	Broadleaf Deciduous Tree - tropical
7	BDT temperate	Broadleaf Deciduous Tree - temperate
8	BDT boreal	Broadleaf Deciduous Tree – boreal
12†	C3 Arctic grass	C3 Arctic grass
13	C3 Grass	C3 grass (cold-season grass)
14	C4 Grass	C4 grass (warm-season grass)

* PFT number 3 (NDT boreal; Needleleaf Deciduous Tree – boreal) is aggregated to PFT number 2 (NET boreal) in the CLM-DGVM

† PFT numbers 9, 10, 11 are shrub types, which are not defined in the CLM-DGVM

Figure 2.1 illustrates the components of the CLM-DGVM and flow of inputs and outputs in the model. The details of these processes are fully described elsewhere (Bonan et al. 2003; Levis et al., 2004), but the details of some chosen processes are discussed here in order to introduce the development of the configuration incorporating seed dispersal mechanisms. At the end of each model year, variables such as percentage of vegetated land area and NPP are updated through seven main modules that are called consecutively: (1) Reproduction; (2) Turnover; (3) Kill due to negative NPP; (4) Allocation; (5) Mortality; (6) Fire; and (7) Establishment (see Figure 2.1).

At the end of each model year, the slow processes in the DGVM are called to update vegetation geography and structure. An important input variable entering the DGVM is Net Primary Production (NPP), and outputs from the DGVMs are the occupied fraction of the naturally vegetated land-unit of each PFT (hereafter called as "fpcgrid"), annual maximum Leaf Area Index (LAI_{max}), height of the tree canopy (H), vegetation carbon and soil carbon. In the model, these output variables are updated in the eight processes consecutively: (1) Reproduction; (2) Turnover; (3) Mortality due to negative NPP; (4) Allocation of carbon; (5) Competition for light; (6) Mortality (background and heat stress); (7) Fire; and (8) Establishment.

In the reproduction process, 10 % of the NPP is consumed for all PFTs. The NPP is updated by 90% with the remaining 10% added to the above-ground litter. In the turnover process that is inversely proportional to the tissue longevities, leaf carbon returns to the above ground litter, root carbon to the below ground litter, and living, sapwood carbon to dead, hardwood carbon. Then if the NPP of a PFT is negative, the PFT is removed because it cannot sustain itself the next year with the negative NPP. The carbon of the killed PFT is moved to litter carbon. For the PFTs whose NPPs are positive, the amount of the NPP is allocated to different parts of the plant; leaves, sapwood, and roots. In the allocation process, fpcgrid, LAI, and H are updated. Then mortalities according to growth efficiency and due to heat stress and fire are applied.

Finally, a set of temperature and moisture conditions determines survival and establishment of the PFT. The processes occur as they set lower and upper limits of temperatures and Growing Degree Days (GDDs) (Levis et al., 2004). For a PFT to survive, the coldest month temperature and GDD should not be lower than the PFT-specific coldest-monthly temperature limit ($T_{c,min}$, second column in Table 2.3). In order to establish or regenerate, first of all, a PFT must satisfy the survival condition (i.e, 20-yr running mean is equal or larger than $T_{c,min}$). Then, in addition to passing the survival condition, the PFT needs to comply with the establishment conditions: the 20-yr running mean temperate should be equal or lower than Tc,max, and the GDD based on 5°C should be at least as many days as $GDD05_{min}$ (third and fourth columns in Table 2.3). The number or population of individual of PFTs (nind) is updated, which depends on the maximum establishment rate, percentage of non-occupied land area, and total number of tree PFTs that could potentially establish according to the climatic rules. Then the fpcgrid of the PFT is updated as the nind changes (Eqn 2.1).

$$fpcgrid_{PFT} = CA \times nind \times fpcgrid_{individual} \quad \text{(Eqn 2.1)}$$

where CA is crown area, nind is number population, $fpcgrid_{individual}$ is the fractional cover of an individual tree of the PFT type. The nind is also a variable that changes as the establishment rate of the grid varies (Eqn 2.2 and Eqn 2.3).

$$nind = nind(of\ the\ previous\ year) + Estab_{grid} \quad \text{(Eqn 2.2)}$$

$$Estab_{grid} = Estab_{PFT} \times [1 - fpcgrid_{Tree\ total}] \quad \text{(Eqn 2.3)}$$

Table 2.3: PFT-specific climatic conditions for survival and establishment (taken from Bonan et al. (2003) and CLM-DGVM 3.5 code)

	Survival	Establishment	
PFT	$T_{c,min}$ [a] [°C]	$T_{c,max}$ [°C]	$GDD05_{min}$ [c]
NET temperate	-2.0	22.0	900
NET boreal	-32.5	-2.0	600
BET tropical	15.5	No limit	0
BET temperate	3.0	18.8	1200
BDT tropical	15.5	No limit	0
BDT temperate	-17.0	15.5	1200
BDT boreal	No limit	-2.0	350
C3 Arctic grass	No limit	-17.0	0
C3 Grass	-17.0	15.5	0
C4 Grass	15.5	No limit	0

[a] PFT-specific limit of the coldest monthly mean temperature for survival

[b,c] Growing Degree Days based upon 0°C and 5°C

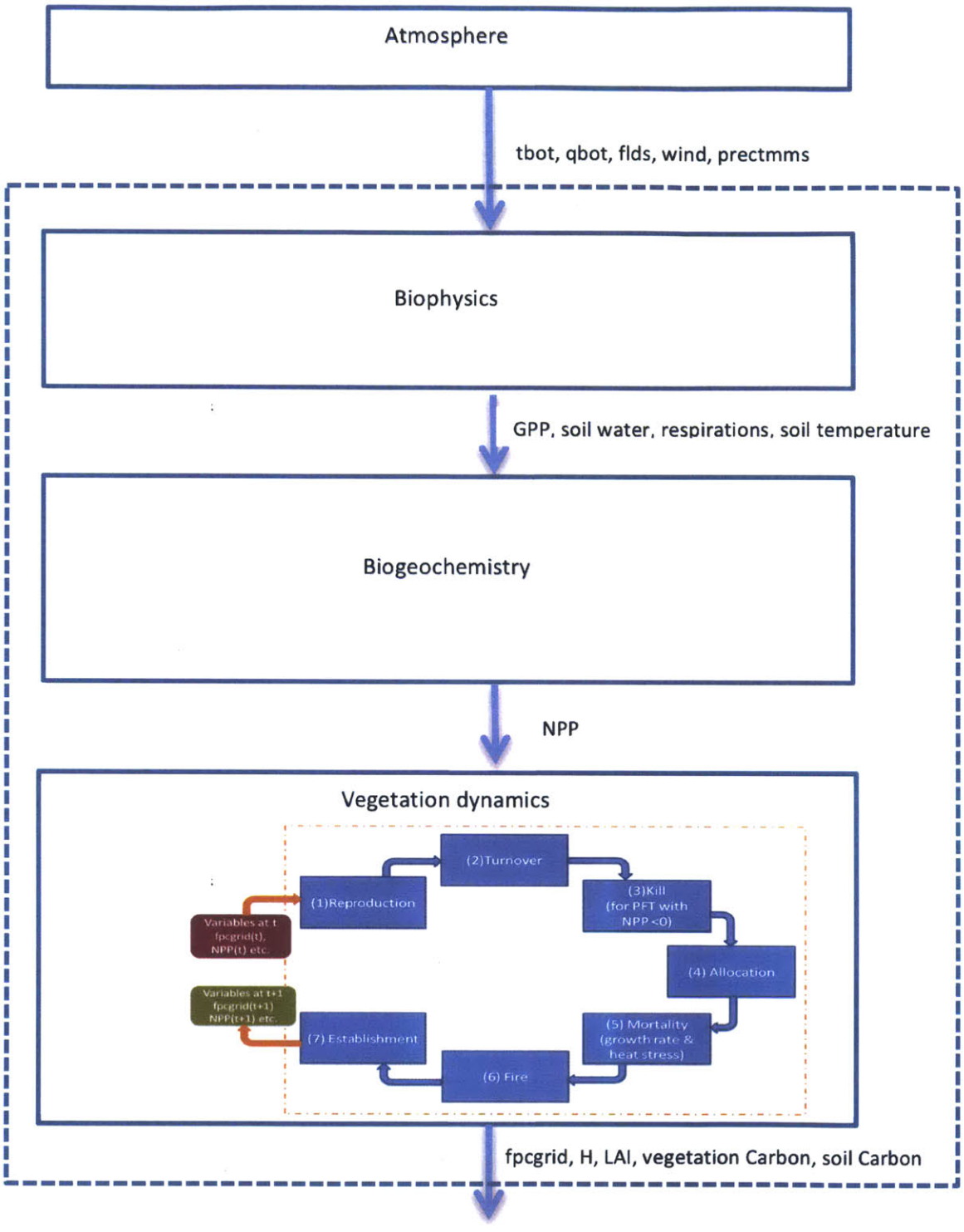

Figure 2.1: Modules describing biogeography in the default CLM –DGVM (version 3.5). The five input variables (tbot, qbot, flds, wind, prectmms) are defined in Table 2.1. GPP means Gross Primary Production, NPP is Net Primary Production. The fpcgrid is the fractional area (%) occupied by a PFT in a grid, H is the height of a PFT, and LAI means Leaf Area Index.

2.4 What is new in the SEED configuration?

As the efforts to include migration process in DGVMs, previous studies applied certain migration scenarios, including gradual **migration** and no migration (model: IMAGE2; van Minnen et al., 2000), and neighboring migration and unlimited grass and shrub migration (model: IBIS; Higgins and Harte, 2006). However, the migration scenarios in these studies are not PFT-specific, and do not include the effect of time-varying meteorology (for example, wind fields) that is an important vehicle for carrying seeds generated from boreal and temperate trees.

To incorporate a more realistic representation of plant migration processes via seed dispersal mechanisms, a configuration (hereafter called as "SEED configuration") is developed, which copes with a dynamic, PFT-specific, and population-dependent seed availability constraint into the CLM-DGVM. The key in this configuration is to determine whether a PFT receives a high number of germinated seeds from surrounding grids. The SEED configuration introduces an idea of probabilistic approach to the process of plant migration into the CLM-DGVM. In the process of computing percentage of occupied area by a PFT, which is PFT fractional coverage relative to the naturally vegetated land-unit area (fpcgrid) in the model, the SEED configuration brings an important condition for seed availability. Note that seed dormancy is not taken into account. The densities of the seeds are computed each year.

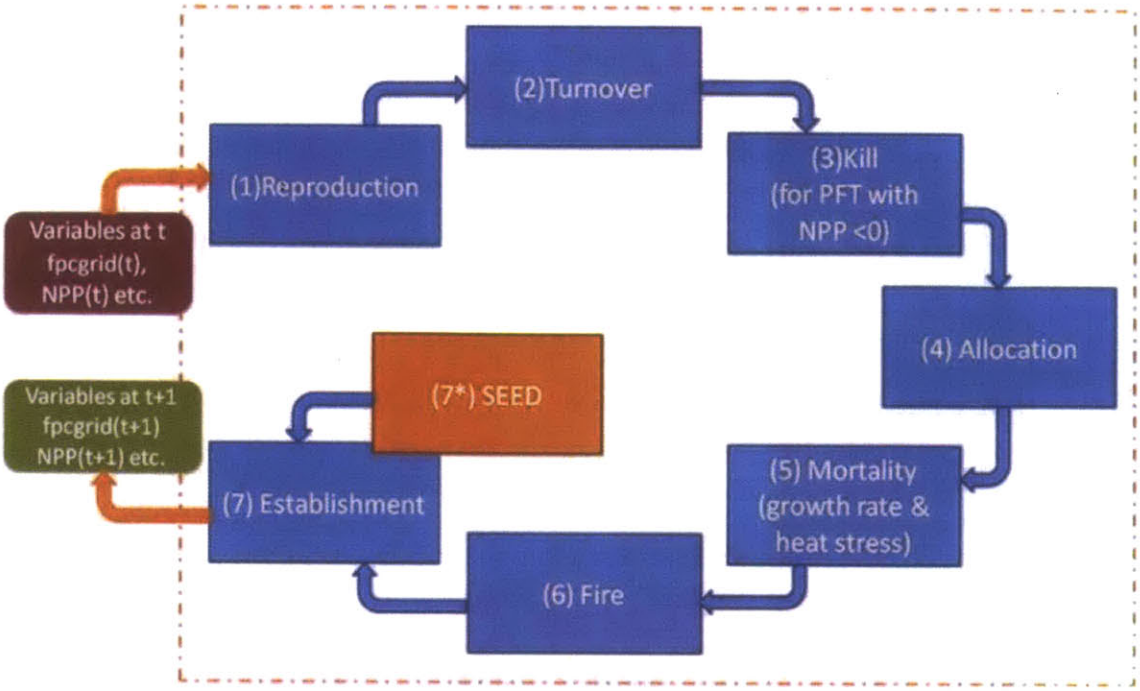

Figure 2.2: Adding another layer of constraints to the establishment process in the CLM-DGVM

The first step is to determine the type of dispersal mechanism for each PFT (wind, neighbor, or no-limit). Next, the type of PFT is scanned, and if the PFT is a tree PFT, then the kind of dispersal mechanism (e.g., wind dispersal for boreal and temperate trees) is assigned to the tree PFT. Since many plants, especially those outside the Tropics, germinate and disperse seeds by wind (Neilson et al., 2005), we assume for boreal trees and temperate trees their inter-grid plant migration process is wind dispersal. Wind dispersal is the dominant seed dispersion mechanism for boreal trees (e.g., willow trees) and temperate trees (e.g., maple trees). For instance, white spruce (*Picea glauca*), a native species to the boreal forests in the North America, are widely found in Western Alaska. Their cones include seeds with brown wings, which are dispersed by wind.

Recently, Long-Distance Dispersal (LDD) mechanisms of plants have gained more attention because of their potentially importance to anticipated climate change. Normally, most plant seeds travel less than a kilometer; however, some seeds travel as far as several hundred kilometers. Updraft winds and turbulence at the top of trees enable seeds to be dispersed by the wind-driven LDD mechanism (Nathan et al, 2002). Considering the spatial scales of the model grid and the LDD, those seeds can be provided from the eight neighboring grids, but not from the grids farther than the neighboring grid cells.

In the tropics, the wind dispersal mechanism is not a major method for seed dispersal, so a loose condition (i.e., neighboring migration constraint) is applied for tropical forests. As long as the tropical tree PFT type exists in at least one adjacent grid, it is assumed that the center grid is able to obtain high enough numbers of geminated seeds from the PFT in the neighboring grid(s).

Three grass types (i.e., C3 grass Arctic, C3 grass and C4 grass) are not limited by wind dispersal or neighboring seed availability and they assumed to freely migrate. Table 2.4 summarizes the dispersal mechanisms for ten PFT types in the SEED configuration.

Table 2.4 Ten PFT types and their seed dispersal mechanisms in the SEED module.

PFT	Category	Seed dispersal mechanism in SEED
NET temperate	Tree	Seeds by wind dispersal
NET boreal	Tree	Seeds by wind dispersal
BET tropical	Tree	Seeds from neighboring grids
BET temperate	Tree	Seeds by wind dispersal
BDT tropical	Tree	Seeds from neighboring grids
BDT temperate	Tree	Seeds by wind dispersal
BDT boreal	Tree	Seeds by wind dispersal
C3 Arctic grass	Grass	Free migration (no-limit)
C3 Grass	Grass	Free migration (no-limit)
C4 Grass	Grass	Free migration (no-limit)

Once the mechanism is determined, then the density of available, germinated seeds for the tree PFTs is computed. For tree PFTs that have wind-dispersed seeds (temperate forests and boreal forests), we take five factors into consideration: (1) fecundity (i.e., number of seeds produced from a tree, denoted as f); (2) population density of the tree PFT type in surrounding grids ($POP_{Neighbor}$); (3) efficiency of dispersal (ε_{disp}); (4) number of days of favored winds to a target grid cell from neighboring grid cells (applied only to boreal forests and temperate forests); and (5) germination rate (*germ*) of seeds.

The number density of potentially germinated seeds (D_{seeds}) for boreal and temperate tree PFTs is then calculated as in Eqn 2.4.

$$D_{seeds} = f \times POP_{Neighbor} \times \varepsilon_{disp} \times \frac{Days\ of\ favorable\ wind}{Total\ days\ in\ autumn} \times germ \qquad \text{(Eqn 2.4)}$$

where 10^4 seeds produced by a tree per year is taken as a typical fecundity rate of a temperate or boreal tree. The efficiency of LDD for boreal forests and temperate forests is 1%~5% (Nathan et al., 2002) and a conservative value of 1% is taken for this study (i.e., $\varepsilon_{disp} = 0.01$). The total number of days in autumn is 90 days, and the typical *germ* is 0.70.

The number of trees (or tree density in a neighboring grid) is calculated by multiplying percentage cover of the tree type with the number of individual trees of the PFT type. The number of days of favorable wind blowing toward a target grid cell is counted only for fall seasons in the Northern hemisphere (September, October and November) and in the Southern hemisphere (March, April and May) because most boreal and temperate forests disperse mature seeds only during the fall season. Finally, the density threshold (10 germinated seed per m^2) is applied.

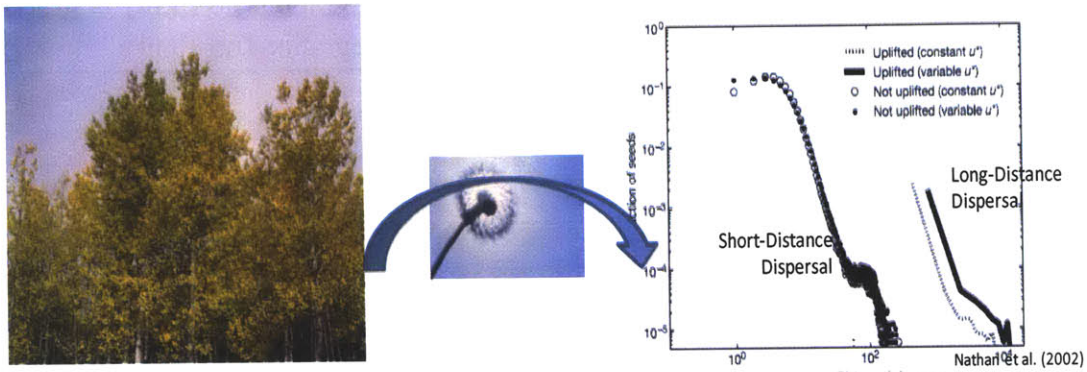

Figure 2.3. Long-Distance Dispersal (LDD) mechanism applied for boreal tree PFTs and temperate tree PFTs. Graph taken from Nathan et al. (2002).

The addition of the above mechanisms is mostly accomplished in the DGVM modules illustrating slow vegetation dynamics. Some minor changes are also made to other parts of the CLM. In the biogeophysics model, the SurfaceAlbedo module is modified in order to expand the options to various climate forcing datasets that may or may not have the same phase of the diurnal cycle as defined in the CLM (e.g., for the case using the IGSM-simulated future climate, discussed later in Chapter 4). The driver module in the main directory is also tailored because the SEED configuration is designed to be called directly from the driver module.

2.5 Calibration and initialization

In order to develop from a bare ground an initial condition of a vegetation distribution map with reasonable plant carbon (e.g., NPP), the CLM-DGVM is initialized by applying a 20-year climate (1951-1970) of the NCEP Corrected by CRU (NCC) dataset repeatedly for 200 years. For this spin-up process, the canonical form of the CLM-DGVM that assumes FREE plant migration is applied because the spin-up begins from a bare ground. A pre-requisite for using the SEED configuration is a map of existing PFTs so that seeds become available from adjacent grids by winds (for boreal forests and temperate forests) or other vehicles (for tropical forests).

First, a suggested set of parameters relating plant physiology from the NCAR CLM-DGVM developers is tested; using these parameters, NPP values from the simulated vegetation are higher than previously reported values in the literature (Kucharik *et al.*, 2001, a hybrid of observation and model data of NPP). This issue of high NPP values is known and reported by developers at NCAR and by previous users. In the CLM-DGVM version 3.5, the vegetation distribution is improved but "Leaf Area Index (LAI) and NPP values remain overestimated" (Oleson et al., 2007). Without modeling the active nitrogen cycle, high Gross Primary Production (GPP) generated in the canopy integration of photosynthesis causes the overproduction of NPP. Especially where boreal forests are dominant, the overproduction is notable. Oleson and others (2007) suggested a set of calibrated nitrogen limitation parameters (Table G1 in their publication); however the NPP values using their parameters still remain somewhat high (Table 2.5).

Table 2.5: Parameters modified for initializing the CLM-DGVM driven by the NCC climate

PFT	Model NPP [gC m^{-2} yr^{-1}] (NCAR calibration using Table G1, Levis et al. (2007))	[a]Observed NPP [gC m^{-2} yr^{-1}]
NET temperate	597	775±500
NET boreal	**1006**	**325±200**
BET tropical	1177	1250±900
BET temperate	590	900±550
BDT tropical	538	825±475
BDT temperate	426	600±325
BDT boreal	486	425±200
C3 Arctic grass	468	150±200
C3 Grass	331	575±475
C4 Grass	1036	N/A

[a] Values taken from Kucharik et al., (2001)

In order to simulate a more reasonable vegetation distribution with acceptable NPP values (i.e, the ranges of the observed NPP (Kucharik et al., 2001) in Table 2.5), further parameterizations are done in this study. The modified parameters include the rate of carbon-fixation reaction of plants' photosynthesis (e.g., V_{cmax25}) and nutrient nitrogen (e.g., fnitr) and carbon allocations (e.g., turnover rates). With the modified V_{cmax25}, *fnitr*, and turnover rates, unreasonably high NPP values are to be adjusted while the vegetation distribution structure is sustained compared to the potential vegetation map by Ramankutty and Foley (1998).

In the photosynthesis process, a five-carbon sugar, which is called ribulose-bisphosphate (RuBP), is converted into two three-carbon sugars using CO_2. This RuBP caboxylation is the rate-limiting step in the carbon-fixation reactions. Therefore lowering V_{cmax} can also bring down the photosynthesis rate, reducing high NPP in the simulations. For the PFT types that simulate unacceptably high NPP, boreal forests and C3 grass Arctic, the V_{cmax} rates at 25 °C are reduced in half: 43.0 μmol $CO_2/m^2/s$ to 21.0 μmol $CO_2/m^2/s$ (NET boreal forest), 51.0 μmol $CO_2/m^2/s$ to 25.0 μmol $CO_2/m^2/s$ (BDT boreal forest), and 43.0 μmol $CO_2/m^2/s$ to 21.0 μmol $CO_2/m^2/s$ (C3 grass Arctic).

fnitr is defined as the nitrogen limitation in the model. Since the CLM-DGVM in version 3.5 does not include modules describing nitrogen dynamics, nitrogen limitation is parameterized using a constant for each PFT. Too low *fnitr* could allow the plant to synthesize unrealistically large amount of carbon through photosynthesis. From a series of test runs, a set of *fnitr* for ten PFTs is suggested, which archive reasonable vegetation distributions and acceptable NPP values. The *fnitr* values are lowered for NET boreal forest (0.62 to 0.30), BDT boreal forest (0.41 to 0.26), C3 grass Arctic (0.39 to 0.23), and C4 grass (0.24 to 0.12). The *fnitr* values for temperate forests and tropical forests do not change, and the value for C3 grass slightly increases (0.24 to 0.34) in order to satisfy the two demands: reasonable vegetation maps and acceptable NPP values (Table 2.6).

Although turnover times do not directly connect to photosynthesis and respiration, they are also linked to NPP by changing the carbon flow from living parts to dead parts of the plant. Assuming the turnover times of boreal forests are slower than temperate forests, lower NPP values are simulated while maintaining crown area and height of the boreal tree. For NET boreal forests, the turnover times of leaves are extended from 2 years to 4 years, and the sapwood turnover period (i.e., sapwood converted to heartwood) from 20 years to 60 years. For BDT boreal forests, slower turnover times of sapwood to heartwood are also assumed (from 20 years to 60 years).

Table 2.6 summarizes V_{cmax25}, *fnitr*, and turnover rates used to simulate the initial condition for the contemporary cases using the NCC climate.

Table 2.6: Parameters modified for initializing the CLM-DGVM with NCC climate (bold fonts).

PFT	V_{cmax25} (NCAR) [μmol $CO_2/m^2 \cdot s$]	V_{cmax25} (MIT) for NCC climate dataset [μmol $CO_2/m^2 \cdot s$]
NET temperate	51.0	51.0
NET boreal	**43.0**	**21.0**
BET tropical	75.0	75.0
BET temperate	69.0	69.0
BDT tropical	40.0	40.0
BDT temperate	51.0	51.0
BDT boreal	**51.0**	**25.0**
C3 grass Arctic	**43.0**	**21.0**
C3 Grass	43.0	43.0
C4 Grass	24.0	24.0

PFT	fnitr ratio (NCAR)	fnitr ratio (MIT) for NCC climate dataset
NET temperate	0.63	0.63
NET boreal	**0.62**	**0.30**
BET tropical	0.69	0.65
BET temperate	0.35	0.36
BDT tropical	0.31	0.31
BDT temperate	0.36	0.36
BDT boreal	**0.41**	**0.26**
C3 grass Arctic	**0.39**	**0.23**
C3 Grass	**0.24**	**0.34**
C4 Grass	**0.24**	**0.12**

Table 2.6 (continued): Parameters modified for initializing the CLM-DGVM with NCC climate (bold fonts).

PFT	Leaf turnover period (NCAR) [years]	Leaf turnover period (MIT) for NCC climate dataset [years]
NET temperate	2.0	2.0
NET boreal	**2.0**	**4.0**
BET tropical	2.0	2.0
BET temperate	1.0	1.0
BDT tropical	1.0	1.0
BDT temperate	1.0	1.0
BDT boreal	1.0	1.0
C3 Arctic grass	1.0	1.0
C3 Grass	1.0	1.0
C4 Grass	1.0	1.0

PFT	Sapwood turnover period (NCAR) [years]	Sapwood turnover period (MIT) for NCC climate dataset [years]
NET temperate	20.0	20.0
NET boreal	**20.0**	**60.0**
BET tropical	20.0	20.0
BET temperate	20.0	20.0
BDT tropical	20.0	20.0
BDT temperate	20.0	20.0
BDT boreal	**20.0**	**60.0**
C3 Arctic grass	1.0	1.0
C3 Grass	1.0	1.0
C4 Grass	1.0	1.0

Another minor change is the mortality of BDT boreal forest. Bonan and co-authors (2003) altered the maximum mortality of the BDT boreal forest in the mortality equation. Their argument for altering the maximum mortality is due to the short longevity of BDT trees. Instead, the coefficient that multiplies the growth efficiency is altered in this study. Because the GPP of BDT trees is reduced by the suggested parameterization of this study, the trees tend to easily die because of lowered NPP; thus their growth is boosted by increasing the mortality coefficient (k_{mort}) that multiplies the growth efficiency. For BDT boreal trees, three times larger k_{mort} is specifically applied.

$$Mortality = \frac{Maximum\ mortality}{[1+ (k_{mort} \times Growth\ efficiency)]} \qquad \text{(Eqn 2.5)}$$

With the new parameterization described above, most of the simulated NPP values result in good agreement with the range of previously reported values (Table 2.7).

Table 2.7: Parameters modified for initializing the CLM-DGVM driven by the NCC climate (bond fonts).

PFT	NPP (NCAR parameterization)	NPP (MIT parameterization for NCC climate dataset	[a]Observed NPP [gC m^{-2} yr^{-1}]
NET temperate	597	546	775±500
NET boreal	**1006**	**674**	325±200
BET tropical	1177	1139	1250±900
BET temperate	590	631	900±550
BDT tropical	538	548	825±475
BDT temperate	426	456	600±325
BDT boreal	**486**	**230**	425±200
C3 Arctic grass	468	422	150±200
C3 Grass	331	501	575±475
C4 Grass	1036	530	N/A

[a] Values taken from Kucharik et al., (2001)

The simulated vegetation distribution is also similar to the potential vegetation distribution of Ramankutty and Foley (1998). The potential vegetation is the vegetation structure that would exist if there were no land use by humans. Using the IBIS model, their potential vegetation includes 15 biome types that cover croplands as well as natural vegetation, whereas this study simulates natural vegetation. Also the classification of the CLM-DGVM includes ten PFTs (seven tree PFTs and three grasses, no shrubs) while they classify natural vegetation with more than 10 types. Finally, their potential vegetation map only shows the most dominant PFT type for the grid, but the simulated vegetation presented here shows the coverage over 5%; therefore, the maps are not expected to be identical. However, the vegetation maps simulated using the new parameterization shown in Figure 2.4 agree with the potential vegetation distribution closely enough.

(a) NET boreal forests

Simulation by CLM-DGVM

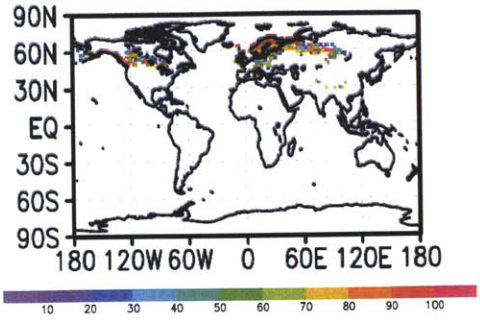

Potential vegetation map

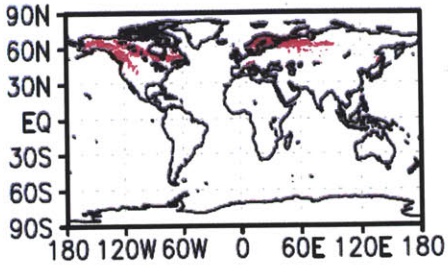

No color scale: NET boreal dominant in pink

(b) BDT boreal forests

Simulation by CLM-DGVM

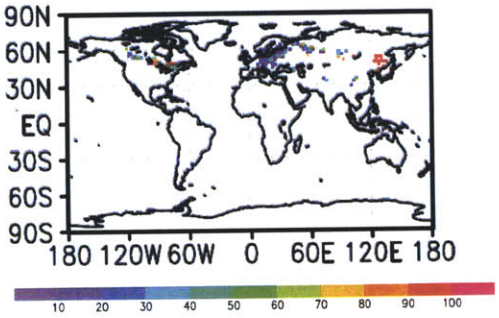

Potential vegetation map

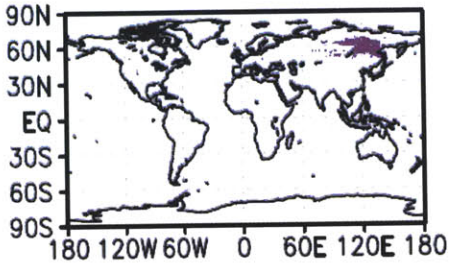

No color scale: BDT boreal dominant in violet

(c) C3 grass Arctic

Simulation by CLM-DGVM

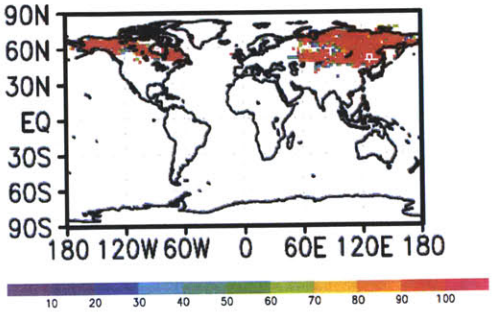

Potential vegetation map (tundra)

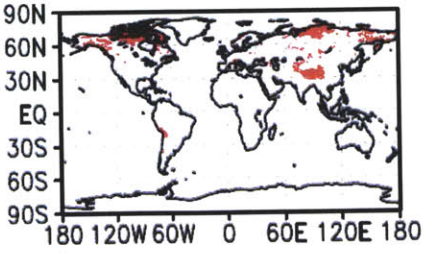

No color scale: C3 grass Arctic dominant in red

Figure 2.4: [Left] Initial distribution maps of ten PFT types simulated using the CLM-DGVM and [Right] potential vegetation maps of matching/similar PFT types by Ramankutty and Foley (1998): (a) NET boreal forests, (b) BDT boreal forests, (c) C3 grass Arctic.

(d) NET temperate forests

Simulation by CLM-DGVM

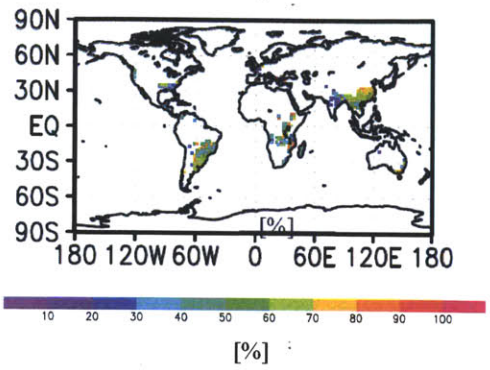

Potential vegetation map

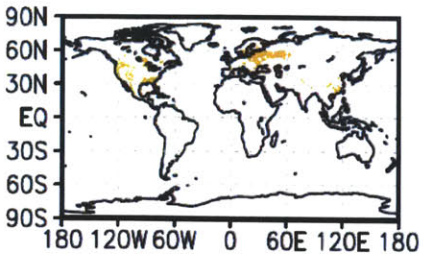

No color scale: NET temperate dominant in yellow

(e) BET temperate forests

Simulation by CLM-DGVM

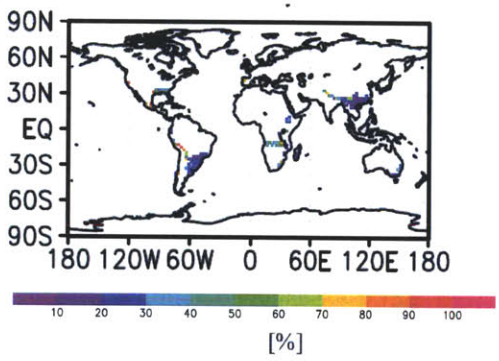

Potential vegetation map

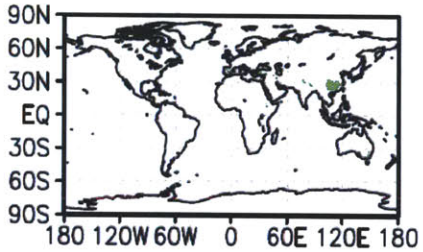

No color scale: BET temperate dominant in green

(f) BDT temperate forests

Simulation by CLM-DGVM

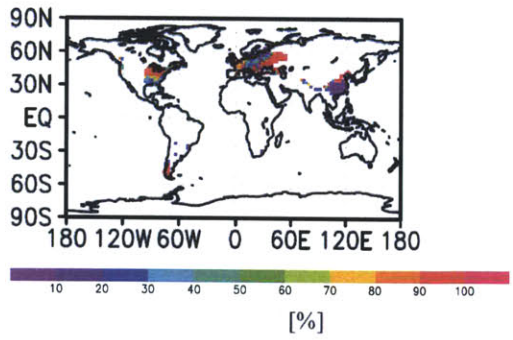

Potential vegetation map

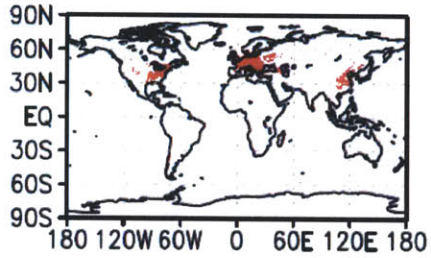

No color scale: BDT temperate dominant in red

Figure 2.4 (continued): [Left] Initial distribution maps of ten PFT types simulated using the CLM-DGVM and [Right] potential vegetation maps of matching/similar PFT types by Ramankutty and Foley (1998): (d) NET temperate forests, (e) BET temperate forests, (f) BDT temperate forests.

(g) C3 grass (cold-season grass)

Simulation by CLM-DGVM

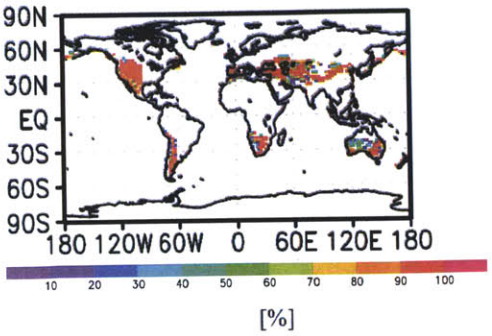

Potential vegetation map (grassland/steppe)

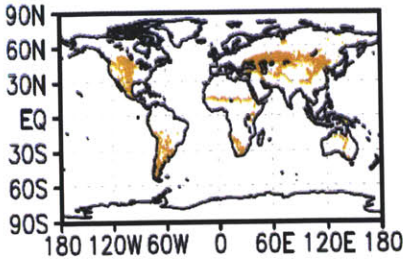

No color scale: C3 grass dominant in yellow

(h) BET tropical forests

Simulation by CLM-DGVM

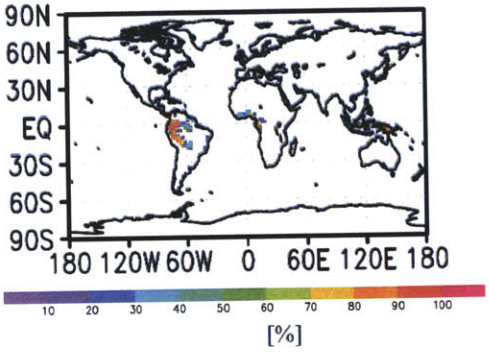

Potential vegetation map

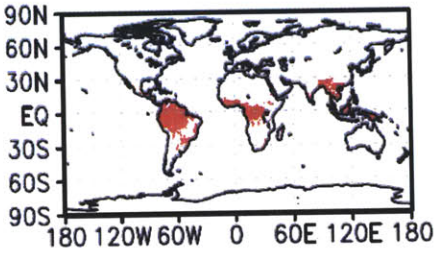

No color scale: BET tropical dominant in red

(i) BDT tropical forests

Simulation by CLM-DGVM

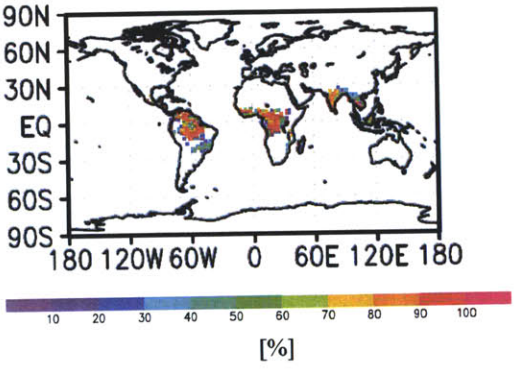

Potential vegetation map

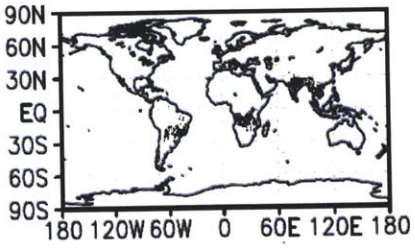

No color scale: BDT tropical dominant in dark grey

Figure 2.4 (continued): [Left] Initial distribution maps of ten PFT types simulated using the CLM-DGVM and [Right] potential vegetation maps of matching/similar PFT types by Ramankutty and Foley (1998): (g) C3 grass, (h) BET tropical forests, (i) BDT tropical forests.

(j) C4 grass (warm-season grass)

Simulation by CLM-DGVM

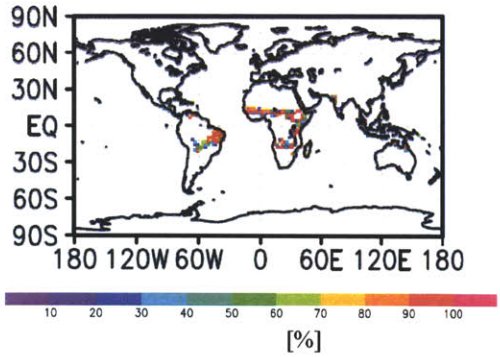

Potential vegetation map (Savanna)

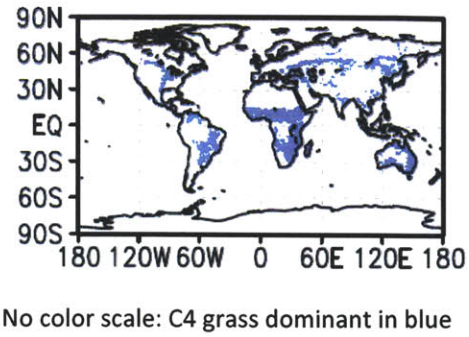

No color scale: C4 grass dominant in blue

Figure 2.4 (continued): [Left] Initial distribution maps of ten PFT types simulated using the CLM-DGVM and [Right] potential vegetation maps of matching/similar PFT types by Ramankutty and Foley (1998): (j) C4 grass.

Chapter 3

Evaluating the effects of seed-dispersal mechanisms on plant migration

3.1 Introduction

In this Chapter, the SEED configuration is evaluated compared to the canonical form of CLM-DGVM (i.e, the FREE configuration). Effects of meteorologically driven seed dispersal for boreal trees and temperate trees and of neighboring grid constraints applied to tropical trees are investigated at the global scale (Section 3.3.1.1) and regional scale (Section 3.3.1.2). In addition, two mechanisms altering competition dynamics among PFTs due to prevailing wind patterns, which are applied to the SEED configuration, are discussed in Section 3.3.2. Finally, comparisons of the simulated vegetation structures to satellite-driven tree covers are described in Section 3.3.3, followed by discussion and a summary of Chapter 3.

3.2 Input datasets and overview of the simulations

To evaluate the development of the SEED configuration, NCEP Corrected by CRU (i.e., NCC) climatology is used to drive two configurations: the canonical form of the CLM-DGVM (i.e., the FREE configuration) and the modified CLM-DGVM (i.e., the SEED configuration). The adjustments made to the NCC climatology are based on observations taken over the past few decades. Over the recent 30 years (1971-2000), the air temperature increased by 1.1 °C in the Northern hemisphere high latitude regions (50N~70N), by 1.0 °C in the Northern hemisphere mid-latitude regions (23.5N~50N), by 0.6 °C in the Tropics (23.5S-23.5N), and by 0.4 °C in the Southern hemisphere mid-latitude regions (50S-23.5S), respectively. The Southern hemisphere high latitude regions (50S~70S) are covered with ocean or no vegetation grows so that they are excluded from the analysis.

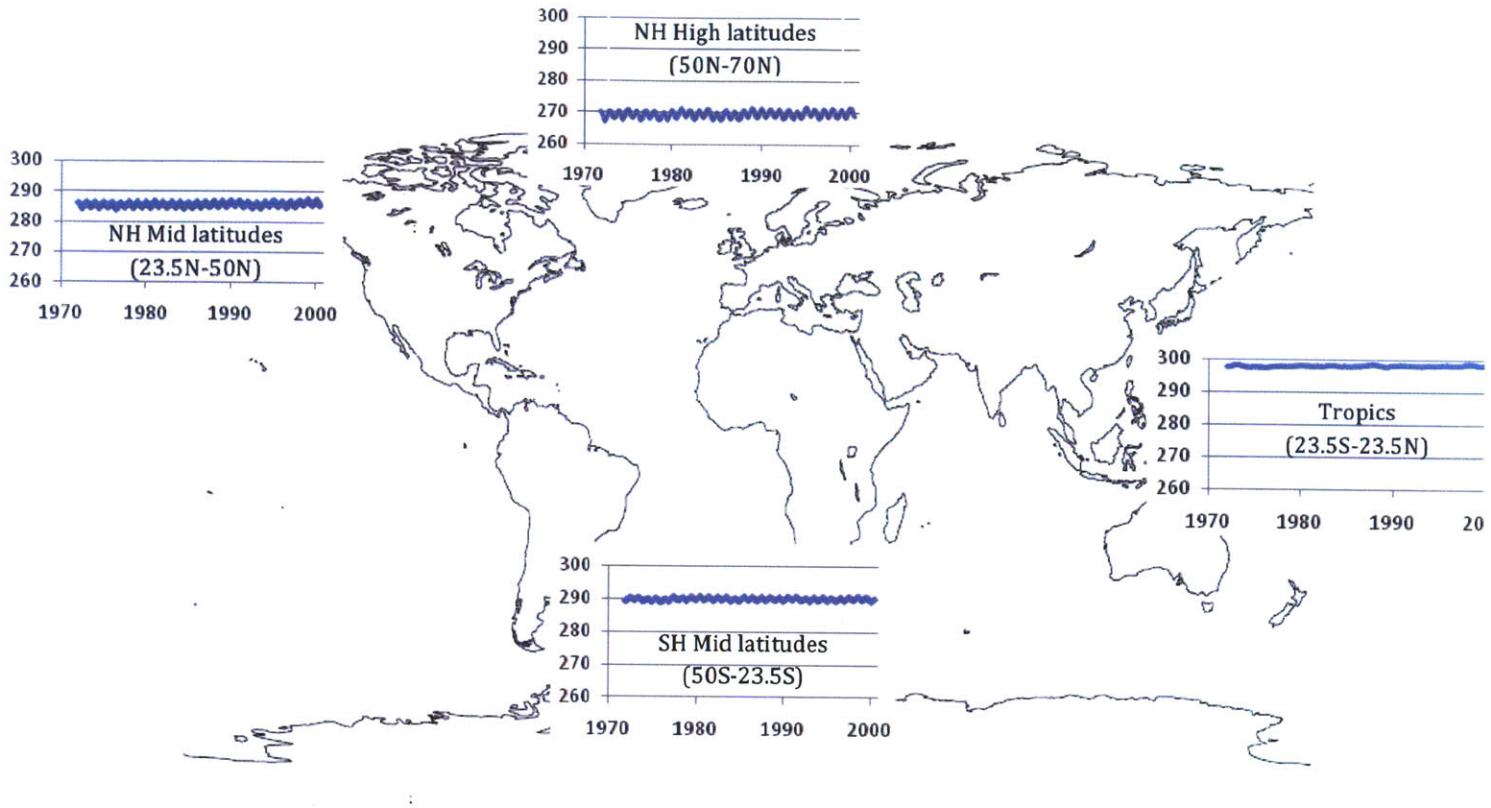

Figure 3.1: The air temperature (unit is K) of the NCC climate dataset. Thirteen-month running average (blue curves) for 1971-2000 are displayed.

The SEED configuration also requires daily wind profiles for 90 days (fall seasons in both hemispheres) to compute the transport density of seeds of boreal trees and temperate trees by wind, daily near-surface winds from the NCEP/NCAR reanalysis dataset are especially used (http://www.esrl.noaa.gov/psd/data/reanalysis/reanalysis.shtml) to confine the availability of seeds dispersed by wind. The reanalysis wind dataset is selected for its consistency with the NCC climate dataset, which is also based upon the NCEP reanalysis dataset.

An example of daily NCEP wind profiles on Oct 15, 1991 is shown in Figure 3.2. The general atmospheric circulation patterns, such as prevailing easterly winds in the high latitudes and westerly winds in the mid-latitudes, are seen in the figure, but local/regional variations of surface wind patterns are also shown, which may be significant in determining the number of seeds dispersed by wind.

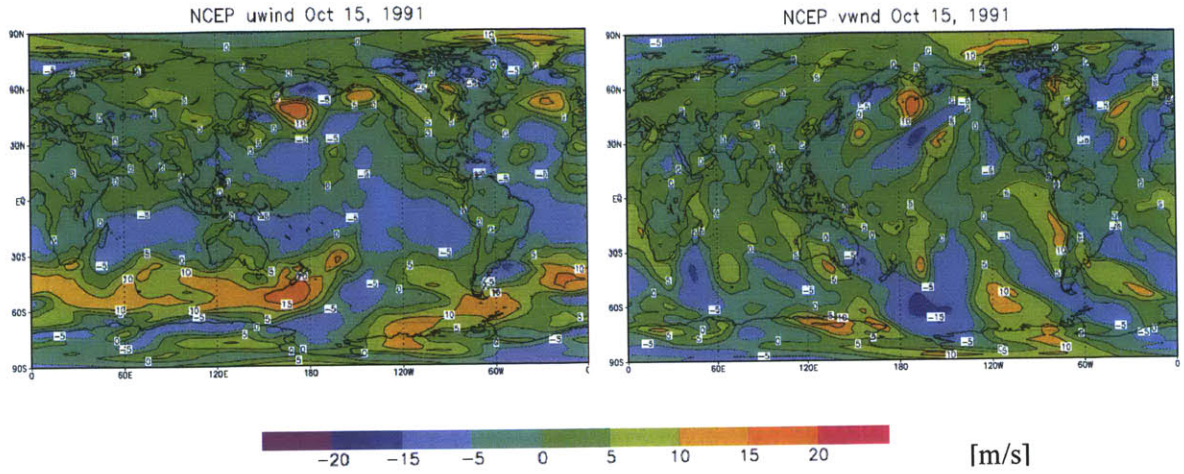

Figure 3.2: An example of wind components of daily NCEP wind vectors used for this study: u-wind (left panel) means east-west component and v-wind (right panel) means north-south component of the wind vector. Unit is in m/s.

The simulations are divided into two steps. In the first step, 50 model years are simulated using the FREE configuration, mimicking a pristine vegetation development from bare ground. For this step, 25-year NCC climate from 1949 to 1973 is cycled twice so that a vegetation map is established from the bare ground, also the initial carbon pools. Since the SEED configuration needs a map of vegetation structure as a pre-requisite, this step is necessary to obtain seeds of the tree PFTs from adjacent grids by winds (for boreal trees and temperate trees) or other vehicles (for tropical trees).

The second step is to simulate an equilibrated state of year 1993 such that it can be evaluated against a satellite-based global mapping of tree-cover. The next set of 20-year NCC climate (1974-1993) is cycled 8 times for 160 years for the FREE configuration and the SEED configuration, respectively. Assuming that reasonable carbon pools and vegetation structures are developed and are also in equilibrium, the resulting vegetation structure of the final model year of this step is analyzed. In this way, the effects of dispersal mechanisms are investigated, which are the wind dispersal of seeds to migration of boreal forests and temperate forests, and the neighbor constraints of seed availability to migration of tropical forests.

The two-step simulation procedure is summarized in Figure 3.3.

1st step: 50-year simulation	2nd step: 160-yr simulation
(2 repetitions of 1949-1973 climate)	(8 repetitions of 1974-1993 climate)
(Initial map: bare ground)	(Initial map: resulting map from the 1st step)
FREE condition only	FREE condition (no wind applied) SEED condition (NCEP reanalysis wind)

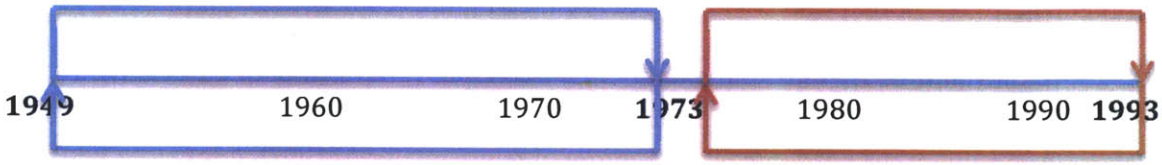

Figure 3.3: Schematic figure of the two-step simulation driven by the NCC climate.

3.3 Model result analysis

3.3.1 Vegetation structure

3.3.1.1 Global scale

At large scales, both of the simulated vegetation structures from the SEED configuration and the FREE configuration at the final model year, which corresponds to the state of year 1993, mimic the characteristics of the current distribution of trees and grasses. Since the overall distribution map of global vegetation structure of each PFT resulting from two configurations look similar, the set of the structures from the SEED configuration only are shown in Figure 3.4. However, in spite of the overall similarity of the global distributions from both configurations, significant differences between the SEED configuration and the FREE configuration are noticeable, and these differences represent the impacts on competition dynamics on plants by implementing seed dispersal constraints. Maps of these differences will be further discussed in the following section 3.3.1.2. Before discussing the regional difference maps, the characteristics of the global vegetation structure of ten PFTs are briefly discussed in this section.

The global vegetation structure maps in Figure 3.4 are provided in the following order: (1) PFTs dominating in the high latitude regions (NET boreal trees and BDT boreal trees and C3 grass Arctic), (2) PFTs dominating in the mid latitude regions (NET

temperate trees, BET temperate trees, BDT temperate trees, and C3 grass), and (3) PFTs dominating in the Tropics (BET tropical trees, BDT tropical trees, and C4 grass).

In Figure 3.4 (a), dense boreal evergreen forests (PFT type = NET boreal forests) in Canada and northern Eurasia are well simulated. Simulated boreal deciduous tree covers are shown (BDT boreal forests, Figure 3.4 (b)) in part of Canada and northern Eurasia but with much less density. Denser BDT boreal forests are found in East Asia and eastern North America from the simulations. C3 grass Arctic (or Tundra) widely dominates most of the area in high latitude regions (50N and above), except for the regions where two boreal tree covers are dense (see Figure 3.4 (c)).

In mid-latitude regions, three temperate tree types (NET temperate trees, BET temperate trees and BDT temperate trees) and C3 grass compete for common resources such as water and other nutrients. Two evergreen temperate trees (NET temperate and BET temperate) are found to overlap in their popularized areas in southern South America, part of western Europe, eastern North America, Southeast Asia, and coastal areas of Australia (Figure 3.4 (d) and (e)). Deciduous temperate trees are dominant in southern Europe, eastern North America, and East Asia (Figure 3.4 (f)). C3 grass (or warm-season grass; see Figure 3.4 (g)) is common in western North America and Central Asia, and also wherever temperate forest covers are not found in the latitude band of 25N-50N.

Tropical forests appear in Amazon (BET tropical trees, Figure 3.4 (h)) and western Africa and southern East Asia (BDT tropical trees, Figure 3.4 (i)). C4 grass (or warm-season grass) is also widespread in Tropics, showing dense grass bands simulated in central Africa (Figure 3.4 (j)).

(a)

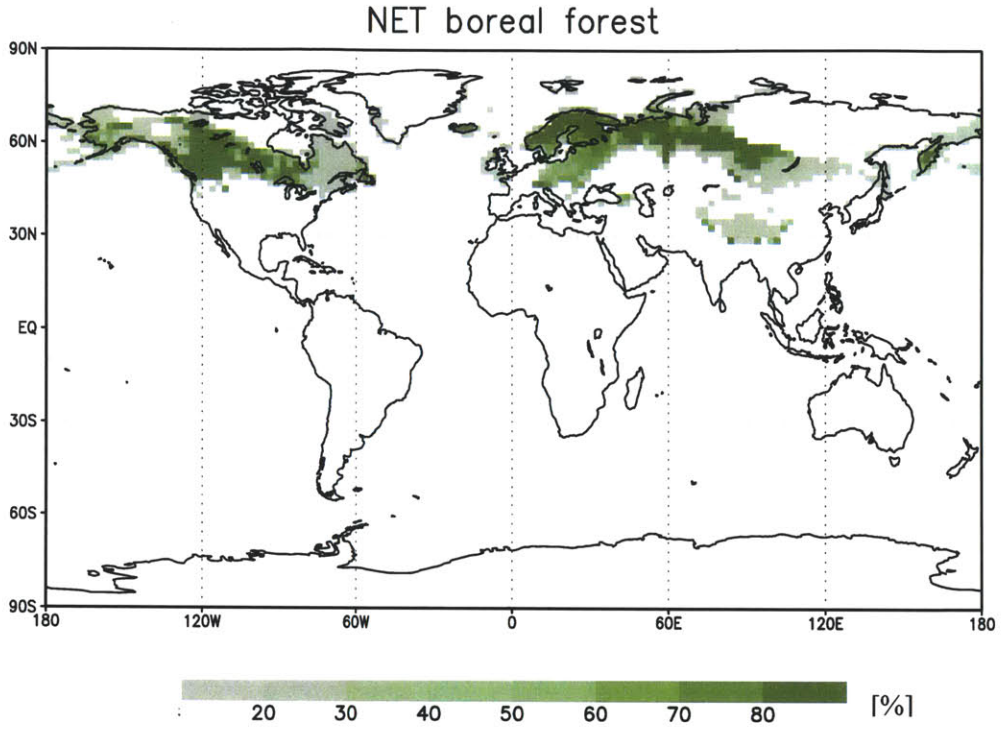

Figure 3.4(a): Global distribution map of popularized area (%) by NET boreal forests from the SEED configuration. The simulated structures are taken at the final model year, which corresponds to the state of year 1993.

(b)

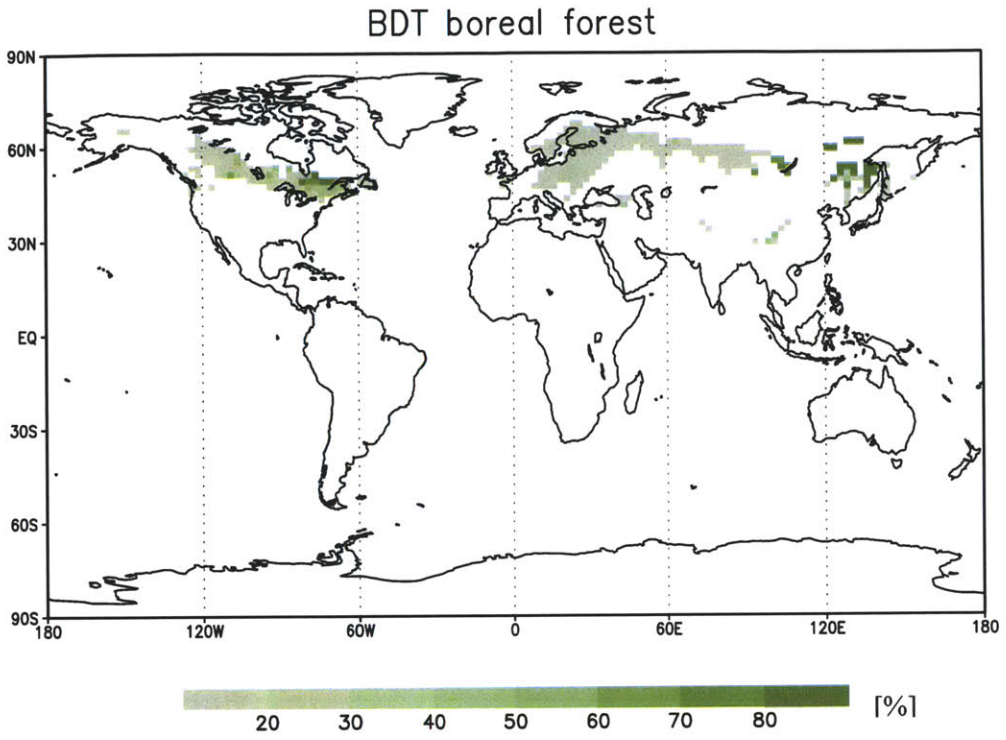

Figure 3.4(b): Global distribution map of popularized area (%) by BDT boreal forests from the SEED configuration. The simulated structures are taken at the final model year, which corresponds to the state of year 1993.

(c)

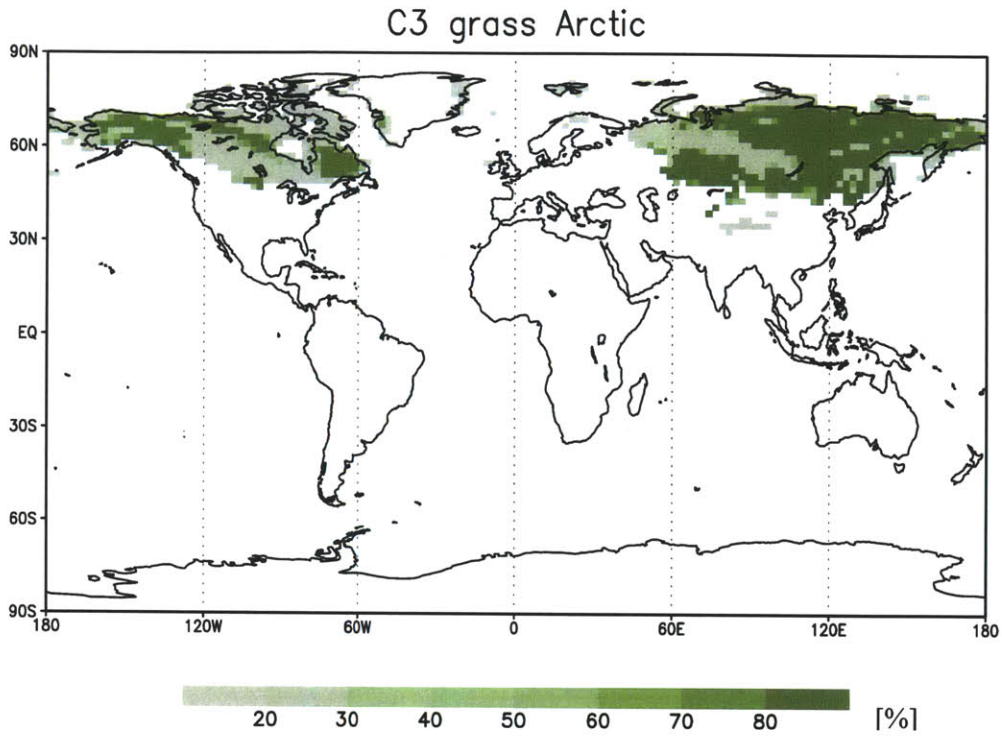

Figure 3.4(c): Global distribution map of popularized area (%) by C3 grass Arctic from the SEED configuration. The simulated structures are taken at the final model year, which corresponds to the state of year 1993.

(d)

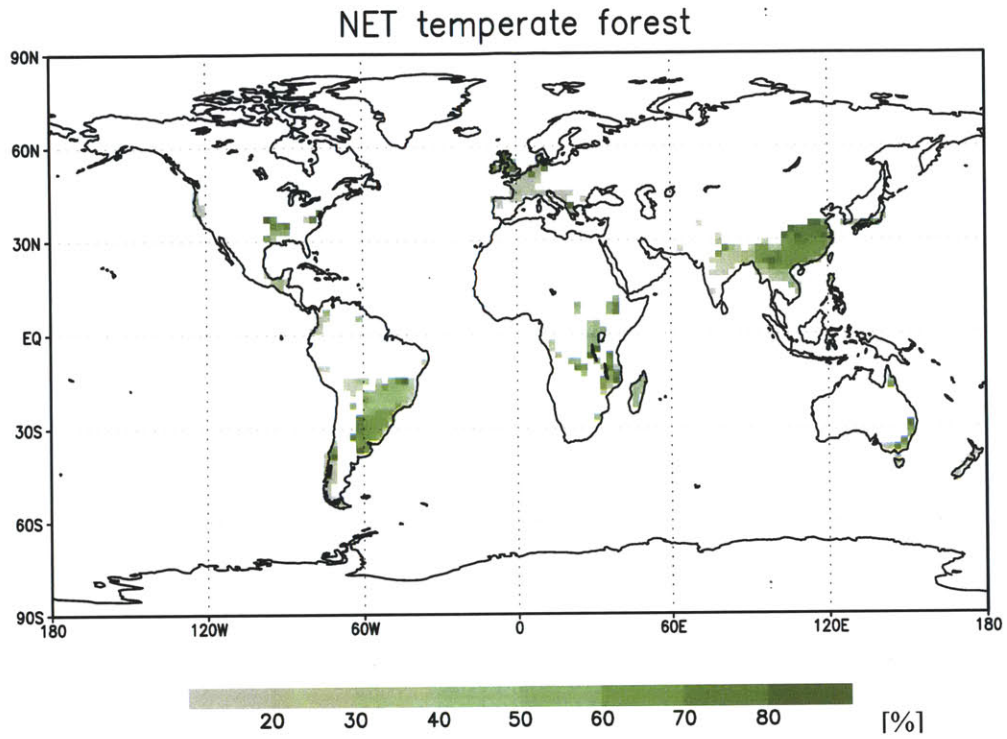

Figure 3.4(d): Global distribution map of popularized area (%) by NET temperate forests from the SEED configuration. The simulated structures are taken at the final model year, which corresponds to the state of year 1993.

(e)

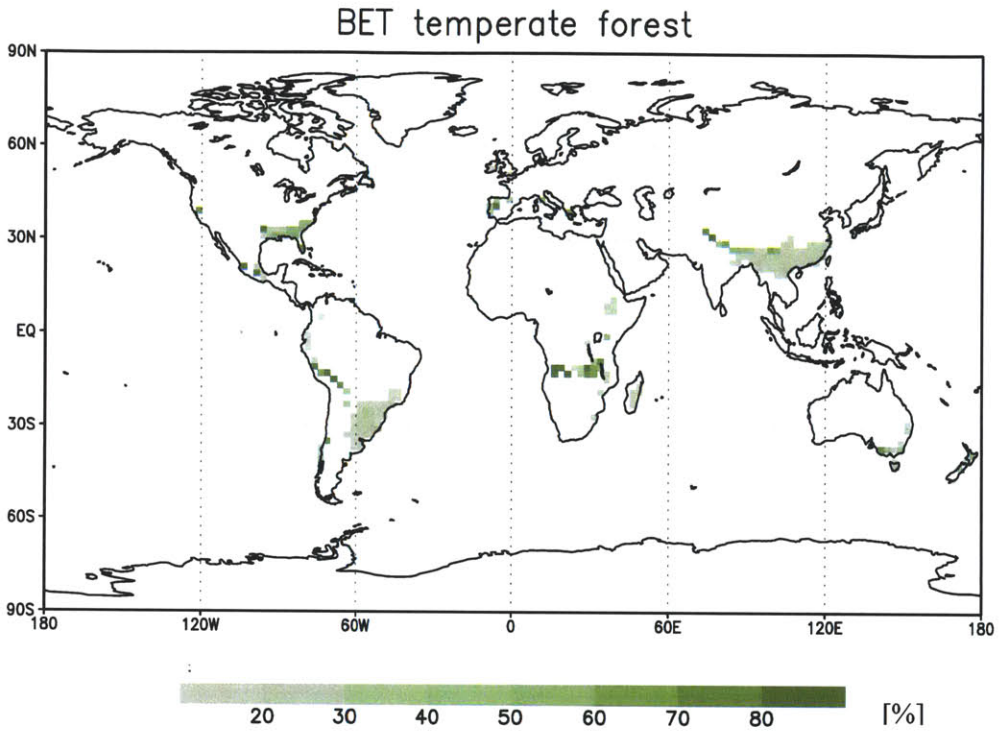

Figure 3.4(e): Global distribution map of popularized area (%) by BET temperate forests from the SEED configuration. The simulated structures are taken at the final model year, which corresponds to the state of year 1993.

(f)

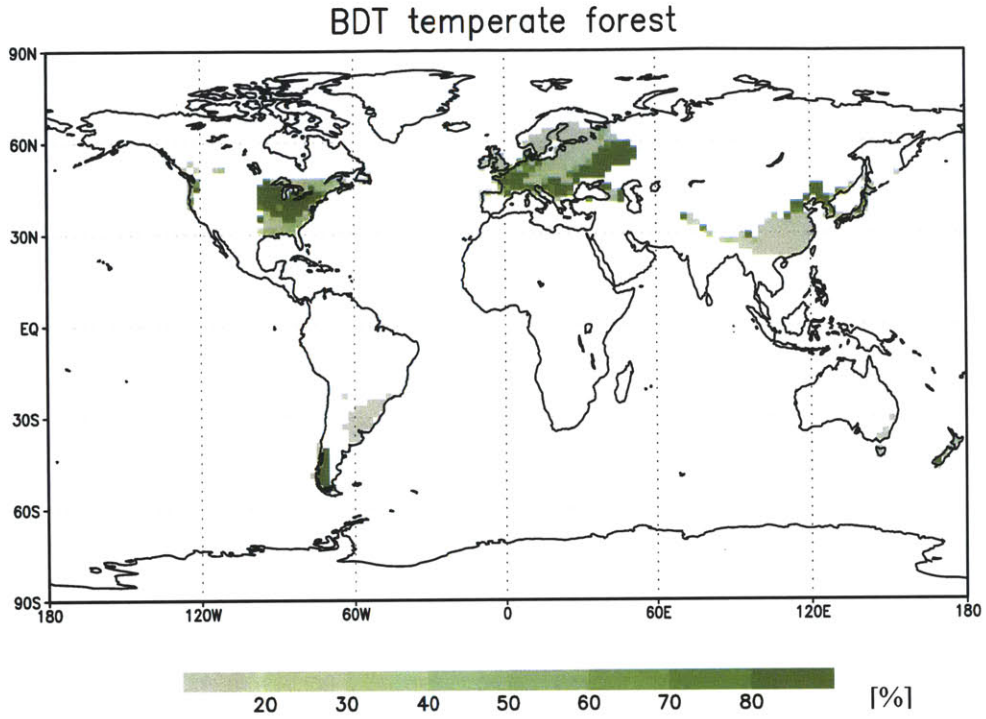

Figure 3.4(f): Global distribution map of popularized area (%) by BDT temperate forests from the SEED configuration. The simulated structures are taken at the final model year, which corresponds to the state of year 1993.

(g)

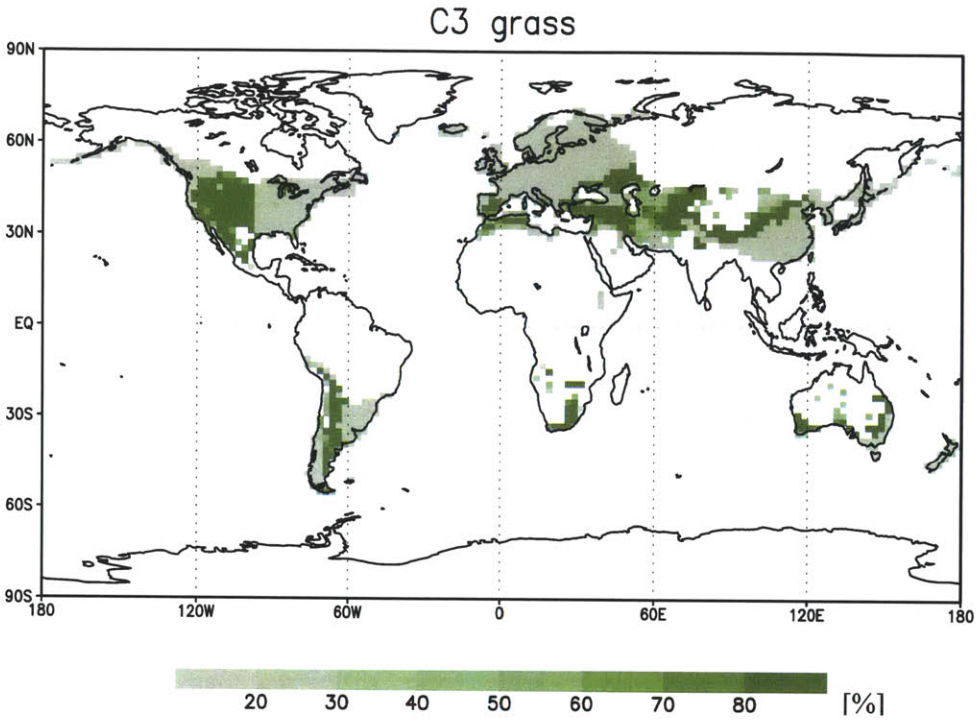

Figure 3.4(g): Global distribution map of popularized area (%) by C3 grass from the SEED configuration. The simulated structures are taken at the final model year, which corresponds to the state of year 1993.

(h)

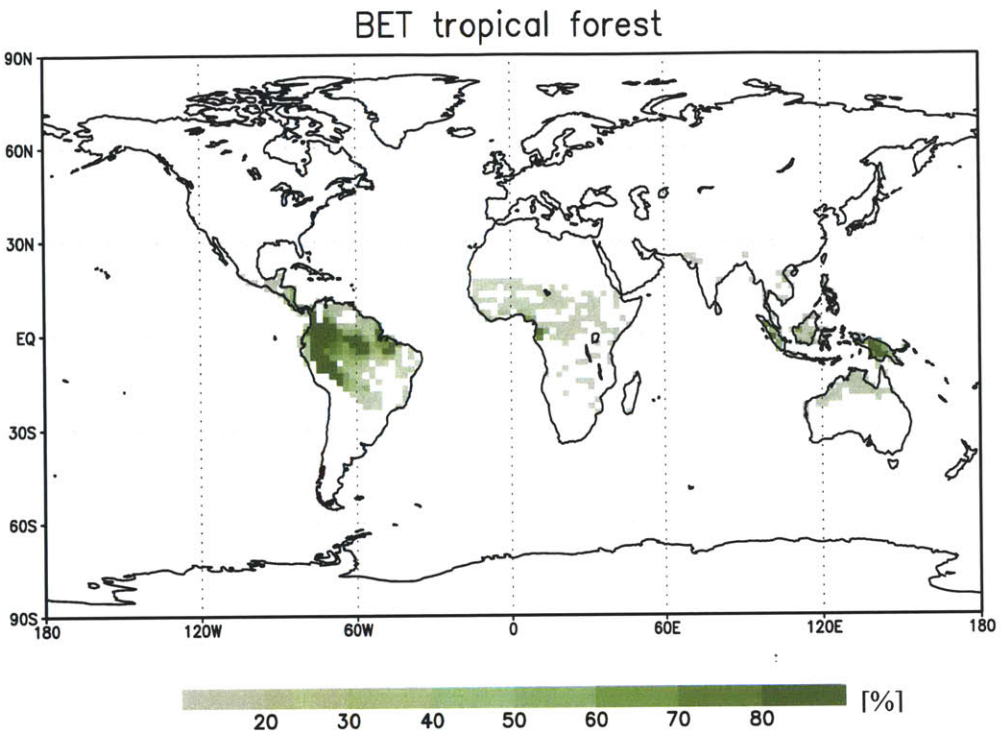

Figure 3.4(h): Global distribution map of popularized area (%) by BET tropical forests from the SEED configuration. The simulated structures are taken at the final model year, which corresponds to the state of year 1993.

(i)

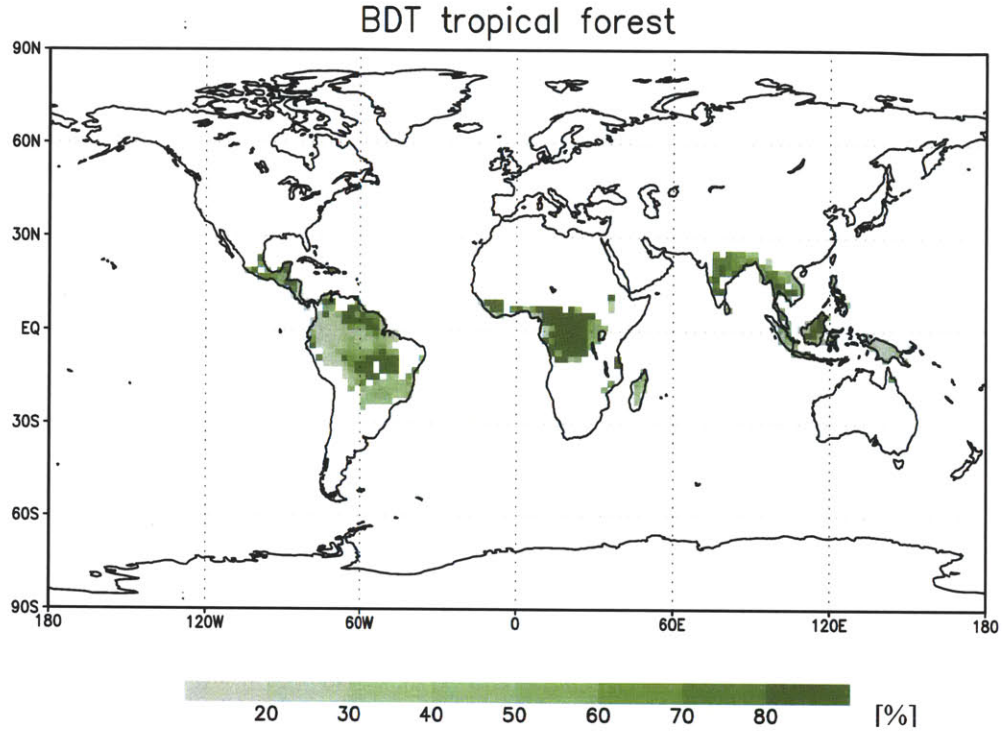

Figure 3.4(i): Global distribution map of popularized area (%) by BDT tropical forests from the SEED configuration. The simulated structures are taken at the final model year, which corresponds to the state of year 1993.

(j)

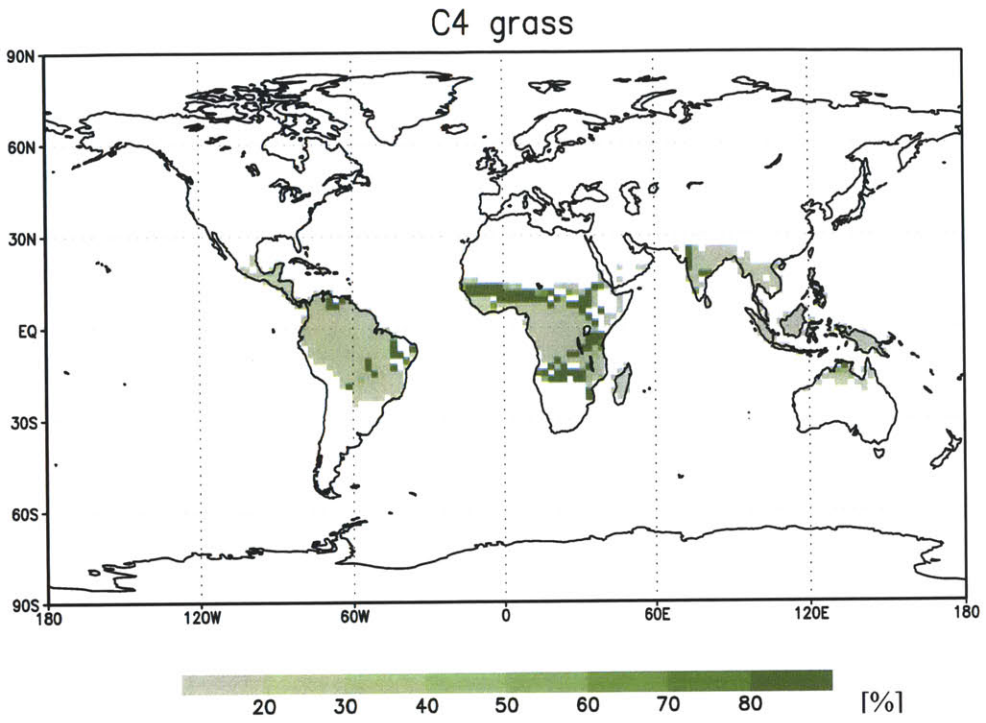

Figure 3.4(j): Global distribution map of popularized area (%) by C4 grass from the SEED configuration. The simulated structures are taken at the final model year, which corresponds to the state of year 1993.

Additionally, in order to provide a summary of the global populations of trees and grasses, the aggregated area of each PFT is also computed. The aggregation is the latitude-weighted average, and any grid cell at which a PFT exists with population over 0.1 percent of the grid cell's land area is taken into consideration (GrADS users guide, http://www.iges.org/grads/). For instance, for BDT temperate trees, all the grid cells that include the PFT occupying greater than 0.1% of their land portion are selected and the areal average that considers the geographical shape of the globe is calculated as a representation of the PFT. The aggregated areas of all ten PFTs are shown in Table 3.1.

Table 3.1: Averaged areas of ten PFTs from the SEED and the FREE configurations.

	SEED (%)	FREE (%)	Delta (%)
NET boreal	35.98	35.93	0.04
BDT boreal	21.01	21.63	-0.62
C3 grass Arctic	51.01	49.24	1.76
NET temperate	42.55	34.73	7.82
BET temperate	30.69	27.34	3.35
BDT temperate	40.14	39.59	0.54
C3 grass	38.25	37.49	0.77
BET tropical	23.59	31.01	-7.42
BDT tropical	53.97	50.18	3.79
C4 grass	21.66	22.15	-0.49

The numbers in Table 3.1 indicate greater coverage of temperate forests from the SEED configuration. Boreal forests seem to have little difference in terms of the aggregated areas, however for the NET boreal forests, significant gains of the tree type in some regions are cancelled out by loss of the type in other regions. In the following section, the differences in the spatial pattern of each PFT between the SEED configuration and the FREE configuration will be discussed.

3.3.1.2 Regional scale

In understanding the role of meteorology in seed dispersal, the changes in the vegetation distribution at regional scale are not negligible, and in fact, are more important than the globally aggregated areas of the PFTs described in the previous section. The difference maps of the vegetated area from the SEED configuration and the FREE configuration indicate salient regional differences more clearly (Figure 3.5).

First of all, as expected, all tree PFTs have widespread but small decreases as a result of the seed constraint. This feature occurs because the SEED configuration eliminates the chances of the universal establishment allowed in the FREE configuration. Some PFTs have a chance to be established for a model year because they satisfy the required establishment climate condition, but at the end of the model year, they do not meet the survival condition so that the PFTs are removed. Each year, this process repeats, which gives very small background coverage for some PFTs simulated by the FREE configuration. The further requirement of a certain seed density for trees does not allow this unrealistic tree cover in the SEED configuration.

In the high latitudes, the SEED configuration tends to simulate more evergreen trees (NET boreal trees) in North America and Northern Eurasia, but less of them in central Siberia (Figure 3.5(a)), compared to the result using the FREE configuration. The changes of the NET boreal trees occur mainly at the expense of C3 grass Arctic (Figure 3.5(b)). Since only tree-PFTs are controlled by the dispersal mechanism (e.g., wind dispersal) but herbaceous PFTs are assumed to migrate freely in the SEED configuration, the C3 grass Arctic compensates in the area where changes of the NET boreal trees are shown. The mechanisms that trigger the major tree cover difference of the NET boreal trees will be discussed in more detail in section 3.3.2. Deciduous trees (BDT boreal trees) in the high latitudes do not show a strong difference between the SEED configuration and the FREE configuration, but generally slightly less predicted in their entire habitats (Figure 3.5(b)). This is because the universal establishment in the background is prohibited in the SEED configuration.

In the mid latitudes, Evergreen trees (NET temperate and BET temperate) show some exchanges in central Africa and southern part of the eastern United States. Greater coverage of BDT temperate trees is estimated in eastern United States at the expense of NET temperate in the southern part of the east United States (Figure 3.5 (d), (e), and (f)) in the SEED configuration. Reduced coverage of BDT temperate trees is estimated in eastern Europe.

Tropical evergreen trees (BET tropical) and deciduous trees (BDT tropical) do not differ much between the FREE configuration and the SEED configuration. For the tropical trees, the applied neighbor constraint only requires that a PFT exists in one of the

eight neighboring grids for the PFT to be established. Given these looser neighboring constraints applied to the tropical forests, the simulated structures between the SEED configuration and the FREE configuration may show smaller differences for the tropical forests.

Bonan and Levis (2006) reported offline simulation results using the canonical form of the CLM-DGVM (i.e., the FREE configuration) driven by NCEP climate, which is very similar to the NCC climate used for this study. They repeated the 20-yr climate dataset (1979-1998) for 80 model years. Considering that this study uses very similar climate forcing data and also cycles 20-yr climate (1974-1993) for 160 model years, comparison between the result of this study and their offline simulation result is reasonable.

For the distribution of boreal trees and temperate trees in the high latitude regions and mid latitude regions, Bonan and Levis (2006) reported that mid-continental parts of boreal forests were underestimated, and tree covers (mainly temperate forests) in the eastern United States were also underestimated by the dominance of grasses. From the simulated vegetation structure from the SEED configuration in this study, greater NET boreal forest cover is estimated largely in northern North America and the western part of Siberia in favor of C3 grass Arctic cover (see Figure 3.5 (a) and (c)), indicating improvement of boreal tree cover.

In addition, the dominance of grasses over tree covers in the eastern United States does not appear in their simulation result. In this study, the dominant tree cover (BDT temperate tree) over grasses is simulated, and this improvement is accomplished by using the modified calibration set of parameters optimized for the NCC climate (see Chapter 2).

Underestimation of BET tropical tree cover due to the dominance of BDT tropical trees was also mentioned in their study. This feature is not improved much in this study either, again because of the loose neighboring constraint applied to the tropical trees being compared. One may not expect a great degree of difference in simulating tropical trees using the FREE configuration and the neighboring constraint in the SEED configuration.

(a)

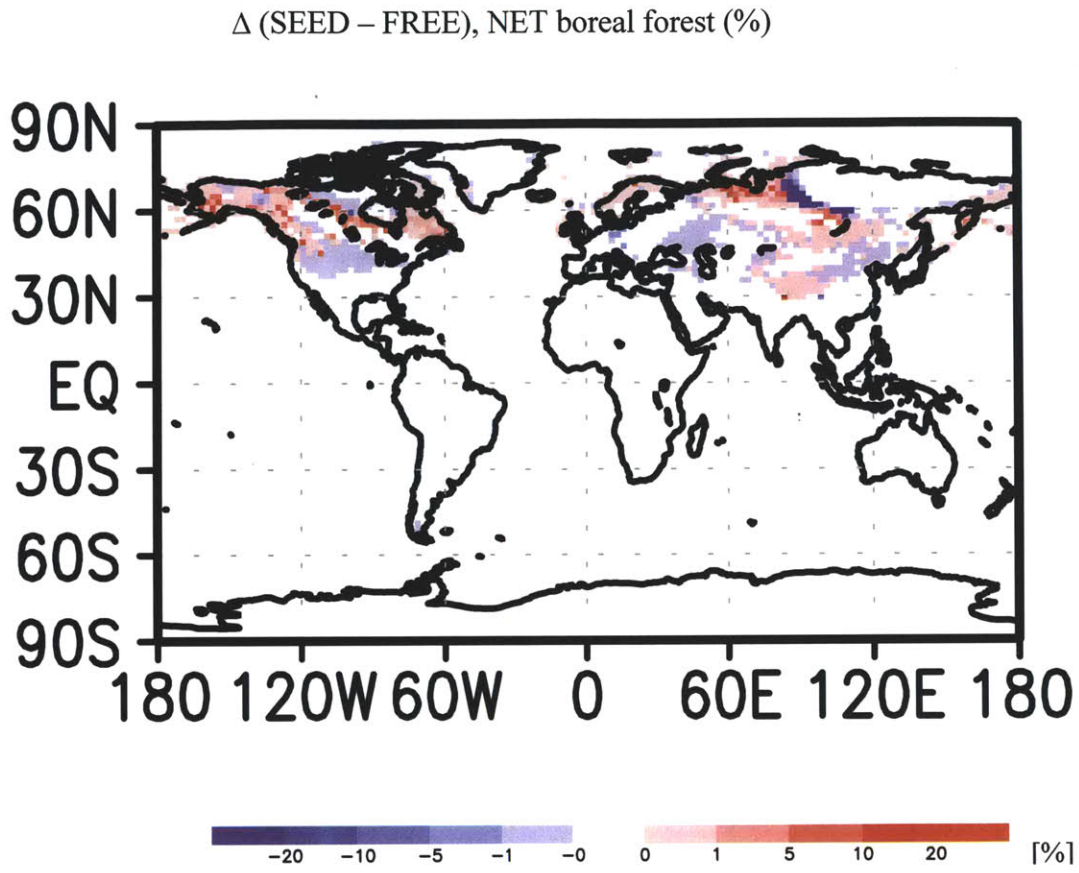

Figure 3.5(a): Difference in occupied area (%) of NET boreal forests. More area simulated in the SEED configuration than in the FREE configuration is shown in red, and less area in the SEED configuration than in the FREE configuration is shown in blue.

(b)

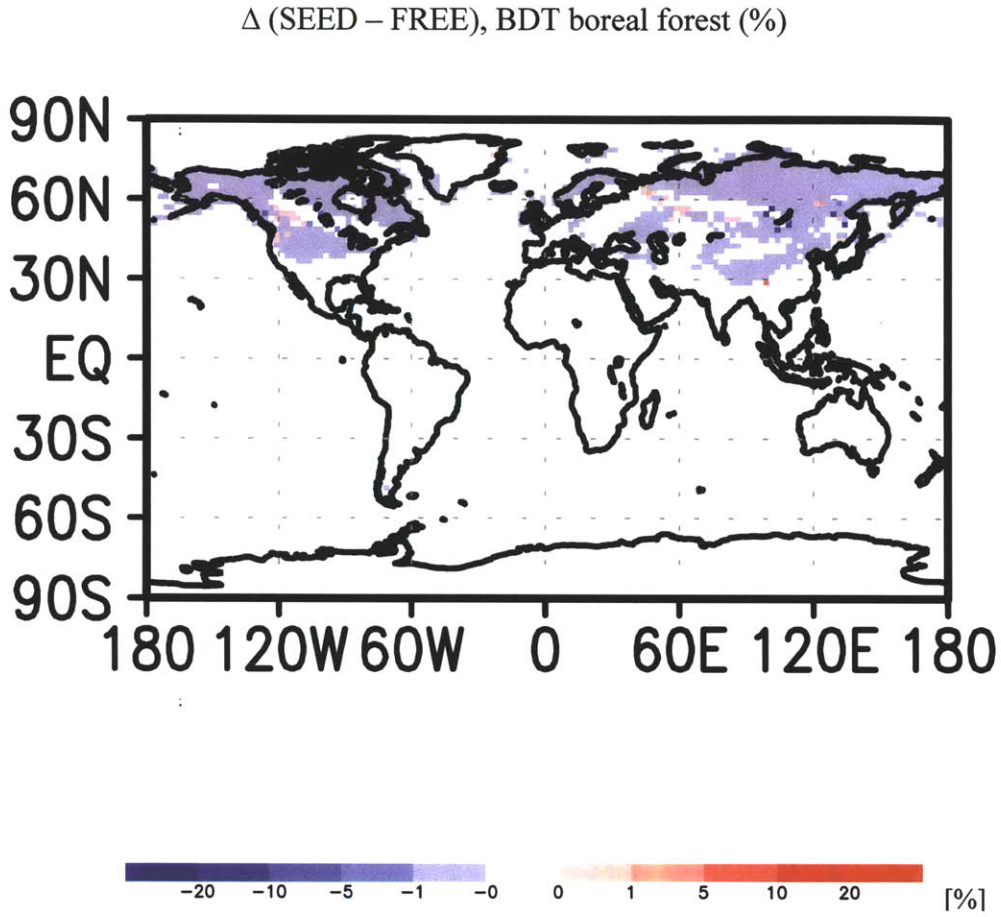

Figure 3.5(b): Difference in occupied area (%) of BDT boreal forests. More area simulated in the SEED configuration than in the FREE configuration is shown in red, and less area in the SEED configuration than in the FREE configuration is shown in blue.

(c)

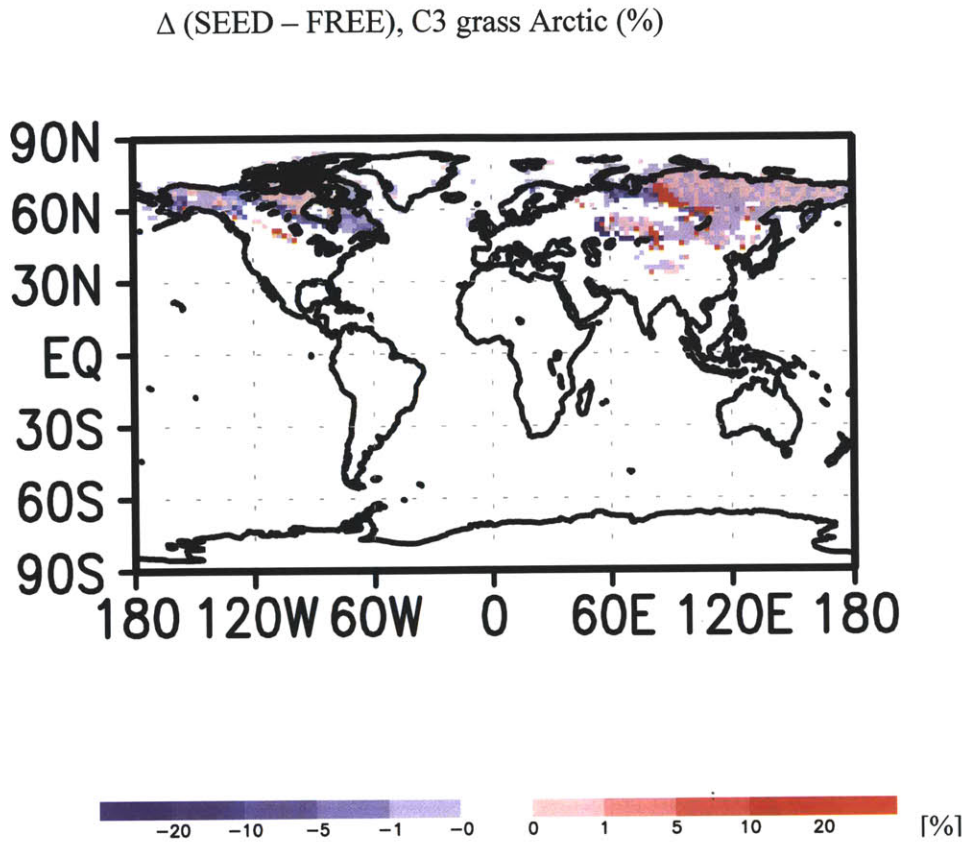

Figure 3.5(c): Difference in occupied area (%) of C3 grass Arctic. More area simulated in the SEED configuration than in the FREE configuration is shown in red, and less area in the SEED configuration than in the FREE configuration is shown in blue.

(d)

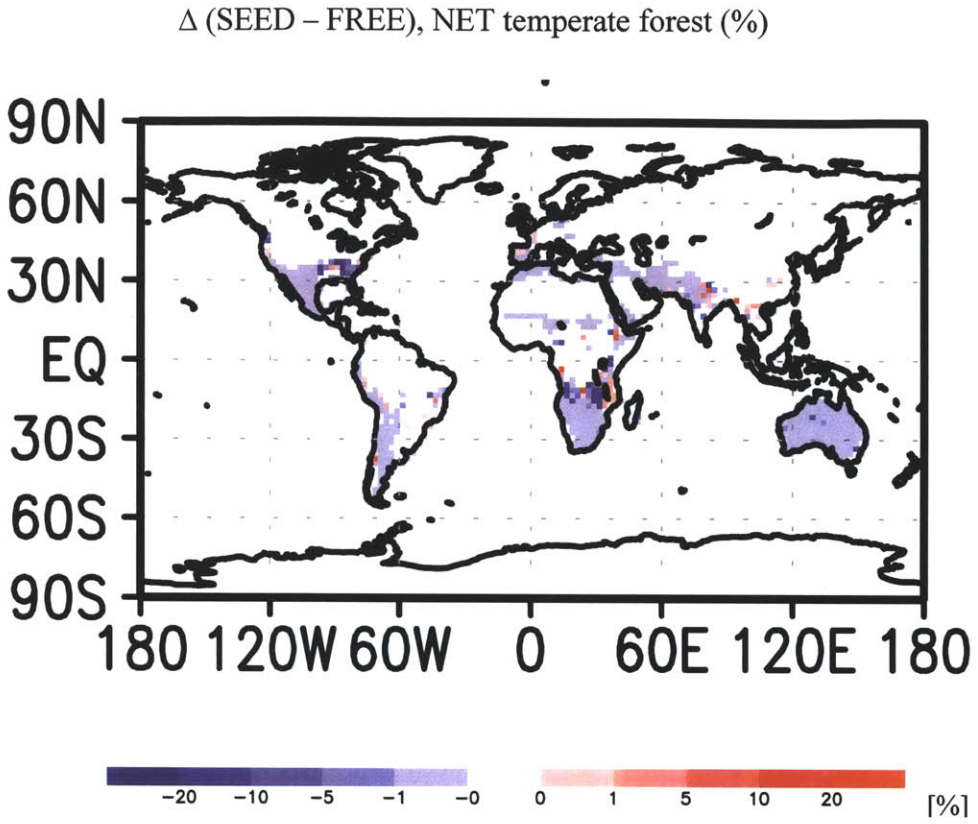

Figure 3.5(d): Difference in occupied area (%) of NET temperate forests. More area simulated in the SEED configuration than in the FREE configuration is shown in red, and less area in the SEED configuration than in the FREE configuration is shown in blue.

(e)

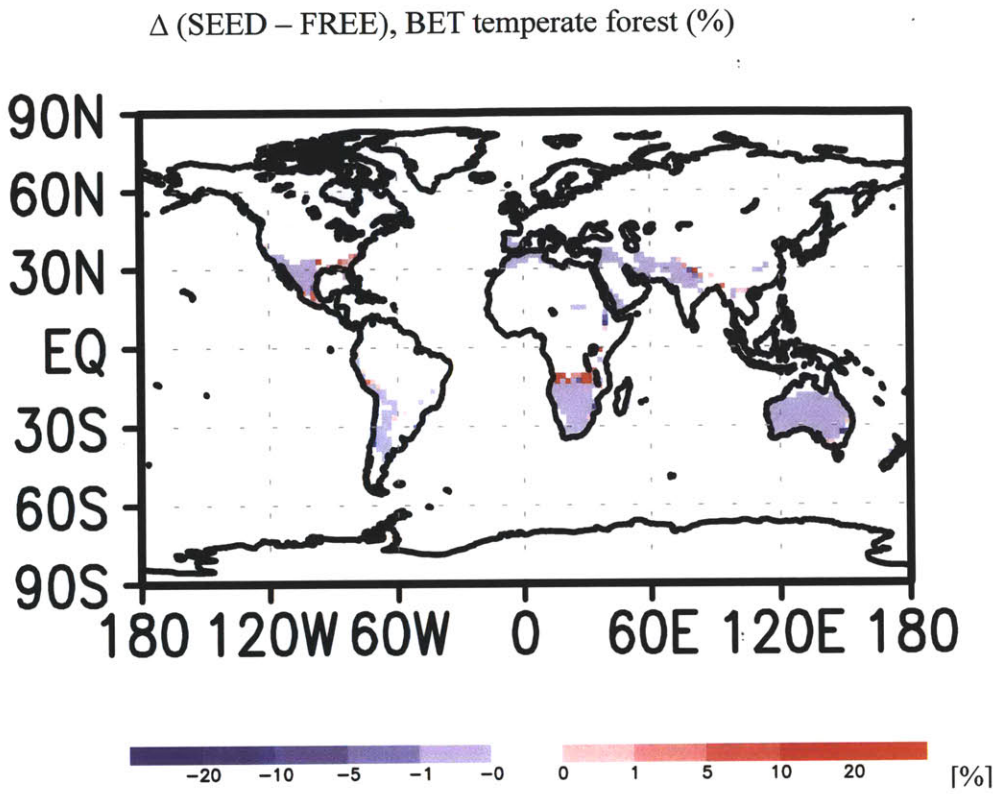

Figure 3.5(e): Difference in occupied area (%) of BET temperate forests. More area simulated in the SEED configuration than in the FREE configuration is shown in red, and less area in the SEED configuration than in the FREE configuration is shown in blue.

(f)

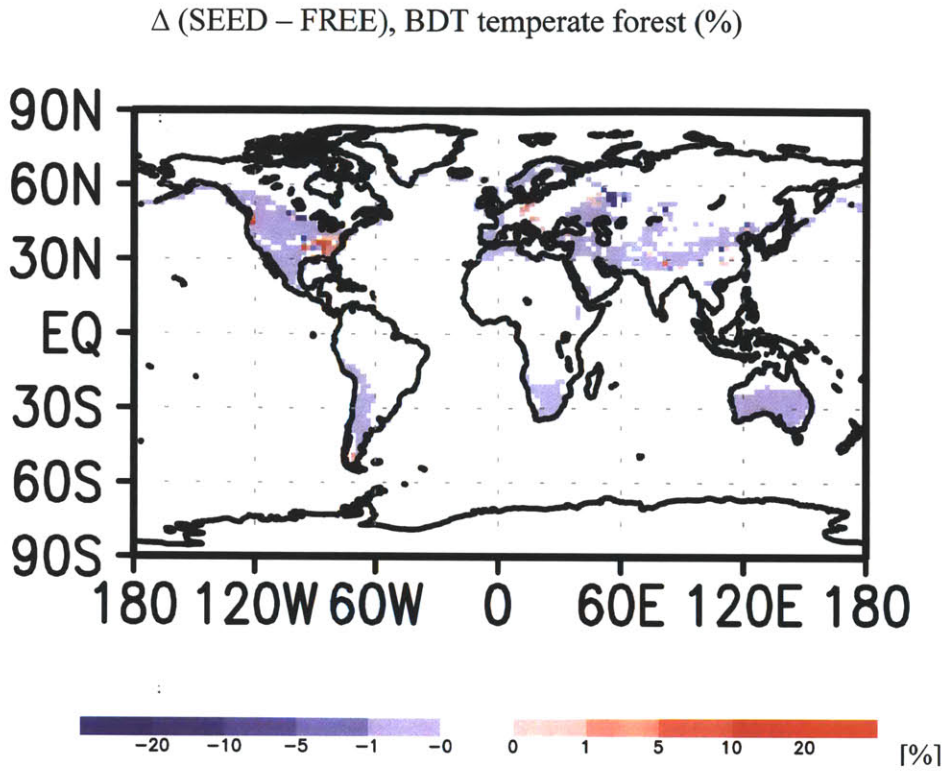

Figure 3.5(f): Difference in occupied area (%) of BDT temperate forests. More area simulated in the SEED configuration than in the FREE configuration is shown in red, and less area in the SEED configuration than in the FREE configuration is shown in blue.

(g)

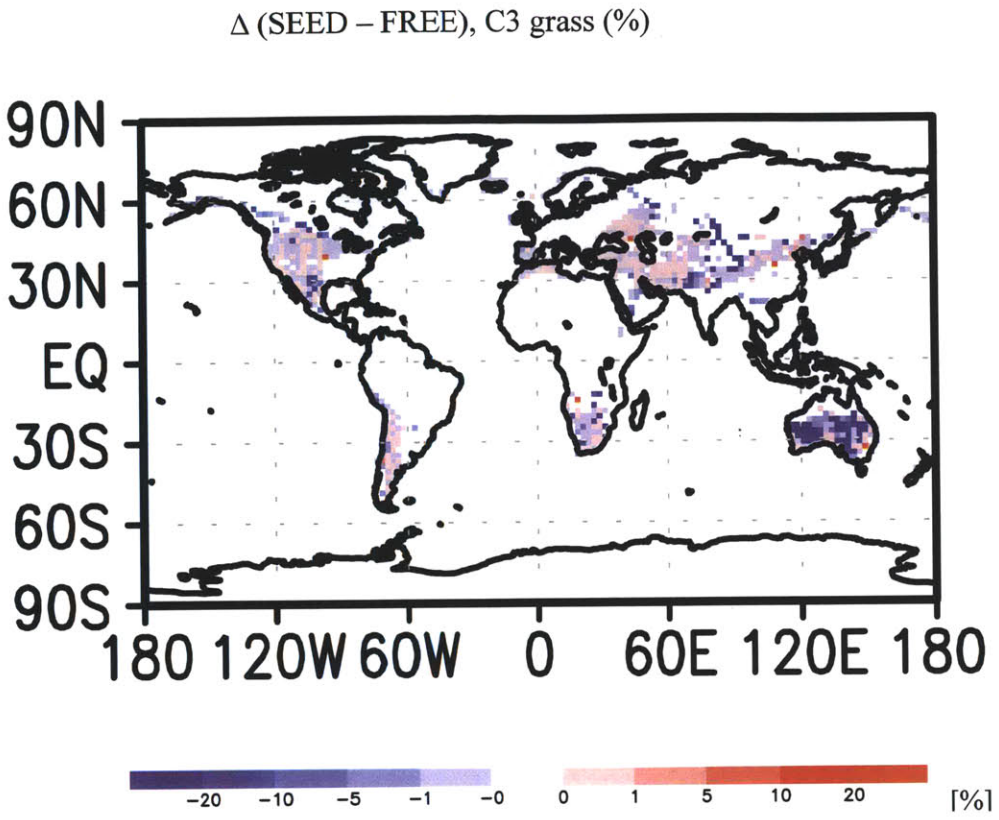

Figure 3.5(g): Difference in occupied area (%) of C3 grass. More area simulated in the SEED configuration than in the FREE configuration is shown in red, and less area in the SEED configuration than in the FREE configuration is shown in blue.

(h)

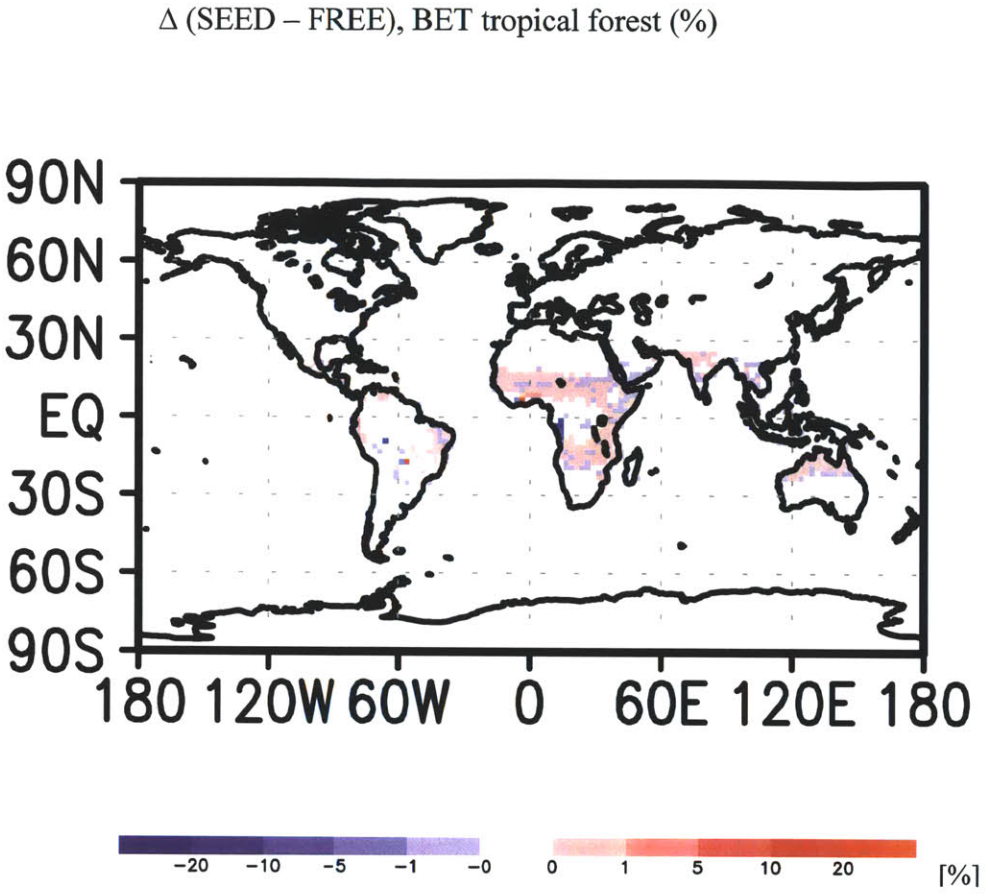

Figure 3.5(h): Difference in occupied area (%) of BDT tropical forests. More area simulated in the SEED configuration than in the FREE configuration is shown in red, and less area in the SEED configuration than in the FREE configuration is shown in blue.

(i)

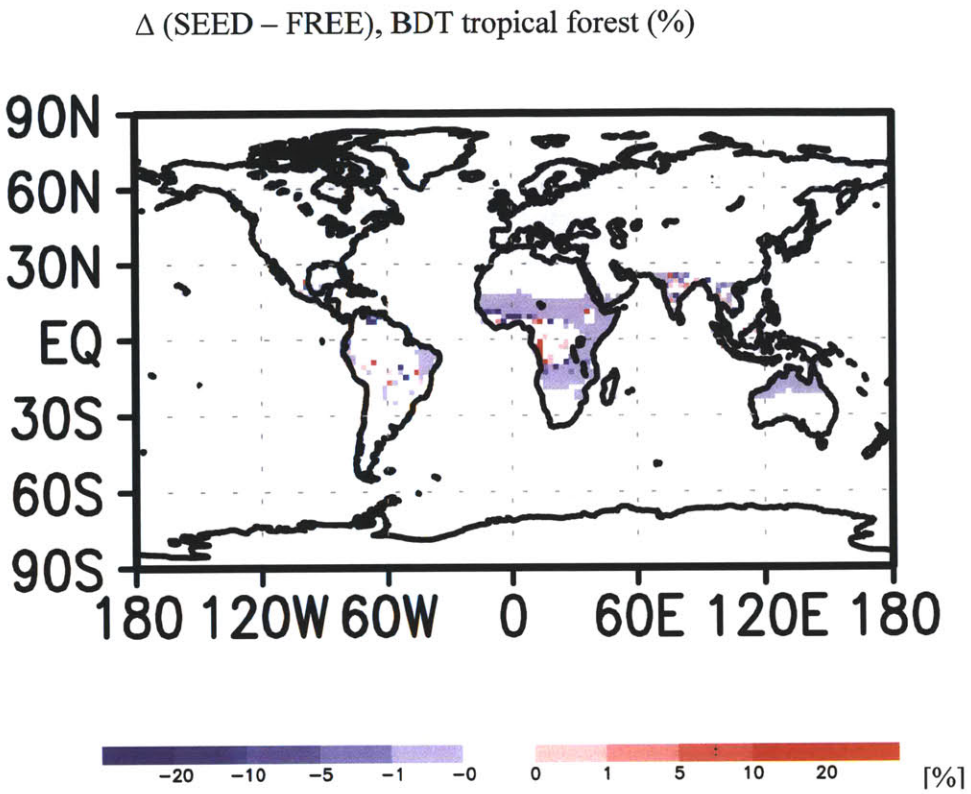

Figure 3.5(i): Difference in occupied area (%) of BDT tropical forests. More area simulated in the SEED configuration than in the FREE configuration is shown in red, and less area in the SEED configuration than in the FREE configuration is shown in blue.

(j)

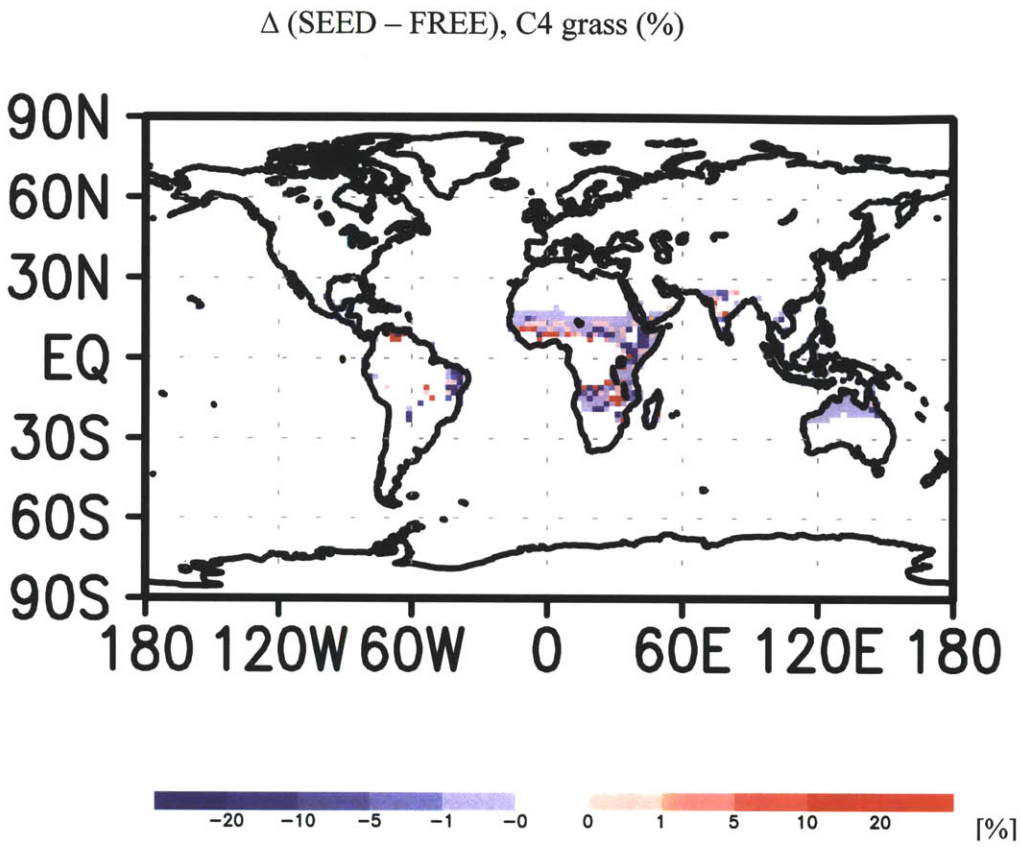

Figure 3.5(j): Difference in occupied area (%) of C4 grass. More area simulated in the SEED configuration than in the FREE configuration is shown in red, and less area in the SEED configuration than in the FREE configuration is shown in blue.

3.3.2 Comparison to the satellite-derived AVHRR tree cover

The simulated vegetation structures from both configurations are now compared to the tree covers derived from the Advanced Very High Resolution Radiometer (AVHRR) satellite observations (DeFries et al., 2000). The satellite-observed reflectance was converted into the normalized difference vegetation index (NDVI) and the NDVI profile converted into the leaf area index (LAI), which was interpolated into tree cover. The dataset uses the satellite observation of NDVI from April 1992 to April 1993 so that the correlation between one of the modeled vegetation structures representing the state of year 1993 and the AVHRR tree cover is comparable. Two categories of tree covers are provided in the AVHRR tree cover dataset: (1) Evergreen vs. Deciduous (according to leaf longevity), and (2) Needleleaf and Broadleaf (according to leaf morphology). Spatial correlation coefficients between a model vegetation distribution of each PFT and the corresponding AVHRR tree cover are shown in Table 3.2.

Table 3.2: Spatial correlation coefficients of the modeled tree covers from the SEED configuraion and the FREE configuration to the satellite-drived AVHRR tree cover. The highlighted pairs indicate the cases for which the spatial correlation is improved in the SEED configuration.

		Leaf Morphology				Leaf Longevity			
		Needleleaf		Broadleaf		Evergreen		Deciduous	
		SEED	FREE	SEED	FREE	SEED	FREE	SEED	FREE
1	NET temperate	**0.15**	**0.12**	-	-	0.07	0.11	-	-
2	NET boreal	0.30	0.30	-	-	0.28	0.28	-	-
4	BET tropical	-	-	0.62	0.63	0.62	0.62	-	-
5	BET temperate	-	-	**0.26**	**0.18**	-0.14	-0.06		
6	BDT tropical	-	-	0.31	0.32	-	-	**0.16**	**0.12**
7	BDT temperate	-	-	**0.33**	**0.31**	-	-	0.39	0.38
8	BDT boreal	-	-	-0.21	-0.25	-	-	**0.12**	**0.07**
	Global	0.30	0.30	0.35	0.30	0.23	0.28	0.25	0.24

For needleleaf tree cover and broadleaf tree cover, according to leaf morphology, the SEED configuration provides better agreement with the AVHRR dataset. The spatial correlation coefficient between the modeled broadleaf tree cover from the SEED configuration and the AVHRR broadleaf tree cover is enhanced to 0.35, compared to 0.30 for the case from the FREE configuration (see the last row of Table 3.2, columns 4 and 5). The overall tighter correlation to the AVHRR broadleaf tree cover are driven by improved correlation of temperate trees (BET temperate and BDT temperate, see also columns 4 and 5 of Table 3.2). This is also consistent with the case of NET temperate trees. In the columns 2 and 3 of Table 3.2, the spatial correlation coefficient increases from 0.12 (NET temperate tree from the FREE configuration vs. the AVHRR needleleaf tree cover) to 0.15 (NET temperate tree from the SEED configuration vs. the AVHRR needleleaf tree cover). Therefore, in terms of leaf morphology category, all three temperate tree PFTs show enhanced spatial correlations to the AVHRR tree cover (Needleleaf or Deciduous), which indicates that the wind disperal mechanism in the SEED configuration provides a better representation of temperate trees. Tropical trees do not show as strong improvement of spatial correlation as temperate trees, (BET tropical trees: 0.62 for the SEED configuration and 0.63 for the FREE configuration; BDT tropical trees: 0.31 for the SEED configuration and 0.32 for the FREE configuration), again due to the looser neighboring constraint in the SEED configuration for these tree types.

Categorized by leaf longevity, evergreen vegetation from the SEED configuration does not agree as well as the FREE configuration to the AVHRR evergreen tree cover, but deciduous tree cover from the SEED configuration still agrees better (columns 6-9 in Table 3.2). For the tree PFTs to which wind disperal mechanism is applied, evergreen temperate trees do not agree well with the AVHRR evergreen tree cover, while boreal trees still agree better. More information about the spatial correlation coefficients for needleleaf and braodleaf trees according to regions of 10 degree latitude x 10 degree longitude can be found in Appendix I.

In addition to the above global correlations, the spatial correlation of some selected regions are further examined. In Table 3.3, the spatial correlation coefficients are illustrated, of selected regions where significant differences in vegetation structure are predicted by the SEED configuration.

Table 3.3: Correlation coefficients of selected regions. Bold fonts indicate improvement using the SEED configuration.

					Correlation coefficient	
		Latitude	Longitude	Category	SEED vs AVHRR	FREE vs AVHRR
NET boreal	Gain	60N-70N	60E-80E	Evergreen	**0.48**	0.45
				Needleleaf	**0.55**	0.49
	Loss	60N-70N	80E-110E	Evergreen	**0.78**	0.62
				Needleleaf	0.63	0.70
BDT temperate	Gain	30N-40N	90W-80W	Deciduous	**0.80**	0.79
				Broadleaf	**0.80**	0.79
	Loss	50N-60N	50E-60E	Deciduous	**0.72**	0.59
				Broadleaf	**0.72**	0.59

The improvement of spatial correlation clearly shows that by implementing the SEED configuration, the gain of NET boreal forests in 60N-70N and 60E-80E and loss of NET boreal forests in 60N-70N and 80E-110E are the better representation of current vegetation structure. Similarly, the gain of BDT temperate forests in 30N-40N and 90W-80W and loss of BDT temperate forests in 50N-60N and 50E-60E are also supported by enhanced correlation in the SEED configuration.

3.3.3 Mechanisms altering competition dynamics in the SEED configuration

3.3.3.1 Mechanism 1: Dispersal forbidden by the prevailing wind pattern

In the SEED configuration, the primary control mechanism is the prevailing wind, which can substantially impede available seeds from dispersing over "up-stream" grids, and thus these grids will not obtain enough seeds of a specific PFT. To investigate this mechanism in detail, a hot spot in central Siberia (60N-70N, 80E-110E) is chosen, which indicates a significantly reduced coverage of NET boreal forest from the SEED configuration. Figure 3.6 illustrates the global difference map of the NET boreal forest and the magnified map of the area of 60N-70N, 80E-110E.

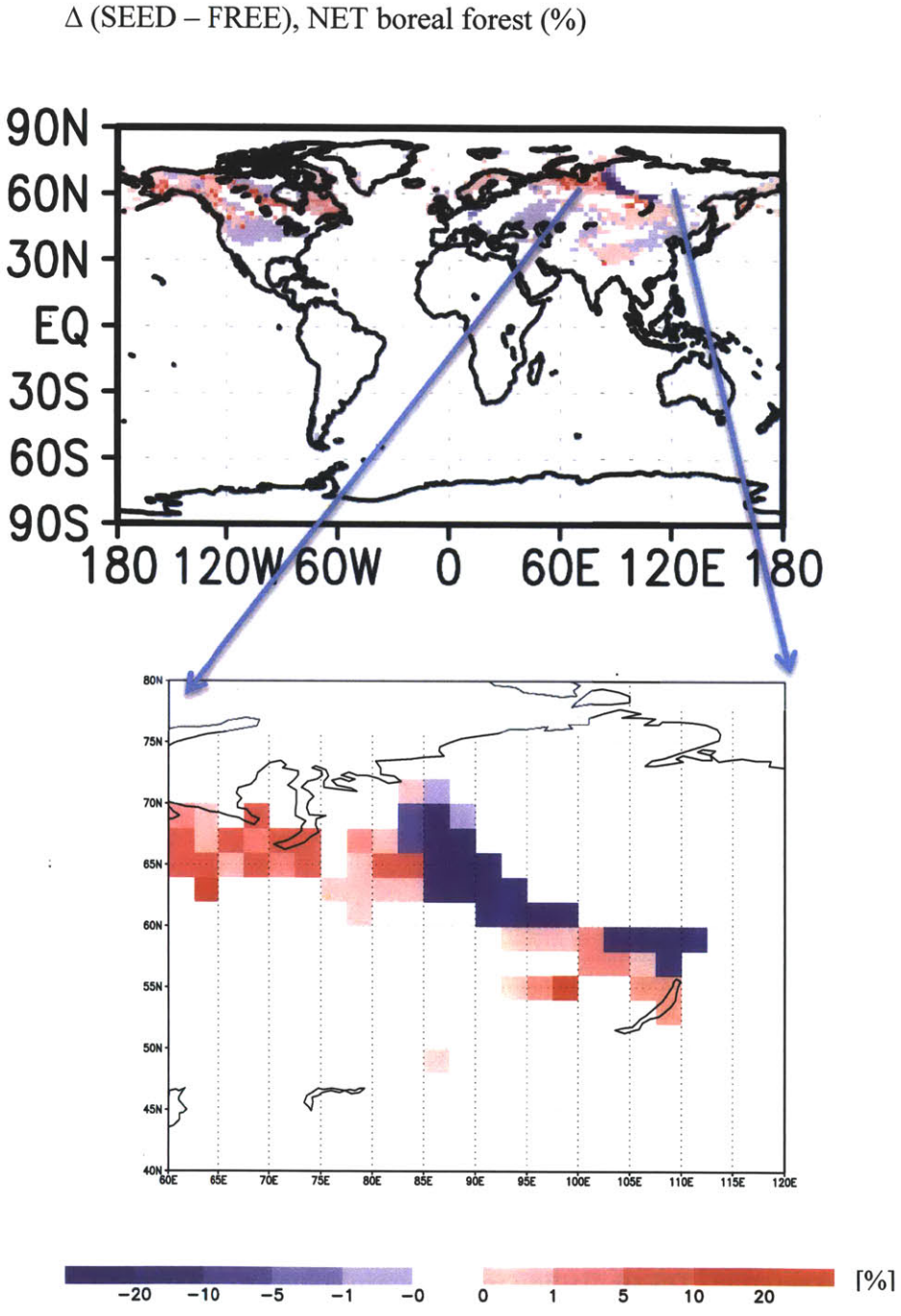

Figure 3.6: Example in Central Siberia where the SEED configuration shows a strong decrease in NET boreal forest. The difference map in the upper panel is same as in Figure 3.5 (a) and is reproduced for explaining Mechanism 1. The lower panel illustrates the magnified map of the region (60N-70N, 80E-110E).

Since the general atmospheric circulation pattern in the high latitude region is dominated by easterly winds, the spot can hardly receive seeds unless NET boreal forest exists in the East, which is not the case. The global distribution of the NET boreal forest affirms this mechanism in the figure below (Figure 3.7).

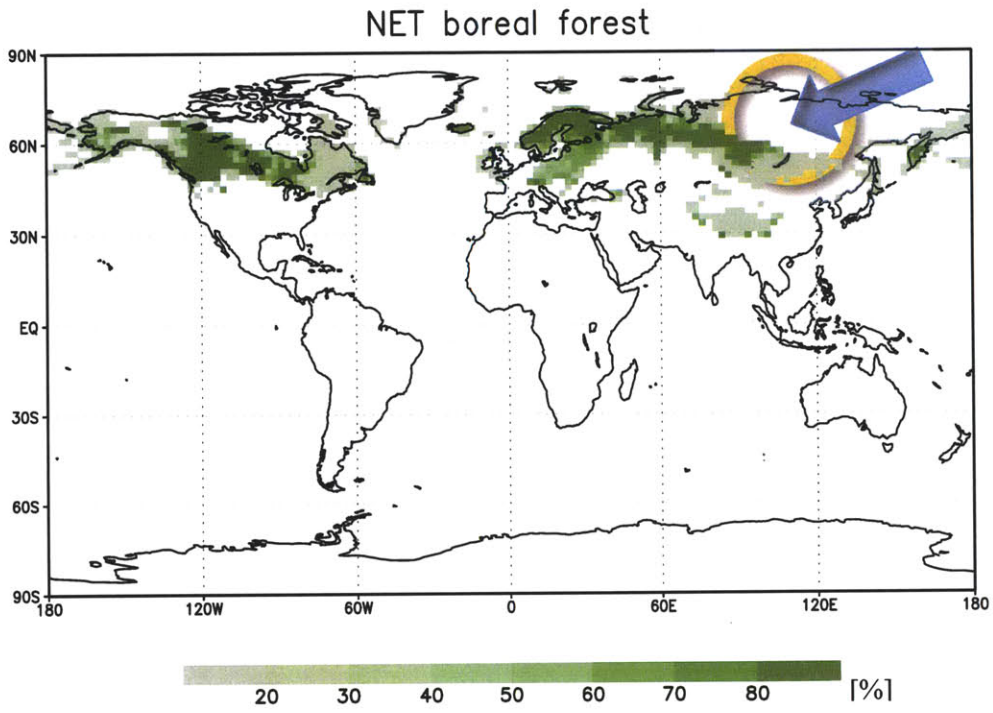

Figure 3.7: Global distribution map of the NET boreal forest (%) simulated in the SEED configuration. The prevailing wind pattern (blue arrow) in the high latitude regions and the existing structure of the NET boreal forest forbid the NET boreal forest to establish and grow in central Siberia.

3.3.3.2 Mechanism 2: One PFT is boosted by competition dynamics, whereas the other is forbidden by prevailing wind

Another important mechanism involves change in the establishment rate due to the altered competition dynamics among PFTs. In Figure 3.8, the southeast United States shows a notable increase in BDT temperate forests in the SEED configuration. The result may seem to be counter-intuitive because the SEED configuration brings another layer of "constraint" to the FREE migration assumption; however, the constraint can alter the competition dynamics where more than two PFTs compete for resources, resulting in boosting growth of a PFT.

In order to explain this behavior, our focus area is restricted to one grid where BDT temperate trees gain more area in the simulation using the SEED configuration. In Figure 3.8, the upper panel illustrates the difference map of BDT temperate trees and the lower panel shows the amplified map around the selected grid whose center is located in 37N, 86W (yellow rectangle).

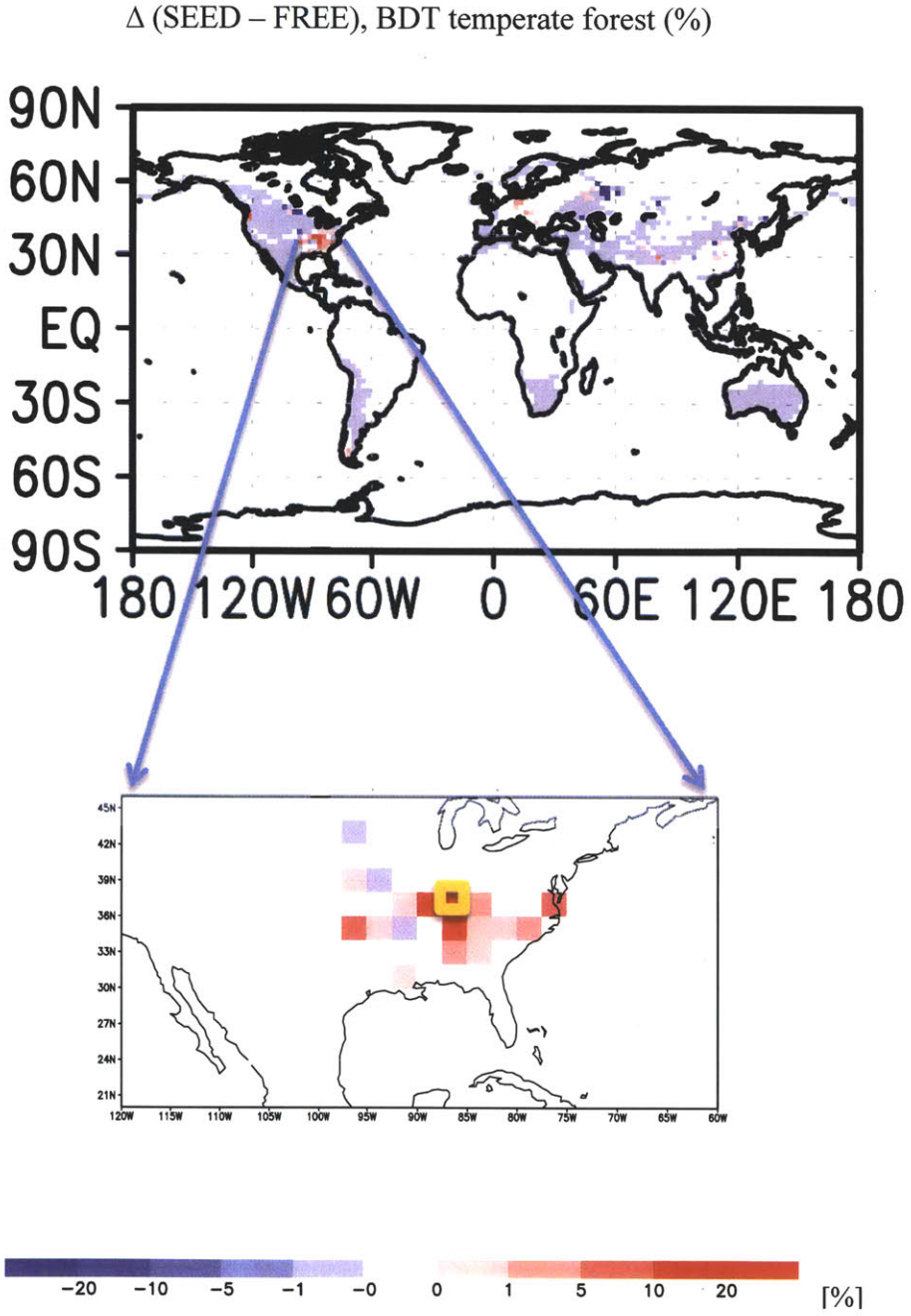

Figure 3.8: Example in eastern United States at which the SEED configuration estimates greater coverage of BDT temperate forest. The difference map in the upper panel is as same as in Figure 3.5 (f) and is reproduced for explaining Mechanism 2. The lower panel illustrates the magnified map of the region centered at 37N,86W (yellow rectangle).

In the grid cell of 37N,86W, there are three co-existing PFTs (NET temperate tree, BDT temperate tree and C3 grass) in the initial vegetation map provided from the first step of the simulation (see Section 3.2 for details of the description of the two-step simulation). In the SEED configuration, the coverage of BDT temperate forest increases at the expense of NET temperate forest in the grid. The competitor, NET temperate tree, is prohibited by the wind dispersal mechanism so that the establishment rate for BDT temperate tree increases, resulting in enhanced coverage of the type. In Figure 3.9, the coverage of BDT temperate forest is 95% in the SEED configuration, compared to 65% in the FREE configuration. The large difference in tree cover (30%) results from the loss of NET temperate forest that would occupy 30% of the land area of the grid cell in the FREE configuration but is wiped out in the SEED configuration for the type does not satisfy the seed dispersal constraint.

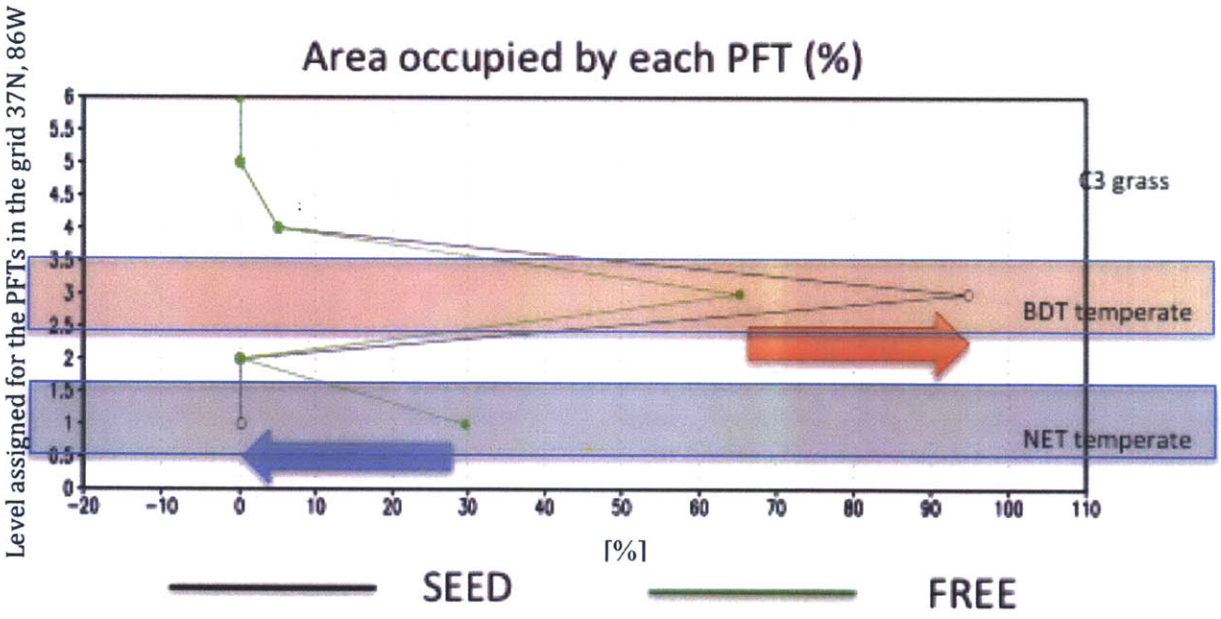

Figure 3.9: Vegetated areas in 37N, 86W grid cell from the SEED configuration (black curve) and the FREE configuration (green curve) at the final model year 1993. BDT temperate forest (assigned to the level 3 in this specific grid 37N, 86W; highlighted in the light red box) gains more area in the SEED configuration at the expense of NET temperate forest (assigned to the level 1 in this specific grid 37N, 86W; highlighted in the light blue box) because NET temperate forest is forbidden by the seed constraint of wind dispersal.

The time series of the evolution of the occupied area by two competing tree PFTs in the grid cell indicate how Mechanism 2 alters competition dynamics more clearly (Figure 3.10). Compared to the gradual development of NET temperate trees in the FREE configuration (green curve at the top panel in Figure 3.10), the growth of NET temperate trees is restricted in the SEED configuration (red curve at the top panel in Figure 3.10). At the expense of NET temperate trees, BDT temperate trees are favored in the SEED configuration. The tree cover of BDT temperate forest increases more rapidly while the growth of NET temperate forest is suppressed, and is later maintained at a higher coverage (95%) in the SEED configuration (red curve at the bottom panel in Figure 3.10). In contrast, the coverage of BDT temperate forest develops at a lower rate and later decreases as NET temperate establishes successfully in the FREE configuration (green curve in the bottom panel in Figure 3.10).

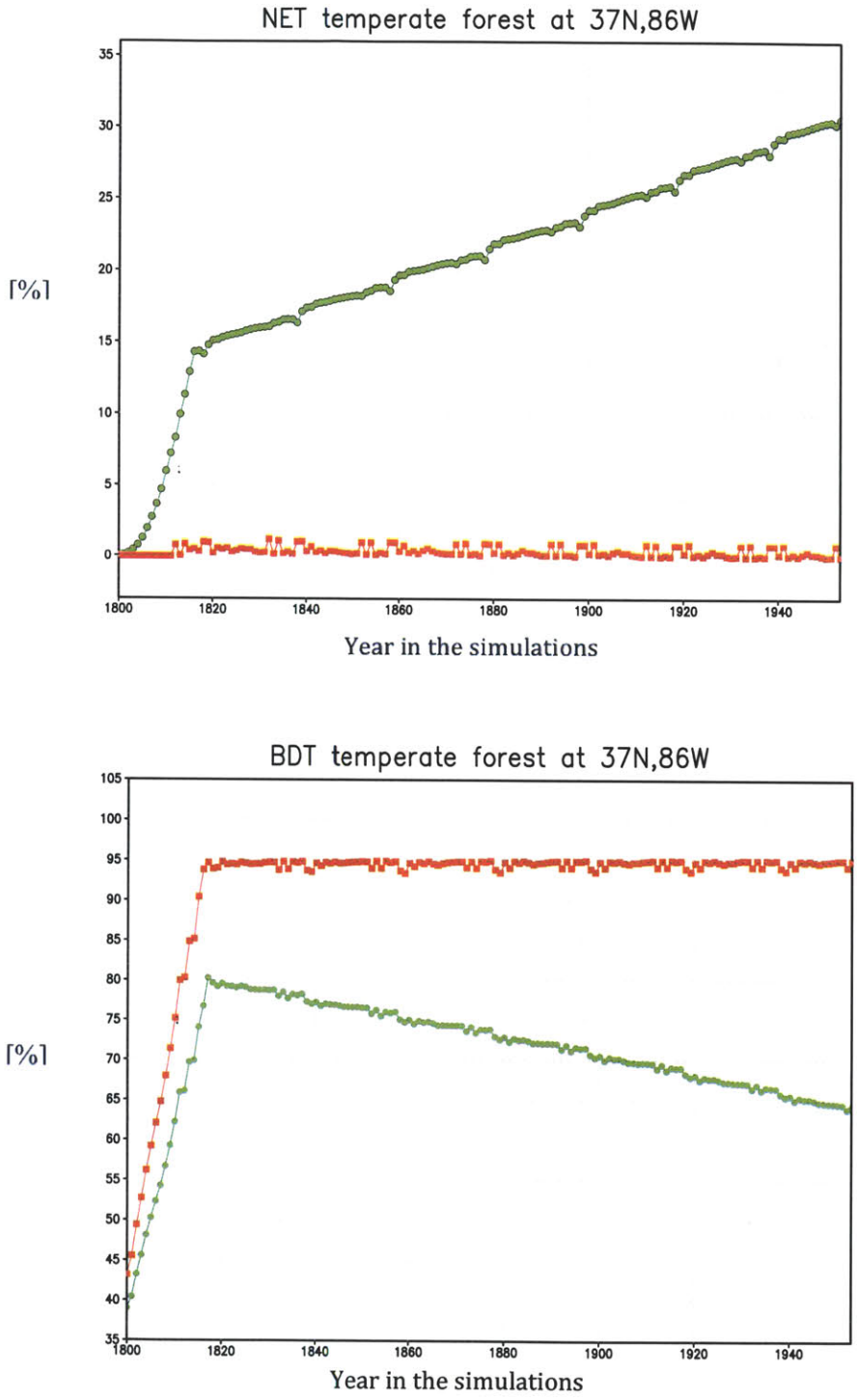

Figure 3.10: Time series of evolution of BDT temperate tree cover in % (upper panel) and NET temperate tree cover in % (lower panel) in 37N, 86W. Green curves give the simulated area of the PFT from the FREE configuration, and red curves from the SEED configuration.

The underlying logical process causing a boosted growth of BDT temperate trees in the SEED configuration is that the seed constraint reduces the competition among saplings that satisfy the establishment condition according to climate. The flow chart in Figure 3.11 illustrates how the competition dynamics may alter the number of competing and establishing PFTs for a given grid cell by applying the seed constraint. In the grid cell of 37N, 86W, the total number of establishing saplings of tree PFTs ($Number_{estab}$) decreases as NET temperate forest is not allowed in the grid cell because of the failure to attain a sufficient seed density for the NET temperate trees. The value of $Number_{estab}$ reduces from 2 (NET temperate tree and BDT temperate tree) in the FREE configuration, to 1 (BDT temperate tree only) in the SEED configuration. Note that grasses are not counted in the number of establishing saplings because they are represented by a group, not by an individual plant type.

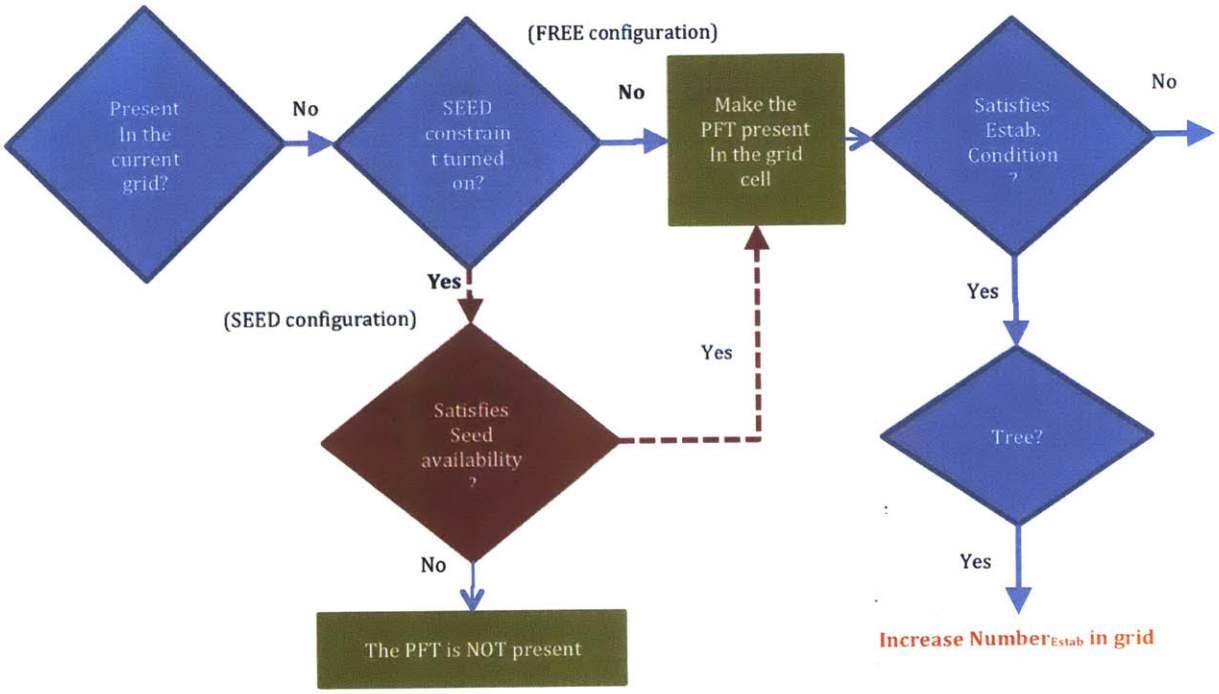

Figure 3.11: Schematic of how the numbers of established PFTs are determined under the FREE configuration and the SEED configuration.

Therefore, the establishment rate in the given grid cell is then adjusted according to the Eqn 3.1 and Eqn 3.2:

$$Estab_{PFT} = Estab_{max} \times \frac{[1 - e^{5(fpcgrid_{Tree\ total} - 1)}]}{Number_{estab}} \quad \text{(Eqn 3.1)}$$

$$Estab_{grid} = Estab_{PFT} \times [1 - fpcgrid_{Tree\ total}] \quad \text{(Eqn 3.2)}$$

where $Estab_{PFT}$ is the establishment rate of existing PFTs in the grid cell, $Estab_{max}$ is the maximum establishment rate (0.24 of individual PFTs/m^2 vegetated land), $fpcgrid_{Tree\ total}$ is total treecover in a given grid cell, and $Estab_{grid}$ is the establishment rate for the grid, equally applied to all the existing PFTs in the grid cell.

In the SEED configuration, a smaller value of $Number_{estab}$ results in a greater establishment rate for the PFTs ($Estab_{PFT}$) that still exist in the grid cell (Equation 3.1) and also a greater grid-wise establishment rate equally applied for all PFT satisfying the seed constraint (Equation 3.2). Compared to the grid-wise establishment rate (0.00133 individual PFTs/m^2 vegetated land) in the FREE configuration, the grid-wise establishment rate in the SEED configuration is enhanced to 0.00265 individual PFTs/m^2 vegetated land, applied solely to BDT temperate trees in the grid cell.

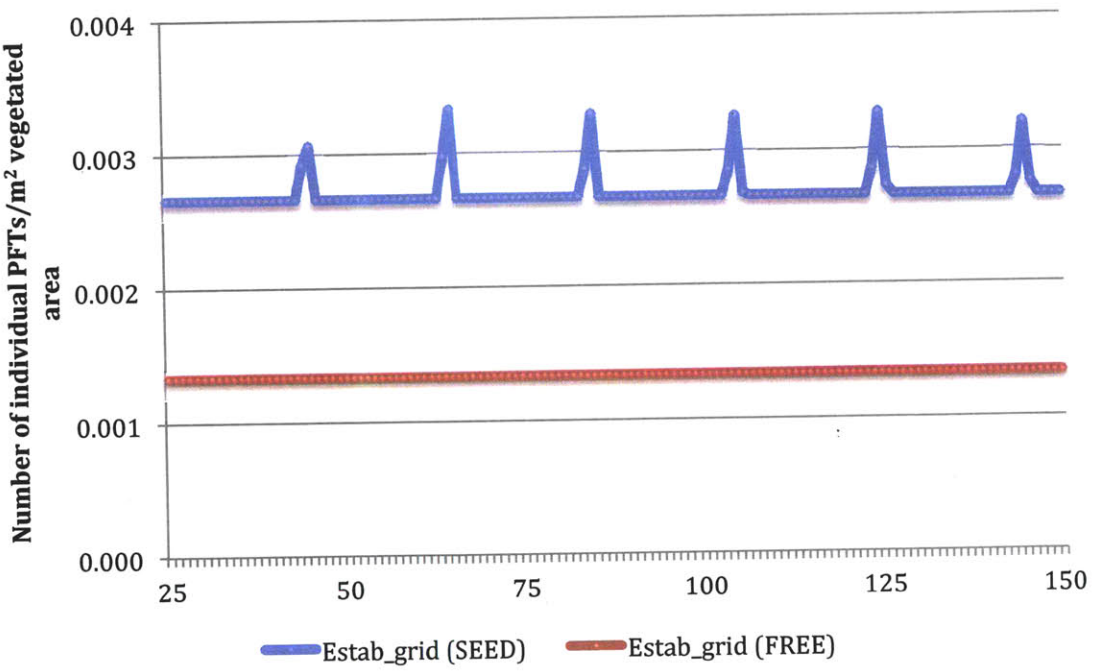

Figure 3.12: Grid-wise establishment rates evenly distributed for all available PFTs satisfying the following conditions: establishment condition only for the FREE configuration (red curve), and both establishment condition and seed constraint for the SEED configuration (blue curve).

3.3.4 Sensitivity of LDD efficiency

Simulated vegetation structure is not sensitive to changes in LDD efficiency (1% to 5%, Nathan et al., (2002)). The resulting structure does not provide any significant difference by applying 1% or 5% of LDD efficiency. When computing the number of available seeds transported by wind, other factors such as the number of days of favorable wind into the grid cell and existing population of the PFTs in neighboring grids play more important roles. The population of existing vegetation from the previous model year, for example, can vary from 0 to 1 so that compared to the impact of existing population, the impact of varying LDD efficiency (0.01 to 0.05) is miniscule.

3.4 Discussion

From the globally aggregated area of each PFT, small changes are estimated between the result using the SEED configuration and the result using the FREE configuration, not wide spread changes. This is because the SEED configuration largely refines the structure by filtering out unrealistic transfers of saplings into a target grid, thereby reducing unnecessary competition among the PFTs. Depending upon the number of PFTs participating in the competition and thereby the altered competition dynamics, a tree PFT may partly gain or lose its habitat area.

If its pre-condition is poorly given, for example, a wrong representation of vegetation structure in the Southern hemisphere, the SEED configuration may drive the model to even amplify the wrong structure to degrade the representation because the configuration reflects the existing population of trees in nearby grid cells as a source of seeds. Note also that the nitrogen cycle is not included and shrub PFTs are not explicitly defined in the CLM-DGVM of version 3.5, which can therefore be sources of errors. It should also be noted that DGVMs are designed to describe the world as if no human influence exists and thus only natural vegetation exists. The models may not represent the vegetation structures of the regions where Land Use and Land Cover (LULC) changes are active.

3.5 Summary and conclusion of Chapter 3

Compared to the satellite-driven AVHRR tree cover, some regions (e.g., boreal forests in the Western Siberia, and temperate forests in Eastern Europe) clearly show significantly improved representation of vegetation using the SEED configuration. The prevailing wind pattern, along with the existing vegetation structure in nearby grid cells, alters the competition dynamics of the trees in these regions by filtering unrealistic saplings out and adjusting their establishment rates.

It should be noted that the SEED configuration is not designed to modify the fundamental climate rules in the CLM-DGVM. Rather, given a rough, but appropriately distributed vegetation map, the SEED configuration takes meteorologically-driven seed dispersal into account, rectifying regional distributions where the free migration assumption does not represent the real competition dynamics among the PFTs.

Chapter 4

Estimation of future vegetation structure under changing climates

4.1 Introduction

Greenhouse emission mitigation policies could make significant differences in future natural vegetation distribution projections. In this Chapter, further simulations are presented, which are designed to estimate the natural vegetation change under two distinct climate mitigation scenarios: No-Policy scenario (hereafter, called the NP scenario) and 450ppm CO_2 stabilization scenario by 2100 (hereafter, called the 450ppm scenario) for the remaining years of the 21st century.

Details of the simulation design are described in section 4.2. Results of future vegetation structure change under the two climate mitigation scenarios are presented at the global scale (section 4.3.1) and also at the regional scale for 22 regions of the global land area (section 4.3.2). In addition, the vulnerability of the 22 regions is assessed according to estimated vegetation structures under changing climates (section 4.3.3). Discussion (section 4.4) and the summary for this Chapter (section 4.5) then follow.

4.2 Description of the IGSM climate with GFDL CM2.1 pattern and wind forcing

In simulating future vegetation structure under the NP scenario and the 450ppm scenario, a hybrid approach of climatology is applied: the NCC climatology for 1994-2000 (17 years), the MIT IGSM merged with the Geophysics Fluid Dynamics Laboratory Coupled Climate Model (GFDL CM 2.1) with median transient climate sensitivity for 2001-2010 (10 years), and finally two distinct merged MIT IGSM-GFDL CM 2.1 climatologies (the NP scenario and the 450ppm scenario) with low transient climate sensitivity (Sokolov et al., 2009) for 2011-2100 (90 years). Driven by the median transient climate sensitivity, the simulations cannot complete the 21st century but crashes, so that the low transient climate sensitivity is applied for 2011-2100. The IGSM climate is zonal so that the longitudinal distribution of precipitation and temperature is mapped following the pattern generated by GFDL CM 2.1 from the IPCC AR4 archive. The zonal distribution pattern does not change over time, but the trend changes over time. In Figure 4.1, annual atmospheric temperature (land only) profiles of the two climate mitigation scenarios are illustrated. Compared to the annual, land-only temperature in year 2011, the NP case shows a rapid increase in temperature by 4 °C at the end of the 21st century, but the 450ppm case shows an increase less than 1 °C.

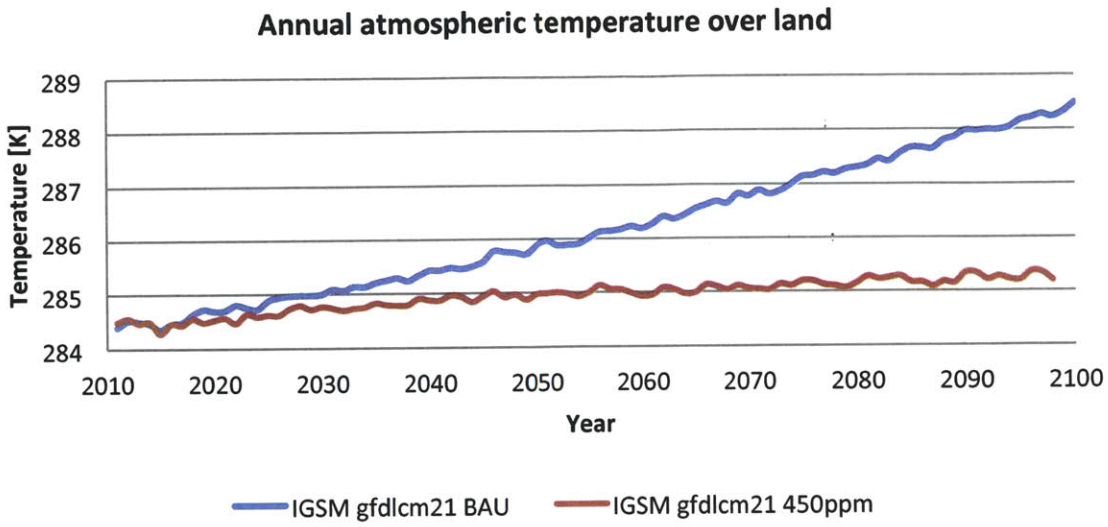

Figure 4.1: Illustrated are atmospheric temperature profiles of the IGSM climate from the NP scenario (blue curve) and the 450ppm scenario (red curve) for 2011-2100.

The simulated vegetation distribution for year 1994, which was generated using the SEED configuration driven by the prescribed NCC meteorological forcing in Chapter 3, is used as the initial vegetation map. The SEED configuration (see Chapter 3 for evaluation of this configuration) continues to be used for the simulations of the 21st century in this Chapter.

In mimicking the meteorology of the 21st century, modeled daily wind profiles are chosen from the IPCC AR4 GCM archive (https://esg.llnl.gov:8443/index.jpg). For the NP scenario, the wind profiles of u-wind (east-west component of wind vector) and v-wind (north-south component of wind vector) simulated by the GFDL CM 2.1 model under the SRESA2 scenario are applied, and for the 450ppm case, the wind profiles simulated under the SRESB1 scenario are used. The complete dataset of daily wind for the entire 21st century is unavailable, but the wind fields of selected years are provided to the public; therefore for years when daily wind datasets are unavailable, the profiles of available years are repeated. The available years for which daily wind dataset are provided by the IPCC AR4 archive, are from year 2046 to year 2065 (20 years) and another set of 20 consecutive years of 2081-2100. Therefore, the daily wind profiles of 2086-2100 are used for the missing years of 2066-2080, and the wind profiles of 2046-2065 are repeated for 2026-2045, and the same profiles of 2051-2065 are repeated for 2011-2025 (Table 4.1).

Table 4.1 Configuration of wind profiles using the available daily wind data from the IPCC AR4 archive.

Time	Daily wind profiles for the NP	Daily wind profiles for the 450ppm	Description
1994-2010	NCEP reanalysis (1994-2010)	NCEP reanalysis (1994-2010)	Reanalyzed observed winds
2011-2025	2051-2065 GFDL CM 2.1 wind (SRES A2)	2051-2065 GFDL CM 2.1 wind (SRES B1)	Repeat of 2051-2065 wind
2026-2045	2046-2065 GFDL CM 2.1 wind (SRES A2)	2046-2065 GFDL CM 2.1 wind (SRES B1)	Repeat of 2046-2065 wind
2046-2065	2046-2065 GFDL CM 2.1 wind (SRES A2)	2046-2065 GFDL CM 2.1 wind (SRES B1)	Available years
2066-2080	2086-2100 GFDL CM 2.1 wind (SRES A2)	2086-2100 GFDL CM 2.1 wind (SRES B1)	Repeat of 2086-2100 wind
2081-2100	2081-2100 GFDL CM 2.1 wind (SRES A2)	2081-2100 GFDL CM 2.1 wind (SRES B1)	Available years

Two sets of calibration parameters are applied to obtain realistic carbon fluxes. The set of calibration parameters, which was used for the simulations driven by the NCC climate in the previous Chapter 3, is also used for time period when the remaining NCC climate is applied (1994-2000). Then another set of calibration parameters, which is optimized for using the IGSM climate, is applied for the time period when the IGSM climate is applied (2001-2100). Similar to the process described in Section 2.5, the calibration is obtained by repeating 20-year IGSM climate (1991-2010) for 200 simulation years, optimizing V_{cmax25}, *fnitr*, and turnover years that are to be tuned for the IGSM climate. Table 4.2 summarizes V_{cmax25}, *fnitr*, and turnover years of the calibration that are applied for the years (2001-2100) using the IGSM climate.

Table 4.2: Parameters modified for initializing the CLM-DGVM with IGSM climate. Modified values in bold font.

PFT	V_{cmax25} (NCAR) [μmol $CO_2/m^2 \cdot s$]	V_{cmax25} (MIT) for IGSM climate dataset [μmol $CO_2/m^2 \cdot s$]
NET temperate	51.0	51.0
NET boreal	**43.0**	**21.0**
BET tropical	75.0	75.0
BET temperate	69.0	69.0
BDT tropical	40.0	40.0
BDT temperate	51.0	51.0
BDT boreal	**51.0**	**25.0**
C3 grass Arctic	**43.0**	**21.0**
C3 Grass	43.0	43.0
C4 Grass	24.0	24.0

PFT	fnitr ratio (NCAR)	fnitr ratio (MIT) for IGSM climate dataset
NET temperate	0.63	0.63
NET boreal	**0.62**	**0.30**
BET tropical	**0.69**	**0.80**
BET temperate	**0.35**	**0.36**
BDT tropical	0.31	0.31
BDT temperate	**0.36**	**0.45**
BDT boreal	**0.41**	**0.33**
C3 grass Arctic	**0.39**	**0.23**
C3 Grass	**0.24**	**0.34**
C4 Grass	**0.24**	**0.17**

Table 4.2 (continued): Parameters modified for initializing the CLM-DGVM with IGSM climate

PFT	Leaf turnover period (NCAR) [years]	Leaf turnover period (MIT) for NCC climate dataset [years]
NET temperate	2.0	2.0
NET boreal	**2.0**	**4.0**
BET tropical	2.0	2.0
BET temperate	1.0	1.0
BDT tropical	1.0	1.0
BDT temperate	1.0	1.0
BDT boreal	1.0	1.0
C3 Arctic grass	1.0	1.0
C3 Grass	1.0	1.0
C4 Grass	1.0	1.0

PFT	Sapwood turnover period (NCAR) [years]	Sapwood turnover period (MIT) for IGSM climate dataset [years]
NET temperate	20.0	20.0
NET boreal	**20.0**	**60.0**
BET tropical	20.0	20.0
BET temperate	20.0	20.0
BDT tropical	20.0	20.0
BDT temperate	20.0	20.0
BDT boreal	**20.0**	**60.0**
C3 Arctic grass	1.0	1.0
C3 Grass	1.0	1.0
C4 Grass	1.0	1.0

The climate data sets, wind profiles, calibration parameters, and two climate mitigation scenarios applied to the two simulations presented in this Chapter are summarized in Table 4.3. Note that only the SEED configuration is applied to these simulations (for the evaluation and details of the SEED configuration and the FREE configuration, see previous Chapter 2 and Chapter 3).

Table 4.3: Summary of climate, wind, calibration and mitigation scenarios used for two simulations presented in this Chapter.

(a) The NP scenario

Time	Climate	Wind	Calibration
1994-2000	NCC climate	NCEP reanalysis (1994-2000)	Optimized for NCC
2001-2010	IGSM climate (*median)	NCEP reanalysis (2001-2010)	Optimized for IGSM
2011-2025	IGSM-GFDL CM 2.1 climate (¶low) NP	2051-2065 GFDL CM 2.1 wind (SRES A2)	Optimized for IGSM
2026-2045	IGSM-GFDL CM 2.1 climate (low) NP	2046-2065 GFDL CM 2.1 wind (SRES A2)	Optimized for IGSM
2046-2065	IGSM-GFDL CM 2.1 climate (low) NP	2046-2065 GFDL CM 2.1 wind (SRES A2)	Optimized for IGSM
2066-2080	IGSM-GFDL CM 2.1 climate (low) NP	2086-2100 GFDL CM 2.1 wind (SRES A2)	Optimized for IGSM
2081-2100	IGSM-GFDL CM 2.1 climate (low) NP	2081-2100 GFDL CM 2.1 wind (SRES A2)	Optimized for IGSM

(b) The 450ppm scenario

Time	Climate	Wind	Calibration
1994-2000	NCC climate	NCEP reanalysis (1994-2000)	Optimized for NCC
2001-2010	IGSM climate (median)	NCEP reanalysis (2001-2010)	Optimized for IGSM
2011-2025	IGSM-GFDL CM 2.1 climate (low) 450ppm	2051-2065 GFDL CM 2.1 wind (SRES B1)	Optimized for IGSM
2026-2045	IGSM-GFDL CM 2.1 climate (low) 450ppm	2046-2065 GFDL CM 2.1 wind (SRES B1)	Optimized for IGSM
2046-2065	IGSM-GFDL CM 2.1 climate (low) 450ppm	2046-2065 GFDL CM 2.1 wind (SRES B1)	Optimized for IGSM
2066-2080	IGSM-GFDL CM 2.1 climate (low) 450ppm	2086-2100 GFDL CM 2.1 wind (SRES B1)	Optimized for IGSM
2081-2100	IGSM-GFDL CM 2.1 climate (low) 450ppm	2081-2100 GFDL CM 2.1 wind (SRES B1)	Optimized for IGSM

* Median: Median transient climate sensitivity

¶ Low: Low transient climate sensitivity

4.3 Model result analysis

4.3.1 Global projections of Natural vegetation distribution

Under the NP scenario and the 450ppm scenario, the resulting global vegetation structures at the end of 21st century show notable differences, both globally and regionally. Since the distribution pattern of each PFT varies depending on time and climate mitigation scenario, global-scale analysis of the difference that is obtained at the end of 21st century for the NP scenario and the 450ppm scenario is discussed first in this section, in order to gauge the impacts of climate on the vegetation structure. More comprehensive and in-depth regional analyses, including the time-series of vegetation area of each PFT, will be discussed in the following section 4.3.2.

Table 4.4 shows globally aggregated areas of 10 PFTs for the year 2011 (starting year), the year 2100 (end year), and their differences (2100 minus 2011). Evergreen trees (NET boreal and BET tropical) will proliferate much more in a warmer world where no climate mitigation policy is implemented (i.e., under the NP scenario). At the end of the 21st century, NET boreal forests in high latitudes and BET tropical in Tropics will increase by 23% and 80% in the NP case, respectively, but will increase only by 2% and 52% in the 450ppm case. Deciduous tree cover will also increase, but the response of deciduous trees to climate is not as sensitive as evergreen trees.

Table 4.4: Averaged areas (%) of ten PFTs, simulated under the NP scenario and the 450ppm scenario.

	Year 2011	Year 2100		Delta (2100-2011)		
		NP	450ppm	NP	450ppm	Trend from 2011 to 2100
NET boreal	29.24	35.86	29.71	**6.63**	**0.48**	Increase
BDT boreal	13.76	20.17	19.70	6.41	5.94	Increase
C3 grass Arctic	43.00	38.60	38.69	-4.40	-4.31	Decrease
NET temperate	11.48	10.38	9.73	-1.10	-1.75	Decrease
BET temperate	11.49	19.57	19.55	8.08	8.06	Increase
BDT temperate	22.19	23.83	24.69	**1.64**	**2.50**	Increase
C3 grass	43.75	40.33	40.74	-3.42	-3.02	Decrease
BET tropical	12.75	22.88	19.40	**10.13**	**6.66**	Increase
BDT tropical	63.67	73.85	73.89	10.18	10.23	Increase
C4 grass	26.69	22.86	21.55	-3.83	-5.14	Decrease

Impacts of climate on the global patterns of plant biogeography are shown in Figure 4.2, assuming the impacts are the greatest in year 2100. Similar to Chapter 3, the maps are shown in the following order from the PFT that is the most abundant in the high latitudes to the PFT most abundant in the low latitudes: NET boreal forest, BDT boreal forest, C3 grass Arctic (i.e., Tundra), NET temperate forest, BET temperate forest, BDT temperate forest, C3 grass, BET tropical forest, BDT tropical forest, and C4 grass.

Under the NP scenario, NET boreal forest expansion is prominent, especially in the high latitudes (50N and above), compared to the 450ppm scenario. Considering the warmer temperature profile of the NP scenario, expected are further northward movement of boreal trees (Figure 4.2 (a) and (b)), replacing C3 arctic grass (or Tundra) in Alaska and East Northern Canada (Figure 4.2 (c)). Also, more NET boreal forest grows in northern Eurasia at the expense of C3 grass Arctic under the NP scenario. In contrast, the habitat of boreal forests shrinks in mid-latitudes under the NP scenario (Figure 4.2 (a) and (b)) because this regions is more favorable for grasses.

Temperate trees provide a mixed pattern of expansion and shrinkage. Roughly, broadleaf temperate trees (BET temperate forest and BDT temperate forest) gain more areas, but needleleaf trees (NET temperate forest) lose some of their habitats. Climate may trigger major shifts of temperate forests in some regions. The warmer climate (i.e., the NP scenario) causes disappearance of NET temperate forest in South Asia, for example, but enhanced coverage of the tree type in Southeast Asia (Figure 4.2 (d)). In addition, BET temperate forest coverage shrinks in South Africa (Figure 4.2 (e)), and BDT temperate becomes less competitive in eastern United States but more favored in South Asia (Figure 4.2 (f)) under the NP scenario, compared to the 450ppm scenario. Northward shift of C3 grass in the mid-latitudes under the NP scenario is clearly shown in Figure 4.2 (g). Details of these regional shifts will be discussed later in the following section 4.3.2.

In the Tropics, evergreen tropical trees (BET tropical forest) favored in warmer climates, especially in Amazon, taking over the habitat areas of broadleaf tropical trees (BDT tropical forest) (Figure 4.2 (h) and (i)). C4 grass is favored under the warmer climate (i.e., the NP scenario), but also loses its cover in western Africa (Figure 4.2 (j)), which is a good example that globally averaged area does not show a noticeable difference but regional changes are significant.

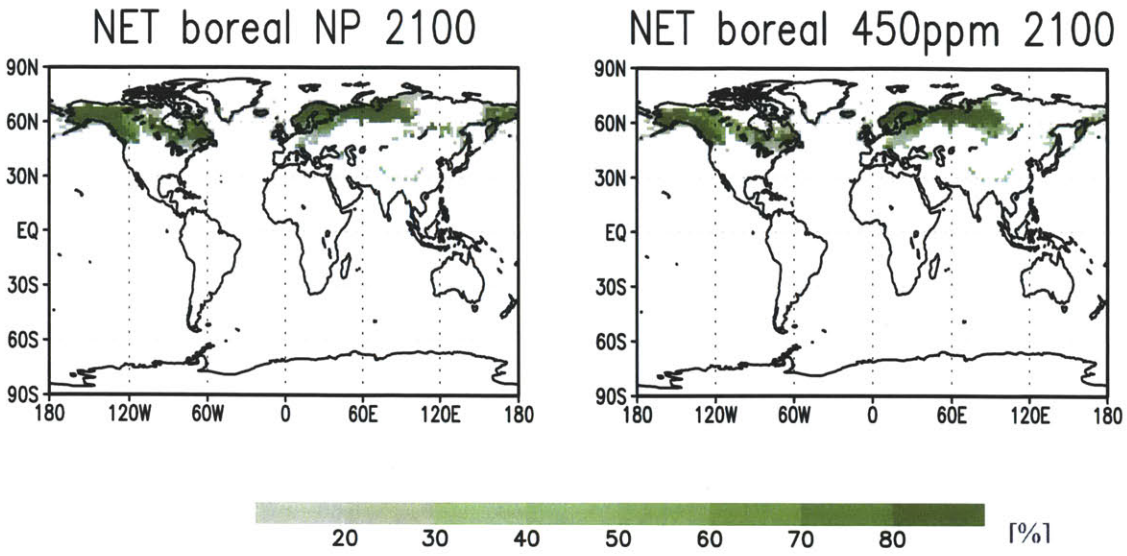

Δ (NP – 450ppm), NET boreal forest at year 2100

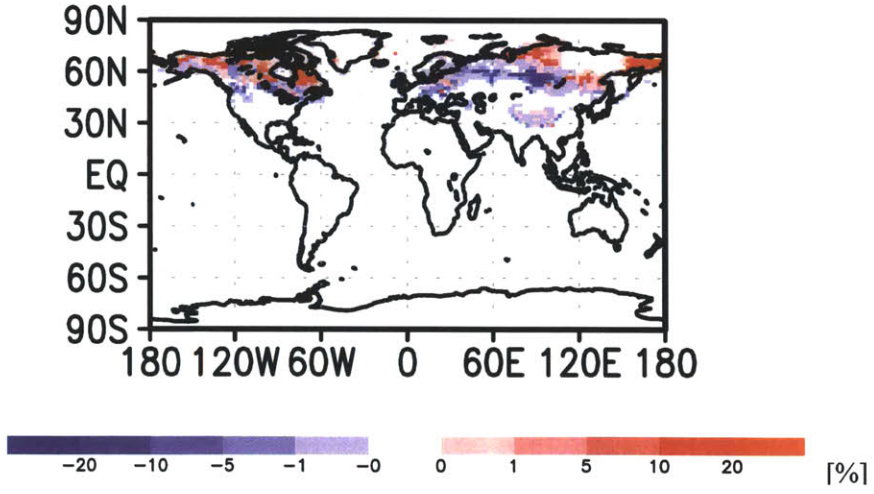

Figure 4.2 (a): Projected distributions of NET boreal forest (%) at year 2100 under the NP scenario (upper left panel) and under the 450ppm scenario (upper right panel). The difference (%) is shown in the lower panel.

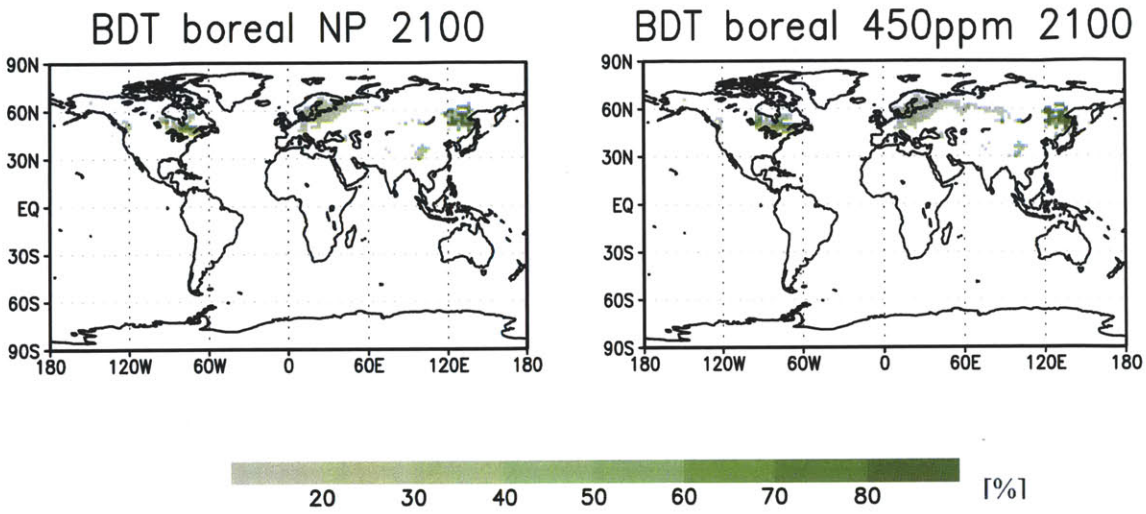

Δ (NP – 450ppm), BDT boreal at year 2100

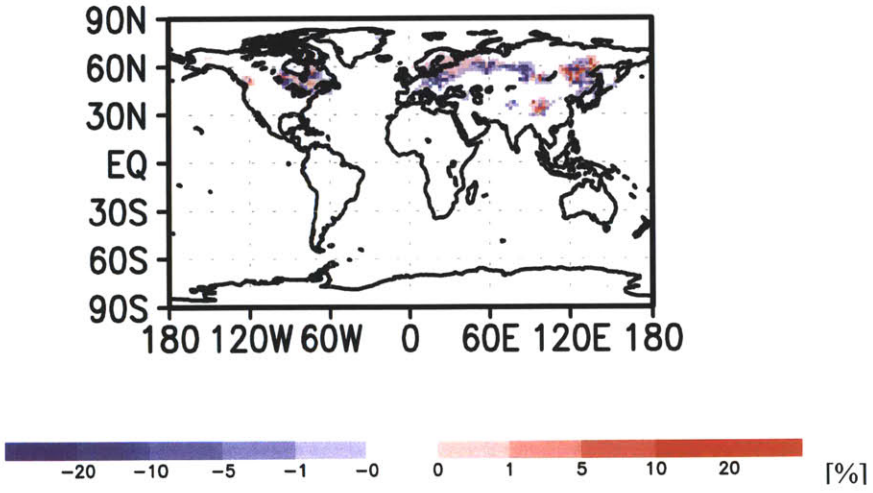

Figure 4.2 (b): Projected distributions of BDT boreal forest (%) at year 2100 under the NP scenario (upper left panel) and under the 450ppm scenario (upper right panel). The difference (%) is shown in the lower panel.

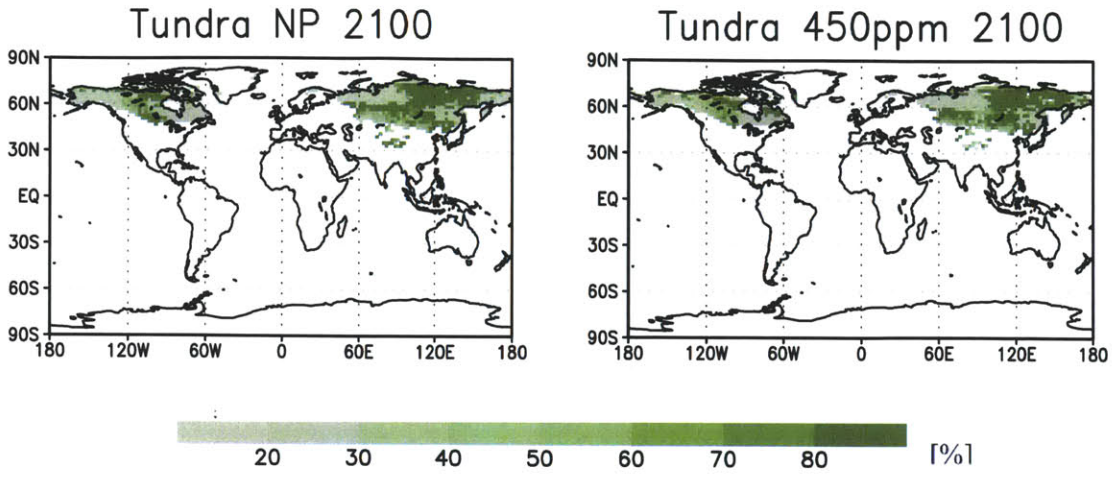

Δ (NP – 450ppm), C3 grass Arctic (Tundra) at year 2100

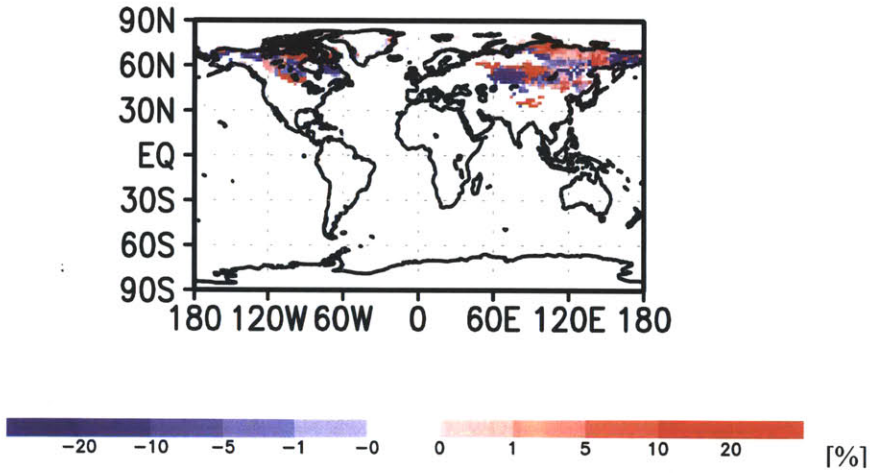

Figure 4.2 (c): Projected distributions of C3 grass Arctic (%) at year 2100 under the NP scenario (upper left panel) and under the 450ppm scenario (upper right panel). The difference (%) is shown in the lower panel.

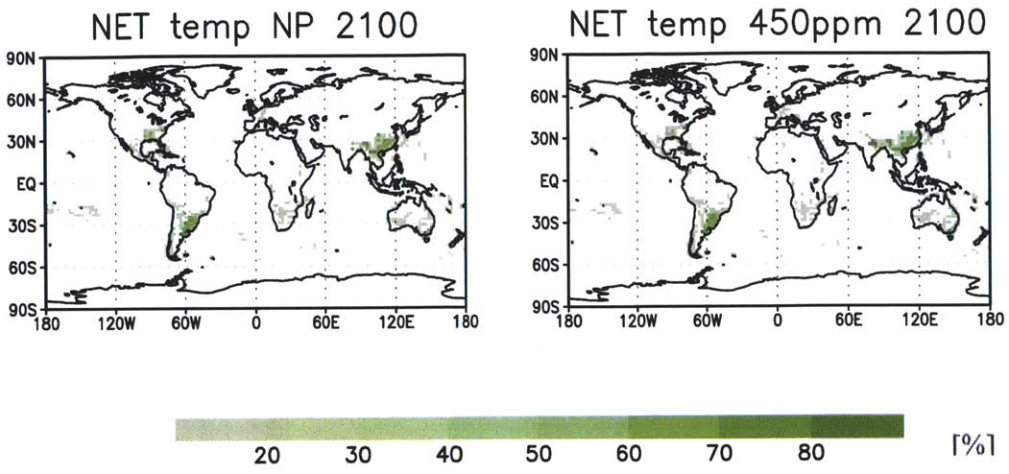

Δ (NP – 450ppm), NET temperate forest at year 2100

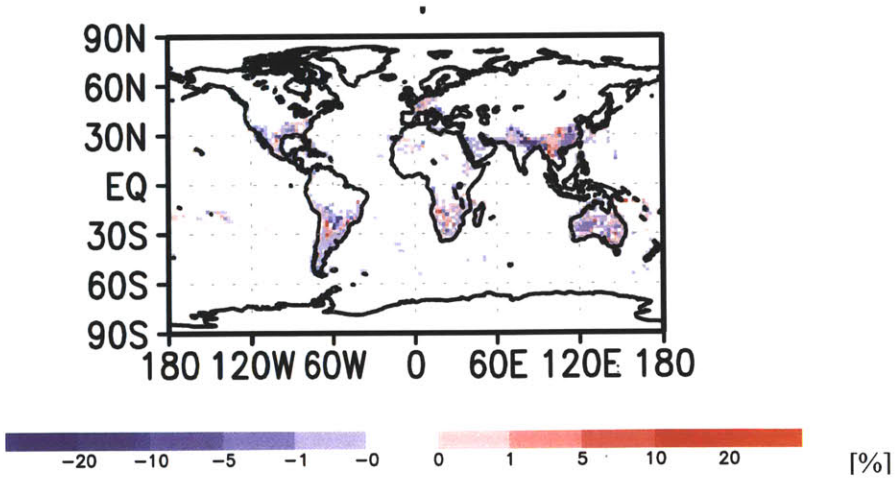

Figure 4.2 (d): Projected distributions of NET temperate forest (%) at year 2100 under the NP scenario (upper left panel) and under the 450ppm scenario (upper right panel). The difference (%) is shown in the lower panel.

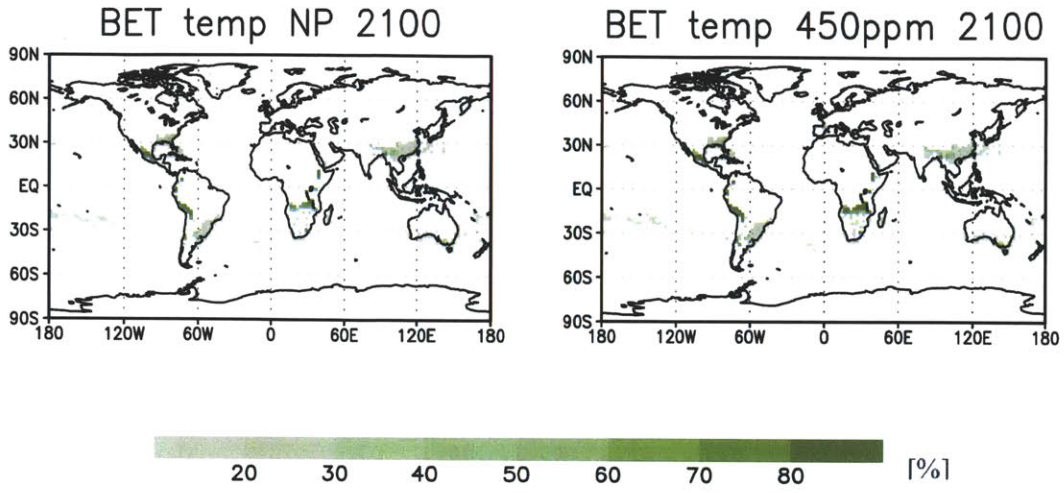

Δ (NP – 450ppm), BET temperate forest at year 2100

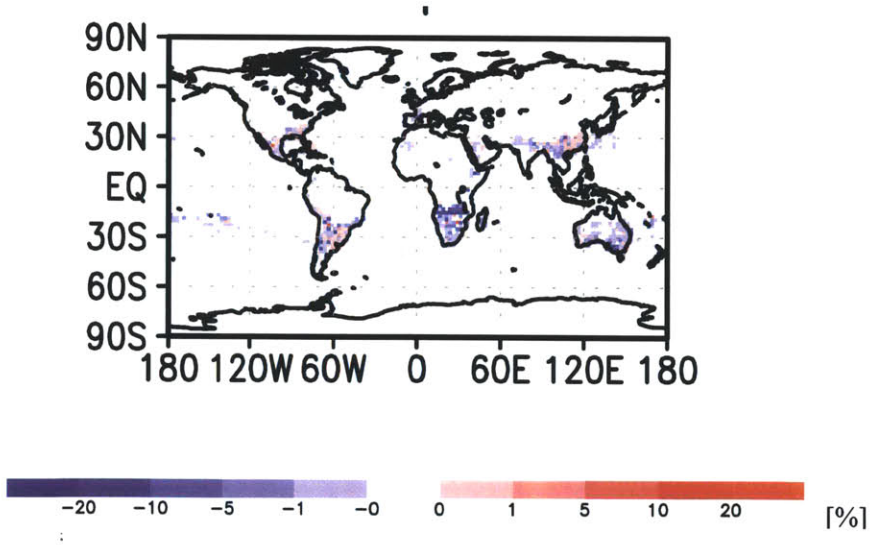

Figure 4.2 (e): Projected distributions of BET temperate forest (%) at year 2100 under the NP scenario (upper left panel) and under the 450ppm scenario (upper right panel). The difference (%) is shown in the lower panel.

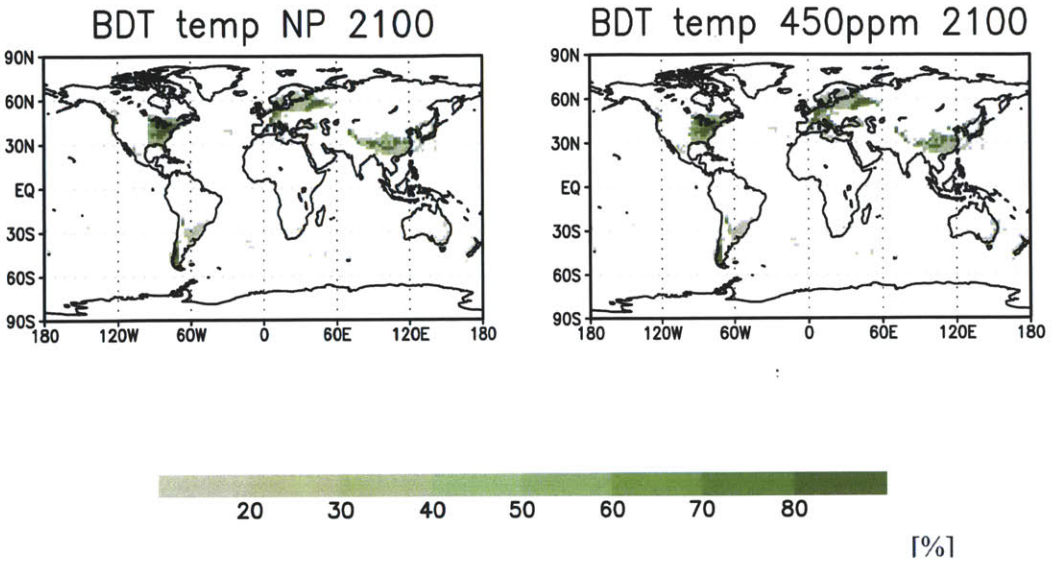

Δ (NP – 450ppm), BDT temperate forest at year 2100

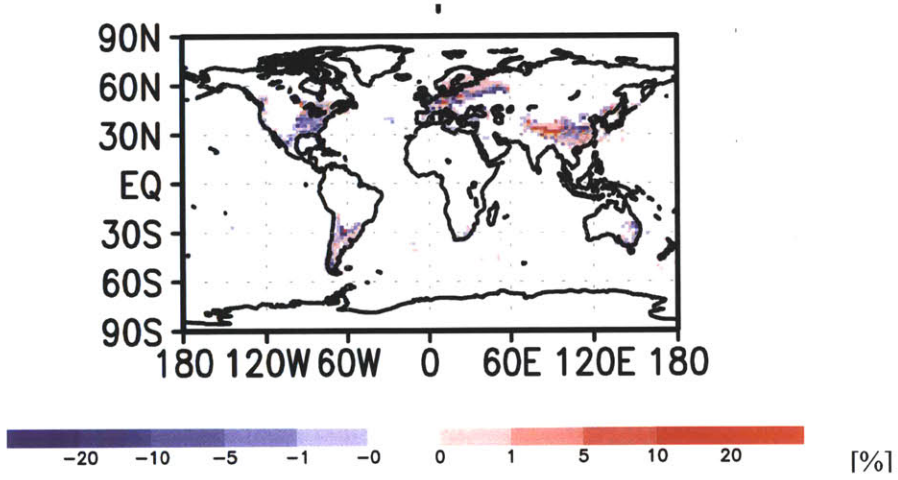

Figure 4.2 (f): Projected distributions of BDT temperate forest (%) at year 2100 under the NP scenario (upper left panel) and under the 450ppm scenario (upper right panel). The difference (%) is shown in the lower panel.

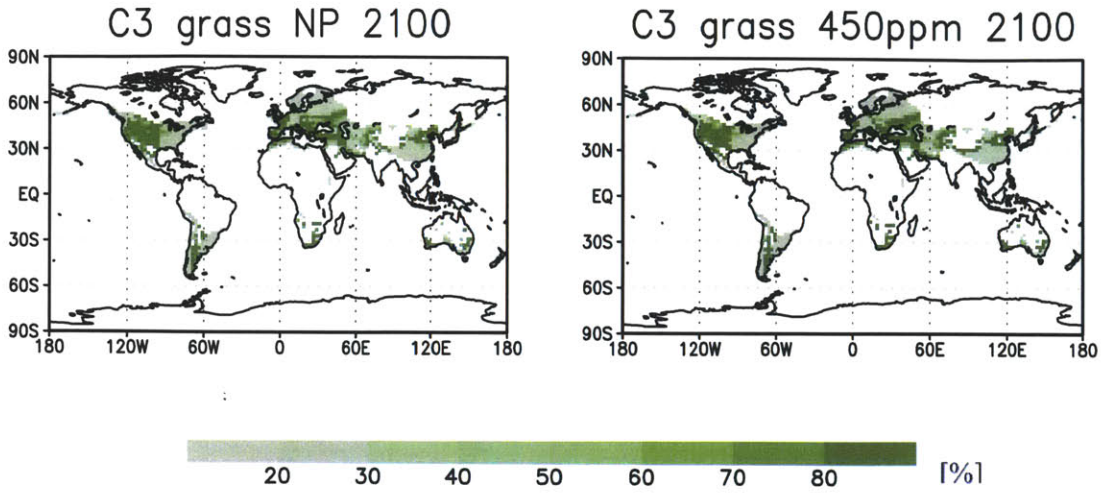

Δ (NP – 450ppm), C3 grass (cold-season) at year 2100

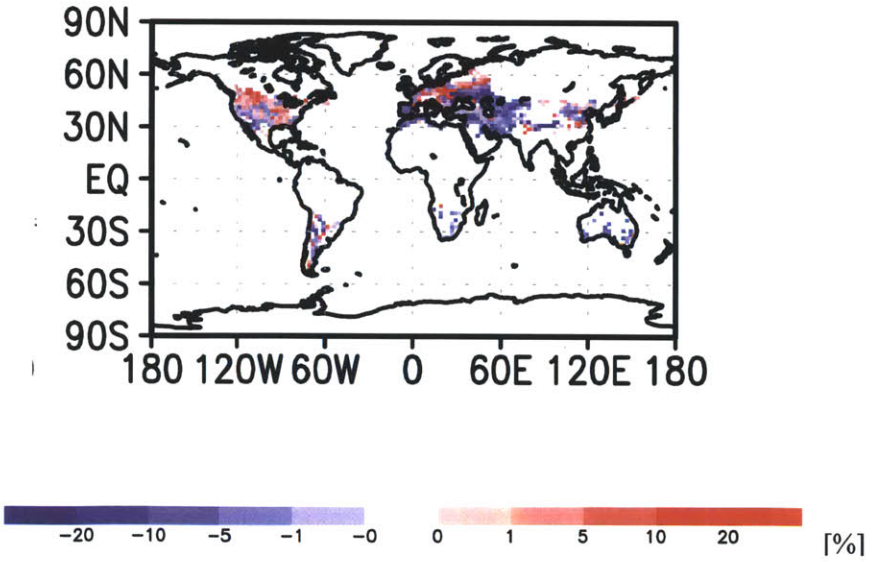

Figure 4.2 (g): Projected distributions of C3 grass (%) at year 2100 under the NP scenario (upper left panel) and under the 450ppm scenario (upper right panel). The difference (%) is shown in the lower panel.

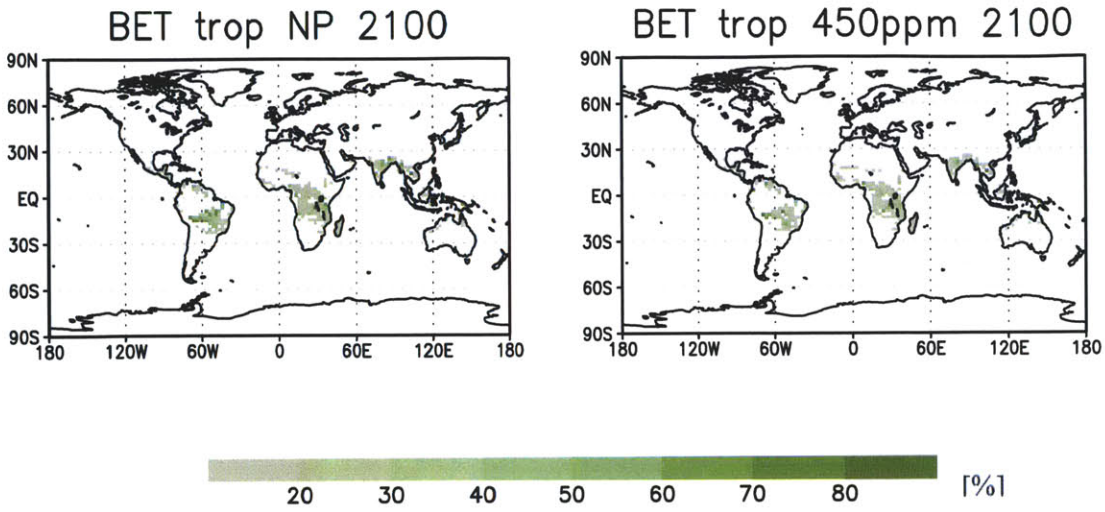

Δ (NP – 450ppm), BET tropical forest at year 2100

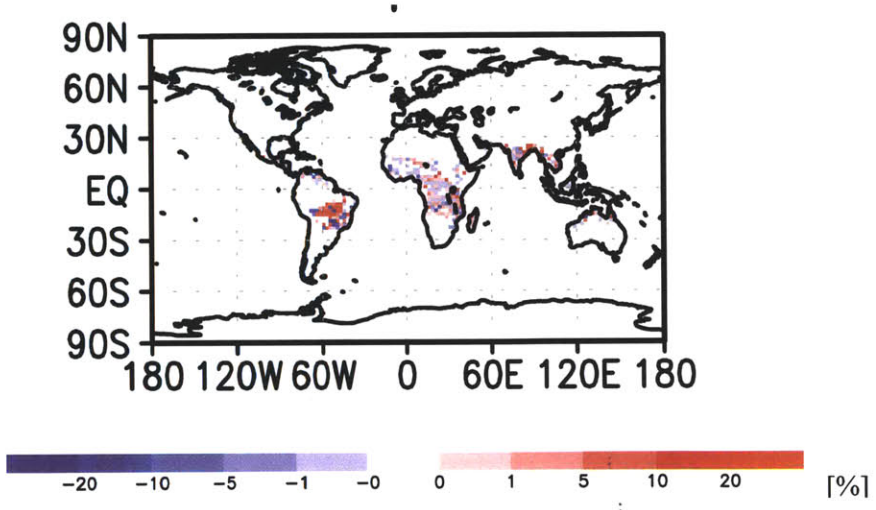

Figure 4.2 (h): Projected distributions of BET tropical forest (%) at year 2100 under the NP scenario (upper left panel) and under the 450ppm scenario (upper right panel). The difference (%) is shown in the lower panel.

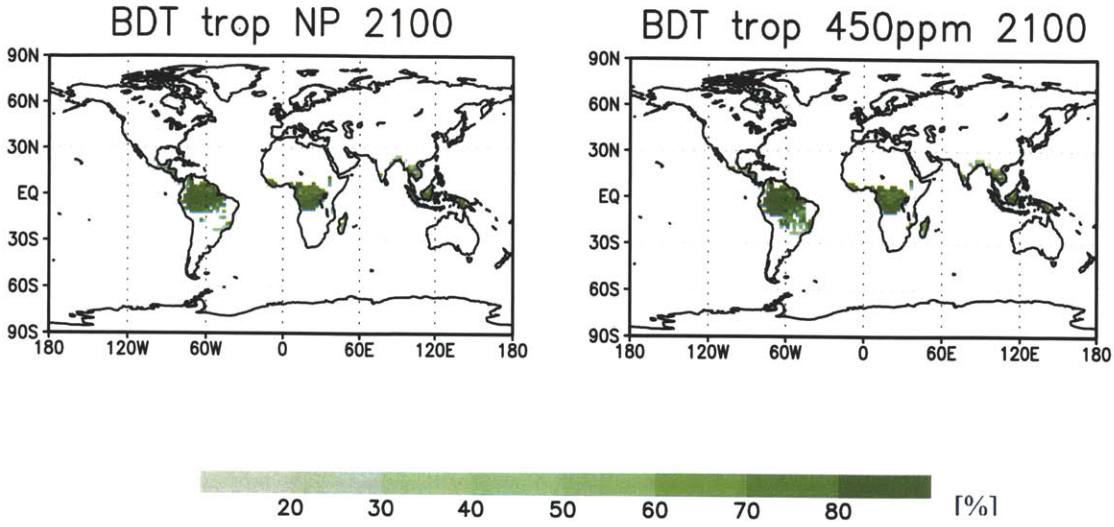

Δ (NP – 450ppm), BDT tropical forest at year 2100

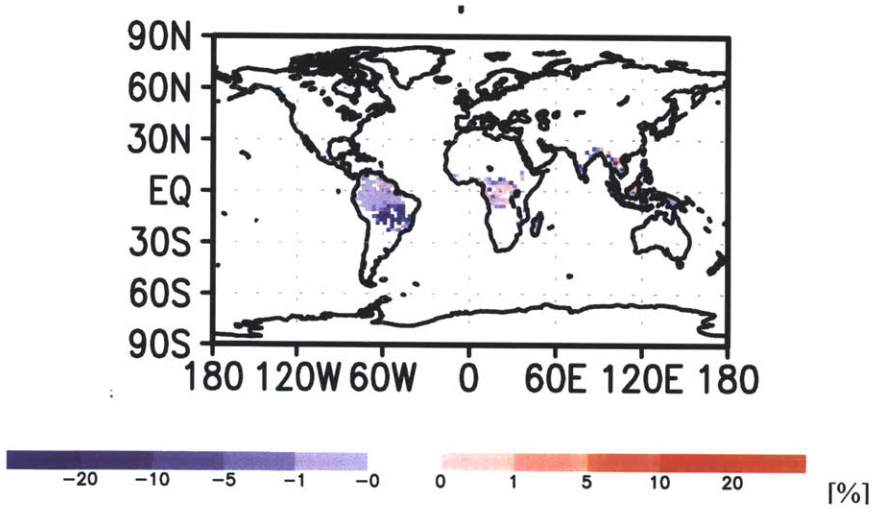

Figure 4.2 (i): Projected distributions of BDT tropical forest (%) at year 2100 under the NP scenario (upper left panel) and under the 450ppm scenario (upper right panel). The difference (%) is shown in the lower panel.

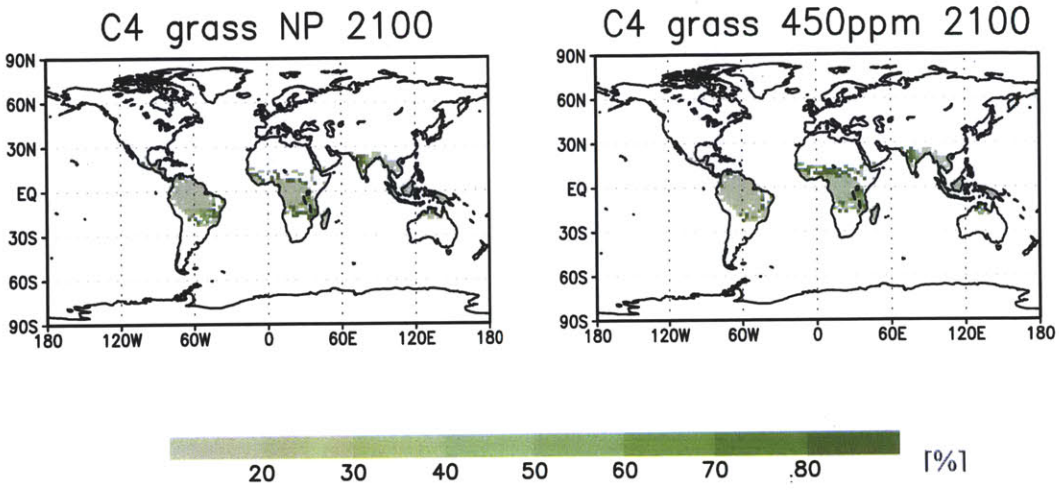

Δ (NP – 450ppm), C4 grass at year 2100

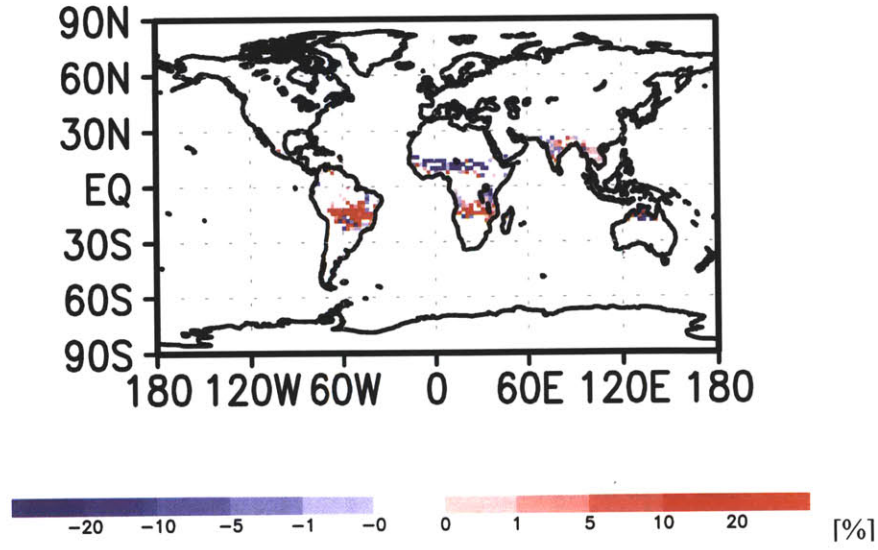

Figure 4.2 (j): Projected distributions of C4 grass (%) at year 2100 under the NP scenario (upper left panel) and under the 450ppm scenario (upper right panel). The difference (%) is shown in the lower panel.

4.3.2 Regional distribution of future natural vegetation

4.3.2.1 Trend of vegetation structure in the 21st century (2011-2100)

As previously discussed, not only the aggregated global change in natural vegetation, but also the spatial distribution of the regional vegetation changes are very informative. Giorgi and Francisco (2000 a, b) divided the global land cover into 22 regions; five in North America, three in South America, two in Europe, four in Africa, six in Asia, two in Australia. In North America, the five regions are Alaska (ALA), Greenland and Northern Territories (GRL), Western North America (WNA), Central North America (CNA), and Eastern North America (ENA). In South America, the three regions are Central America (CAM), Amazon basin (AMZ), Southern South America (SSA). The two regions in Europe are Northern Europe (NEU) and Southern Europe (SEU), and the four regions in Africa are Sahara (SAR), Western Africa (WAF), Eastern Africa (EAF), and Southern Africa (SAF). In Asia, the six regions are: North Asia (NAS), Central Asia (CAS), Tibet (TIB), East Asia (EAS), South Asia (SAS), and Southeast Asia (SEA). The two regions in Australia are North Australia (NAU) and South Australia (SAU).

Definitions of these rectangular regions by coordinate (longitude and latitude) are listed in Table 4.5.

Table 4.5: List of 22 regions used for this analysis by Giorge and Francisco (2000 a, b) (also in Hegerl et al., 2007, SPM 9-9, Note 2)

Region	Name	Longitude, Latitude coverage
Global	GLO	180W to 180E, 90S to 90N
North America	ALA	170W to 103W, 60N to 72N
	GRL	103W to 10W, 50N to 85N
	WNA	130W to 103W, 30N to 60N
	CNA	103W to 85W, 30N to 50N
	ENA	85W to 50W, 25N to 50N
South America	CAM	116W to 83W, 10N to 30N
	AMZ	82W to 34W, 20S to 12N
	SSA	76W to 40W, 56S to 20S
Europe	NEU	10W to 40E, 48N to 75N
	SEU	10W to 40E, 30N to 48N
Africa	SAR	20W to 65E, 18N to 30N
	WAF	20W to 22E, 12S to 18N
	EAF	22E to 52E, 12S to 18N
	SAF	10E to 52E, 35S to 12S
Asia	NAS	40E to 180E, 50N to 70N
	CAS	40E to 75E, 30N to 50N
	TIB	75E to 100E, 30N to 50N
	EAS	100E to 145E, 20N to 50N
	SAS	65E to 100E, 5N to 30N
	SEA	95E to 155E, 11S to 20N
Australia	NAU	110E to 155E, 30S to 11S
	SAU	110E to 155E, 45S to 30S

Following the definitions of these characteristic regions in the Table 4.5, the time-series of area occupied by each PFT from 2011 to 2100 are illustrated in Figure 4.3. The spatial patterns of change in vegetation structure (at year 2100, compared to the starting year 2011), are shown in Figure 4.4.

NET boreal forest continues to dominate (over 20%) at the regions ALA, GRL, WNA, NEU and NAS (Figure 4.3 (a)). In ALA, GRL, and NAS, the area covered by NET boreal forest expands over time throughout the 21st century. In WNA and NEU, however, NET boreal tree cover shrinks, or the density of the forest is reduced. NET boreal forests in ALA and GRL respond to climate change more promptly (from 2040s and later years in the 21st century), increasing more rapidly under the NP scenario. In ALA, the forest coverage is up to 60% under the NP scenario, but under the 450ppm scenario, the coverage is only up to 42%. Similarly, the NET boreal forests in GRL increase much more under the NP scenario (up to 30% in 2100), but the expansion lingers

under the 450ppm scenario, maintaining 20% of the region. Although the tree cover in NEU, WNA, and NAS changes in response to climate, the change is slow and gradual, and is not sensitive to the two different mitigation scenarios.

Another boreal tree type (i.e., BDT boreal tree) shows a different pattern of shift (Figure 4.3 (b)). Although BDT boreal forest overall occupies less area than the NET boreal forest, their habitats are very focused on certain regions and show some notable responses upon changing climates at the end of 21st century. In short, BDT boreal forests do not lose their habitats under the 450ppm scenario. Their migration is either zero or slow under changing climates over time. In CNA and ENA, the population change of this type does not strongly respond to climate change but maintains its population until the later years of the 21st century. Then in these later years of the century, under the warmer climate (the NP scenario) its northward expansion is limited or even causes a reduction of its population. In Europe, BDT boreal forest coverage increases but the expansion is very slow. Similar to CNA and ENA, its expansion is more favored under the mild warming scenario (i.e., the 450ppm scenario). In NAS, its northward shift occurs for later years of the 21st century (after 2050), in part because of the disappearance of C3 grass Arctic in the region. Populations in EAS are maintained.

As a counterpart to the boreal forests, C3 grass Arctic shows significant reduction in the high latitudes, especially in ALA and NAS (Figure 4.3 (c)). This grass type disappears as NET boreal forest expands in ALA, and is also reduced as NET boreal forest gains in Central Siberia and BDT boreal forest expands at the east corner of NAS (also see Figure 4.4 (a), (b), and (c)). Since boreal forests expand more rigorously under the NP scenario (blue curves, in Figure 4.3 (a) and (b)), the degree of loss in C3 grass Arctic is greater (Figure 4.3 (c)) in ALA and NAS. In WNA and in CNA, its coverage increases as warming causes northward shifts of NET boreal forests, transforming the regions more favorable to C3 grass Arctic. In TIB, C3 grass Arctic also expands more under the NP scenario because warming provides a better environment for this type to grow, where no other competing tree PFTs exist.

NET temperate coverage is not sensitive to changing climates, except in South Asia (SAS) (Figure 4.3 (d)). In regions such as CAN, CAM, SSA, NEU, EAS, and SAU, this temperate tree type maintains its coverage throughout the 21st century. NET temperate forests do not show a strong dependency upon climate scenarios (Figure 4.4 (d)). However, extreme warming under the NP scenario adversely affects NET temperate forest, for example in SAS and CAM. In these regions, NET temperate forest eventually disappears under the NP scenario (blue curve in Figure 4.3 (d)), compared to the 450ppm scenario (red curve in Figure 4.3 (d)). Although the spatial patterns of difference in Figure 4.4 (d) are shown to be similar to each other, an opposite sign of change is indicated in SAS.

Patterns of change in BET temperate forest (Figure 4.3 (e)) indicate a gradual response in the regions located in the northern hemisphere mid-latitudes including CNA, ENA, EAS, and in the regions in the Tropics (CAM, AMZ. SAS and EAF). The responses in SSA, SAF and SAU are more sensitive to changing climate over time and also to the two mitigation scenarios (Figure 4.4 (e)). BDT temperate forest shows slow and gradual expansion in most of its populated regions such as CNA, ENA, and NEU, except for EAS (Figure 4.3 (f)). In EAS, the change is rapid in the early 21st century, almost doubling the initial population by the year 2011, and after that the area is maintained. Dependency upon the climate scenarios is not strong for this type (Figure 4.4 (f)). C3 grass expands eastward in North America (Figure 4.3 (g) and Figure 4.4 (g)). It loses its coverage in WNA, but gain more in CAN. The pattern of change is gradual. In NEU and SEU, C3 grass expands partly because of the decrease in BDT temperate forest in these regions. In CAS and TIB, overall the coverage of C3 grass slowly decreases although some oscillating patterns are found over time. The degree of shrinkage is accelerated under the NP scenario. In Australia (NAU and SAU) and southern South America (SSA), C3 grass is also found to disappear.

In AMZ, BET tropical forest cover rapidly decreases in the early 21st century, being replaced with BDT tropical forest and partly with C4 grass (Figure 4.3 (h)). It slowly recovers its occupied area in AMZ for later years of the century. In other tropical regions such as CAM, WAF, EAF, SAS and SEA, BET tropical forests expand over time, except for SAF that shows a gradual reduction. Rapid increase of BET tropical forest is seen in SAS, and the expansion is accelerated under the NP scenario (see also Figure 4.4 (h)). BDT tropical forest shows a mirror image of the trend seen in BET tropical forest, with an opposite sign in AMZ (Figure 4.3 (i)). The area occupied by this tree type rapidly increases in the early 21st century. The tree cover is maintained at its high coverage (~ 50%) under the 450ppm scenario (red curve in Figure 4.3 (i)), but retreats to the level of year 2011 (~ 40 %) under the NP scenario. Compared to year 2011, BDT tropical forest in year 2100 forms denser forest in the upper west part of the continent of South America, while losing some of its habitat in the southern east part of AMZ (Figure 4.4 (i)). In SAS, BDT tropical is replaced by BET tropical forest (Figure 4.3 (i) and Figure 4.4 (i)). For other tropical regions, including CAM, WAF, EAF and SEA, the coverage by BDT tropical trees is either static or shows a slow reduction.

Responding to changes by BET tropical forest and BDT tropical forest, C4 grasses show complicated time series (oscillations in AMZ, WAF, EAF, and SAF: see Figure 4.3 (j)). In SAS, C4 grass gradually expands; however, for other tropical regions, especially in WAF, the loss of its coverage is notable, and a strong dependency on climate scenarios is also shown (red curve and blue curve in Figure 4.3 (j)) and also see Figure 4.4 (j)).

(a) NET boreal (y-axis scale: 0%~60%)

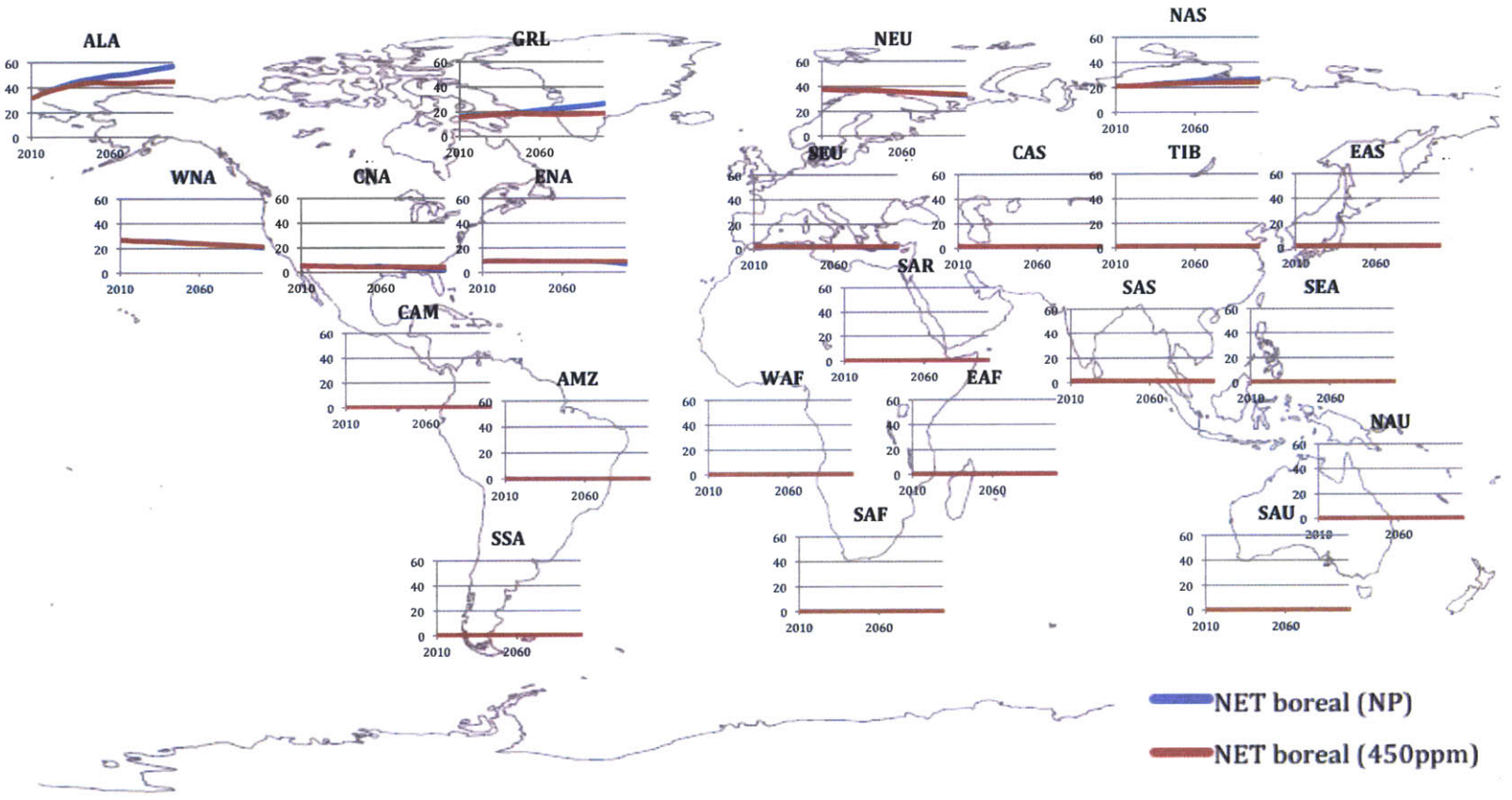

Figure 4.3(a): Aggregated vegetation area change (%) from year 2011 to year 2100 for NET boreal forests in 22 regions. Both the NP scenario (blue) and the 450ppm scenario (red) are illustrated.

(b) BDT boreal (y-axis scale: 0%~15%)

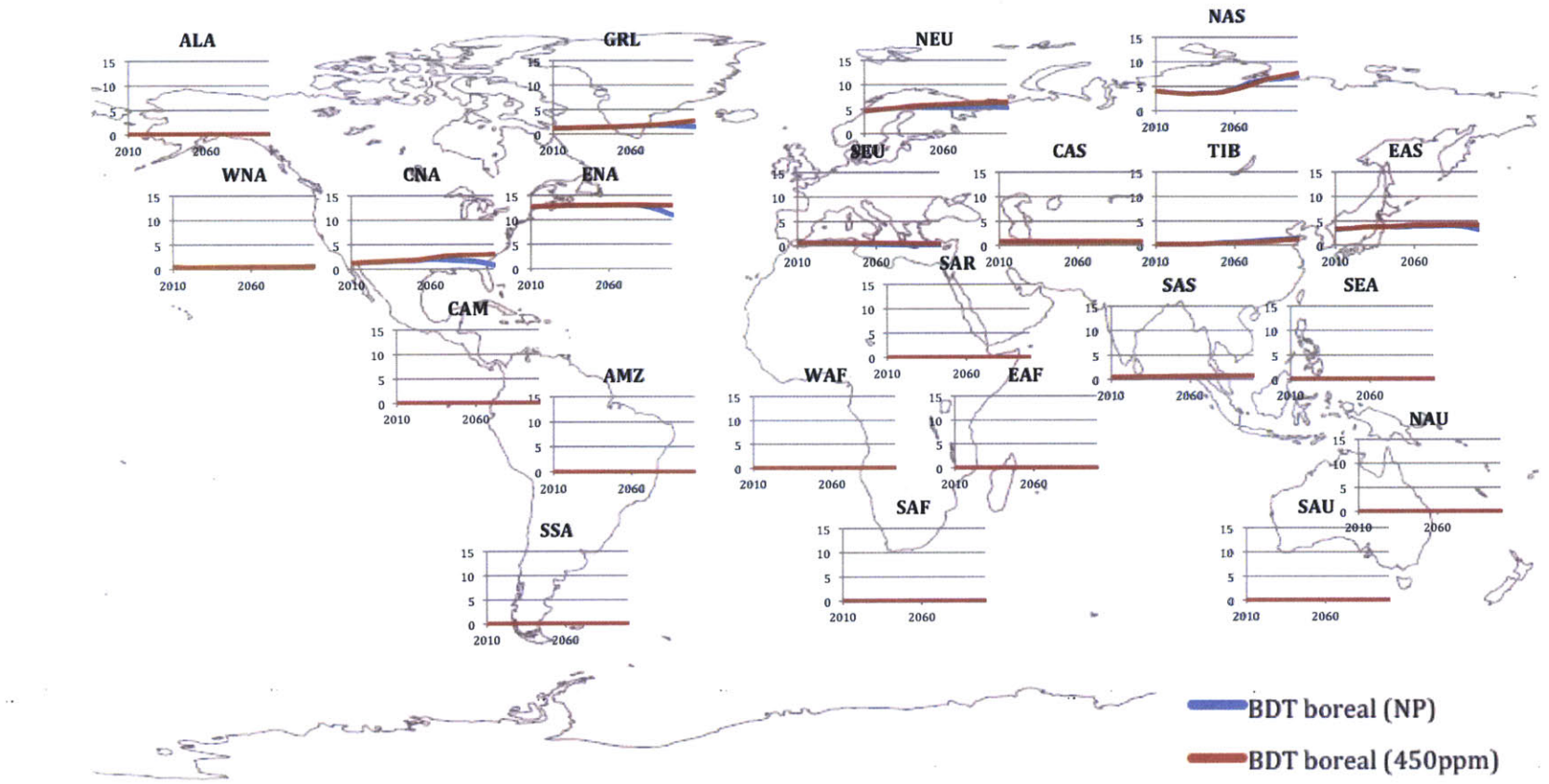

Figure 4.3(b): Aggregated vegetation area change (%) from year 2011 to year 2100 for BDT boreal forests in 22 regions. Both the NP scenario (blue) and the 450ppm scenario (red) are illustrated.

(c) C3 grass Arctic (y-axis scale: 0%~60%)

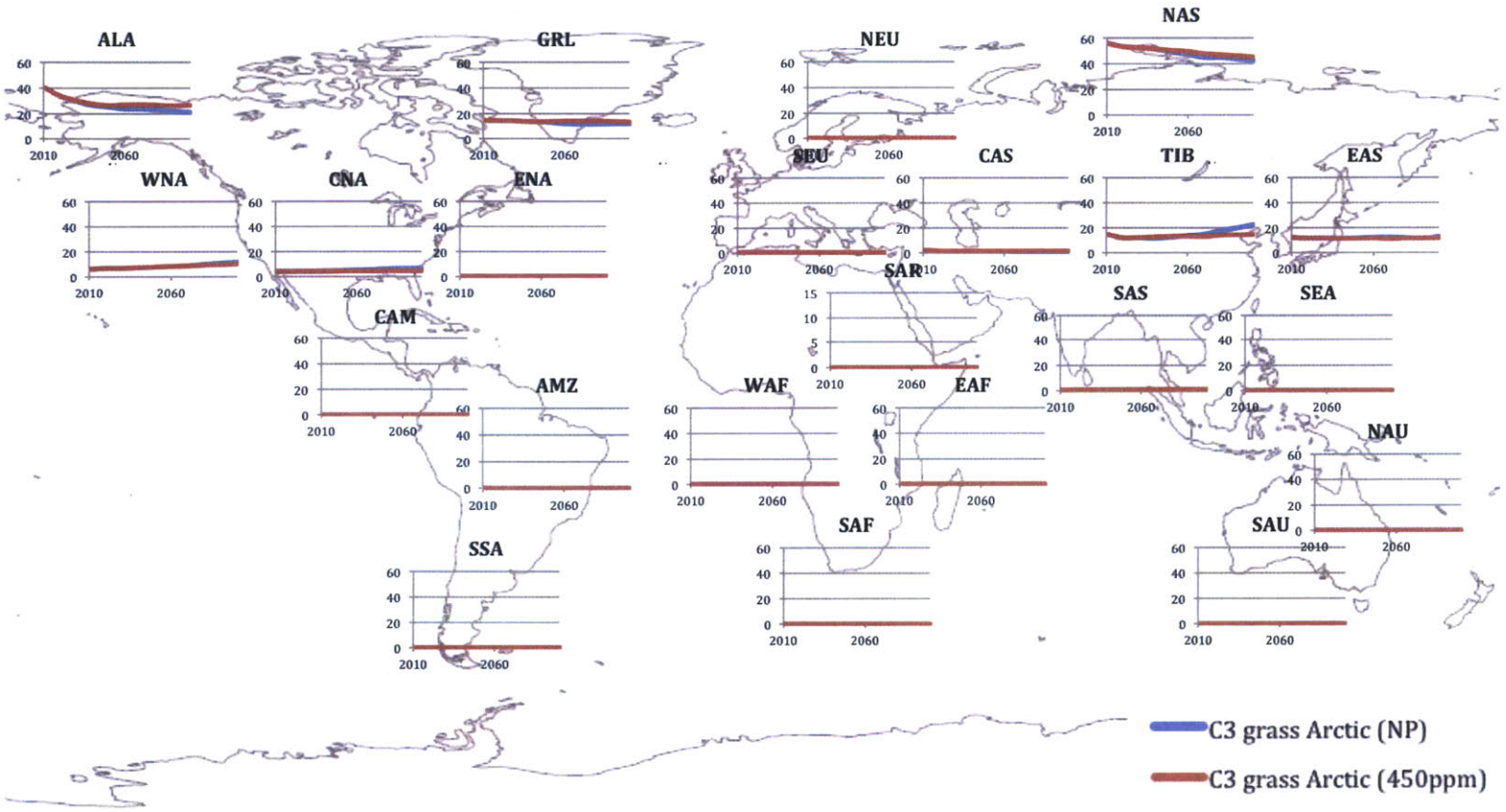

Figure 4.3(c): Aggregated vegetation area change (%) from year 2011 to year 2100 for C3 grass Arctic in 22 regions. Both the NP scenario (blue) and the 450ppm scenario (red) are illustrated.

(d) NET temperate forest (y-axis scale: 0%~30%)

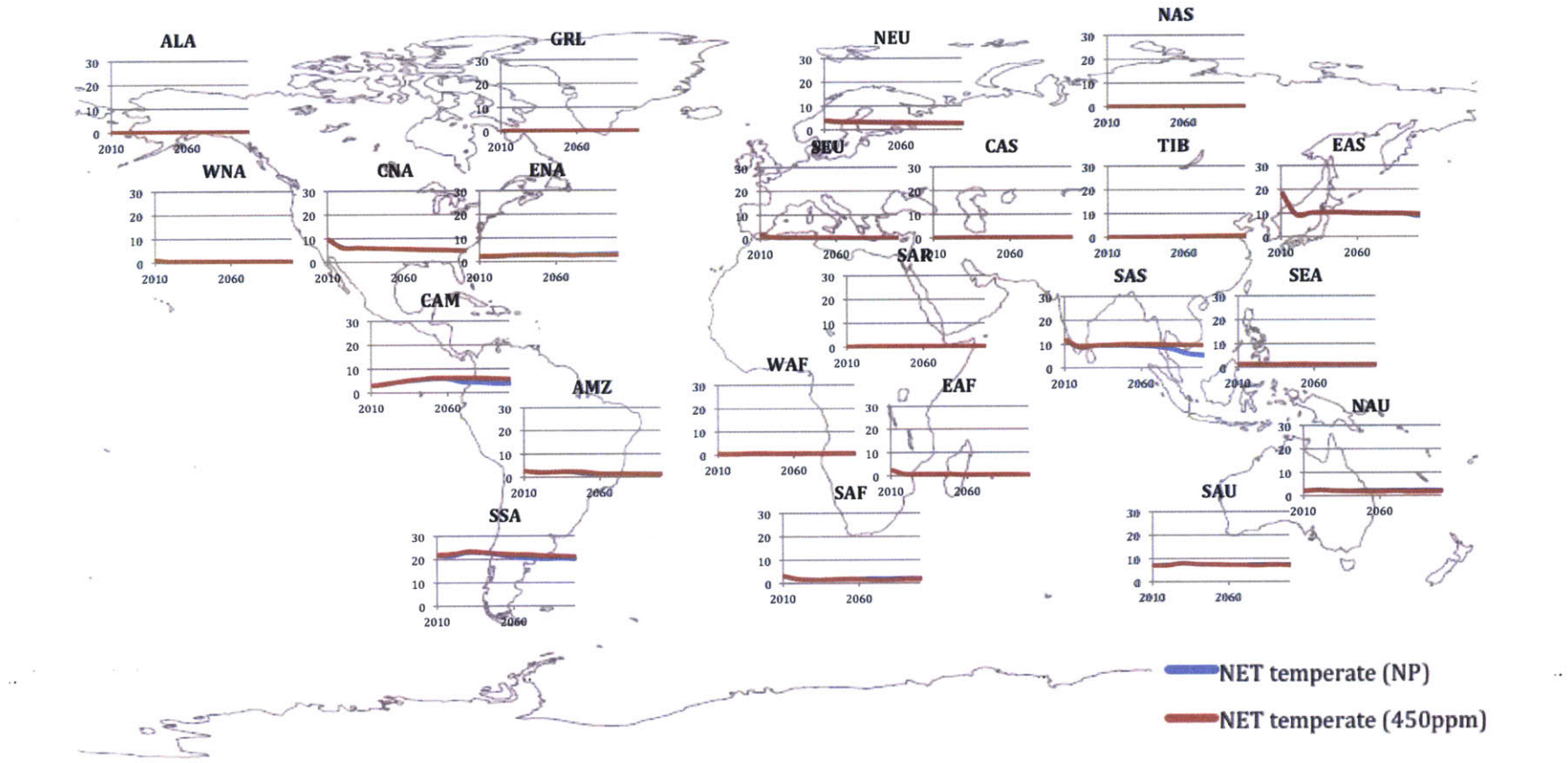

Figure 4.3(d): Aggregated vegetation area change (%) from year 2011 to year 2100 for NET temperate forests in 22 regions. Both the NP scenario (blue) and the 450ppm scenario (red) are illustrated.

(e) BET temperate forest (y-axis scale: 0%~15%)

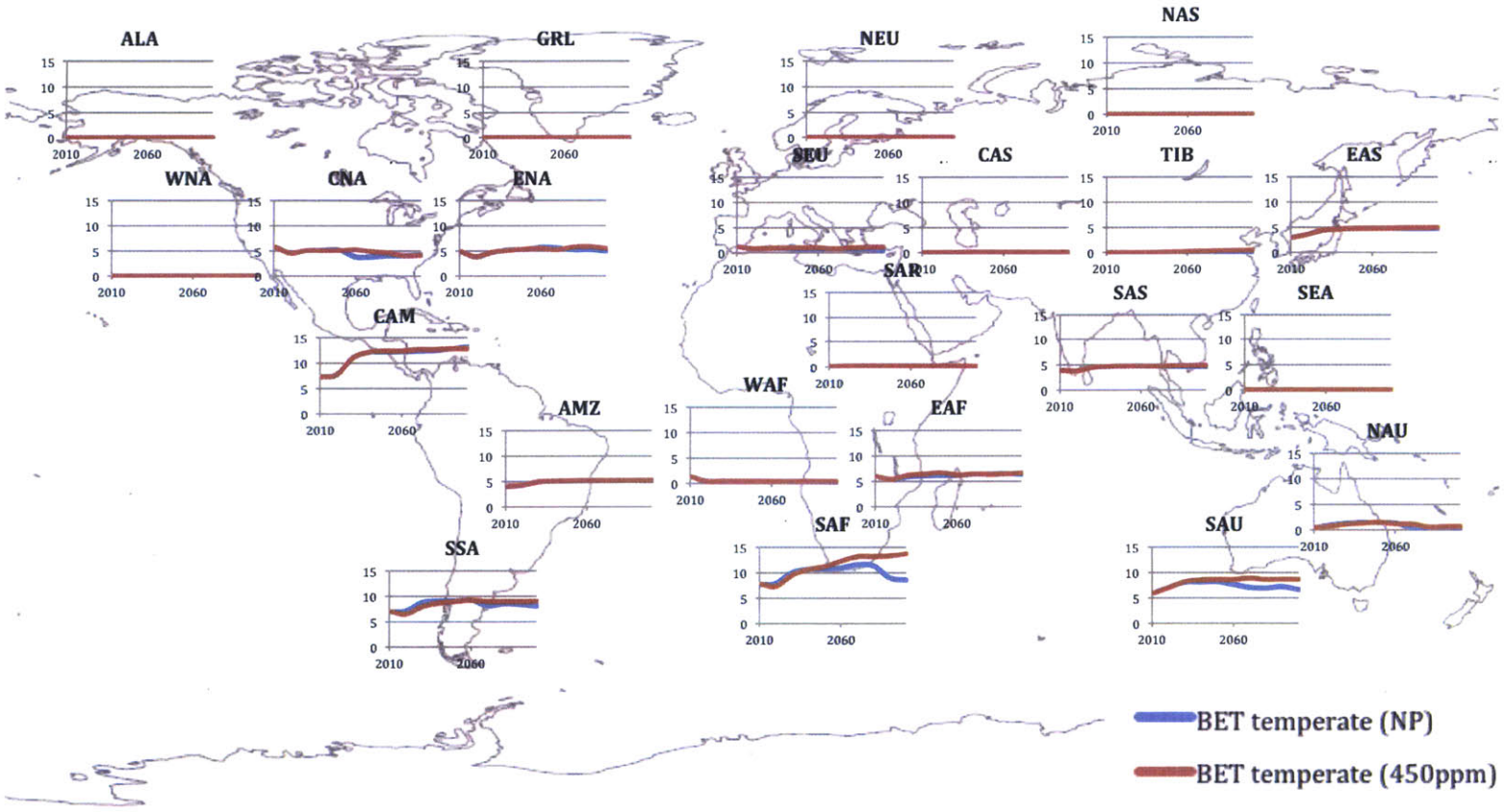

Figure 4.3(e): Aggregated vegetation area change (%) from year 2011 to year 2100 for BET temperate forests in 22 regions. Both the NP scenario (blue) and the 450ppm scenario (red) are illustrated.

(f) BDT temperate forest (y-axis scale: 0%~40%)

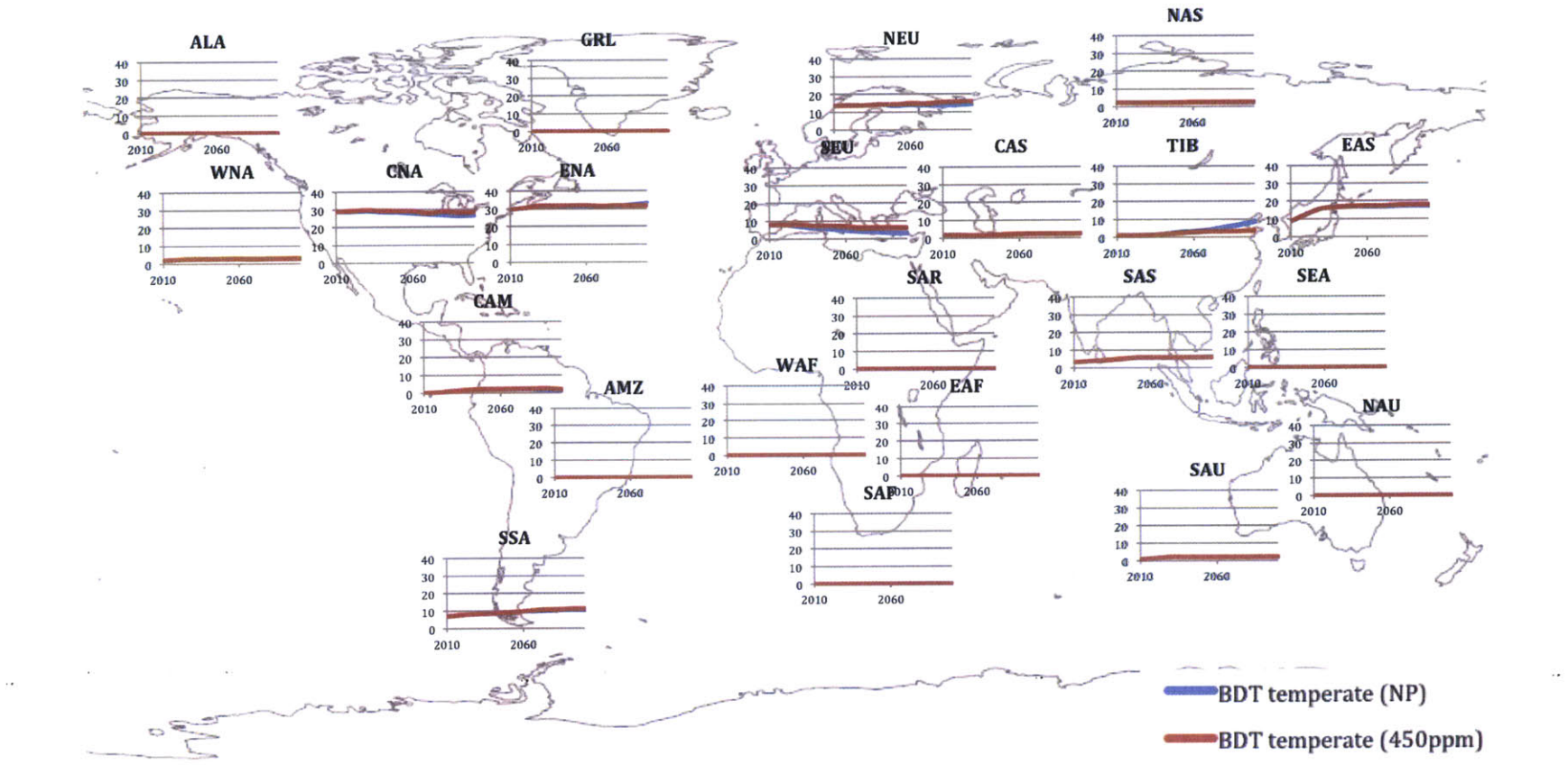

Figure 4.3(f): Aggregated vegetation area change (%) from year 2011 to year 2100 for BDT temperate forests in 22 regions. Both the NP scenario (blue) and the 450ppm scenario (red) are illustrated.

(g) C3 grass (y-axis scale: 0%~60%)

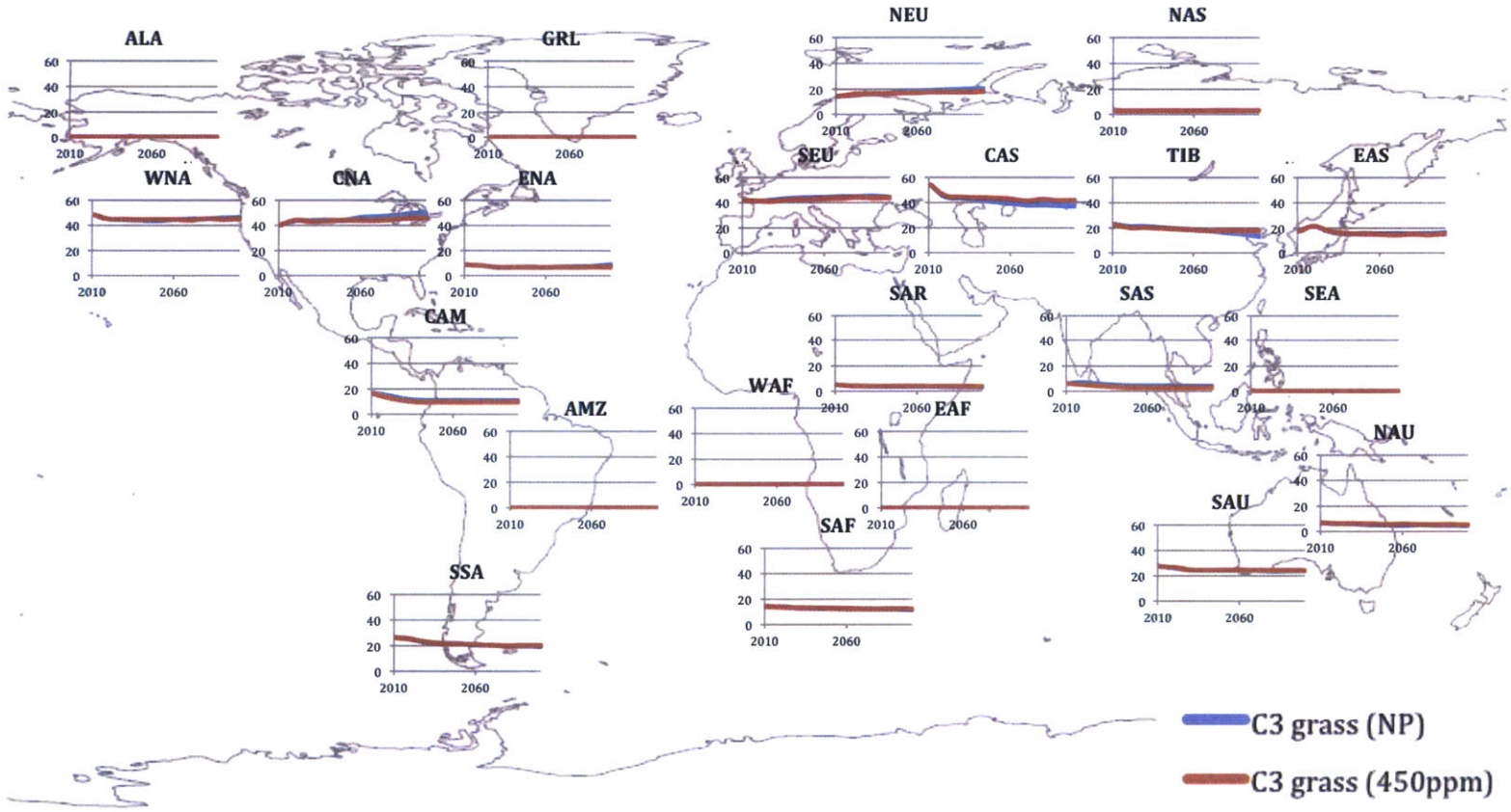

Figure 4.3(g): Aggregated vegetation area change (%) from year 2011 to year 2100 for C3 grass in 22 regions. Both the NP scenario (blue) and the 450ppm scenario (red) are illustrated.

(h) BET tropical forest (y-axis scale: 0%~30%)

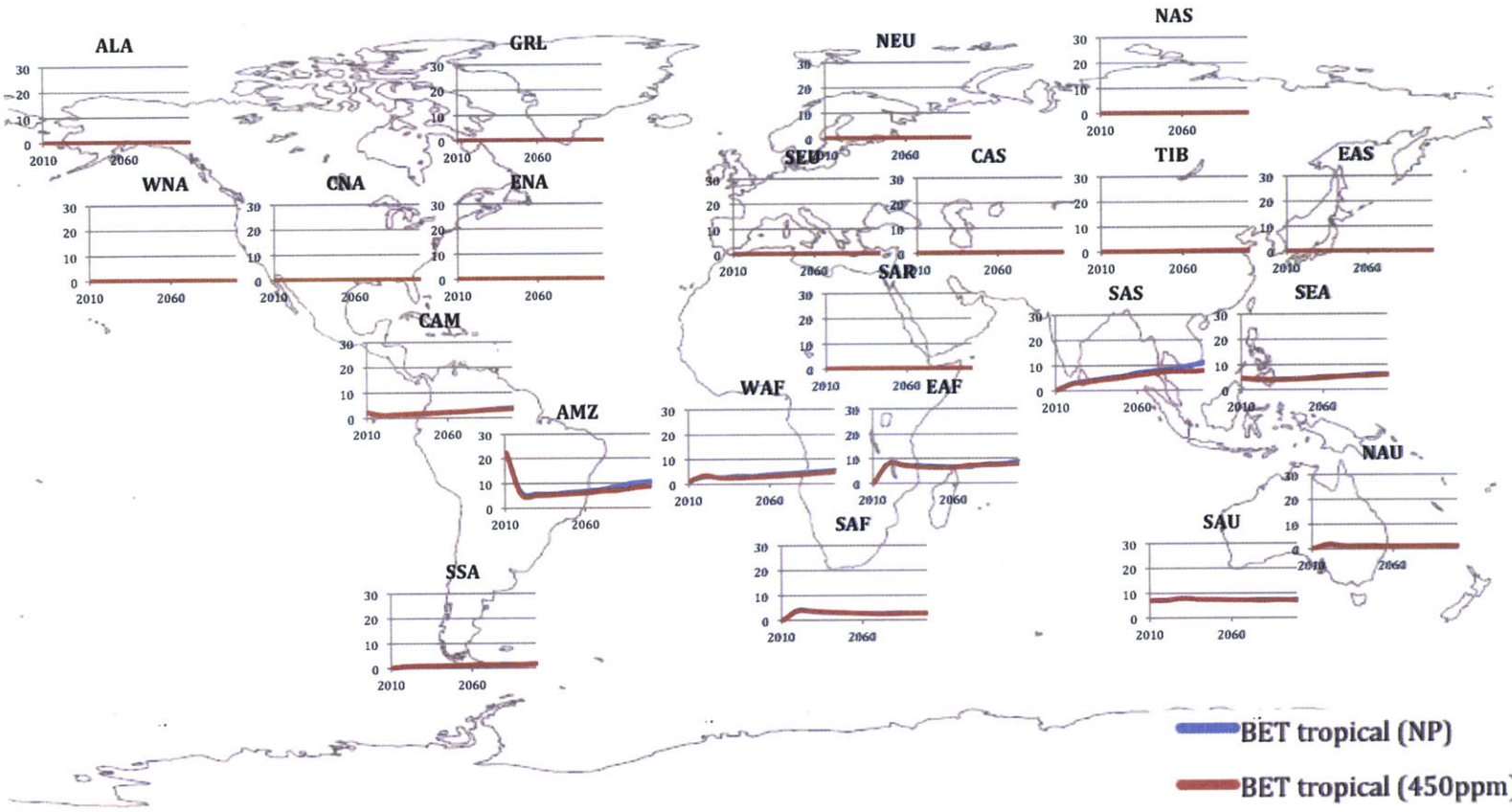

Figure 4.3(h): Aggregated vegetation area change (%) from year 2011 to year 2100 for BET tropical forests in 22 regions. Both the NP scenario (blue) and the 450ppm scenario (red) are illustrated.

(i) BDT tropical forest (y-axis scale: 0%~60%)

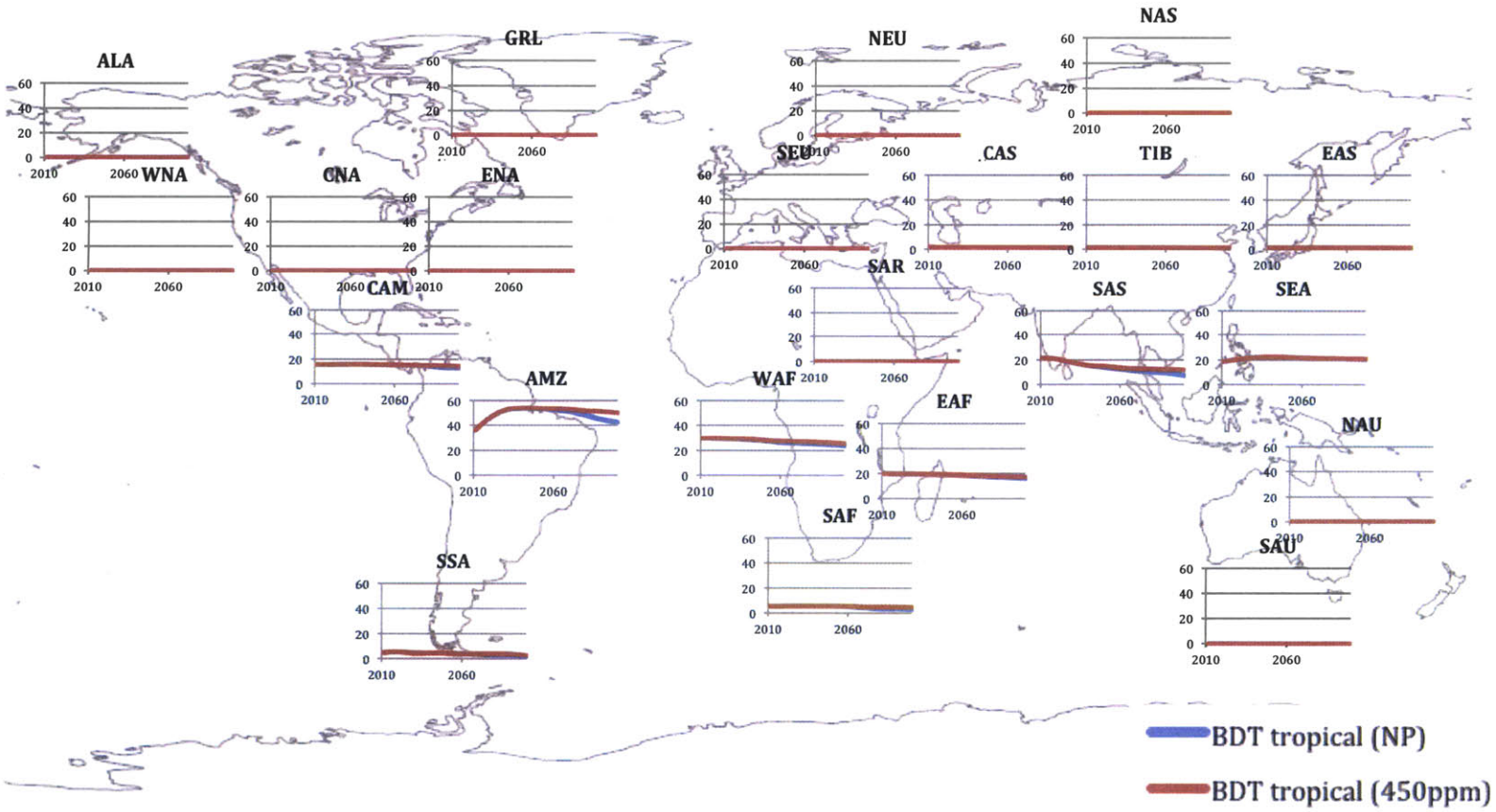

Figure 4.3(i): Aggregated vegetation area change (%) from year 2011 to year 2100 for BDT tropical forests in 22 regions. Both the NP scenario (blue) and the 450ppm scenario (red) are illustrated.

(j) C4 grass (y-axis scale: 0%~30%)

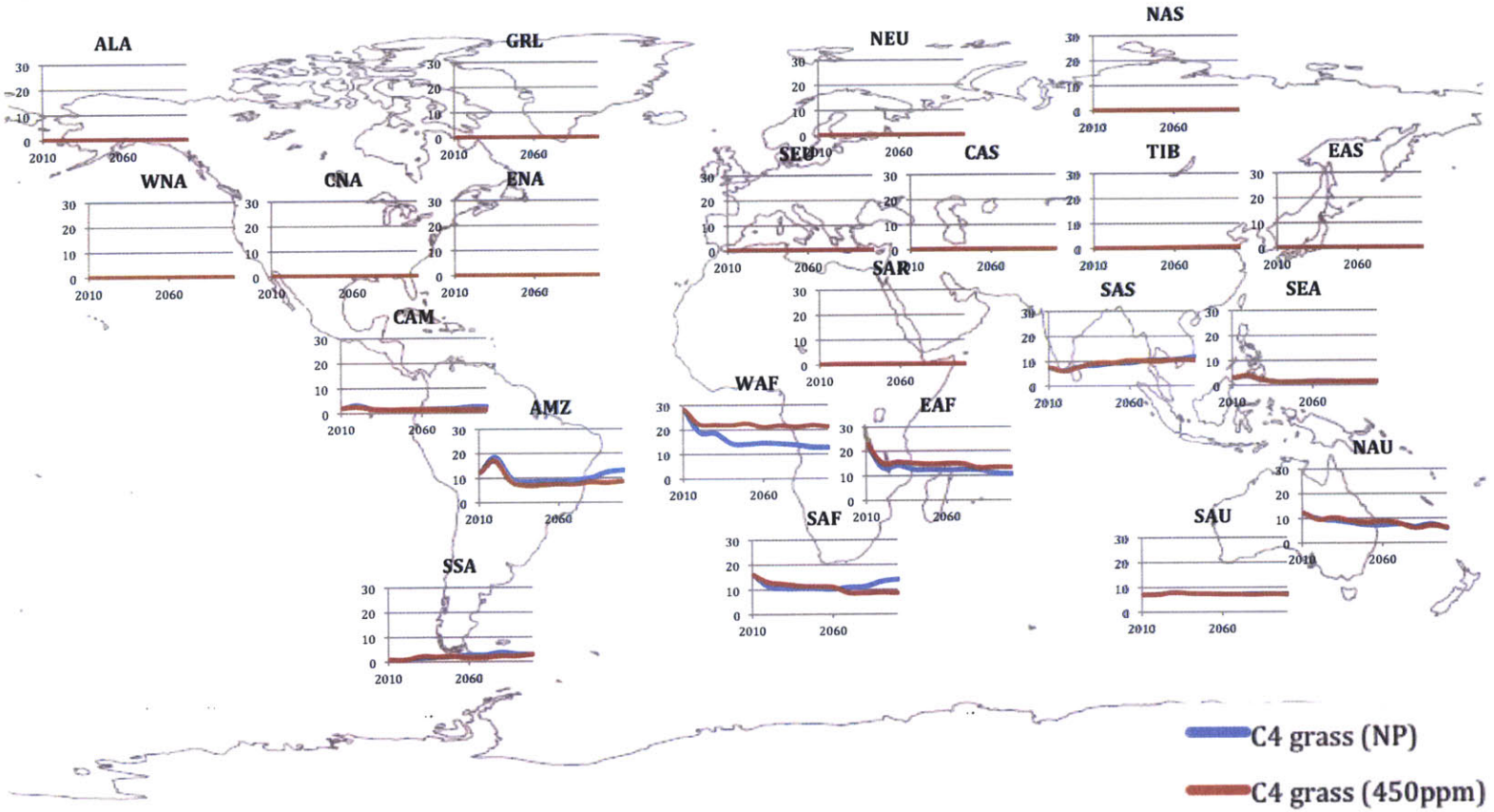

Figure 4.3(j): Aggregated vegetation area change (%) from year 2011 to year 2100 for C4 grass in 22 regions. Both the NP scenario (blue) and the 450ppm scenario (red) are illustrated.

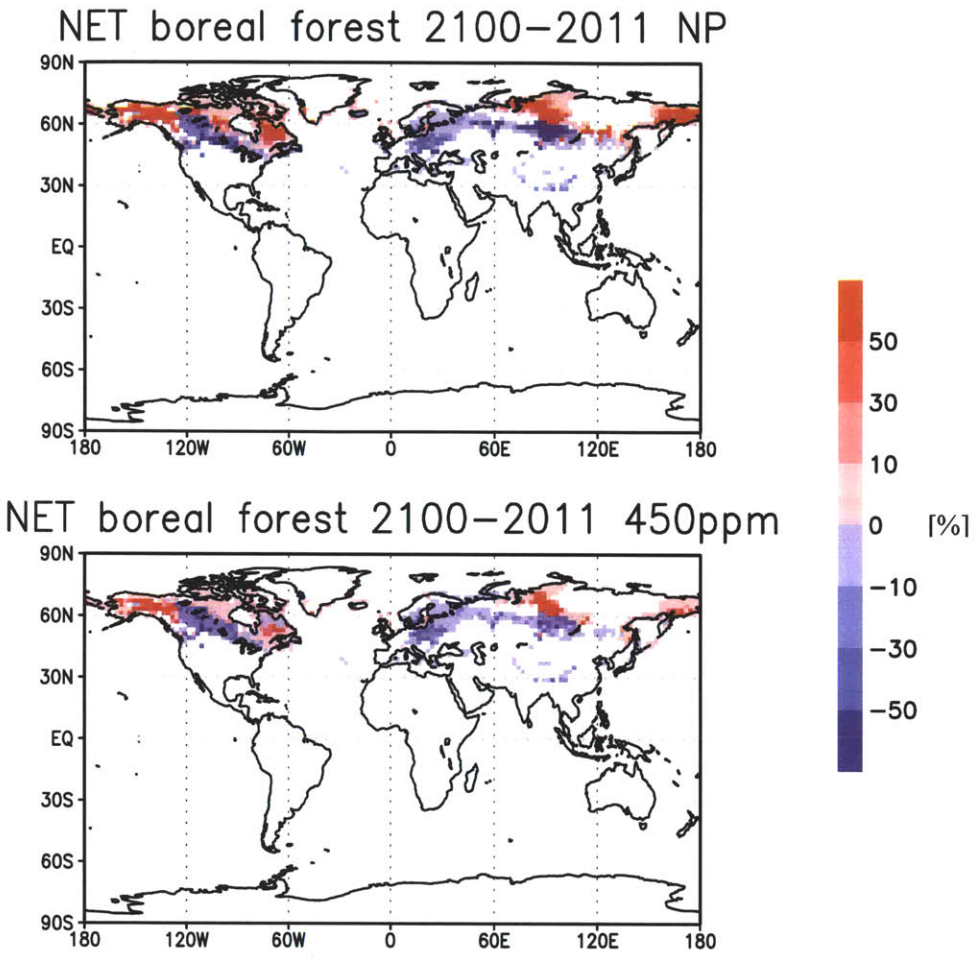

Figure 4.4 (a): Change in NET boreal forest (%) in the 21st century (coverage in 2100 minus coverage in 2011) under the NP scenario (upper panel) and the 450ppm scenario (lower panel). Blue indicates a decrease and red indicates an increase from 2011 to 2100.

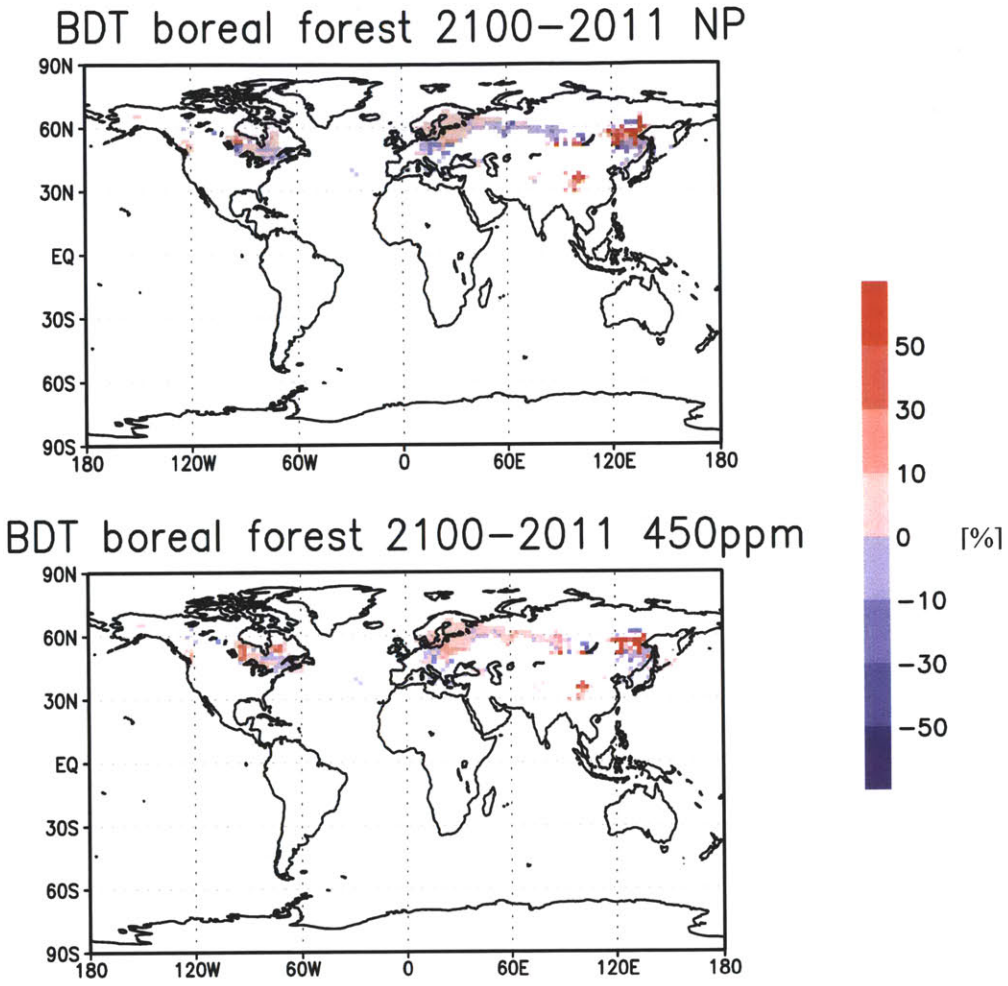

Figure 4.4 (b): Change in BDT boreal forest (%) in the 21st century (coverage in 2100 minus coverage in 2011) under the NP scenario (upper panel) and the 450ppm scenario (lower panel). Blue indicates a decrease and red indicates an increase from 2011 to 2100.

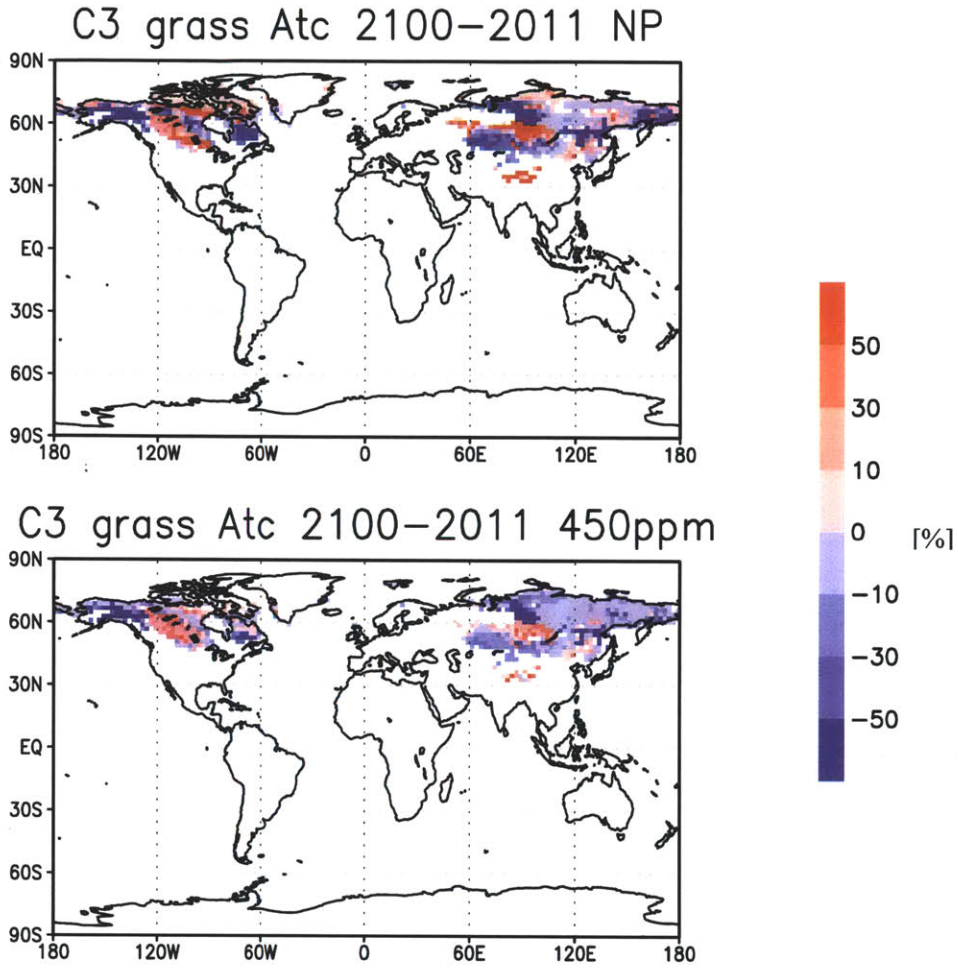

Figure 4.4 (c): Change in C3 grass Arctic (%) in the 21st century (coverage in 2100 minus coverage in 2011) under the NP scenario (upper panel) and the 450ppm scenario (lower panel). Blue indicates a decrease and red indicates an increase from 2011 to 2100.

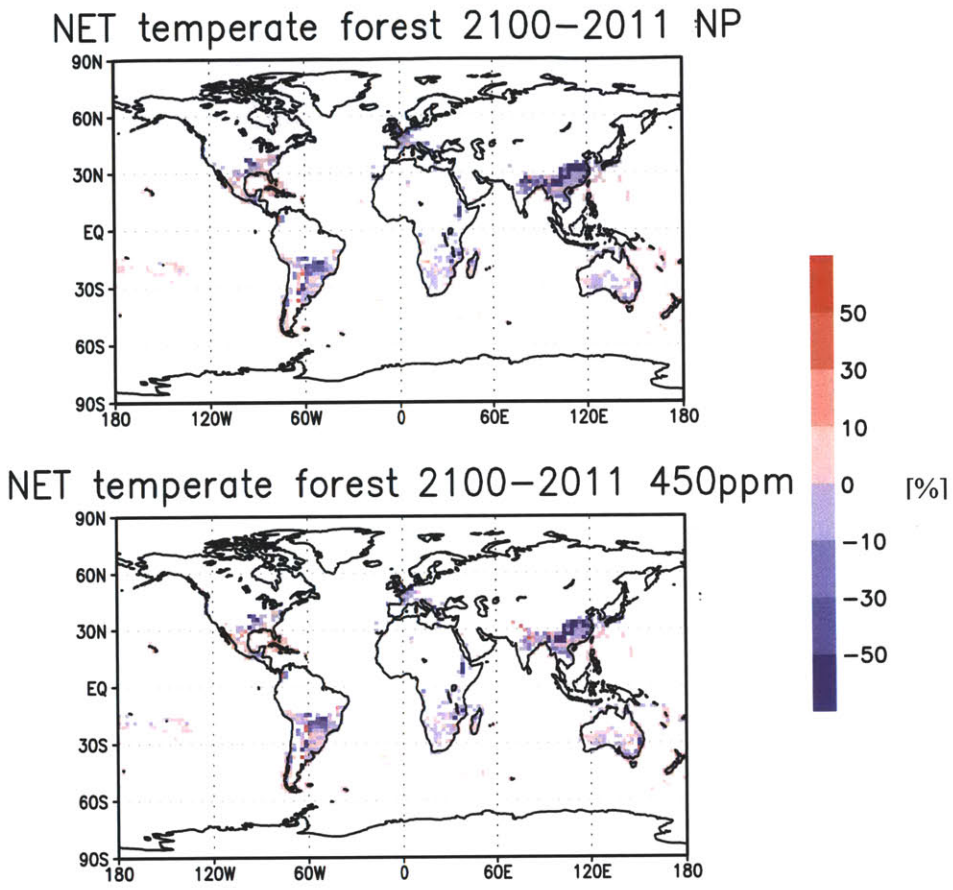

Figure 4.4 (d): Change in NET temperate forest (%) in the 21st century (coverage in 2100 minus coverage in 2011) under the NP scenario (upper panel) and the 450ppm scenario (lower panel). Blue indicates a decrease and red indicates an increase from 2011 to 2100.

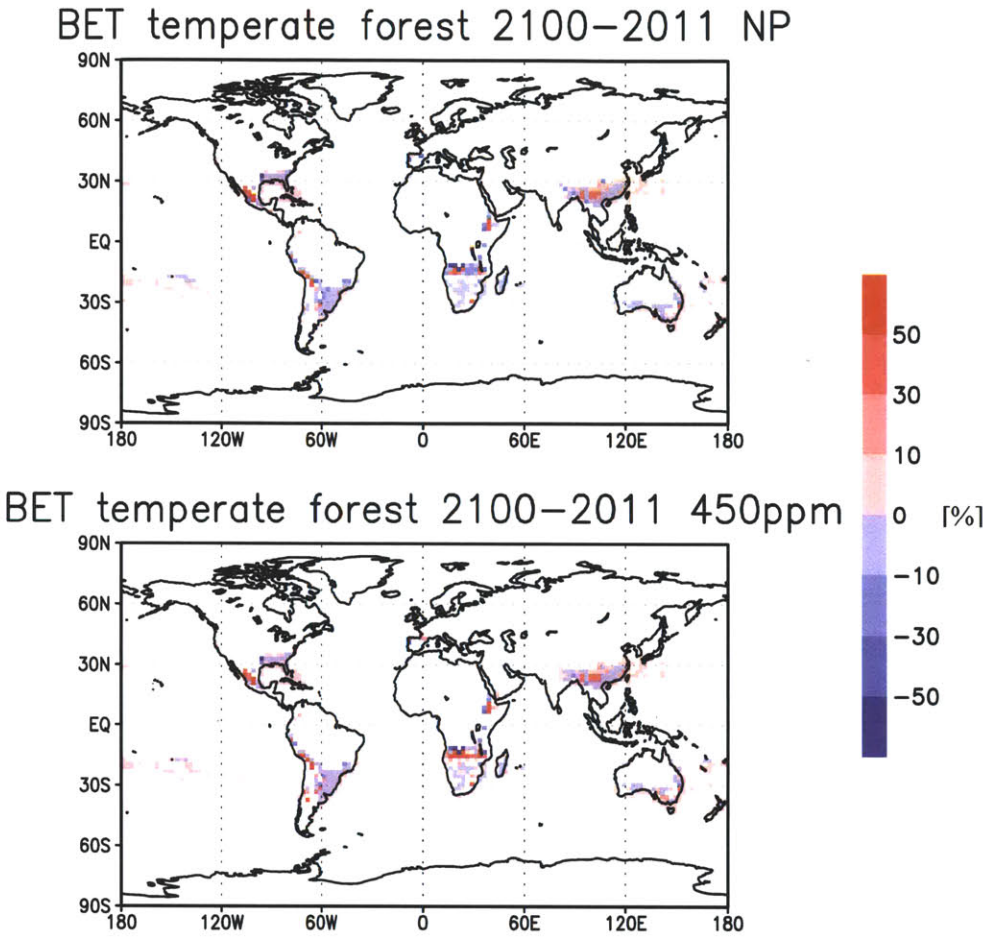

Figure 4.4 (e): Change in BET temperate forest (%) in the 21st century (coverage in 2100 minus coverage in 2011) under the NP scenario (upper panel) and the 450ppm scenario (lower panel). Blue indicates a decrease and red indicates an increase from 2011 to 2100.

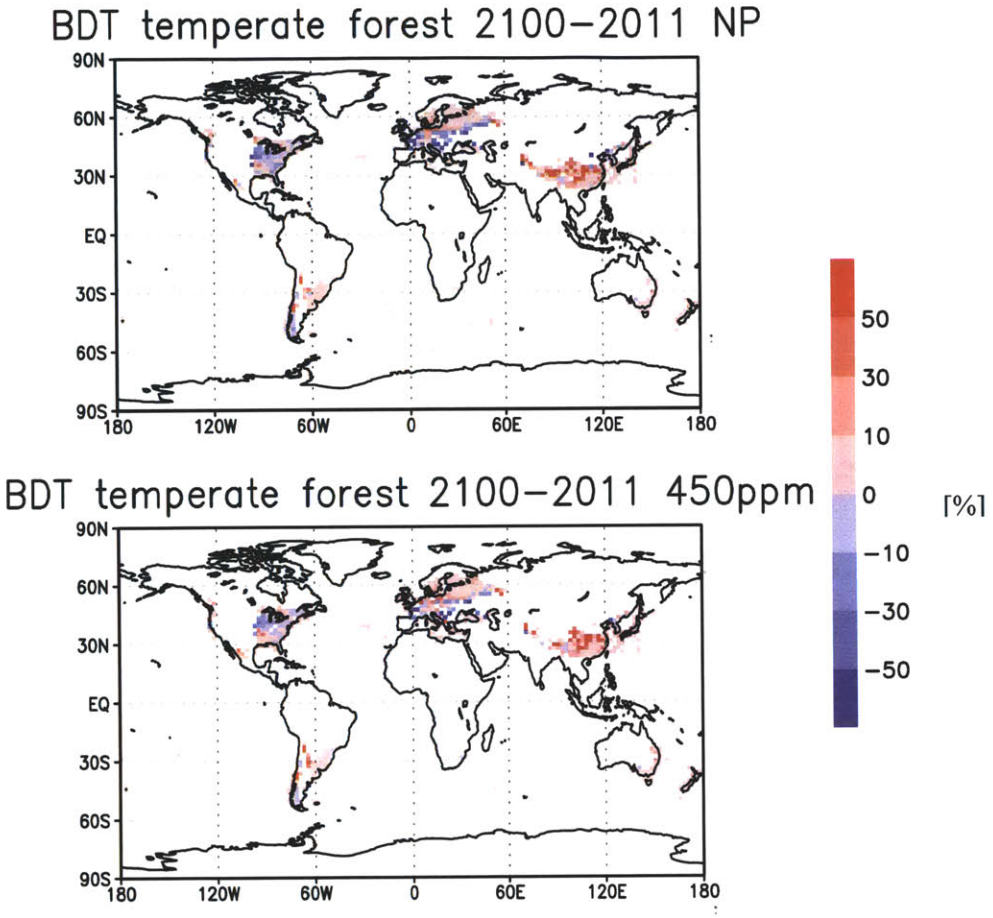

Figure 4.4 (f): Change in BDT temperate forest (%) in the 21st century (coverage in 2100 minus coverage in 2011) under the NP scenario (upper panel) and the 450ppm scenario (lower panel). Blue indicates a decrease and red indicates an increase from 2011 to 2100.

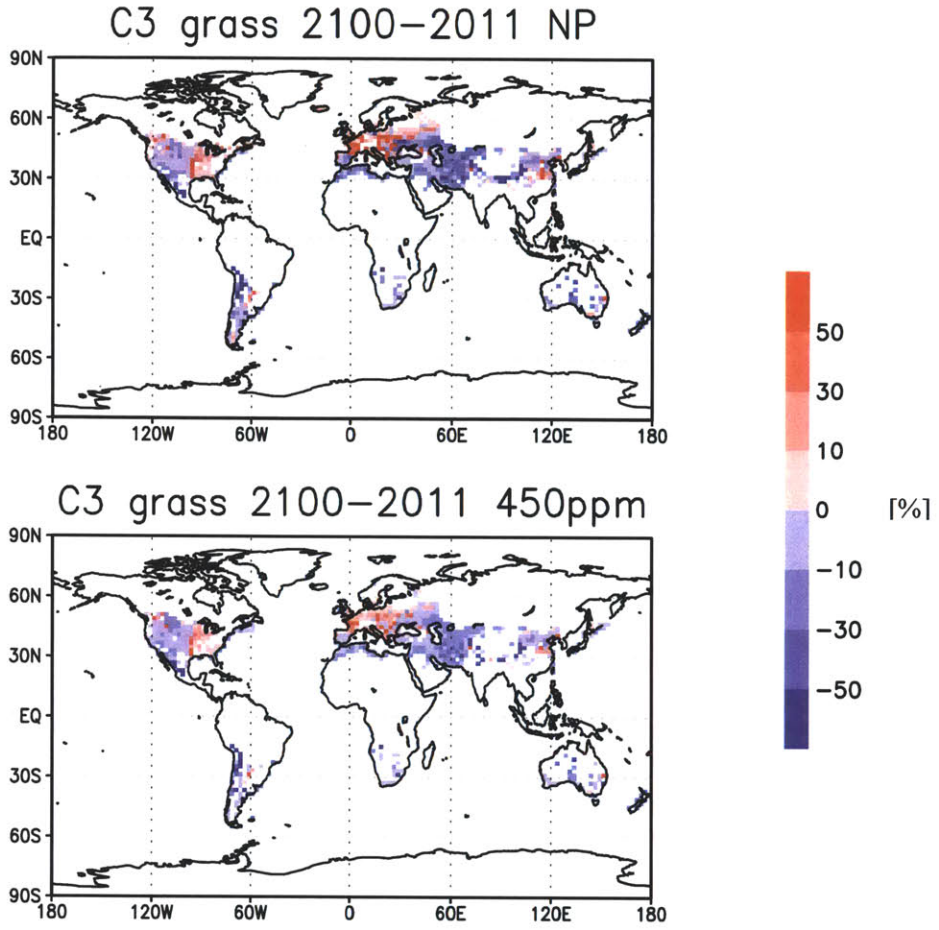

Figure 4.4 (g): Change in C3 grass (%) in the 21st century (coverage in 2100 minus coverage in 2011) under the NP scenario (upper panel) and the 450ppm scenario (lower panel). Blue indicates a decrease and red indicates an increase from 2011 to 2100.

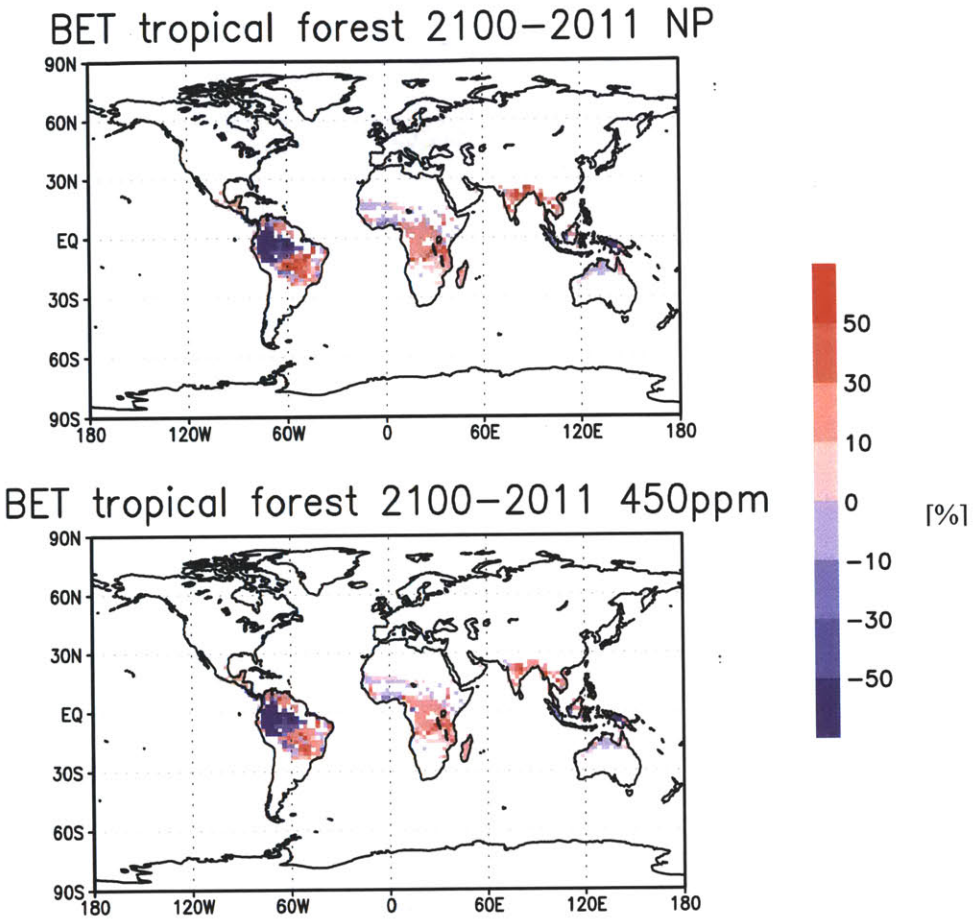

Figure 4.4 (h): Change in BET tropical forest (%) in the 21st century (coverage in 2100 minus coverage in 2011) under the NP scenario (upper panel) and the 450ppm scenario (lower panel). Blue indicates a decrease and red indicates an increase from 2011 to 2100.

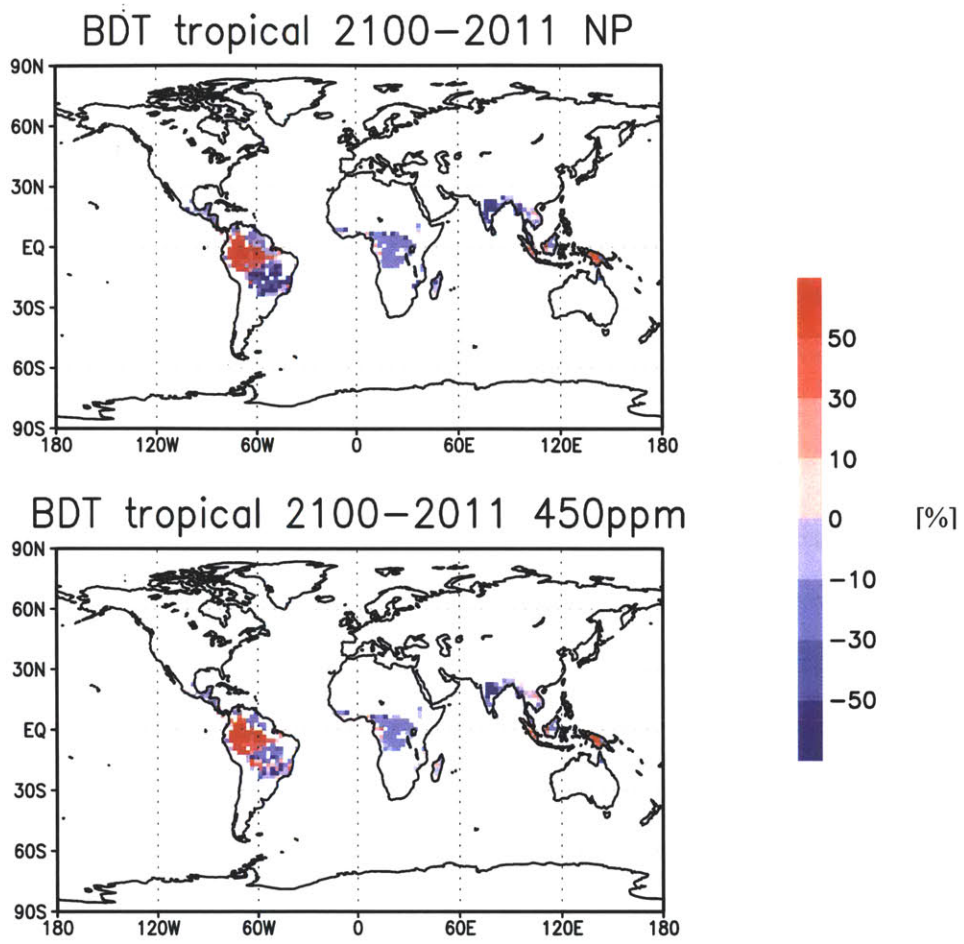

Figure 4.4 (i): Change in BDT tropical forest (%) in the 21st century (coverage in 2100 minus coverage in 2011) under the NP scenario (upper panel) and the 450ppm scenario (lower panel). Blue indicates a decrease and red indicates an increase from 2011 to 2100.

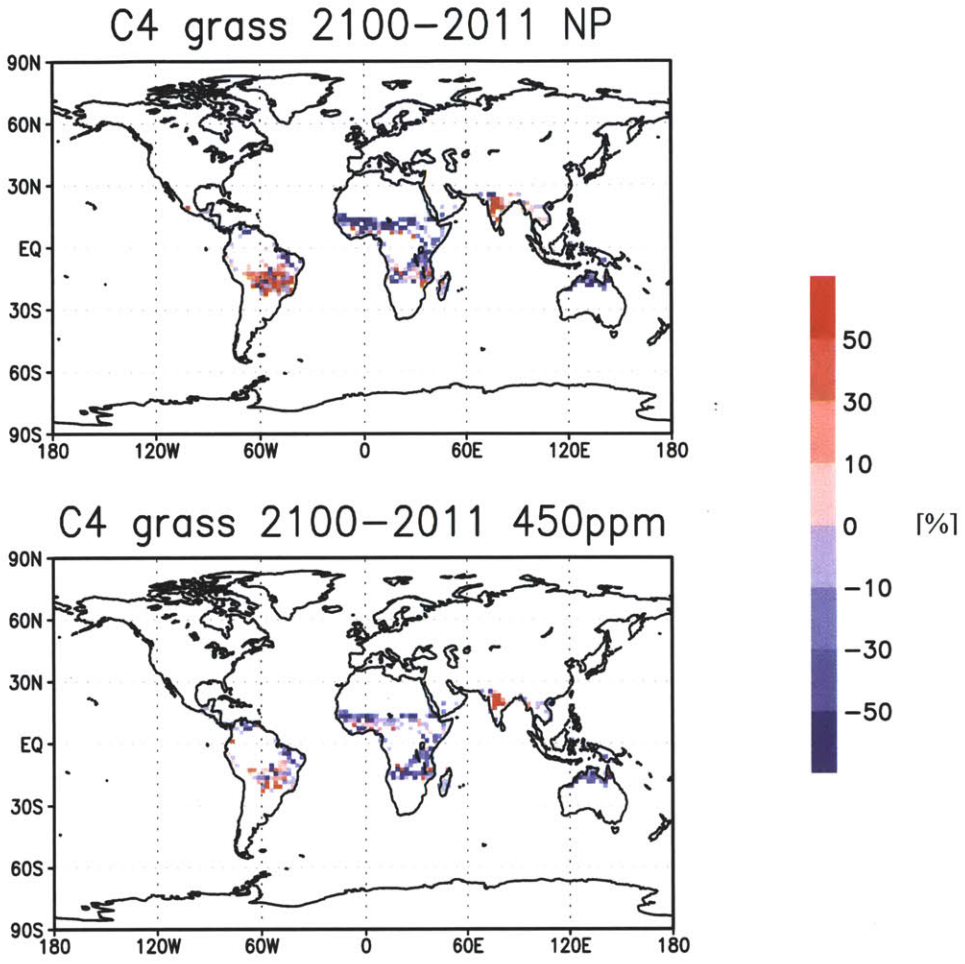

Figure 4.4 (j): Changes in C4 grass (%) in the 21st century (coverage in 2100 minus coverage in 2011) under the NP scenario (upper panel) and the 450ppm scenario (lower panel). Blue indicates a decrease and red indicates an increase from 2011 to 2100.

4.3.3 Assessing vulnerability according to future vegetation structure in the 21st century

As the results of the regional analysis of future vegetation structure indicate in the previous section, some regions are expected to experience a great degree of change. Vulnerability is defined as "the degree to which a system is susceptible to, and unable to cope with, adverse effects of climate change (IPCC, 2007, in Appendix I: Glossary). Recently, Chaturvedi et al. (2011) suggested a vulnerability index for analysis of impacts of climate change on forestry ecosystems in India. From 1 to 7, they assigned a vulnerability index for forest grids in India, based upon forest diversity, forest crown density, and vegetation type change. By adopting their vulnerability index, a modified but more comprehensive description of vulnerability is suggested in this study for assessment of the chosen 22 regions in the global land.

Vulnerability can be expressed as a function of the structural characteristics of the system, the magnitude of change, and the rate of change and adaptive capacity (IPCC, 2007, in Appendix I: Glossary). Therefore, as a simple but useful tool to assess vulnerability of a region, a vulnerability index is proposed according to the degree of vegetation structure change. This suggested vulnerability index considers three categories as follows: characteristic of forests at the starting year (2011), magnitude of change from 2011 to 2100, and forest density (see Table 4.6).

First, the characteristic of the forest in the starting year (2011) is considered. If the forest is a monoculture (i.e., only one PFT type exists), the region is very likely to be vulnerable, because one-type of vegetation structure is highly susceptible to climate change. Therefore, a higher number for vulnerability index is assigned (12,11 or 10), depending upon the forest area density (low is less than 20%, medium is from 20% to 40%, and high is over 40%) of the selected region.

For regions that have mixed-culture vegetation structures, lower numbers (1 through 9) are assigned. The magnitude of change is then applied to further determine the level of vulnerability. From 2011 to 2100, if the shift of dominant PFT occurs (e.g., C3 grass Arctic dominating for year 2011 but NET boreal forest dominating for year 2100), the region falls into the category of a significant vegetation structure change. Depending upon the forest area density (low, medium or high), a number between 7~9 is assigned, representing the vulnerability for a region experiencing shift of major PFT.

For the regions maintaining their dominant PFT throughout the 21st century, they are less likely to be susceptible to climate change. However, if the change in occupied area by the dominant PFT is large (over 50%) so that either substantial expansion or reduction of forest coverage is possible, then it is considered to be sensitive to climate change and its adaptive capacity is small. For this case, a number of 4, 5 or 6 is assigned,

also based upon the area density of the forest. If the change in occupied area is minor (less than 50%), the region is considered as one of the least vulnerable so that the regions are assigned the lower numbers (1,2 or 3).

The method is summarized in Table 4.6 in which the 22 regions are given a number from 1 through 12, which represents the level of vulnerability.

Table 4.6: Vulnerability Index (originally suggested in Table 4 of Chaturvedi et al. (2011) for regions in India and modified for purposes of this study)

Forest diversity at year 2011	Change in dominant PFT type from 2011 to 2100	Level of change	Forest density at year 2011	Vulnerability Index
Yes	N/A	N/A	Low (<20%)	12
Yes	N/A	N/A	Medium (20%~40%)	11
Yes	N/A	N/A	High (>40%)	10
No	Yes	N/A	Low (<20%)	9
No	Yes	N/A	Medium (20%~40%)	8
No	Yes	N/A	High (>40%)	7
No	No	Major (>50%)	Low (<20%)	6
No	No	Major (>50%)	Medium (20%~40%)	5
No	No	Major (>50%)	High (>40%)	4
No	No	Minor (<50%)	Low (<20%)	3
No	No	Minor (<50%)	Medium (20%~40%)	2
No	No	Minor (<50%)	High (>40%)	1

Applying the Table 4.6 recipe in the NP scenario, seven regions that include ALA, CAM, SSA, EAF, TIB, EAS, and SAS are likely to be highly vulnerable to climate change in the 21st century (Table 4.7), while the 450ppm scenario, six regions including ALA, CAM, SSA, EAF, SAF, and EAS are expected to be vulnerable to the climate change (Table 4.8).

If the 450ppm scenario is implemented, vulnerability will be much alleviated in the four regions GRL (from 6 to 3), TIB (from 9 to 3), SAS (from 7 to 1), and NAU (from 6 to 3) (see Table 4.9). Two regions (NEU and SAF) are reported to increase their vulnerability under the 450ppm scenario compared to the NP scenario; however SAF is a real concern, increasing from 3 to 9, but the expected change for NEU is negligible because NEU is still highly stable either under the NP scenario (index is 1) or under the 450ppm scenario (index is 2).

Table 4.7: Assessment of vulnerability for the 22 regions in the NP scenario

Region	Monoculture	Change in Dominant PFT	Change in %	Forest density	Vulnerability index
ALA	No	Yes	N/A	32.0	8
GRL	No	No	61.6	17.6	6
WNA	No	No	-4.6	30.6	2
CNA	No	No	22.8	51.1	1
ENA	No	No	10.4	58.7	1
CAM	No	Yes	N/A	27.8	8
AMZ	No	No	17.5	65.0	1
SSA	No	Yes	N/A	40.9	7
NEU	No	No	-13.8	59.8	1
SEU	No	No	5.7	13.3	3
SAR	No	No	-35.2	0.1	3
WAF	No	No	-19.9	32.7	2
EAF	No	Yes	N/A	28.1	8
SAF	No	No	-10.8	15.8	3
NAS	No	No	-23.2	27.7	2
CAS	No	No	-30.9	4.4	3
TIB	No	Yes	N/A	3.0	9
EAS	No	Yes	N/A	34.6	8
SAS	No	Yes	N/A	42.4	7
SEA	No	No	9.7	24.6	2
NAU	No	No	-51.1	3.1	6
SAU	No	No	-12.2	14.0	3

Table 4.8: Assessment of vulnerability for the 22 regions in the 450ppm scenario

Region	Monoculture	Change in Dominant PFT	Change in %	Forest density	Vulnerability index
ALA	No	Yes	N/A	32.0	8
GRL	No	No	15.2	17.6	3
WNA	No	No	-6.0	30.6	2
CNA	No	No	13.6	51.1	1
ENA	No	No	6.7	58.7	1
CAM	No	Yes	N/A	27.8	8
AMZ	No	No	38.8	65.0	1
SSA	No	Yes	N/A	40.9	7
NEU	No	No	-11.7	59.8	2
SEU	No	No	5.0	13.3	3
SAR	No	No	-23.2	0.1	3
WAF	No	No	-14.1	32.7	2
EAF	No	Yes	N/A	28.1	8
SAF	No	Yes	N/A	15.8	9
NAS	No	No	-18.4	27.7	2
CAS	No	No	-22.4	4.4	3
TIB	No	No	-21.7	3.0	3
EAS	No	Yes	N/A	34.6	8
SAS	No	No	-43.7	42.4	1
SEA	No	No	11.9	24.6	2
NAU	No	No	-47.9	3.1	3
SAU	No	No	-11.4	14.0	3

Table 4.9: Comparison of the vulnerability index for the NP scenario and the 450ppm scenario.

Region	NP scenario	450ppm scenario	
ALA	8	8	
GRL	6	3	Less vulnerable under the 450ppm
WNA	2	2	
CNA	1	1	
ENA	1	1	
CAM	8	8	
AMZ	1	1	
SSA	7	7	
NEU	1	2	More vulnerable under the 450ppm
SEU	3	3	
SAR	3	3	
WAF	2	2	
EAF	8	8	
SAF	3	9	More vulnerable under the 450ppm
NAS	2	2	
CAS	3	3	
TIB	9	3	Less vulnerable under the 450ppm
EAS	8	8	
SAS	7	1	Less vulnerable under the 450ppm
SEA	2	2	
NAU	6	3	Less vulnerable under the 450ppm
SAU	3	3	

4.4 Discussion

The change in future vegetation patterns derived in this study generally agrees with results from previous studies (Lucht et al., 2006; Schaphoff et al., 2006), including a northward shift of boreal forests, disappearing C3 grass Arctic in northern Eurasia, and expansion of deciduous temperate trees in southern Africa.

In addition, the modeled vegetation structures using the SEED configuration are compared to the structures simulated using the FREE configuration that are forced by the same IGSM climate forcing (2011-2100) of the NP scenario (see section 4.2) and the same calibration (see Table 4.2) but using the FREE configuration. The two sets of vegetation distribution maps show that the SEED and the FREE configurations provide regionally distinct estimates of future PFT distributions, especially in the high latitudes. In Figure 4.5, for example, more NET boreal forests using the SEED configuration are expected in North America (10%~15%, compared to the FREE configuration), but less of this type are expected in central Siberia (i.e., < -15%, compared to the FREE configuration) in 2100. These patterns of regional differences are similar to the difference patterns using the contemporary climates (see Chapter 3 for more details), thus reaffirming that the two mechanisms that are applied to the SEED configuration modify regional vegetation structures by altering the competition dynamics either by simply suppressing the growth of a tree PFT by prevailing winds (e.g., central Siberia) or by boosting growth of a tree PFT by filtering out unrealistic saplings (e.g., North America). Changes in NET boreal forests are mostly at the expense of C3 grass Arctic, and a few regions are at the expense of BDT boreal forests (e.g., central Canada). More information of the difference maps can be found in Appendix II.

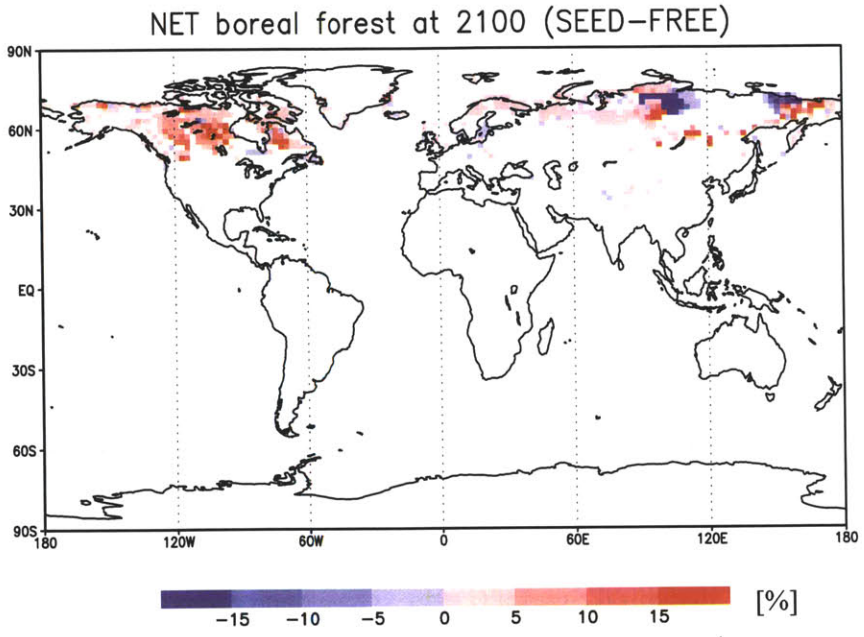

Figure 4.5: Difference in occupied areas (%) by NET boreal forest computed as the SEED configuration map minus the FREE configuration map in 2100. The areas in the red color scales illustrate more NET boreal forests from the SEED configuration, and the areas in the blue color scales show less NET boreal forests from the SEED configuration.

As the SEED and FREE configurations simulate natural vegetation dynamics each year, they provide distributions of plants in the future that would result from natural plant migration in the absence of any direct human interference (such as land use). Note that both model structures do not explicitly account for changes in mortality rates that would result from disease and/or insect infestations (although the prescribed mortality rates themselves do, in principle, reflect these sorts of processes in a static sense). Therefore, one should interpret these model results with these conditions in mind. Granted the limitations and characteristics of these models, the vegetation structure analysis can serve as an approximate indicator to assess the vulnerability of forestry and plant biogeography for policy-makers.

4.5 Summary and conclusion of Chapter 4

Under two climate mitigation scenarios for the 21st century, regions in the high latitudes are expected to experience greater changes in their composition of plant types, characterized by expansion of NET boreal forests and shrinkage of C3 grass Arctic. Regions such as Alaska and Siberia are expected to experience big shifts of forestry structure, which is an alert to the people who live in these regions as well as an indicator of the risks for animals that rely on these PFTs for survival.

Temperate trees are likely to expand in South America, South Africa, and East Asia. They show sensitive responses to climate change for later years of the 21st century, especially in South Asia. In the Tropics (e.g., Amazon and regions in Africa) there may be a great degree of change in their vegetation distribution patterns.

Regardless of the two mitigation scenarios, vegetation structures in Alaska, Greenland, Central America, the southern part of South America, East Africa and East Asia are expected to be vulnerable to changing climates. The vulnerability assessment also indicates that Greenland, Tibet, South Asia and Northern Australia can be alleviated from their high risk of vulnerability if the 450ppm scenario is implemented. In providing ecosystem goods and services, the possibility of such changes should be taken into consideration. More analysis assessing changes in these ecosystems are discussed in the following Chapter 5.

Chapter 5

Assessing ecosystem change due to evolving vegetation structure under changing climates

5.1 Introduction

As the structure of vegetation cover changes, corresponding changes to ecosystems due to this vegetation structure change are expected to occur in the 21st century. A previous study by Feddema et al. (2005), for example, suggested that the influence of land-cover change is significant in simulating future climates because impacts of the land-cover change can be diverse, altering many aspects of biogeochemical and biogeophysical processes of the ecosystem. To assess this topic, the simulations described in Section 5.2 are carried out.

By altering biogeophysical processes, future vegetation structure change can lead to a change in the radiation budget, especially the capacity and the pattern of absorption of solar radiation at the land surface. In section 5.3.1, impacts of vegetation structure change on absorbed solar radiation and terrestrial surface albedo are investigated. Along with a change in climate, tree cover change may also alter the hydrologic cycle of the ecosystem. Changes in hydrologic features including evapotranspiration and runoff are discussed in section 5.3.2. Furthermore, a different structure in the vegetation distribution may result in a change in biogeochemical variables such as net primary production and vegetation carbon pool (section 5.3.3).

The results are the first estimates from simulations that apply the SEED configuration that incorporates impacts of meteorology on changes in future vegetation structure. The estimates presented here in this chapter, therefore, can be viewed as more comprehensive results than previous estimates using DGVMs that do not consider the seed dispersal mechanism and plant migration processes, and may therefore serve better the growing, active field of research in assessing impacts of land-cover change on future ecosystems and climates.

5.2 Description of the simulations and analysis method

In this chapter, the results from the No-Policy scenario and the 450ppm scenario continue to be used to assess their impacts on ecosystems. Details about the simulation design can be found in section 4.2. For purposes of comparison, simulation results using a static vegetation map (courtesy of Xiang Gao) are also analyzed. The simulations are

driven by the same IGSM-GFDL CM 2.1 climate forcings but the vegetation map does not change over time so that the effect of dynamic vegetation change is excluded. These simulations will be called the SV (i.e., Static Vegetation) and the simulations using the SEED configuration will be called the DV (i.e., Dynamic Vegetation). Table 5.1 summarizes the four simulations analyzed in this chapter and their abbreviations.

Table 5.1: Matrix of four simulations presented in this Chapter.

	*Dynamic Vegetation	Static Vegetation
No-Policy	NPDV	NPSV
450ppm CO_2 stabilization	450ppmDV	450ppmSV

* Simulations using the SEED configuration. See section 4.2 for details

In order to isolate the effect of vegetation, a linearity assumption is made to approximate the attributions of climate and vegetation. For a biophysical or biogeochemical variable X, the impacts of climate and vegetation are expressed as in Equation 5.1.

$$\frac{dX}{dt} = \underbrace{\frac{\partial X}{\partial C}\cdot\frac{dC}{dt}}_{\text{Term (a)}} + \underbrace{\frac{\partial X}{\partial V}\cdot\frac{dV}{dt}}_{\text{Term (b)}} + \underbrace{\frac{\partial X}{\partial t}}_{\text{Term (c)}} \qquad \text{(Equation 5.1)}$$

where X is a variable such as albedo, evapotranspiration and net primary production, C stands for climate, and V means vegetation.

Also, although the DV simulations and the SV simulations are driven by the same IGSM-GFDL CM 2.1 pattern climatology, the initializing conditions can differ from each other. To prevent the potential bias, the change in a variable X, which is an average in 2091-2100 minus an average in 2011-2020 is considered in this analysis.

5.3 Model result analysis

5.3.1 Assessing radiation change due to change in future vegetation structure

5.3.1.1 Effect on absorbed solar radiation

Absorbed solar radiation can be directly influenced by vegetation change. Forests absorb more sunlight than grass. Therefore expansion of NET boreal forests in the high latitudes, for example, may lead to a regional increase of absorbed solar energy.

Figure 5.1 shows for the NPDV case, the average absorbed solar radiation for 2011-2020, and the average radiation for 2091-2100, and the difference from (2091-2100) minus (2011-2020). In the high latitudes, the pattern of the difference in absorbed solar radiation varies regionally, showing a prominent increase (e.g., North Asia) and a noticeable decrease (e.g., northern Canada and northern Europe). The difference pattern in the mid-latitudes is moderate, indicating a regional increase in central Asia and a decrease in eastern North America and central North America. In the Tropics, absorption of solar radiation is expected to be larger in central South America, but smaller in the Amazon basin and central Africa.

In contrast, without dynamic vegetation change, the spatial pattern of the difference in absorbed solar radiation for the NPSV case, for the same time periods (2091-2100 minus 2011-2020), illustrates a more uniform distribution (see Figure 5.2) because the vegetation distribution pattern does not change and only the direct climate affects on vegetation albedo are included.

(a)

(b)

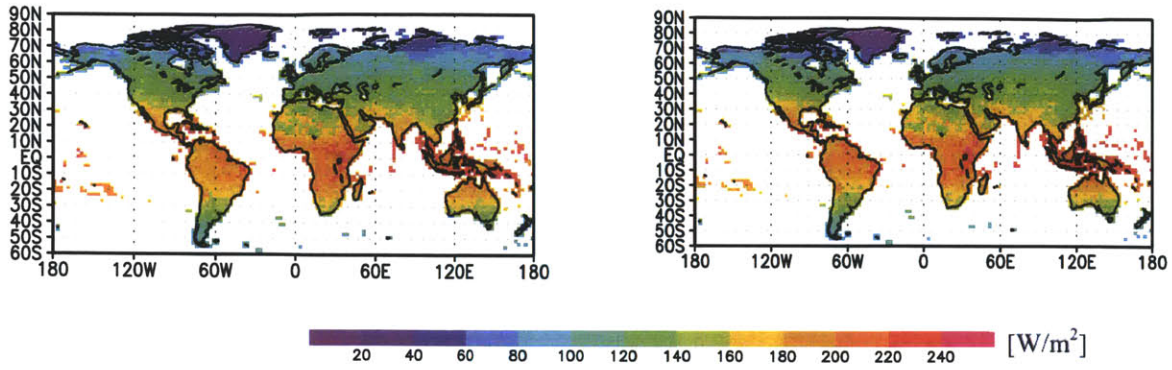

(c)

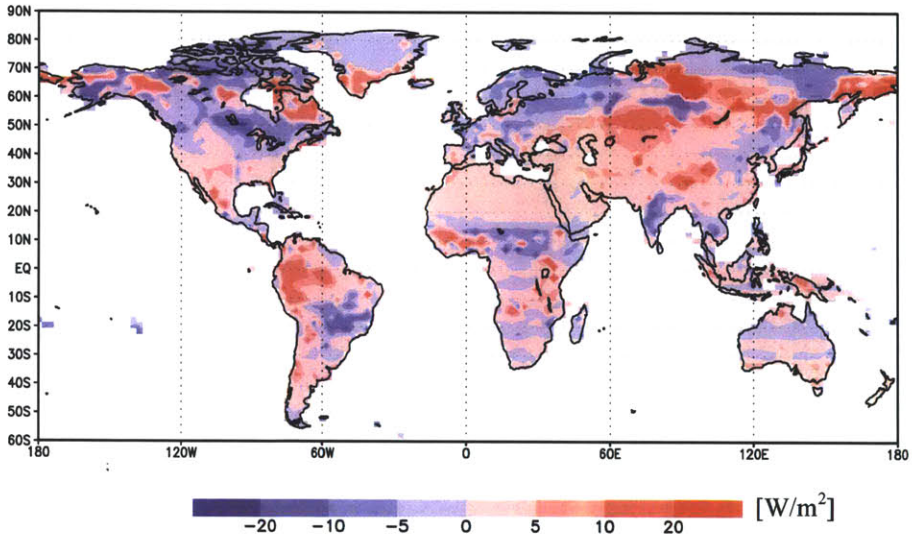

Figure 5.1: (a) Average of absorbed solar radiation for 2011-2020, (b) average of absorbed solar radiation for 2091-2100, and (c) the difference in absorbed solar radiation (i.e., (a) minus (b)) due to the combined effect of direct climate (Term (a) in the Eqn 5.1), vegetation (Term (b) in the Eqn 5.1) and the random change (Term (c) in the Eqn 5.1) of the NPDV case.

(a) (b)

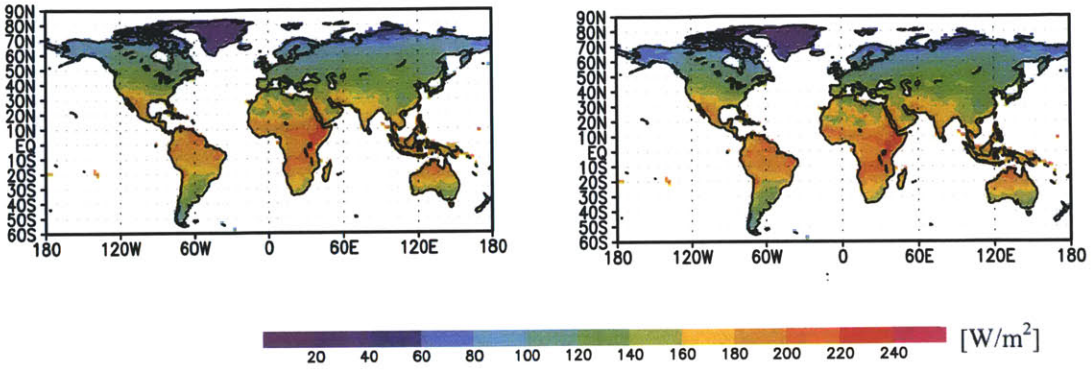

(c)

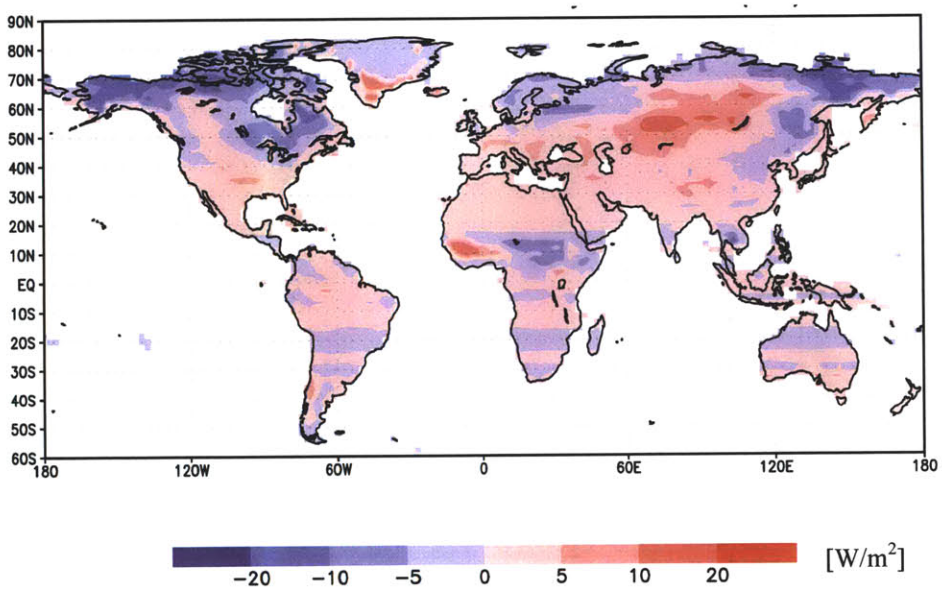

Figure 5.2: (a) Average of absorbed solar radiation for 2011-2020, (b) average of absorbed solar radiation for 2091-2100, and (c) the difference in absorbed solar radiation (i.e., (a) minus (b)) due to the effect of direct climate (Term (a) in the Eqn 5.1) and the random change (Term (c) in the Eqn 5.1) of the NPSV case.

The net effect of vegetation structure to the absorbed solar radiation is estimated as the difference between the NPDV and NPSV cases (Figure 5.3). The spatial pattern in Figure 5.3 indicates that the heterogeneous pattern of absorbed solar radiation shown in Figure 5.1(c) is mostly due to vegetation structure change. It corresponds very well with the vegetation re-distribution such as the northward expansion of boreal forests and shrinking C3 grass Arctic found in Alaska, northeastern North America, North Asia (Siberia) and northeastern Asia. Because a piece of land covered by grass can reflects more solar radiation than the land covered by trees, the transition from C3 grass Arctic to boreal forests leads to more absorption of solar radiation. Therefore, under the NP scenario, more absorption of solar radiation due to boreal forest expansion in the high latitude regions may accelerate warming in high latitudes. This result also reaffirms the strong positive feedback to high-latitude warming suggested by Higgins and Harte (2006).

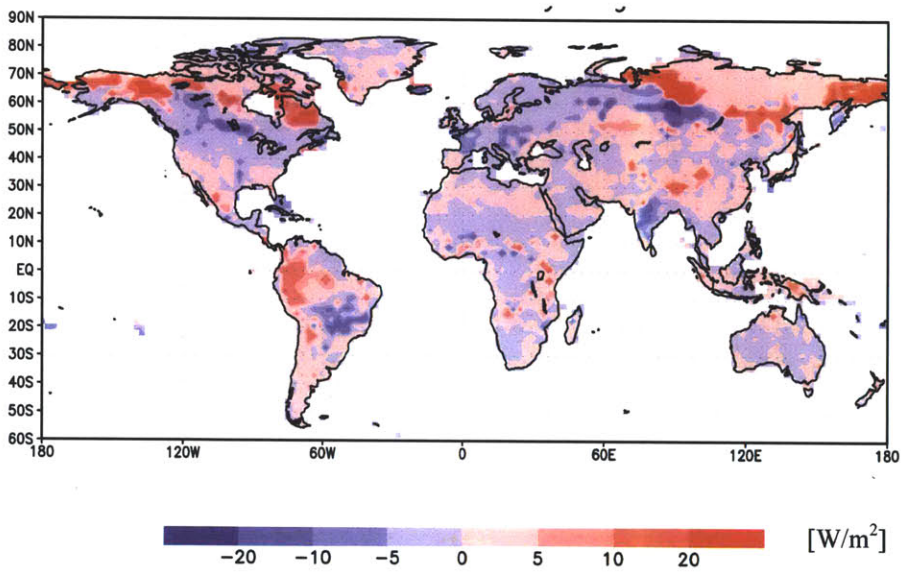

Figure 5.3: Contribution of vegetation structure change (Term (b) in the Eqn 5.1) to change in absorbed solar radiation in the NP scenario. Shown is specifically the NPDV change (Fig 5.1 (c)) minus the NPSV change (Fig 5.2 (c)). Unit is W/m^2

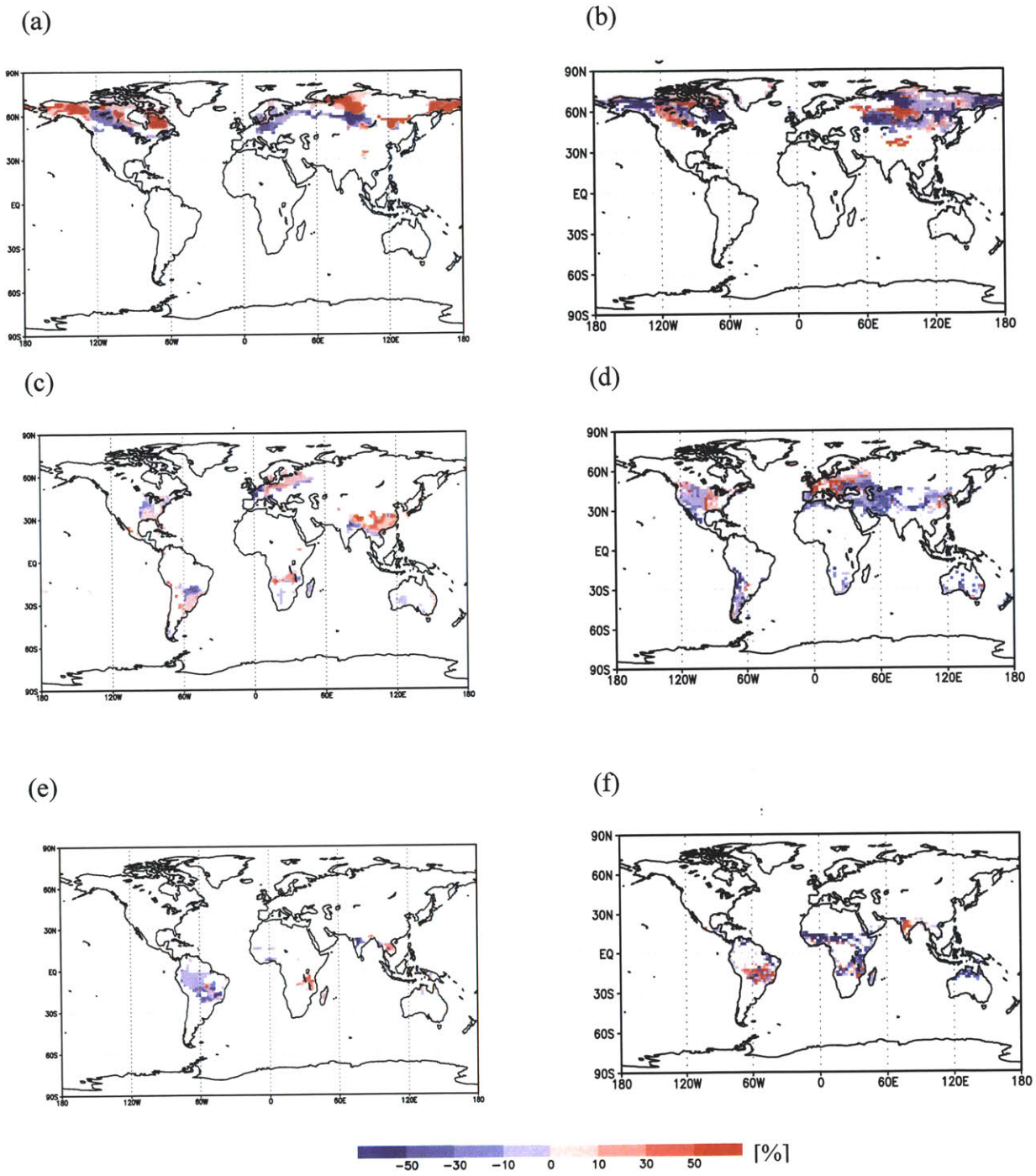

Figure 5.4: Vegetation structure change of (2091-2100) minus (2011-2020) in the NP scenario: forest covers (panels on the left column) and grass covers (panels on the right column): (a) Difference in boreal forests, (b) Difference in C3 grass Arctic, (c) Difference in temperate forests, (d) Difference in C3 (cold-season) grass, (e) Difference in tropical forests, and (f) Difference in C4 (warm-season) grass. All units are in %.

5.3.1.2 Effect on albedo

Terrestrial surface albedo may be also influenced as the vegetation distribution is modified under changing climates. The albedo is defined and calculated as reflected radiation divided by incoming solar radiation (Equation 5.2)

$$Albedo = \frac{Reflected\ solar\ radiation}{Incident\ solar\ radiation} \quad \text{(Equation 5.2)}$$

Similar to the analysis shown in the previous section 5.3.1.1, the impact of vegetation structure on albedo is isolated for both the NP scenario and the 450ppm scenario, and the results of the estimated albedo change from (2091-2100) minus (2011-2022) are shown in Table 5.2.

Table 5.2: Change in estimated albedo (2091-2100) minus (2011-2020) of four latitude bands under the NP scenario and the 450ppm scenario.

		NP			450ppm		
Region	Latitudes	*C+V+R	#C+R	¶V	*C+V+R	#C+R	¶V
High latitude	50N-90N	-0.0357	-0.0187	-0.0171	-0.0145	-0.0187	0.0042
Mid latitude (NH)	23.5N-50N	0.0013	-0.0013	0.0025	-0.0007	-0.0013	0.0006
Tropics	23.5S-23.5N	0.0002	0.0008	-0.0005	-0.0014	0.0008	-0.0021
Mid latitude (SH)	50S-23.5S	0.0005	0.0016	-0.0011	0.0008	0.0016	-0.0008

* C+V +R: Term (a) + Term (b) + Term (c) in Eqn 5.1

C+ R: Term (a) + Term (c) in Eqn 5.1

¶ V: Term (b) in Eqn 5.1 (i.e., isolated impact by vegetation change)

Under the NP scenario, the terrestrial surface albedo change attributed to vegetation structure change in 50N-90N is V = -0.0171, which implies a positive vegetation-albedo feedback in high latitudes. In the Northern hemisphere mid-latitude regions (23.5N-50N), surface albedo due to vegetation change is expected to increase by V = 0.0025 by the last decade of the 21st century under the NP scenario; however, it cannot reverse the sign of the reduction in albedo in the high latitudes (V = -0.0171). Likewise, contributions of the Tropics and the Southern hemisphere mid-latitudes to the total change in surface albedo (V = -0.0005 and V = -0.0011, respectively) are negligible under the NP scenario.

Under the 450ppm scenario, the impact of vegetation change on surface albedo is much less than in the NP scenario. At high latitudes, the change of vegetation structure serves to increase the albedo by V = 0.0042. This albedo change is very small, and more importantly, the sign of its feedback is negative, alleviating otherwise positive feedbacks in the high latitudes. This result implies a very crucial point that at a certain degree of climate mitigation (i.e., 450ppm scenario), vegetation structure change may be able to buffer the warming trend; however, if no mitigation policy is implemented, the expansion of boreal forests and retreat of C3 grass Arctic may not offset the warming any more but accelerate warming in high latitudes.

The changes in reflected radiation, (2091-2100) minus (2011-2020) in Figure 5.5 also support the conclusion that the albedo change is driven by change in high latitudes, showing relatively greater decrease in reflected radiation in high latitudes under the NP scenario (Figure 5.5 (a)) and much less change in reflected radiation under the 450ppm scenario (Figure 5.5 (b)).

(a)

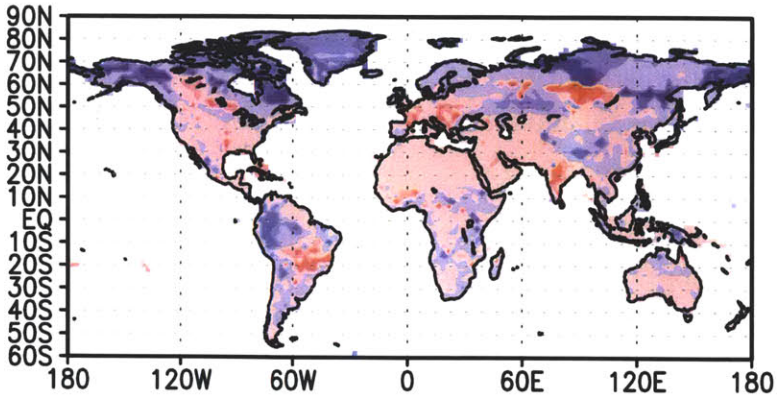

(b)

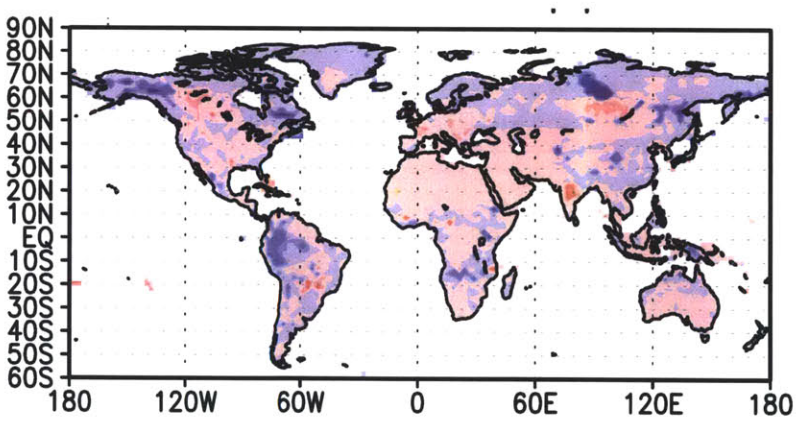

Figure 5.5: Contribution of vegetation structure change to the change in reflected radiation, decade of (2091-2100) minus decade of (2011-2020) in the units of W/m^2: (a) Change in reflected radiation (W/m^2) due to vegetation under the NP scenario), and (b) Change in reflected radiation (W/m^2) due to vegetation under the 450ppm scenario.

5.3.2 Assessing hydrologic change due to change in future vegetation structure

Hydrologic features can be altered indirectly by structural changes in vegetation under changing climates. In this section, the impacts of vegetation structure on the hydrologic cycle are further investigated. Because hydrologic changes do vary regionally and uncertainties are large, qualitative results only from the NP scenario are analyzed and discussed here.

As warming occurs, higher temperature is expected to cause more precipitation globally, as well as more variability in precipitation patterns (i.e., regionally enhanced precipitation but also more droughts), because the warmer atmosphere can hold more water vapor (Trenberth et al., 2003). In Figure 5.6, the difference in precipitation, which is the averaged precipitation for 2091-2100 minus the averaged precipitation of 2011-2020 is illustrated. More precipitation (i.e., rainfall + snowfall) in high latitudes, and more rainfall in central Asia, East Asia, and the eastern United States is expected. The degree of increase in precipitation in the Tropics is expected to be more intense than in other parts of the globe. The Southern hemisphere mid-latitudes as well as southern Europe, the Middle East and western United States are projected to receive less rainfall during the last decade of the 21st century.

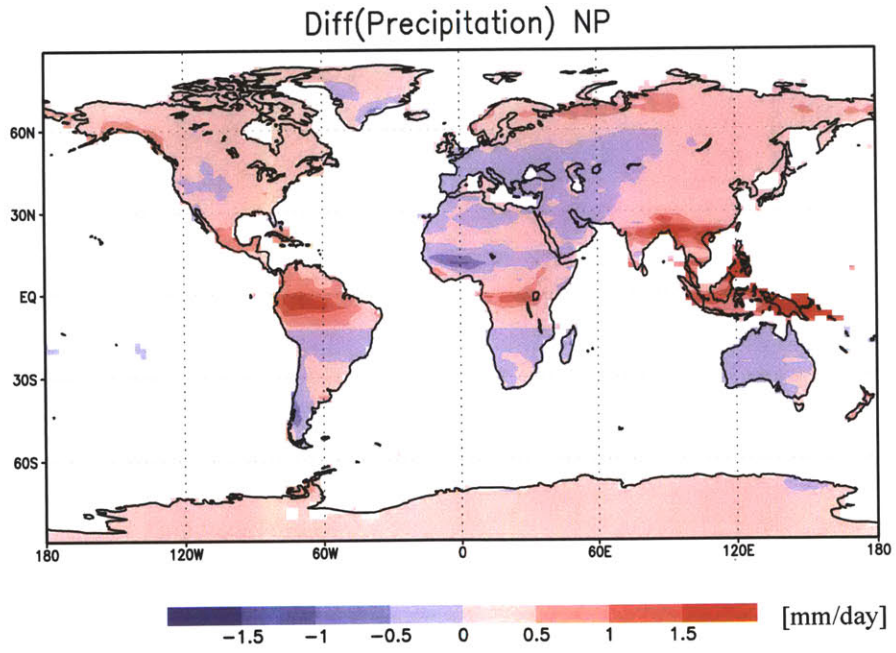

Figure 5.6: Change in precipitation computed as the decade of (2091~2100) minus the decade of (2011-2020). The same profile of precipitation is applied to force both the NPDV case and the NPSV case. Unit is mm/day.

When rainfall occurs over a land region covered by forests, it first reaches the layer of the tree canopy. Some of the water is intercepted by the canopy and does not reach the ground. As more forest expands to the North in high latitudes, for example, a greater amount of water is intercepted at the forest canopy level. Figure 5.7 shows the differences in fluxes of interception, considering (a) both climate change and dynamic vegetation, (b) climate change only without vegetation change, and (c) vegetation change only, which is the subtraction of Figure 5.7 (b) from Figure 5.7 (a). As expected, expansion of boreal forests at the expense of C3 grass Arctic in the high latitude regions, the increase in the temperate forest cover in South Asia and Southeast Asia, and the tropical tree cover changes in South America (also see Figure 5.4 for details of vegetation structure change) are well captured in Figure 5.7 (c), which implies that vegetation structure change modifies the amount of water intercepted at the canopy layer.

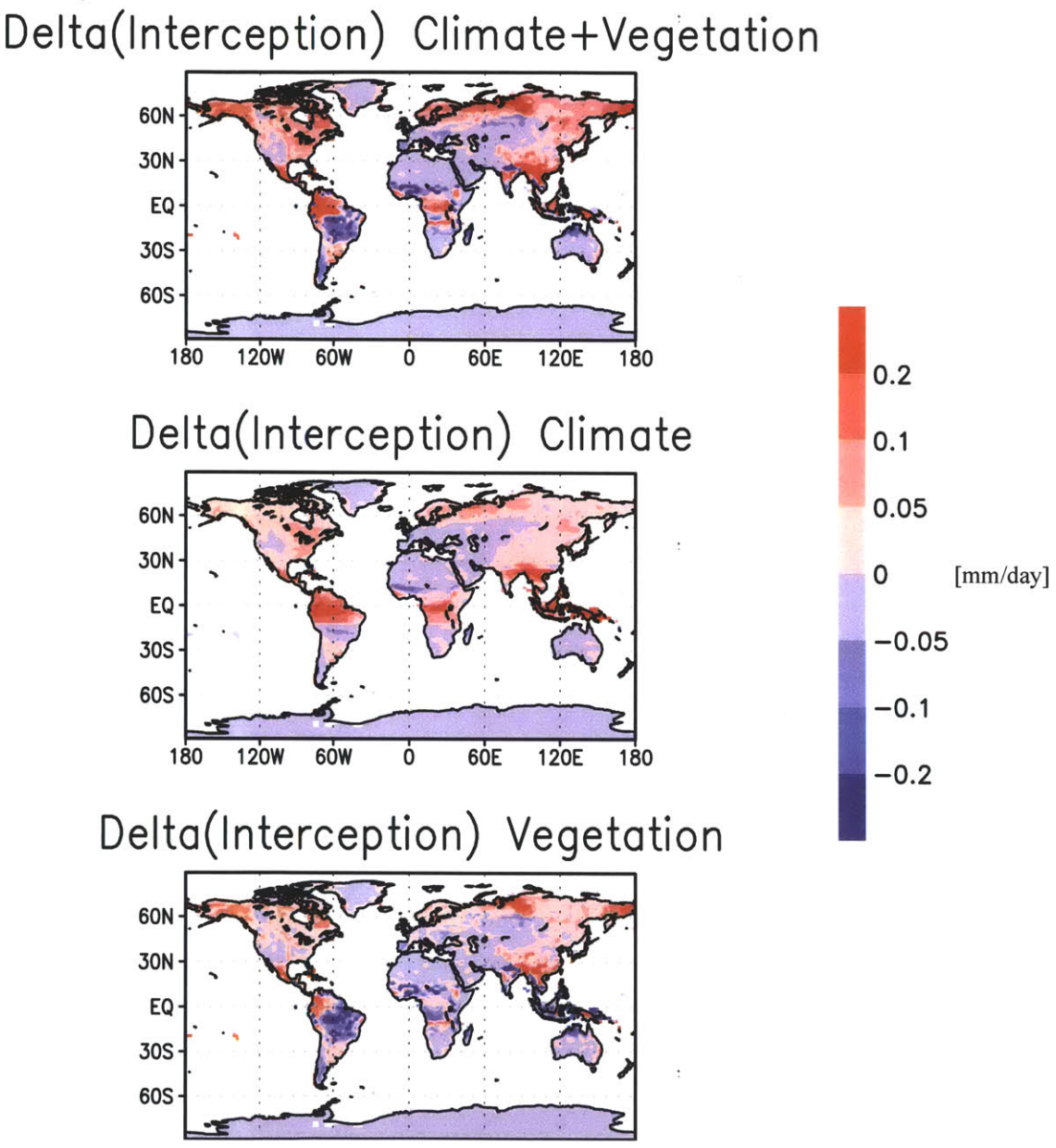

Figure 5.7: Changes in flux of interception measured as the flux in (2091~2100) minus the flux in (2011-2020) in units of mm/day under the NP scenario: (Top panel) the combined effect of climate and dynamic vegetation, (Middle panel) the effect of climate only without vegetation change, and (Bottom panel) the isolated effect of vegetation only.

Before the remaining water that is filtered through the canopy layer reaches the ground, some of the water returns back to the atmosphere through evapotranspiration process, which includes evaporation at the canopy and on the ground, and the removal of water by transpiration through the stomata of plants.

Transpiration by plants accounts for about 10 percent of the global atmospheric moisture flux. Under changing climates, both atmospheric CO_2 concentration and temperature contribute to changes in the transpiration rates of plants, but in opposite directions. One mechanism is called "physiological forcing", which means that under an elevated atmospheric CO_2 concentration, plants will open their stomata less, thus reducing the rate of transpiration. As a result, more water will remain on land (Betts et al., 2007). Another mechanism, which is also expected under warming, relates to the elevation of the temperature. In the warmer environment, healthy plants cool themselves by opening their stomata more widely, thus enhancing the transpiration rate and lowering the amount of runoff. Because the atmospheric CO_2 concentration remains the same for the simulations done for this analysis, the physiological forcing is not considered but the effect of temperature on the rate of transpiration via vegetation structure change is shown here.

Differences in the fluxes of transpiration are illustrated in Figure 5.8, and differences in fluxes of evaporanspiration (i.e., the sum of canopy transpiration, canopy evaporation and ground evaporation) are shown in Figure 5.9. In high latitudes, expansion of boreal forests leads to a greater transpiration flux (Figure 5.8 (c)), and thus also to more evapotranspiration (Figure 5.9 (c)) where the forests proliferate at the expense of C3 grass Arctic. In addition, more solar energy is absorbed due to the spread of boreal forests, accelerating the transpiration and evapotranspiration processes (see Figure 5.3 for the pattern of change in absorbed solar radation by vegetation structure change). Enhanced transpiration and evepotranpiration in South Asia and Southeast Asia (Figure 5.8 (c) and Figure 5.9 (c)) are driven by the spread of temperate forests (see also Figure 5.4). Most notably, the pattern of changes in transpiration rates in the Tropics (Figure 5.8(c)) clearly resonates with the structure change of the tropical forests. Reduction of the tranpiration in the Amazon basin is due to the forest type changing from BET tropical forests to BDT tropical forests. Leaves of the evergreen trees are active year-long, whereas leaves of the deciduous trees become active for only a part of year (i.e., seasonal). Replacing BET tropical forests by BDT tropical forests results in reductions of transpiration and evapotranspiration (Figure 5.8 (c) and Figure 5.9 (c)). In contrast, the southeastern part of the Amazon shows an increase in transpiration and evapotranspiration because C4 grass is replaced by the BET tropical forests as the forests become more favored in this region.

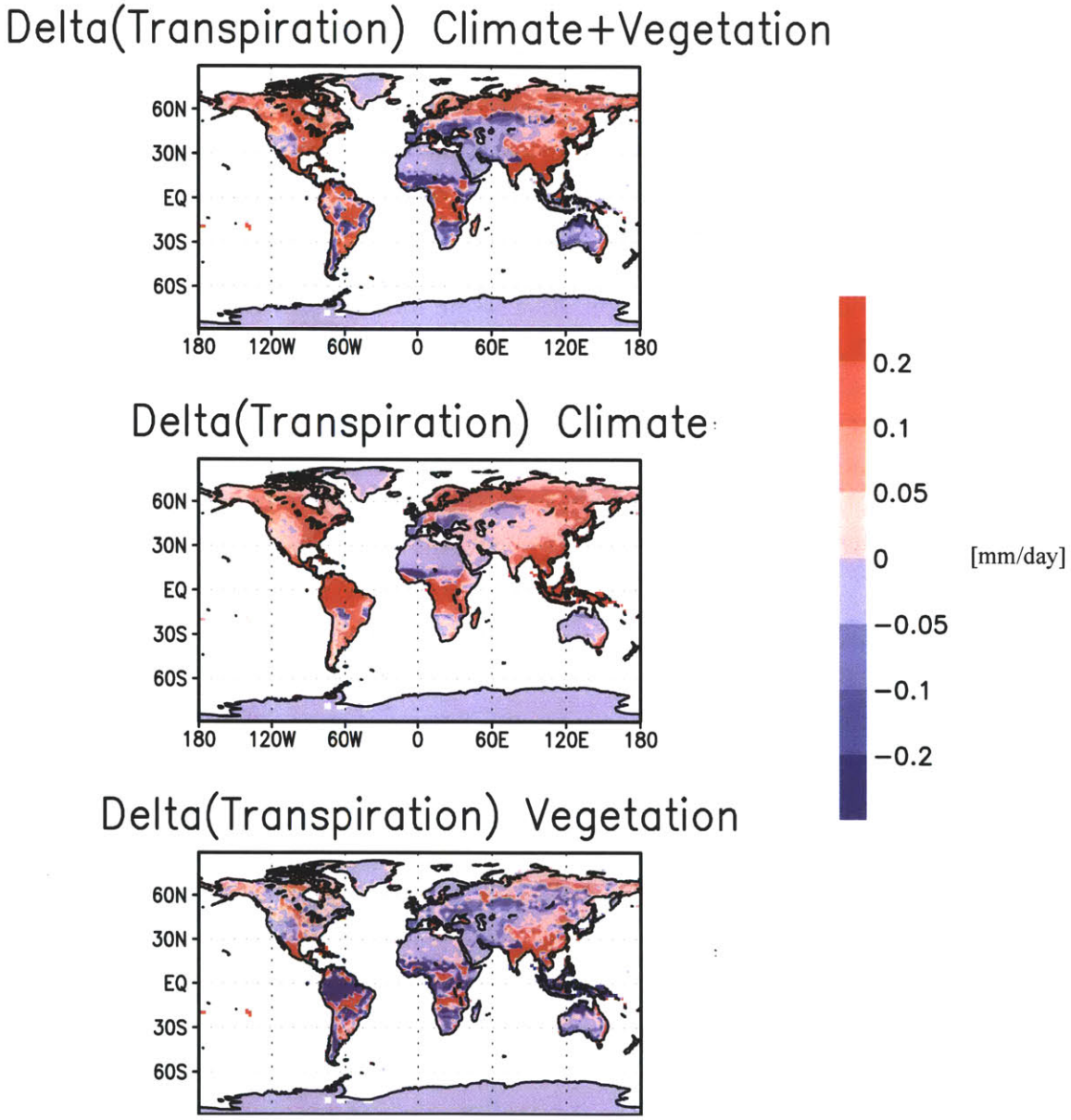

Figure 5.8: Changes in the flux of transpiration, measured as the flux in (2091~2100) minus the flux in (2011-2020), in units of mm/day under the NP scenario: (Top panel) the combined effect of climate and dynamic vegetation, (Middle panel) the effect of climate only without vegetation change, and (Bottom panel) the isolated effect of vegetation only.

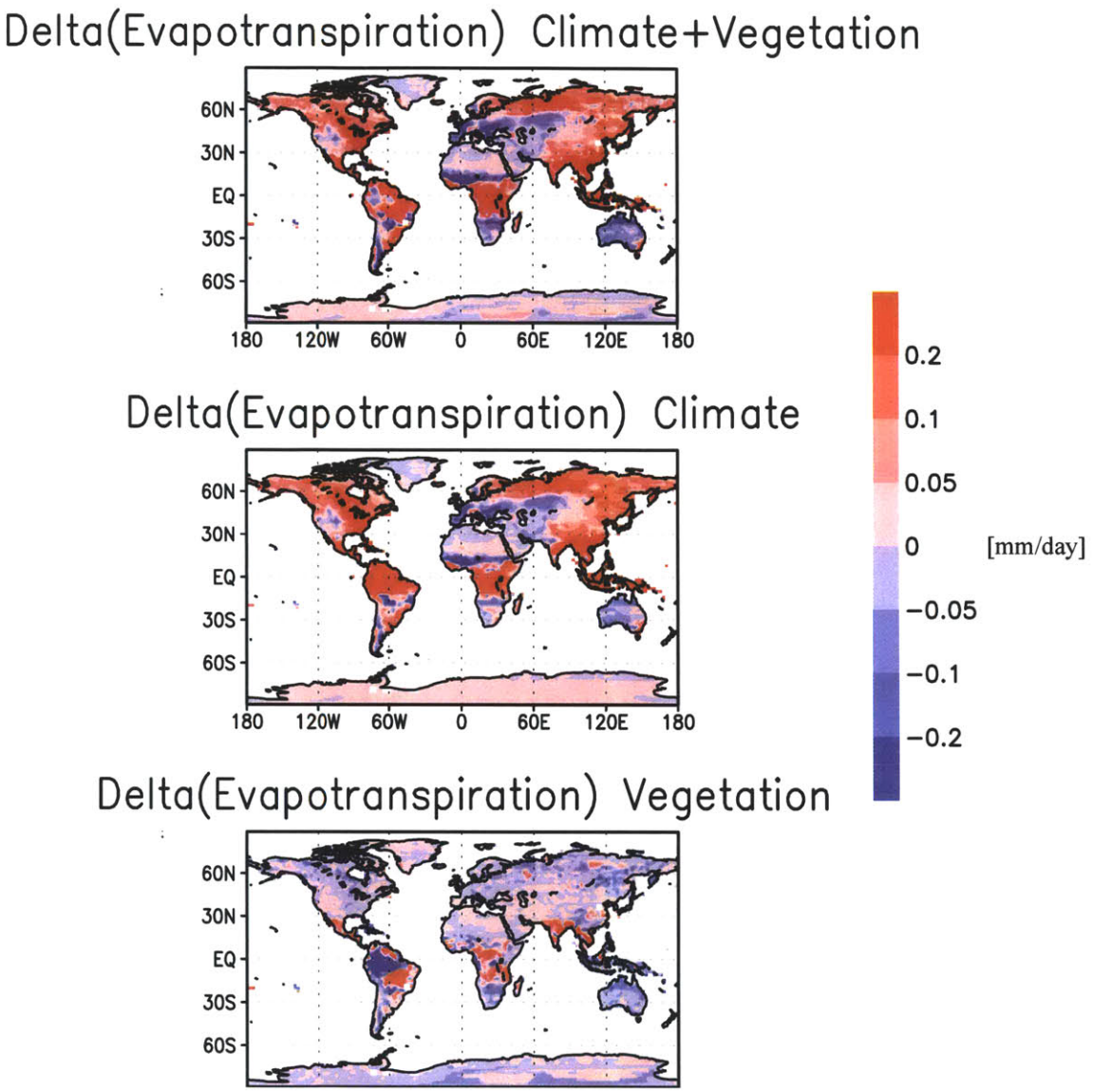

Figure 5.9: Changes in the flux of evapotranspiration, measured as the flux in (2091~2100) minus the flux in (2011-2020), in units of mm/day under the NP scenario: (Top panel) the combined effect of climate and dynamic vegetation, (Middle panel) the effect of climate only without vegetation change, and (Bottom panel) the isolated effect of vegetation only.

Finally, the water reaching the ground is either being absorbed into the soil column, or if the soil is saturated, the excess water runs away along the surface (i.e., runoff). The runoff change (Figure 5.10 and also Figure 5.11) indicates that the impacts of vegetation offset the increase in runoff due to the enhanced precipitation (Figure 5.6), especially where trees are expected to expand at the expense of grasses (e.g., South Asia). In addition, forests can hold more water in the soil column, therefore inducing higher water table depth (Figure 5.12 (c)). It should be noted, however, that considering the heterogeneity of the vegetation structure change and the series of relevant processes (i.e., interception, evapotranspiration) that may modify the amount of water reaching the ground, regional variations in runoff are also expected to be large.

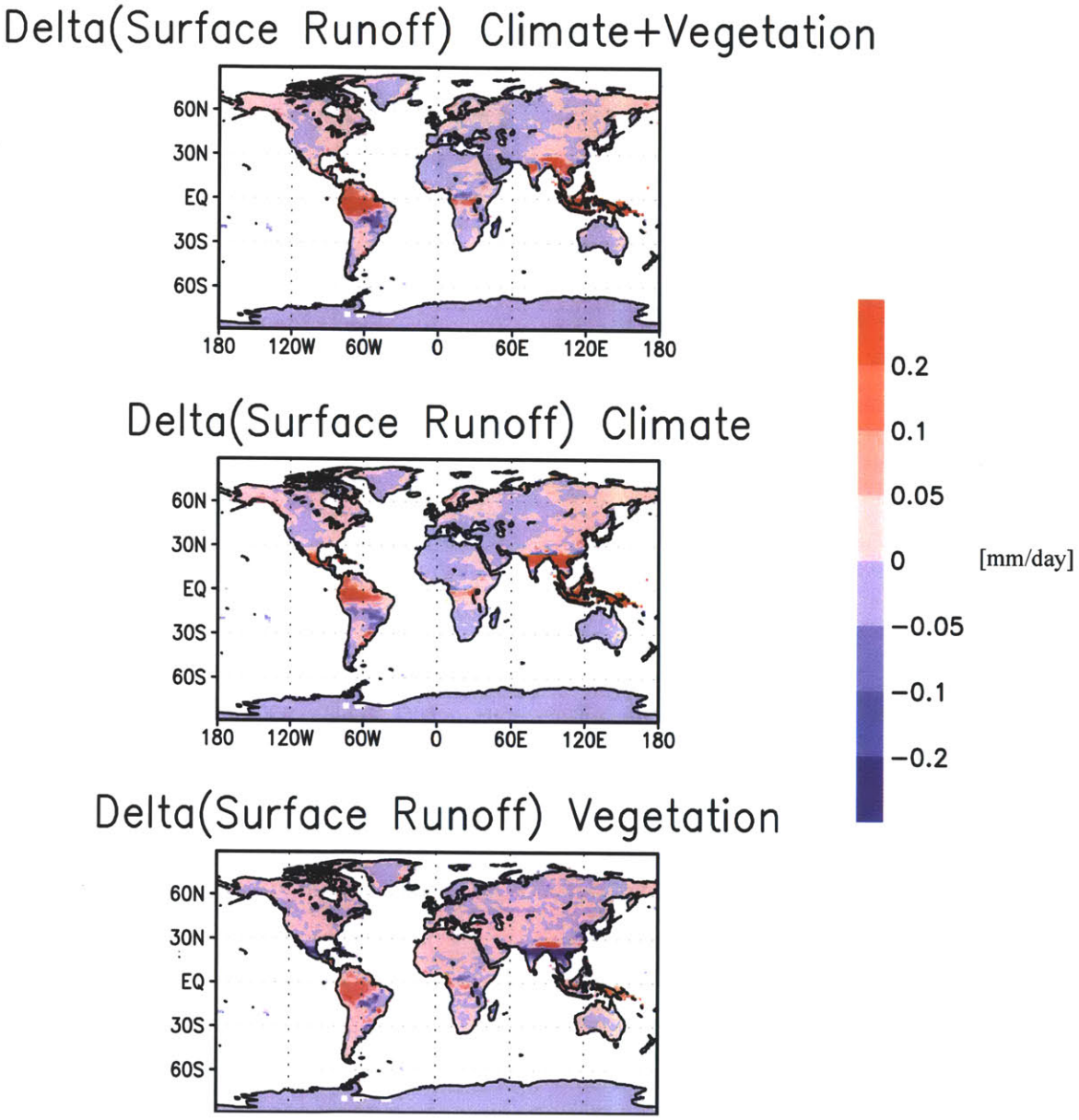

Figure 5.10: Changes in the flux of surface runoff, measured as the flux in (2091~2100) minus the flux in (2011-2020), in units of mm/day under the NP scenario: (Top panel) the combined effect of climate and dynamic vegetation, (Middle panel) the effect of climate only without vegetation change, and (Bottom panel) the isolated effect of vegetation only.

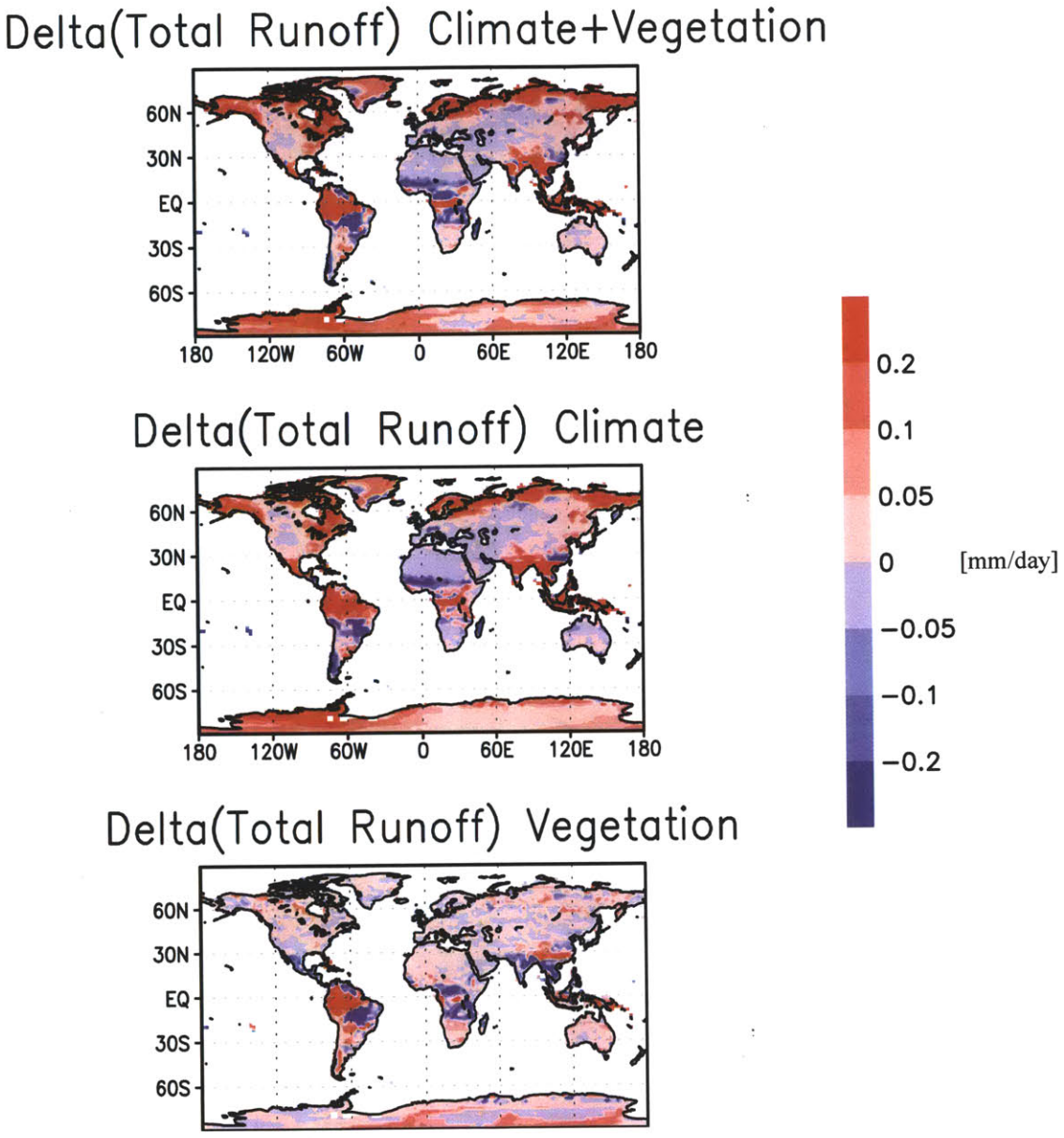

Figure 5.11: Changes in the flux of total runoff, measured as the flux in (2091~2100) minus the flux in (2011-2020), in units of mm/day under the NP scenario: (Top panel) the combined effect of climate and dynamic vegetation, (Middle panel) the effect of climate only without vegetation change, and (Bottom panel) the isolated effect of vegetation only.

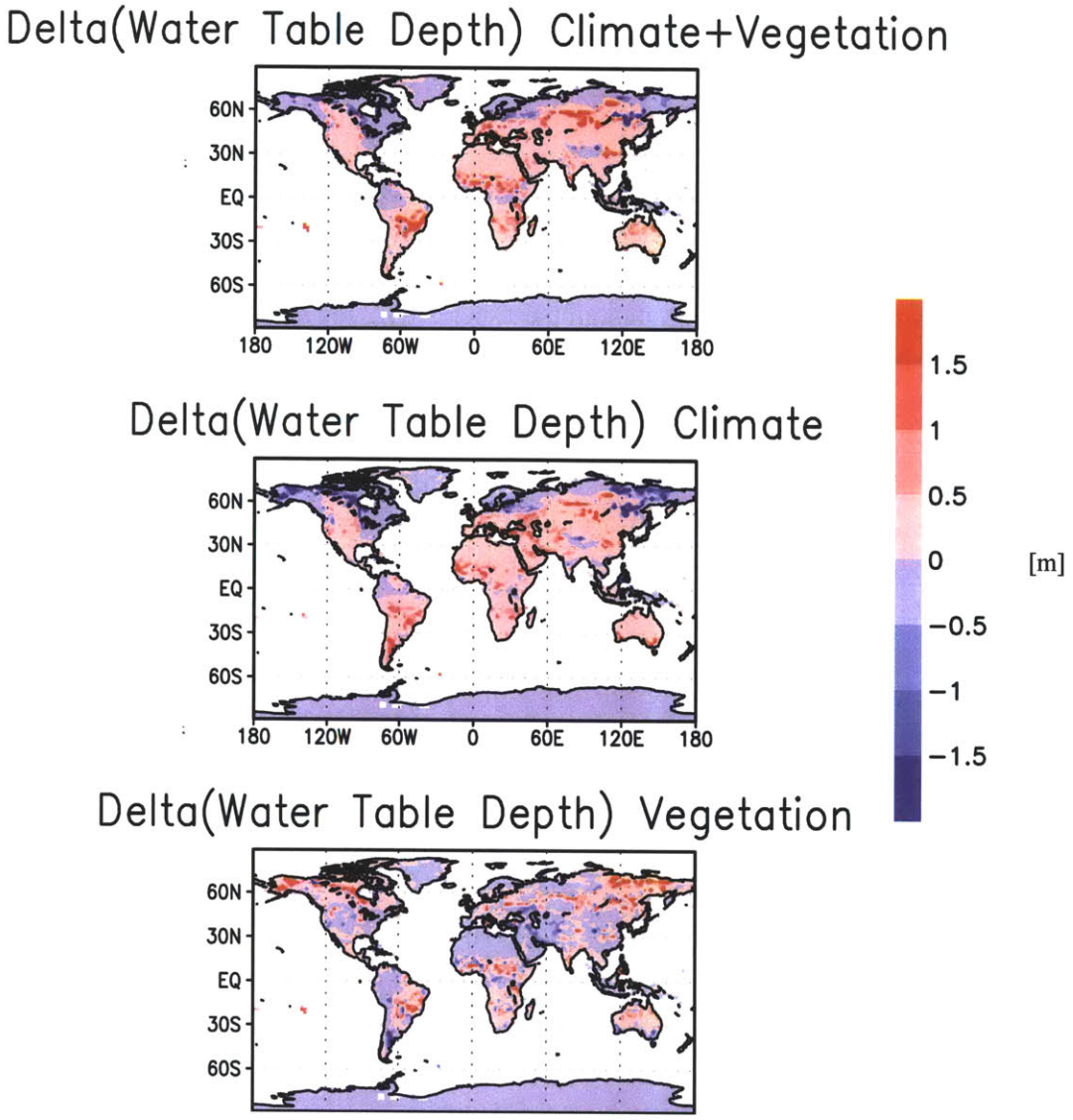

Figure 5.12: Changes in the water table depth, measured as the depth in (2091~2100) minus the depth in (2011-2020), in units of meters under the NP scenario: (Top panel) the combined effect of climate and dynamic vegetation, (Middle panel) the effect of climate only without vegetation change, and (Bottom panel) the isolated effect of vegetation only.

5.3.3 Assessing biogeochemical change due to change in future vegetation structure

Recently, Arneth et al. (2010) concluded that the magnitude of biogeochemical feedbacks of the terrestrial biosphere to the atmosphere may be as large as the feedbacks of the physical climate system, emphasizing the role of terrestrial biogeochemical feedbacks to climate.

Figure 5.13 shows globally aggregated annual NPP from 2021 to 2100. The first ten years (i.e., 2011-2020) of the simulations are not considered in analyzing biogeochemical variables because the SEED configuration needs time to adjust to the transitions made in simulation design (see section 4.2 for details of the hybrid design). Under the NP scenario (blue curve in Figure 5.13), NPP gradually decreases from 2021 to 2100 (from 62 PgC/yr down to 54 PgC/yr), leading to a loss of about 8 PgC/yr, whereas NPP under the 450ppm scenario does not vary to a great extent. It maintains NPP at about 60PgC/yr for 2020-2100 (red curve in Figure 5.13). Warming of the atmosphere may increase the respiration rates of plants, resulting in reduction of global NPP, especially in Amazonian forests according to other DGVMs such as Hyland, TRIFFID, and LPJ (Galbraith, 2010). The result is also consistent with estimates by other DGVMs in a previous study by Sitch et al. (2008), falling into the range of change in NPP of -20PgC/yr to 0PgC/yr for a 3 °C surface temperature increase (similar to temperature increase under the NP scenario in this study). The CO_2 fertilization effect does not apply to the simulations in this study, which may have counteracted the loss of NPP if it had been considered in the simulations.

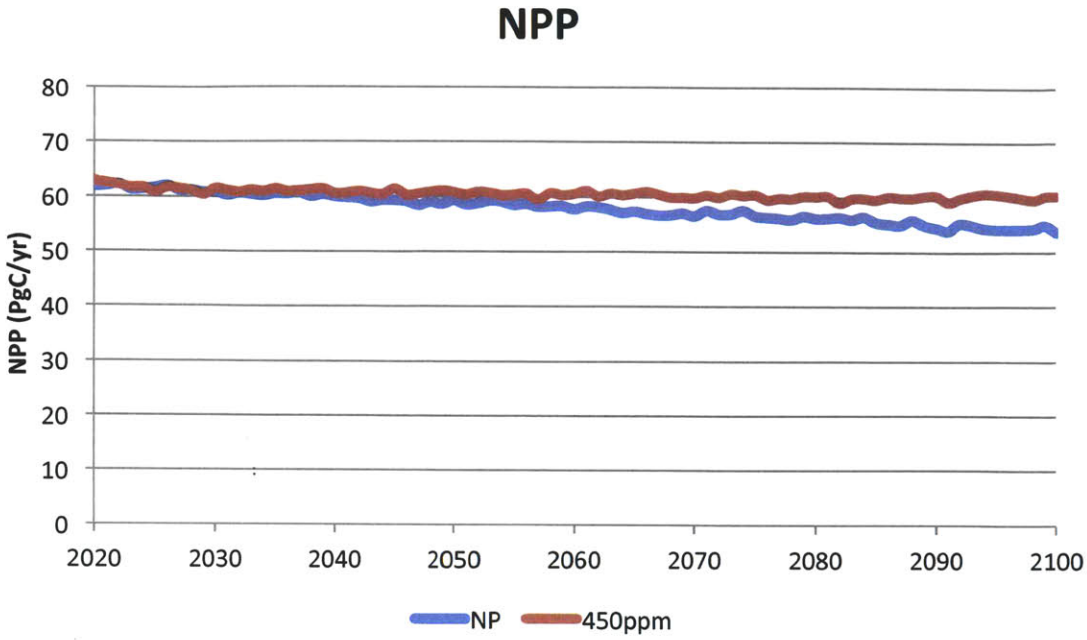

Figure 5.13: Annual global NPP (PgC/yr) for the NP scenario (blue curve) and the 450ppm scenario (red curve).

Total vegetation carbon is expected to increase in the 21st century, but the rate of increase under the NP scenario (blue curve in Figure 5.14) is seen to be slower than the 450ppm scenario (red curve in Figure 5.14). Because the CO_2 fertilization effect is not considered in the simulations in this study, temperature and precipitation are the main drivers for modifying total vegetation carbon. Compared to previous studies using DGVMs that do not incorporate any plant migration constraints (and thus potentially overestimate terrestrial carbon sequestration capacity), the increments of increase in total vegetation carbon from 2021 to 2100 in this study (24 PgC for the NP scenario and 37 PgC for the 450ppm scenario) may be conservative (Table 5.3 and Table 5.4).

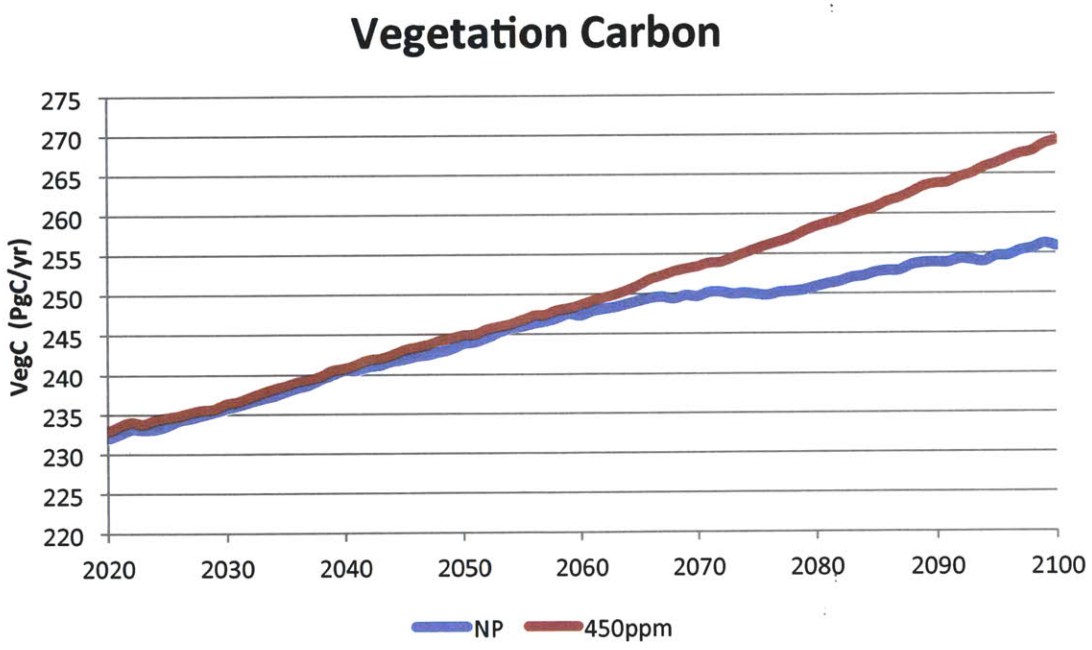

Figure 5.14: Change in terrestrial vegetation carbon for the NP scenario (blue curve) and the 450ppm scenario (red curve).

Table 5.3: Comparisons of vegetation carbon (PgC) from this study for the NP scenario using the SEED configuration and from other DGVMs using the similar SRES A2 emissions scenario (reconstructed using the values from Sitch et al (2008) Table 3).

Source	VegC (PgC)	DGVM	Migration Configuration	Climate forcing	Scenario	Target years	CO_2 fertilization
This study	**24**	CLM-DGVM	SEED	IGSM-GLDL CM 2.1 pattern (offline)	No policy	2100 minus 2021	NO
Sitch et al. (2008)	344	HyLand	FREE	HadCM3LC (coupled)	A2	2100 minus 2000	YES
	60	LPJ	FREE	HadCM3LC	A2	2100 minus 2000	YES
	278	ORCHEE	FREE	HadCM3LC	A2	2100 minus 2000	YES
	294	Sheffield-DGVM	FREE	HadCM3LC	A2	2100 minus 2000	YES
	-8	TRIFFID	FREE	HadCM3LC	A2	2100 minus 2000	YES

Table 5.4: Comparisons of vegetation carbon (PgC) from this study for the 450ppm scenario using the SEED configuration and from other DGVMs using the similar SRES B1 emissions scenario (reconstructed using the values from Sitch et al (2008) Table 3).

Source	VegC (PgC)	DGVM	Migration Configuration	Climate forcing	Scenario	Target years	CO_2 fertilization
This study	**37**	CLM-DGVM	SEED	IGSM-GLDL CM 2.1 pattern (offline)	450 ppm	2100 minus 2021	NO
Sitch et al. (2008)	277	HyLand	FREE	HadCM3LC (coupled)	B1	2100 minus 2000	YES
	66	LPJ	FREE	HadCM3LC	B1	2100 minus 2000	YES
	217	ORCHEE	FREE	HadCM3LC	B1	2100 minus 2000	YES
	168	Sheffield-DGVM	FREE	HadCM3LC	B1	2100 minus 2000	YES
	7	TRIFFID	FREE	HadCM3LC	B1	2100 minus 2000	YES

5.4 Discussion

Betts (2000) suggested that the increase in radiative forcing caused by reducing the albedo in expanding boreal forests can offset the advantage from enhanced carbon sequestration capacity by the CO_2 fertilization effect. Arneth et al. (2010) also argued that the contribution by the terrestrial biosphere to the total radiative forcing budget is up to 0.9 or 1.5 W/m^2, which offsets and may even eliminate the suggested cooling induced by the CO_2 fertilization effect. As shown in section 5.3.1.2, the changes to albedo (or radiative forcing) caused by vegetation structure change depend upon the climate mitigation scenario. Especially in the high latitudes, the reduction of albedo due to the expansion of boreal forests under the NP scenario may not offset the warming trend but instead contribute to accelerating warming (i.e., a positive feedback).

The CO_2 fertilization effect is not considered, and the nitrogen cycle is not fully incorporated in these simulation results. With higher atmospheric CO_2 concentrations, productivity increases result in higher primary production; however with inclusion of the nitrogen cycle, productivity may decrease because nitrogen is a limiting nutrient, especially in the high latitudes. Therefore, the overall productivity may be greater or smaller than the estimates provided in this study. This study is the first effort to incorporate the impacts of meteorology on vegetation structure (through the seed dispersal mechanism and resultant altered competition dynamics), so that better estimating NPP and carbon storage will also be contributing to estimating the carbon cycle more accurately.

5.5 Summary and conclusion of Chapter 5

Assessment of the impacts of vegetation structure change in ecosystems has been done for the first time using the SEED configuration that incorporates the meteorology-driven seed dispersal mechanism. Potential impacts of the vegetation structure change to the ecosystem functions are investigated in three areas: (1) radiation budget, (2) water cycle and (3) terrestrial carbon cycle.

The results from this study suggest that the influence of future vegetation change to the radiation budget cannot be neglected. Depending upon the climate mitigation scenarios, the induced change in albedo will either accelerate or alleviate the warming under changing climates. Under the NP scenario, proliferation of boreal forests in high latitudes is expected to cause a positive vegetation-albedo feedback to climate, whereas under the 450ppm scenario, it can buffer the warming trend (i.e., a negative feedback). The impacts to albedo may even offset the increase in carbon uptake by the expansion of forests.

Interception of rainfall by the forest canopy, evapotranspiration, and runoff are all influenced by changes in future vegetation structure. Replacement of grasses by forests, along with the enhanced absorption of solar radiation caused by expansion of forests, may result in greater rates of interception of water at the tree canopy level and increases in evapotranspiration, thus eventually altering the pattern of runoff. The impacts of vegetation structure on runoff are confined primarily to the Tropics and sub-Tropics. Globally, the runoff change due to vegetation change may partially offset or amplify the change in runoff due to climate change with enhanced precipitation accompanying global warming. In the time horizon considered in this study (through the end of the 21st century), the magnitude of the runoff response by the vegetation change does not exceed the direct response from the hydro-climate change.

Since forestation is suggested as a way to mitigate climate change due to greenhouse gases, the assessment of this action and its implications need to be carefully evaluated. Changing forest structure is a complicated process that includes many indirect feedbacks such as albedo, transpiration, and carbon sequestration capacity. Some of them may act as offsets to each other. Also regionally, forestation may help to mitigate warming locally but it may not help much to mitigate it in other regions. More comprehensive modeling studies that couple meteorology, dynamic vegetation change, biogeophysical processes, and biogeochemical processes are needed for assessing the impacts of forestation on global carbon budget and the global radiation budget in the future.

Chapter 6

Conclusions, closing discussions, and suggestions for future work

6.1 Major findings of this study

Major findings of this study include:

- The SEED configuration developed in this study, which incorporates the meteorology-driven seed dispersal mechanism for boreal trees and temperate trees, provides a more realistic representation of vegetation structure, for example, in the boreal forests in western Siberia and the temperate forests in Eastern Europe.
- The prevailing wind pattern, along with the existing vegetation structure in nearby grid cells, alters the competition dynamics of the trees by filtering out unrealistic transfers of saplings and thereby adjusting their establishment rates in the SEED configuration.
- New estimates of future vegetation structure using the SEED configuration generally agree with the expected trend of expansion of boreal trees in the high latitudes, and suggests that more regions in the world are expected to experience a greater degree of change in tree species and grasses, especially if no climate mitigation policy is implemented. The vulnerability assessment carried out in this study suggests that for the regions including Greenland, Tibet, South Asia and Northern Australia, their risk of experiencing a rapid transition in vegetation structure can be alleviated if a stringent policy like the 450ppm scenario is implemented.
- Impacts of the land cover change induced by future vegetation structure change in natural ecosystems may be significant. Because of the heterogeneity of change in vegetation structure, regional impacts to ecosystems under changing climate may vary and may be more significant than change at the global scale. In the high latitudes, the vegetation-albedo feedback is driven by expansion of boreal trees, and the sign of the feedback depends on the climate mitigation scenarios. If no mitigation policy is implemented, the vegetation change in the high latitudes may amplify warming, whereas under the 450ppm scenario, the policy may offset warming of the region.

6.1.1 Development of the SEED configuration

The newly developed seed dispersal process (i.e., the SEED configuration) incorporates the wind-driven seed dispersal mechanism into the CLM-DGVM. This modified CLM-DGVM has been applied for boreal and temperate trees and a different neighboring constraint has been applied for tropical trees. To compute the density of available germinated seeds dispersed by winds, five factors are considered: the fecundity of a tree, the population density of the tree PFT type in surrounding grids, the efficiency of the long-distance dispersal, the number of days of favored winds to a target grid cell from neighboring grid cells, and the germination rate of seeds. A density threshold of 10 germinated seeds per m^2 is applied to determine whether saplings of a tree PFT are allowed to develop in the target grid or not.

6.1.2 Evaluation of the SEED configuration

For evaluation of the SEED configuration, the simulated vegetation structures from the SEED configuration and from the canonical form of CLM-DGVM (i.e, the FREE configuration) have been compared to the satellite-driven AVHRR tree covers. The vegetation structure simulated by the SEED configuration shows better spatial correlations with the AVHRR tree covers than the structure simulated by the FREE configuration. This implies an improved representation of vegetation structure (e.g., of boreal forests in western Siberia and temperate forests in Eastern Europe), when the dynamics include the meteorology-driven seed dispersal mechanism. In the SEED configuration, the competition dynamics of the trees are also modified, which suppresses unrealistic transfers of saplings into a target grid and thus reduces unrealistic competition among the PFTs.

6.1.3 Assessing future vegetation structure under changing climates

Projections of future vegetation structure suggest that greater changes in vegetation distributions are expected in the high latitudes and the mid-latitudes. Shifts in forestry structure by expansion of NET boreal forests and shrinkage of C3 grass Arctic can occur in some high latitude regions, for example, in Alaska and Siberia. In the mid-latitudes, temperate trees are likely to become more favorable in South America, South Africa, and East Asia for later years of the 21st century. Alterations in vegetation structure may also occur in the Tropics between tree PFTs, and also between a tree PFT and a grass PFT. Using an assessment method based on projected changes in future vegetation structure, six regions including Alaska, Greenland, Central America, southern South America, East Africa and East Asia are expected to be vulnerable under both the NP

climate policy scenario and the 450ppm scenario. Greenland, Tibet, South Asia and Northern Australia may become less vulnerable if the 450ppm scenario is implemented.

6.1.4 Assessing changes in the ecosystems induced by changes in vegetation structure

Depending upon the climate mitigation scenarios, the induced change in albedo due to vegetation change is expected to accelerate or alleviate the warming trend of the 21st century under changing climates. Under the NP scenario, proliferation of boreal forests in the high latitudes is expected to cause a positive vegetation-albedo feedback to climate, whereas under the 450ppm scenario, it can buffer the warming trend, since it has a negative feedback. Interception of rainfall by the forest canopy, evapotranspiration, and runoff are all expected to be influenced by changes in future vegetation structure. Replacement of grasses by forests may result in greater rates of interception of water at the tree canopy level, and along with the enhanced absorption of solar radiation by expansion of forests, the vegetation structure change may lead to alterations in evapotranspiration and runoff. The impacts to runoff attributed to vegetation structure change are mostly confined to the Tropics and sub-Tropics, either offsetting or amplifying the increasing trend of runoff by enhanced precipitation due to warming. Calculated NPP and vegetation carbon stock using the SEED configuration agree with the range of estimates from previous studies using DGVMs that make the assumption of ubiquitous and free plant migration; however, the values of this study do not exceed the upper boundary of productivity and vegetation carbon from the previously-reported estimates.

6.2 Remaining limitations and sources of errors

6.2.1 Daily wind profiles

The full IPCC AR4 ensemble dataset of the model-projected future daily wind fields are not available, so that the wind profiles of the available years are repeated for the missing years as surrogates in the simulations of future vegetation structures of the 21st century. The partially-repeated wind profiles may have caused some errors when applying the wind-driven seed mechanisms of the SEED configuration to simulate future vegetation structures.

Use of another model wind dataset from other GCM models from the IPCC AR4 archive can possibly change the result, but even if so, given the similarity of prevailing winds across most GCMs, the change is likely to be negligible. Because the SEED configuration considers only directions of wind vectors, not magnitudes of wind speeds,

it is not expected that the simulated vegetation distributions using the SEED configuration are sensitive to the more subtle differences between differing GCM winds.

Shifts of future wind vectors may also occur due to changes in storm tracks. Bengtsson et al. (2006) reported regional shifts of the future storm tracks such as poleward shifts of storm tracks in both hemispheres, and equatorward shift in the eastern Pacific under the SREA A1B emissions scenario by the end of the 21st century. With the poleward shifts, the seeds of temperate trees may be delivered more effectively to the high latitude regions thus accelerating invasion of temperate trees with the anticipated warming. The equatorward shift may not cause a big difference because the shift of the storm track occurs mainly in the Pacific and makes little impacts on the transfer of seeds.

6.2.2 CO_2 fertilization effect

The CO_2 fertilization effect, which may cause an increase in NPP and decrease in the rate of transpiration, is not taken into account; therefore, potential alterations to the carbon cycle and the water cycle under the influence of the elevated atmospheric CO_2 concentrations are not included in the results of this study. From the model comparison study by Sitch et al. (2008), productivities simulated from five DGVMs are enhanced as the atmospheric CO_2 concentration is elevated (i.e., CO_2 fertilization effect). Further experiments considering both the SEED configuration and the CO2 fertilization effect may provide insights to meteorology-climate-carbon feedbacks of the terrestrial ecosystem.

6.2.3 Nitrogen cycle

The CLM-DGVM version 3.5 does not include the nitrogen cycle. Thus, in the absence of nitrogen dynamics, some estimates of variables such as NPP may have been overestimated. This is especially true at the high latitudes at which the role of nitrogen as a limiting nutrient is reported to be significant (Mitchell and Chandler, 1939; Tamm et al., 1982). Also, as the warming progresses, the carbon-nitrogen interactions are expected to constrain terrestrial carbon uptake in complicated ways (Melillo et al., 1993; Sokolov et al., 2008).

Instead of the full carbon-nitrogen interactions, the CLM-DGVM version 3.5 introduces parameters that mimic nitrogen dynamics such as a nitrogen limitation factor (*fnitr*). In this study, further adjustments are made for the initial condition to provide more realistic NPP values (see Section 2.4 for details of the calibration); however, without describing the full dynamics of carbon-nitrogen interactions, the resulting

biogeochemical variables, especially NPP, may have been estimated with some modest errors. This may have also affected to the simulations of vegetation structures because a couple of processes such as reproduction and mortality in the DGVM are directly associated with the annual NPP value. With more complete nitrogen dynamics coupled to the CLM-DGVM in the future, the simulation results may be improved.

Recently, the CLM version 4 (released on April 2010 to public) considers both carbon and nitrogen dynamics that can be coupled to the DGVM. If combined to the most recent version of the CLM, the SEED configuration could provide more realistic maps of vegetation structure.

6.2.4 Observational datasets and classification of vegetation type

The AVHRR tree cover dataset is obtained from the satellite data of 1992-1993, and the spatial resolution of the dataset is finer (1km) than the resolution of the model (2° x 2.5°) used for this study. In addition, tree types defined in the dataset are categorized either as needleleaf vs. broadleaf (according to leaf morphology), or evergreen vs. deciduous (according to leaf longevity), whereas the CLM-DGVM simulates vegetation structures with seven tree PFTs. Therefore, aggregation of the modeled area of seven tree PFTs to the groups of tree types according to the AVHRR categories may have caused some errors.

Moreover, the CLM-DGVM does not distinguish needleleaf deciduous boreal tree (NDT boreal) and needleleaf evergreen boreal tree (NET boreal), but aggregates the boreal tree types to be NET boreal trees. Therefore, a part of the simulated area occupied by NET boreal forests may actually be designated to NDT boreal forests, which can cause a bias toward overestimation of evergreen trees and underestimation of deciduous trees in the high latitudes in the simulation.

6.2.5 Effect of land use

As the rules in the DGVMs only apply to natural vegetation dynamics, land-use changes influenced by humans (e.g., agriculture) are not simulated. Therefore, projections of vegetation structure in regions where agriculture is dominant and/or large-scale deforestation occurs will not represent land cover change accurately.

6.3 Suggestions for future research

6.3.1 Effect of non-climate, external disturbance of large areas

Recent studies reported the effects of fires to the changes in successional dynamics (Euskirchen et al., 2009), especially for the high latitudes ecosystems (e.g., Euskirchen et al., 2007), and to the terrestrial carbon cycle and ecosystems (e.g., Balshi et al., 2009a, b; Trainor et al., 2009; Yi et al., 2009). The effectiveness and costs of the policy scenario called Reducing Emissions from Deforestation and forest Degradation (REDD) (e.g., Miles and Kapos, 2008), especially applied to the tropical forests, are also in the category of large-scale, non-climate disturbances. With the assumption of land-clearing by non-climate disturbances, further projections of vegetation distributions using the SEED configuration may help improve understanding of the altered dynamics of competition and migration of plants, as well as providing useful information for the calculation of the carbon credits due to forestry change.

6.3.2 Simulations with CO_2 fertilization effect and carbon-nitrogen interactions

As mentioned in Section 6.2.2, the direct effect of elevated CO_2 concentration in the atmosphere on plant functions is not considered in this study. In the absence of these direct effects of the elevated atmospheric CO_2 concentration, productivity may have been underestimated. Another set of simulations forced by increasing atmospheric CO_2 concentration profile is thus desirable to gauge the degree of impacts of physiology forcing to the rate of transpiration (Betts et al., 2007), along with the future vegetation cover change using the SEED configuration.

Furthermore, without consideration of carbon-nitrogen interactions, the potential of terrestrial carbon sequestration capacity may have been overestimated (Hungate et al., 2003), and depending upon the degree of warming in the future climate, terrestrial carbon uptake changes may be negative or positive (Sokolov et al., 2008). Therefore, additional simulations including the CO_2 fertilization effect and/or the nitrogen dynamics, using the SEED configuration, can provide improved estimates of the direction and size of each effect (i.e., elevated CO_2 and carbon-nitrogen interactions) to terrestrial carbon accumulation under changing climates.

6.4 Concluding remarks

This study demonstrates that a series of simulations using the new CLM-DGVM-SEED configuration differs from the simulations in previous studies that exclude the impacts of meteorology-driven seed dispersal mechanisms. Inclusion of the SEED configuration to DGVMs can provide a better representation of current vegetation structure and can help to better understand competition mechanisms and plant migration processes. Furthermore, in projecting future vegetation structure under changing climates, the SEED configuration may provide more comprehensive projections of future plant distribution and its impacts on biogeochemical and biogeophysical processes. As a growing number of studies stress the importance of land-cover change affecting future climates, it is very crucial to include as many essential processes (such as seed dispersal constraints) as possible to current DGVMs.

As forestation is suggested as a way to mitigate greenhouse gases, possible outcomes induced by large-scale tree cover change need to be carefully evaluated because as shown in this study, change in vegetation structure is associated with many other biophysical and biogeochemical processes such as albedo, transpiration, and carbon sequestration changes, which implies potential feedbacks to the climate. Forestation may help to mitigate regional-scale warming but may not help much to mitigate the warming at other neighboring regions. More comprehensive modeling studies that couple meteorology, dynamic vegetation change, biogeophysical processes and biogeochemical processes are needed for assessing the impacts of forestation on the global carbon budget and global radiation budget in the future.

BIBIOGRAPHY

Arnell, N. W., Effects of IPCC SRES emissions scenarios on river runoff: a global perspective, *Hydrology and Earth System Sciences*, **7**, 619-641, 2003.

Arneth. A., S. P. Harrison, S. Zaehle, K. Tsigaridis, S. Menon, P. J. Bartlein, J. Feichter, A. Korhola, M. Kulmala, D. O'Donnell, G. Schrgers, S. Sorvari, and T. Vesala, Terrestrial biogeochemical feedbacks in the climate system, *Nature Geoscience*, **3**, 525-532, 2010.

Balshi, M.S., A.D. McGuire, P. Duffy, D.W. Kicklighter, and J. Melillo. Vulnerability of carbon storage in North American boreal forests to wildfires during the 21st Century. *Global Change Biology*, **15**, 1491-1510, 2009.

Balshi, M.S., A.D. McGuire, P. Duffy, M. Flannigan, J. Walsh, and J. Melillo, Assessing the response of area burned to changing climate in western boreal North America using a, Multivariate Adaptive Regression Splines (MARS) approach. *Global Change Biology*, **15**, 578-600, 2009.

Bengtsson, L., K. I. Hodges, and E. Roeckner, Storm Tracks and Climate Change, *Journal of Climate,* **19**, 3518-3543, 2006.

Betts, R. A., Offset of the potential carbon sink from boreal forestation by decreases in surface albedo, *Nature*, 408, 187-190, 2000.

Betts, R. A., O. Boucher, M. Collins, P. M. Cox, P. D. Falloon, N. Gedney, D. L. Hemming, C. Huntingford, C. D. Jones, D. M. H. Sexton, and M. J. Webb, Projected increase in continental runoff due to plant responses to increasing carbon dioxide, *Nature*, 448, 1037-1041, 2007.

Bonan, G. B., S. Levis, L. Kergoat, and K. W. Oleson, Landscapes as patches of plant functional types: An integrating concept for climate and ecosystem models, Global Biogeochemical Cycles, **16 (2)**, 10.1029/2000GB001360, 2002.

Bonan, G. B., S. Levis, S. Sitch, M. Vertenstein, and K. W. Oleson, A dynamic global vegetation model for use with climate models: concepts and description of simulated vegetation dynamics. *Global Change Biology*, **9**, 1543-1566, 2003.

Bonan, G. B., and S. Levis, Evaluating Aspects of the Community Land and Atmosphere Models (CLM3 and CAM3) Using a Dynamic Global Vegetation Model, *Journal of Climate*, **19**, 2290-2301, 2006.

Bonan, G. B., Forests and Climate Change: Forcings, Feedbacks, and the Climate Benefits of Forests, *Science*, **320**, 1444-1449, 2008.

Canadell, J. G. and M. R. Raupach, Managing Forests for Climate Change Mitigation, *Science*, **320**, 1456-1457, 2008.

Chapin III, F. S., M. Strum, M.C. Serreze, J. P. McFadden, J. R. Key, A. H. Lloyd, A. D. McGuire, T. S. Rupp, A. H. Lynch, J. P. Schimel, J. Beringer, W. L. Chapman, H. E. Epstein, E. S. Euskirchen, L. D. Hinzman, G. Jia, C. –L, Ping, K. D. Tape, C. D. C. Thompson, D. A. Walker and J. M. Welker, Role of Land-Surface Changes in Arctic Summer Warming, *Science*, **310**, 657-660, 2005.

Clark, J. S., C. Fastie, G. Hurtt, S. T. Jackson, C. Johnson, G. A. King, M. Lewis, K. Lynch, S. Pacala, C. Prentice, E. W. Schupp, T. Webb III, and P. Wyckoff, Reid's Paradox of Rapid Plant Migration, *Bioscience*, **48(1)**, 1998.

Cox, P. M., R. A. Betts, C. D. Jones, S. A. Spall and I. J. Totterdell, Acceleration of global warming due to carbon-cycle feedbacks in a coupled climate model, *Nature*, **408**, 184-187, 2000.

Cox, P. M., Description of the "TRIFFID" dynamic global vegetation model, Hadley center technical note 24, 2001.

Davis, M. B., Lags in vegetation response to greenhouse warming, *Climatic Change*, **15**, 75-82, 1989.

DeFries, R. S. M. C. Hansen, J. R. G. Townshend, A. C. Janetos, and T. R. Loveland, A new global 1-km dataset of percentage tree cover derived from remote sensing, *Global Change Biology*, 6, 247-254, 2000.

Devi, N., F. Hagedorn, P. Moiseev, H. Bugman, S. Shiyatov, V. Mazepa, and A. Rigling, Expanding forests and changing growth forms of Siberian larch at the Polar Urals treeline during the 20th century, *Global Change Biology*, 14, 1581-1591, 2008.

Dickinson, R. E., K. W. Oleson, G. Bonan, F. Hoffman, P. Thornton, M. Vertenstein, Z.-L. Yang, and X. Zeng, The Community Land Model and its climate statistics as a component of the Community Climate System Model, *Journal of Climate*, 19, 2302– 2324, 2006.

Esper, J., and F. H. Schweingruber, Large-scale treeline changes recorded in Siberia. *Geophysical Research Letters*, 31, L06202, 2004: doi: 10.1029/2003GL019178.

Euskirchen, E. S., A. D. McGuire, F. S. Chapin, S. Yi, and C. C. Thompson, Changes in vegetation in northern Alaska under scenarios of climate change, 2003–2100: implications for climate feedbacks, *Ecological Applications*, 19, 1022–1043, 2009.

Euskirchen, E. S., A. D. McGuire, T. S. Rupp, F. S. Chapin, and J. E. Walsh, Projected changes in atmospheric heating due to changes in fire disturbance and the snow season in the western Arctic, 2003–2100, *Journal of Geophysical Research*, 114, 2009, doi:10.1029/2009JG001095.

Feddema, J. J., K. W. Oleson, G. B. Bonan, L. O. Mearns, L. E. Buja, G. A. Meehl, and W. M. Washington, The importance of land-cover change in simulating future climates, *Science*, 310, 1674-1678, 2005.

Foley, J. A., I. C. Prentice, N. Ramankutty, S. Levis, D. Pollard, S. Sitch, and A. Haxeltine, An integrated biosphere model of land surface processes, terrestrial carbon balance, and vegetation dynamics, *Global Biogeochem. Cycles*, *10*(4), 603–628, 1996, doi:10.1029/96GB02692.

Gerten, D., W. Lucht, S. Schaphoff, W. Cramer, T. Hickler, and W. Wagner, Hydrologic resilience of the terrestrial biosphere, *Geophys. Res. Lett.*, *32*, L21408, 2005, doi:10.1029/2005GL024247.

Giorgi, F., and R. Francisco, Evaluating uncertainties in the prediction of regional climate change, *Geophysical Research Letters*, 27(9), 1295-1298, 2000.

Giorgi, F. and R. Francisco, Uncertainties in regional climate change predictions. A regional analysis of ensemble simulations with the HADCM2 GCM, *Climate Dynamics*, 16, 169-182, 2000.

Hack, J. J., J. M. Caron, S. G. Yeager, K. W. Oleson, M. M. Holland, J. E. Truesdale, and P. J. Rasch, Simulation of the global hydrological cycle in the CCSM Community Atmosphere Model version 3 (CAM3): mean features, *Journal of Climate*,19, 2199– 2221, 2006.

Hegerl, G.C., F. W. Zwiers, P. Braconnot, N.P. Gillett, Y. Luo, J.A. Marengo Orsini, N. Nicholls, J.E. Penner and P.A. Stott, 2007: Understanding and Attributing Climate Change. In: *Climate Change 2007: The Physical Science Basis. Contribution of Working Group I to the Fourth Assessment Report of the Intergovernmental Panel on Climate Change* [Solomon, S., D. Qin, M. Manning, Z. Chen, M. Marquis,K.B. Averyt, M. Tignor and H.L. Miller (eds.)]. Cambridge University Press, Cambridge, United Kingdom and New York, NY, USA.

Higgins, P.A.T., and J. Harte, Biophysical and Biogeochemical Responses to Climate Change Depend on Dispersal and Migration, *BioScience*, 56 (5), 407-417, 2006.

Hungate, B. A., J. S. Dukes, M. R. Shaw, Y. Luo, Nitrogen and climate change, *Science*, 302, 2003.

Huntingford, C., R. A. Fisher, L. Mercado, B. B. B. Booth, S. Sitch, P. P. Harris, P. M. Cox, C. D. Jones, R. A. Betts, Y. Malhi, G. R. Harris, M. Collins, and P. Moorcroft, Towards quantifying uncertainty in predictions of Amazon 'dieback', *Phil. Trans. R. Soc. B*, 363 (1498), 2008, 1857-1864.

IPCC, 2007: Climate Change 2007: Impacts, Adaptations and Vulnerability. Contribution of Working Group II to the Fourth Assessment Report of the Intergovernmental Panel on Climate Change, M. L. Parry, O. F. Canziani, J. P. Palutikof, P. J. van der Linden and C. E. Hanson, Eds., Cambridge University Press, Cambridge, UK, pp976.

Iversen, J., The late-glacial flora of Denmark and its relation to climate and soil, *Danm. Geol. Unders*, 1954.

Krinner, G., N. Viovy, N. de Noblet-Ducoudre´, J. Oge´e, J. Polcher, P. Friedlingstein, P. Ciais, S. Sitch, and I. C. Prentice, A dynamic global vegetation model for studies of the coupled atmosphere-biosphere system, *Global Biogeochemical Cycles*, 19, 2005, GB1015,

doi:10.1029/2003GB002199.

Kucharik, C. J., J. A. Foley, C. Delire, V. A. Fisher, M. T. Coe, J. D. Lenters, C. Young-Molling, N. Ramankutty, J. M. Norman, and S. T. Gower, Testing the performance of a Dynamic Global Ecosystem Model: Water balance, carbon balance, and vegetation structure, *Global Biogeochemical Cycles*, 14 (3), 795-825, 2000.

Kullman, L., Rapid recent range-margin rise of tree and shrub species in the Swedish Scandes. *Journal of Ecology*, 90, 68–77, 2002.

Lawrence, D. M., P. E. Thornton, K. W. Oleson, and G. B. Bonan , The partitioning of evapotranspiration into transpiration, soil evaporation, and canopy evaporation in a GCM: Impacts on land-atmosphere interaction, *Journal of Hydrometeorology*, 8, 862–880, 2007.

Levis, S., M. Vertenstein, and K. W. Oleson, The Community Land Model's dynamic global vegetation model (CLM-DGVM): Technical description and user's guide. NCAR Tech. Note TN-459_IA, 2004.

Lucht, W., S. Schaphoff, T. Erbrecht, U. Heyder, and W. Cramer, Terrestrial vegetation redistribution and carbon balance under climate change, *Carbon Balance and Management*, 1-6, 2006.

Lloyd, A. H., Ecological histories from Alaskan tree lines provide insight into future change, *Ecology*, 86, 1687–1695, 2005.

MacDonald, G. M., T. W. D. Edwards, K. A. Moser, R. Pienitz, and J. P. Smol, Rapid response of treeline vegetation and lakes to past climate warming, *Nature*, 361, 243-246, 1993.

Moiseev, P. A. and S. G. Shiyatov, Vegetation dynamics at the treeline ecotone in the Ural Highlands, Russia. *Ecological Studies*, 167, 423–435, 2003.

Nathan, R., G. G. Katul, H. S. Horn, S. M. Thomas, R. Oren, R. Avissar, S. W. Pacala, and S. A. Levin, Mechanisms of long-distance dispersal of seeds by wind, *Nature*, 418, 409-413, 2002.

Neilson, R. P., L.F. Pitelka, A. M. Solomon, R. Nathan, G. F. Midgley, J. M. V. Fragoso, H. Lischke, and K. Thompson, Forecasting Regional to Global Plant Migration in Response to Climate Change, *BioScience*, 55(9), 749-759, 2005.

Oleson, K .W., G. –Y. Niu, Z. –L. Yang, D. M. Lawrence, P. E. Thornton, P. J. Lawrence, R. Stockli, R. E. Dickinson, G. B. Bonan, and S. Levis, CLM 3.5 Documentation, National Center for Atmospheric Research, Boulder, CO, USA, 2007.

Schaphoff, S., W. Lucht, D. Gerten, S. Sitch, W. Cramer, and I. Prentice, Terrestrial biosphere carbon storage under alternative climate projections, *Climatic Change*, 74, 97-122, 2006.

Sauer, J. D., Plant Migration: the Dynamics of Geograpjic Patterning in Seed Plant Species, University of California Press, Berkley and Los Angeles, CA, 1988.

Sitch, S., B. Smith, I. C. Prentice, A. Arneth, A. Bondeau, W. Cramer, J. O. Kaplan, S. Levis, W. Lucht, M. T. Sykes, K. Thonicke, and S. Venevsky, Evaluation of ecosystem dynamics, plant geography, and terrestrial carbon cycling in the LPJ dynamic global vegetation model, *Global Change Biology*, 9, 161-185, 2003.

Sitch, S, C. Huntington, N. Gedney, P. E. Levy, M. Lomas, S. L. Piao, R. Betts, P. Ciais, P. Cox, P. Friedlingstein, C. D. Jones, I. C. Prentice, and F. I. Woodward, Evaluation of the terrestrial carbon cycle, future plant geography and climate-carbon cycle feedbacks using five Dynamic Global Vegetation Models (DGVMs), *Global Change Biology*, 14, 2015-2039, 2008.

Sokolov, A. P., P. H. Stone, C. E. Forest, R. Prinn, M. C. Sarofim, M. Webster, S. Paltsev, C. A. Schlosser, D. Kicklighter, S. Dutkiewicz, J. Reilly, C. Wang, B. Felzer, J. M. Melillo, and H. D. Jacoby, Probabilistic Forecast for Twenty-First-Century Climate Based on Uncertainties in Emissions (Without Policy) and Climate Parameters, *Journal of Climate*, **22**, 5175–5204, 2009: doi: 10.1175/2009JCLI2863.1.

Sokolov, A. P., D. W. Kicklighter, J. M. Melillo, B. S. Felzer, C. A. Schlosser, T. W. Cronin, Consequences of Considering Carbon–Nitrogen Interactions on the Feedbacks between Climate and the Terrestrial Carbon Cycle. *Journal of Climate*, **21**, 3776–3796, 2008: doi: 10.1175/2008JCLI2038.1

Swann, A. L., I. Y. Fung, S. Levis, G. B. Bonan, and S. C. Doney, Changes in Arctic vegetation amplify high-latitude warming through the greenhouse effect, *Proceedings of the National Academy of Sciences*, 107 (4), 1295-1300.

Solomon, A. M. and A. P. Kirilenko, Climate change and terrestrial biomass: what if trees do not migration?, *Global Ecology and biogeography letters*, 6, 139-148, 1997.

Trainor, S.F., M. Calef, D. Natcher, F.S. Chapin III, A.D. McGuire, O. Huntington, P. Duffy, T.S. Rupp, L. DeWilde, M. Kwart, N. Fresco, and A.L. Lovecraft. 2009. Vulnerability and adaptation to climate-related fire impacts in rural and urban interior Alaska, *Polar Research*, 28,100-118.

Trenberth, K. E., A. Dai, R. M. Rasmussen, and D. B. Parsons, The changing character of precipitation, *Bulletin of American Meteorological Society*, 1205-1217, 2003.

Van Minnen, J.G., R. Leemans, and F. Ihle, Defining the importance of including transient ecosystem responses to simulate C-cycle dynamics in a global change model, *Global Change Biology*, 6, 595-611, 2000.

Woodward, F. I. and M. R. Lomas, Simulating vegetation processes along the Kalahari transect, *Global Change Biology*, 10(3), 383–392, 2004.

Yi, S., A.D. McGuire, J. Harden, E. Kasaschke, K. Manies, L. Hinzman, A. Liljedahl, J. Randerson, H. Liu, V. Romanovsky, S. Marchenko, and Y Kim, Interactions between soil thermal and hydrological dynamics in the response of Alaska ecosystems to fire disturbance. *Journal of Geophysical Research – Biogeosciences*, 114, G02015, 2009: doi:10.1029/2008JG000841.

Zeng, X., Evaluating the dependence of vegetation on climate in an improved dynamic global vegetation model, *Advances in Atmospheric Sciences*, 27 (5), 977-991, 2010.

Spatial correlation coefficients of NET boreal forest from the SEED configuration vs. AVHRR needleleaf treecover (180W-0W)

SD vs NOBL	180W-170W	170W-160W	160W-150W	150W-140W	140W-130W	130W-120W	120W-110W	110W-100W	100W-90W	90W-80W	80W-70W	70W-60W	60W-50W	50W-40W	40W-30W	30W-20W	20W-10W	10W-0W
80N-90N	-	-	-	-	-	-	-	-	-	-	-	-	-	-	-	-	-	-
70N-80N	-	-	-	-	-	-	-	-	-	-	-	-	-	-	-	-	-	-
60N-70N	-	0.22	0.74	0.24	0.11	-0.01	0.47	0.97	-	-	-	-	-	-	-	1.00	1.00	-
50N-60N	-	-1.00	0.50	-	0.48	0.84	0.65	0.34	0.23	0.68	0.67	-0.34	0.39	-	-	-	-	-1.00
40N-50N	-	-	-	-	-	0.93	0.95	-	0.33	0.15	-0.17	0.24	0.92	-	-	-	-	-
30N-40N	-	-	-	-	-	-	-	-	-	-	-	-	-	-	-	-	-	-
20N-30N	-	-	-	-	-	-	-	-	-	-	-	-	-	-	-	-	-	-
10N-20N	-	-	-	-	-	-	-	-	-	-	-	-	-	-	-	-	-	-
0N-10N	-	-	-	-	-	-	-	-	-	-	-	-	-	-	-	-	-	-
10S-0S	-	-	-	-	-	-	-	-	-	-	-	-	-	-	-	-	-	-
20S-10S	-	-	-	-	-	-	-	-	-	-	-	-	-	-	-	-	-	-
30S-20S	-	-	-	-	-	-	-	-	-	-	-	-	-	-	-	-	-	-
40S-30S	-	-	-	-	-	-	-	-	-	-	-	-	-	-	-	-	-	-
50S-40S	-	-	-	-	-	-	-	-	-	-	-	-	-	-	-	-	-	-
60S-50S	-	-	-	-	-	-	-	-	-	-	-	-	-	-	-	-	-	-
70S-60S	-	-	-	-	-	-	-	-	-	-	-	-	-	-	-	-	-	-
80S-70S	-	-	-	-	-	-	-	-	-	-	-	-	-	-	-	-	-	-
90S-80S	-	-	-	-	-	-	-	-	-	-	-	-	-	-	-	-	-	-

Spatial correlation coefficients of NET boreal forest from the SEED vs. AVHRR needleleaf treecover (0E-180E)

SD vs NOBL	0E-10E	10E-20E	20E-30E	30E-40E	40E-50E	50E-60E	60E-70E	70E-80E	80E-90E	90E-100E	100E-110E	110E-120E	120E-130E	130E-140E	140E-150E	150E-160E	160E-170E	170E-180E
80N-90N	-	-	-	-	-	-	-	-	-	-	-	-	-	-	-	-	-	-
70N-80N	-	-	0.01	-	-	-	-	-	-	-	-	-	-	-	-	-	-	-
60N-70N	0.97	0.70	0.20	0.08	0.80	-0.28	0.67	0.51	0.63	-	-	-	-	-	-	-	-	-
50N-60N	-1.00	0.46	0.39	0.51	-	-0.68	-	0.88	-0.50	0.32	0.60	-	-	-	1.00	0.83	0.98	-
40N-50N	-	0.82	-0.32	-	0.11	-	-	-	-	-	-	-	-	-	-	-	-	-
30N-40N	-	-	-	-	-	-	-	1.00	-	-	-0.53	-	-	-	-	-	-	-
20N-30N	-	-	-	-	-	-	-	-	-	1.00	-	-	-	-	-	-	-	-
10N-20N	-	-	-	-	-	-	-	-	-	-	-	-	-	-	-	-	-	-
0N-10N	-	-	-	-	-	-	-	-	-	-	-	-	-	-	-	-	-	-
10S-0S	-	-	-	-	-	-	-	-	-	-	-	-	-	-	-	-	-	-
20S-10S	-	-	-	-	-	-	-	-	-	-	-	-	-	-	-	-	-	-
30S-20S	-	-	-	-	-	-	-	-	-	-	-	-	-	-	-	-	-	-
40S-30S	-	-	-	-	-	-	-	-	-	-	-	-	-	-	-	-	-	-
50S-40S	-	-	-	-	-	-	-	-	-	-	-	-	-	-	-	-	-	-
60S-50S	-	-	-	-	-	-	-	-	-	-	-	-	-	-	-	-	-	-
70S-60S	-	-	-	-	-	-	-	-	-	-	-	-	-	-	-	-	-	-
80S-70S	-	-	-	-	-	-	-	-	-	-	-	-	-	-	-	-	-	-
90S-80S	-	-	-	-	-	-	-	-	-	-	-	-	-	-	-	-	-	-

Spatial correlation coefficients of NET boreal forest from the FREE vs. AVHRR needleleaf treecover (180W-0W)

FR vs NOBL	180W - 170W	170W - 160W	160W - 150W	150W - 140W	140W - 130W	130W - 120W	120W - 110W	110W - 100W	100W -90W	90W- 80W	80W- 70W	70W- 60W	60W- 50W	50W- 40W	40W- 30W	30W- 20W	20W- 10W	10W- 0W
80N-90N	-	-	-	-	-	-	-	-	-	-	-	-	-	-	-	-	-	-
70N-80N	-	-	-	-	-	-	-	-	-	-	-	-	-	-	-	-	-	-
60N-70N	-	-0.07	0.72	0.19	0.13	-0.05	0.52	0.95	-	-	-	-	-	-	-	-	1.00	-
50N-60N	-	-1.00	0.28	-	0.44	0.76	0.65	0.35	0.40	0.76	0.72	1.00	0.04	-	-	-	-	-1.00
40N-50N	-	-	-	-	-	0.93	-1.00	-	0.27	0.15	-0.17	0.24	0.92	-	-	-	-	-
30N-40N	-	-	-	-	-	-	-	-	-	-	-	-	-	-	-	-	-	-
20N-30N	-	-	-	-	-	-	-	-	-	-	-	-	-	-	-	-	-	-
10N-20N	-	-	-	-	-	-	-	-	-	-	-	-	-	-	-	-	-	-
0N-10N	-	-	-	-	-	-	-	-	-	-	-	-	-	-	-	-	-	-
10S-0S	-	-	-	-	-	-	-	-	-	-	-	-	-	-	-	-	-	-
20S-10S	-	-	-	-	-	-	-	-	-	-	-	-	-	-	-	-	-	-
30S-20S	-	-	-	-	-	-	-	-	-	-	-	-	-	-	-	-	-	-
40S-30S	-	-	-	-	-	-	-	-	-	-	-	-	-	-	-	-	-	-
50S-40S	-	-	-	-	-	-	-	-	-	-	-	-	-	-	-	-	-	-
60S-50S	-	-	-	-	-	-	-	-	-	-	-	-	-	-	-	-	-	-
70S-60S	-	-	-	-	-	-	-	-	-	-	-	-	-	-	-	-	-	-
80S-70S	-	-	-	-	-	-	-	-	-	-	-	-	-	-	-	-	-	-
90S-80S	-	-	-	-	-	-	-	-	-	-	-	-	-	-	-	-	-	-

Spatial correlation coefficients of NET boreal forest from the FREE vs. AVHRR needleleaf treecover (0E-180E)

FR vs NOBL	0E-10E	10E-20E	20E-30E	30E-40E	40E-50E	50E-60E	60E-70E	70E-80E	80E-90E	90E-100E	100E-110E	110E-120E	120E-130E	130E-140E	140E-150E	150E-160E	160E-170E	170E-180E
80N-90N	-	-	-	-	-	-	-	-	-	-	-	-	-	-	-	-	-	-
70N-80N	-	-	0.01	-	-	-	-	-	-	-	-	-	-	-	-	-	-	-
60N-70N	0.97	0.70	0.27	0.09	0.80	-0.23	0.61	0.52	0.69	0.79	-	-	-	-	-	-	-	-
50N-60N	-1.00	0.45	0.39	0.51	-	-0.68	-	0.88	-0.50	0.29	0.66	-	-	-	-	0.66	1.00	-
40N-50N	-	0.84	-0.32	-	0.11	-	-	-	-	-	-	-	-	-	-	-	-	-
30N-40N	-	-	-	-	-	-	-	1.00	-	-	-0.53	-	-	-	-	-	-	-
20N-30N	-	-	-	-	-	-	-	-	-	1.00	-	-	-	-	-	-	-	-
10N-20N	-	-	-	-	-	-	-	-	-	-	-	-	-	-	-	-	-	-
0N-10N	-	-	-	-	-	-	-	-	-	-	-	-	-	-	-	-	-	-
10S-0S	-	-	-	-	-	-	-	-	-	-	-	-	-	-	-	-	-	-
20S-10S	-	-	-	-	-	-	-	-	-	-	-	-	-	-	-	-	-	-
30S-20S	-	-	-	-	-	-	-	-	-	-	-	-	-	-	-	-	-	-
40S-30S	-	-	-	-	-	-	-	-	-	-	-	-	-	-	-	-	-	-
50S-40S	-	-	-	-	-	-	-	-	-	-	-	-	-	-	-	-	-	-
60S-50S	-	-	-	-	-	-	-	-	-	-	-	-	-	-	-	-	-	-
70S-60S	-	-	-	-	-	-	-	-	-	-	-	-	-	-	-	-	-	-
80S-70S	-	-	-	-	-	-	-	-	-	-	-	-	-	-	-	-	-	-
90S-80S	-	-	-	-	-	-	-	-	-	-	-	-	-	-	-	-	-	-

Difference of spatial correlation between NET boreal (SEED) vs. AVHRR needleleaf and NET boreal (FREE) vs. AVHRR needleleaf (180W-0W). Stronger correlations by the SEED are highlighted in yellow and less stronger correlation by the SEED in pink.

DIFF	180W-170W	170W-160W	160W-150W	150W-140W	140W-130W	130W-120W	120W-110W	110W-100W	100W-90W	90W-80W	80W-70W	70W-60W	60W-50W	50W-40W	40W-30W	30W-20W	20W-10W	10W-0W
80N-90N	-	-	-	-	-	-	-	-	-	-	-	-	-	-	-	-	-	-
70N-80N	-	-	-	-	-	-	-	-	-	-	-	-	-	-	-	-	-	-
60N-70N	-	**0.29**	**0.01**	**0.05**	-0.02	**0.05**	-0.05	**0.02**	-	-	-	-	-	-	-	**1.00**	-	-
50N-60N	-	-	**0.22**	-	**0.03**	**0.08**	-	-0.01	-0.17	-0.08	-0.05	-1.34	**0.35**	-	-	-	-	-
40N-50N	-	-	-	-	-	-	**1.95**	-	**0.07**	-	-	-	-	-	-	-	-	-
30N-40N	-	-	-	-	-	-	-	-	-	-	-	-	-	-	-	-	-	-
20N-30N	-	-	-	-	-	-	-	-	-	-	-	-	-	-	-	-	-	-
10N-20N	-	-	-	-	-	-	-	-	-	-	-	-	-	-	-	-	-	-
0N-10N	-	-	-	-	-	-	-	-	-	-	-	-	-	-	-	-	-	-
10S-0S	-	-	-	-	-	-	-	-	-	-	-	-	-	-	-	-	-	-
20S-10S	-	-	-	-	-	-	-	-	-	-	-	-	-	-	-	-	-	-
30S-20S	-	-	-	-	-	-	-	-	-	-	-	-	-	-	-	-	-	-
40S-30S	-	-	-	-	-	-	-	-	-	-	-	-	-	-	-	-	-	-
50S-40S	-	-	-	-	-	-	-	-	-	-	-	-	-	-	-	-	-	-
60S-50S	-	-	-	-	-	-	-	-	-	-	-	-	-	-	-	-	-	-
70S-60S	-	-	-	-	-	-	-	-	-	-	-	-	-	-	-	-	-	-
80S-70S	-	-	-	-	-	-	-	-	-	-	-	-	-	-	-	-	-	-
90S-80S	-	-	-	-	-	-	-	-	-	-	-	-	-	-	-	-	-	-

Difference of spatial correlation between NET boreal (SEED) vs. AVHRR needleleaf and NET boreal (FREE) vs. AVHRR needleleaf (0E-180E). Stronger correlations by the SEED are highlighted in yellow and less stronger correlation by the SEED in pink.

DIFF	0E-10E	10E-20E	20E-30E	30E-40E	40E-50E	50E-60E	60E-70E	70E-80E	80E-90E	90E-100E	100E-110E	110E-120E	120E-130E	130E-140E	140E-150E	150E-160E	160E-170E	170E-180E
80N-90N	-	-	-	-	-	-	-	-	-	-	-	-	-	-	-	-	-	-
70N-80N	-	-	-	-	-	-	-	-	-	-	-	-	-	-	-	-	-	-
60N-70N	-	-	-0.07	-	-0.01	-0.05	**0.06**	-0.02	-0.07	-0.29	-	-	-	-	-	-	-	-
50N-60N	-	**0.01**	-	-	-	-	-	-	-	**0.03**	-0.06	-	-	-	**1.00**	**0.17**	-0.01	-
40N-50N	-	-0.01	-	-	-	-	-	-	-	-	-	-	-	-	-	-	-	-
30N-40N	-	-	-	-	-	-	-	-	-	-	-	-	-	-	-	-	-	-
20N-30N	-	-	-	-	-	-	-	-	-	-	-	-	-	-	-	-	-	-
10N-20N	-	-	-	-	-	-	-	-	-	-	-	-	-	-	-	-	-	-
0N-10N	-	-	-	-	-	-	-	-	-	-	-	-	-	-	-	-	-	-
10S-0S	-	-	-	-	-	-	-	-	-	-	-	-	-	-	-	-	-	-
20S-10S	-	-	-	-	-	-	-	-	-	-	-	-	-	-	-	-	-	-
30S-20S	-	-	-	-	-	-	-	-	-	-	-	-	-	-	-	-	-	-
40S-30S	-	-	-	-	-	-	-	-	-	-	-	-	-	-	-	-	-	-
50S-40S	-	-	-	-	-	-	-	-	-	-	-	-	-	-	-	-	-	-
60S-50S	-	-	-	-	-	-	-	-	-	-	-	-	-	-	-	-	-	-
70S-60S	-	-	-	-	-	-	-	-	-	-	-	-	-	-	-	-	-	-
80S-70S	-	-	-	-	-	-	-	-	-	-	-	-	-	-	-	-	-	-
90S-80S	-	-	-	-	-	-	-	-	-	-	-	-	-	-	-	-	-	-

Spatial correlation coefficients of NET temperate forest from the SEED vs. AVHRR needleleaf treecover (180W-0W)

SD vs NOBL	180W-170W	170W-160W	160W-150W	150W-140W	140W-130W	130W-120W	120W-110W	110W-100W	100W-90W	90W-80W	80W-70W	70W-60W	60W-50W	50W-40W	40W-30W	30W-20W	20W-10W	10W-0W
80N-90N	–	–	–	–	–	–	–	–	–	–	–	–	–	–	–	–	–	–
70N-80N	–	–	–	–	–	–	–	–	–	–	–	–	–	–	–	–	–	–
60N-70N	–	–	–	–	–	–	–	–	–	–	–	–	–	–	–	–	–	–
50N-60N	–	–	–	–	–	–	–	–	–	–	–	–	–	–	–	–	–	0.83
40N-50N	–	–	–	–	–	1.00	–	–	–	–	–	–	–	–	–	–	–	–
30N-40N	–	–	–	–	–	–	–	–	-0.56	-1.00	1.00	–	–	–	–	–	–	–
20N-30N	–	–	–	–	–	–	–	–	–	–	–	–	–	–	–	–	–	–
10N-20N	–	–	–	–	–	–	–	–	–	–	–	–	–	–	–	–	–	–
0N-10N	–	–	–	–	–	–	–	–	–	–	–	–	–	–	–	–	–	–
10S-0S	–	–	–	–	–	–	–	–	–	–	–	–	–	–	–	–	–	–
20S-10S	–	–	–	–	–	–	–	–	–	–	–	–	–	–	–	–	–	–
30S-20S	–	–	–	–	–	–	–	–	–	–	–	–	–	–	–	–	–	–
40S-30S	–	–	–	–	–	–	–	–	–	–	–	–	–	–	–	–	–	–
50S-40S	–	–	–	–	–	–	–	–	–	–	–	–	–	–	–	–	–	–
60S-50S	–	–	–	–	–	–	–	–	–	–	–	–	–	–	–	–	–	–
70S-60S	–	–	–	–	–	–	–	–	–	–	–	–	–	–	–	–	–	–
80S-70S	–	–	–	–	–	–	–	–	–	–	–	–	–	–	–	–	–	–
90S-80S	–	–	–	–	–	–	–	–	–	–	–	–	–	–	–	–	–	–

Spatial correlation coefficients of NET temperate forest from the SEED vs. AVHRR needleleaf treecover (0E-180E)

SD vs NOBL	0E-10E	10E-20E	20E-30E	30E-40E	40E-50E	50E-60E	60E-70E	70E-80E	80E-90E	90E-100E	100E-110E	110E-120E	120E-130E	130E-140E	140E-150E	150E-160E	160E-170E	170E-180E
80N-90N	_	_	_	_	_	_	_	_	_	_	_	_	_	_	_	_	_	_
70N-80N	_	_	_	_	_	_	_	_	_	_	_	_	_	_	_	_	_	_
60N-70N	_	_	_	_	_	_	_	_	_	_	_	_	_	_	_	_	_	_
50N-60N	0.32	_	_	_	_	_	_	_	_	_	_	_	_	_	_	_	_	_
40N-50N	0.95	_	1.00	_	_	_	_	_	_	_	_	_	_	_	_	_	_	_
30N-40N	_	_	_	_	_	_	_	_	_	_	0.47	0.29	-0.30	0.96	1.00	_	_	_
20N-30N	_	_	_	_	_	_	_	_	-1.00	-0.46	0.25	0.71	_	_	_	_	_	_
10N-20N	_	_	_	_	_	_	_	_	_	_	_	_	_	_	_	_	_	_
0N-10N	_	_	_	_	_	_	_	_	_	_	_	_	_	_	_	_	_	_
10S-0S	_	_	_	_	_	_	_	_	_	_	_	_	_	_	_	_	_	_
20S-10S	_	_	_	_	1.00	_	_	_	_	_	_	_	_	_	_	_	_	_
30S-20S	_	_	_	_	_	_	_	_	_	_	_	_	_	_	_	_	_	_
40S-30S	_	_	_	_	_	_	_	_	_	_	_	_	_	_	_	_	_	_
50S-40S	_	_	_	_	_	_	_	_	_	_	_	_	_	_	_	_	-1.00	_
60S-50S	_	_	_	_	_	_	_	_	_	_	_	_	_	_	_	_	_	_
70S-60S	_	_	_	_	_	_	_	_	_	_	_	_	_	_	_	_	_	_
80S-70S	_	_	_	_	_	_	_	_	_	_	_	_	_	_	_	_	_	_
90S-80S	_	_	_	_	_	_	_	_	_	_	_	_	_	_	_	_	_	_

Spatial correlation coefficients of NET temperate forest from the FREE vs. AVHRR needleleaf treecover (180W-0W)

FR vs NOBL	180W-170W	170W-160W	160W-150W	150W-140W	140W-130W	130W-120W	120W-110W	110W-100W	100W-90W	90W-80W	80W-70W	70W-60W	60W-50W	50W-40W	40W-30W	30W-20W	20W-10W	10W-0W
80N-90N	–	–	–	–	–	–	–	–	–	–	–	–	–	–	–	–	–	–
70N-80N	–	–	–	–	–	–	–	–	–	–	–	–	–	–	–	–	–	–
60N-70N	–	–	–	–	–	–	–	–	–	–	–	–	–	–	–	–	–	–
50N-60N	–	–	–	–	–	–	–	–	–	–	–	–	–	–	–	–	–	0.83
40N-50N	–	–	–	–	–	0.08	–	–	–	–	–	–	–	–	–	–	–	–
30N-40N	–	–	–	–	–	–	–	–	-0.14	0.01	-0.23	–	–	–	–	–	–	–
20N-30N	–	–	–	–	–	–	–	–	–	–	–	–	–	–	–	–	–	–
10N-20N	–	–	–	–	–	–	–	–	–	–	–	–	–	–	–	–	–	–
0N-10N	–	–	–	–	–	–	–	–	–	–	–	–	–	–	–	–	–	–
10S-0S	–	–	–	–	–	–	–	–	–	–	–	–	–	–	–	–	–	–
20S-10S	–	–	–	–	–	–	–	–	–	–	–	–	–	–	–	–	–	–
30S-20S	–	–	–	–	–	–	–	–	–	–	–	–	–	–	–	–	–	–
40S-30S	–	–	–	–	–	–	–	–	–	–	–	–	–	–	–	–	–	–
50S-40S	–	–	–	–	–	–	–	–	–	–	–	–	–	–	–	–	–	–
60S-50S	–	–	–	–	–	–	–	–	–	–	–	–	–	–	–	–	–	–
70S-60S	–	–	–	–	–	–	–	–	–	–	–	–	–	–	–	–	–	–
80S-70S	–	–	–	–	–	–	–	–	–	–	–	–	–	–	–	–	–	–
90S-80S	–	–	–	–	–	–	–	–	–	–	–	–	–	–	–	–	–	–

Spatial correlation coefficients of NET temperate forest from the FREE vs. AVHRR needleleaf treecover (0E-180E)

FR vs NOBL	0E-10E	10E-20E	20E-30E	30E-40E	40E-50E	50E-60E	60E-70E	70E-80E	80E-90E	90E-100E	100E-110E	110E-120E	120E-130E	130E-140E	140E-150E	150E-160E	160E-170E	170E-180E
80N-90N	–	–	–	–	–	–	–	–	–	–	–	–	–	–	–	–	–	–
70N-80N	–	–	–	–	–	–	–	–	–	–	–	–	–	–	–	–	–	–
60N-70N	–	–	–	–	–	–	–	–	–	–	–	–	–	–	–	–	–	–
50N-60N	0.32	–	–	–	–	–	–	–	–	–	–	–	–	–	–	–	–	–
40N-50N	0.95	–	1.00	–	–	–	–	–	–	–	–	–	–	–	–	–	–	–
30N-40N	–	–	–	–	–	–	–	–	–	–	0.47	0.29	-0.30	0.96	1.00	–	–	–
20N-30N	–	–	–	–	–	–	–	–	-1.00	-0.66	0.27	0.72	–	–	–	–	–	–
10N-20N	–	–	–	–	–	–	–	–	–	–	–	–	–	–	–	–	–	–
0N-10N	–	–	–	–	–	–	–	–	–	–	–	–	–	–	–	–	–	–
10S-0S	–	–	–	–	–	–	–	–	–	–	–	–	–	–	–	–	–	–
20S-10S	–	–	–	–	1.00	–	–	–	–	–	–	–	–	–	–	–	–	–
30S-20S	–	–	–	–	–	–	–	–	–	–	–	–	–	–	–	–	–	–
40S-30S	–	–	–	–	–	–	–	–	–	–	–	–	–	–	–	–	–	–
50S-40S	–	–	–	–	–	–	–	–	–	–	–	–	–	–	–	–	-1.00	–
60S-50S	–	–	–	–	–	–	–	–	–	–	–	–	–	–	–	–	–	–
70S-60S	–	–	–	–	–	–	–	–	–	–	–	–	–	–	–	–	–	–
80S-70S	–	–	–	–	–	–	–	–	–	–	–	–	–	–	–	–	–	–
90S-80S	–	–	–	–	–	–	–	–	–	–	–	–	–	–	–	–	–	–

Difference of spatial correlation between NET temperate (SEED) vs. AVHRR needleleaf and NET temperate (FREE) vs. AVHRR needleleaf (180W-0W). Stronger correlations by the SEED are highlighted in yellow and less stronger correlation by the SEED in pink.

DIFF 1	180W-170W	170W-160W	160W-150W	150W-140W	140W-130W	130W-120W	120W-110W	110W-100W	100W-90W	90W-80W	80W-70W	70W-60W	60W-50W	50W-40W	40W-30W	30W-20W	20W-10W	10W-0W
80N-90N	–	–	–	–	–	–	–	–	–	–	–	–	–	–	–	–	–	–
70N-80N	–	–	–	–	–	–	–	–	–	–	–	–	–	–	–	–	–	–
60N-70N	–	–	–	–	–	–	–	–	–	–	–	–	–	–	–	–	–	–
50N-60N	–	–	–	–	–	–	–	–	–	–	–	–	–	–	–	–	–	–
40N-50N	–	–	–	–	–	**0.92**	–	–	–	–	–	–	–	–	–	–	–	–
30N-40N	–	–	–	–	–	–	–	–	**-0.42**	**-1.01**	**1.23**	–	–	–	–	–	–	–
20N-30N	–	–	–	–	–	–	–	–	–	–	–	–	–	–	–	–	–	–
10N-20N	–	–	–	–	–	–	–	–	–	–	–	–	–	–	–	–	–	–
0N-10N	–	–	–	–	–	–	–	–	–	–	–	–	–	–	–	–	–	–
10S-0S	–	–	–	–	–	–	–	–	–	–	–	–	–	–	–	–	–	–
20S-10S	–	–	–	–	–	–	–	–	–	–	–	–	–	–	–	–	–	–
30S-20S	–	–	–	–	–	–	–	–	–	–	–	–	–	–	–	–	–	–
40S-30S	–	–	–	–	–	–	–	–	–	–	–	–	–	–	–	–	–	–
50S-40S	–	–	–	–	–	–	–	–	–	–	–	–	–	–	–	–	–	–
60S-50S	–	–	–	–	–	–	–	–	–	–	–	–	–	–	–	–	–	–
70S-60S	–	–	–	–	–	–	–	–	–	–	–	–	–	–	–	–	–	–
80S-70S	–	–	–	–	–	–	–	–	–	–	–	–	–	–	–	–	–	–
90S-80S	–	–	–	–	–	–	–	–	–	–	–	–	–	–	–	–	–	–

Difference of spatial correlation between NET temperate (SEED) vs. AVHRR needleleaf and NET temperate (FREE) vs. AVHRR needleleaf (0E-180E). Stronger correlations by the SEED are highlighted in yellow and less stronger correlation by the SEED in pink.

DIFF 1	180W-170W	170W-160W	160W-150W	150W-140W	140W-130W	130W-120W	120W-110W	110W-100W	100W-90W	90W-80W	80W-70W	70W-60W	60W-50W	50W-40W	40W-30W	30W-20W	20W-10W	10W-0W
80N-90N	–	–	–	–	–	–	–	–	–	–	–	–	–	–	–	–	–	–
70N-80N	–	–	–	–	–	–	–	–	–	–	–	–	–	–	–	–	–	–
60N-70N	–	–	–	–	–	–	–	–	–	–	–	–	–	–	–	–	–	–
50N-60N	–	–	–	–	–	–	–	–	–	–	–	–	–	–	–	–	–	–
40N-50N	-0.01	–	–	–	–	–	–	–	–	–	–	–	–	–	–	–	–	–
30N-40N	–	–	–	–	–	–	–	–	–	–	–	–	–	–	–	–	–	–
20N-30N	–	–	–	–	–	–	–	–	–	0.20	-0.02	–	–	–	–	–	–	–
10N-20N	–	–	–	–	–	–	–	–	–	–	–	–	–	–	–	–	–	–
0N-10N	–	–	–	–	–	–	–	–	–	–	–	–	–	–	–	–	–	–
10S-0S	–	–	–	–	–	–	–	–	–	–	–	–	–	–	–	–	–	–
20S-10S	–	–	–	–	–	–	–	–	–	–	–	–	–	–	–	–	–	–
30S-20S	–	–	–	–	–	–	–	–	–	–	–	–	–	–	–	–	–	–
40S-30S	–	–	–	–	–	–	–	–	–	–	–	–	–	–	–	–	–	–
50S-40S	–	–	–	–	–	–	–	–	–	–	–	–	–	–	–	–	–	–
60S-50S	–	–	–	–	–	–	–	–	–	–	–	–	–	–	–	–	–	–
70S-60S	–	–	–	–	–	–	–	–	–	–	–	–	–	–	–	–	–	–
80S-70S	–	–	–	–	–	–	–	–	–	–	–	–	–	–	–	–	–	–
90S-80S	–	–	–	–	–	–	–	–	–	–	–	–	–	–	–	–	–	–

Spatial correlation coefficients of BET tropical forest from the SEED vs. AVHRR broadleaf treecover (180W-0W)

SD4 vs. BOBL	180W-170W	170W-160W	160W-150W	150W-140W	140W-130W	130W-120W	120W-110W	110W-100W	100W-90W	90W-80W	80W-70W	70W-60W	60W-50W	50W-40W	40W-30W	30W-20W	20W-10W	10W-0W
80N-90N	–	–	–	–	–	–	–	–	–	–	–	–	–	–	–	–	–	–
70N-80N	–	–	–	–	–	–	–	–	–	–	–	–	–	–	–	–	–	–
60N-70N	–	–	–	–	–	–	–	–	–	–	–	–	–	–	–	–	–	–
50N-60N	–	–	–	–	–	–	–	–	–	–	–	–	–	–	–	–	–	–
40N-50N	–	–	–	–	–	–	–	–	–	–	–	–	–	–	–	–	–	–
30N-40N	–	–	–	–	–	–	–	–	–	–	–	–	–	–	–	–	–	–
20N-30N	–	–	–	–	–	–	–	–	–	–	–	–	–	–	–	–	–	–
10N-20N	–	–	–	–	–	–	–	–	–	-0.21	–	–	–	–	–	–	–	–
0N-10N	–	–	–	–	–	–	–	–	–	-1.00	0.75	0.46	-0.54	–	–	–	–	-0.68
10S-0S	–	–	–	–	–	–	–	–	–	–	0.87	0.23	0.33	0.66	–	–	–	–
20S-10S	–	–	–	–	–	–	–	–	–	–	1.00	-0.15	0.21	–	–	–	–	–
30S-20S	–	–	–	–	–	–	–	–	–	–	–	–	–	–	–	–	–	–
40S-30S	–	–	–	–	–	–	–	–	–	–	–	–	–	–	–	–	–	–
50S-40S	–	–	–	–	–	–	–	–	–	–	–	–	–	–	–	–	–	–
60S-50S	–	–	–	–	–	–	–	–	–	–	–	–	–	–	–	–	–	–
70S-60S	–	–	–	–	–	–	–	–	–	–	–	–	–	–	–	–	–	–
80S-70S	–	–	–	–	–	–	–	–	–	–	–	–	–	–	–	–	–	–
90S-80S	–	–	–	–	–	–	–	–	–	–	–	–	–	–	–	–	–	–

Spatial correlation coefficients of BET tropical forest from the SEED vs. AVHRR broadleaf treecover (0E-180E)

SD4 vs. BOBL	0E-10E	10E-20E	20E-30E	30E-40E	40E-50E	50E-60E	60E-70E	70E-80E	80E-90E	90E-100E	100E-110E	110E-120E	120E-130E	130E-140E	140E-150E	150E-160E	160E-170E	170E-180E
80N-90N	_	_	_	_	_	_	_	_	_	_	_	_	_	_	_	_	_	_
70N-80N	_	_	_	_	_	_	_	_	_	_	_	_	_	_	_	_	_	_
60N-70N	_	_	_	_	_	_	_	_	_	_	_	_	_	_	_	_	_	_
50N-60N	_	_	_	_	_	_	_	_	_	_	_	_	_	_	_	_	_	_
40N-50N	_	_	_	_	_	_	_	_	_	_	_	_	_	_	_	_	_	_
30N-40N	_	_	_	_	_	_	_	_	_	_	_	_	_	_	_	_	_	_
20N-30N	_	_	_	_	_	_	_	_	_	_	_	_	_	_	_	_	_	_
10N-20N	_	_	_	_	_	_	_	_	_	_	0.64	_	_	_	_	_	_	_
0N-10N	0.23	0.07	_	_	_	_	_	_	_	_	0.99	1.00	_	_	_	_	_	_
10S-0S	_	1.00	_	_	_	_	_	_	_	_	0.61	0.56	-1.00	0.87	0.93	_	_	_
20S-10S	_	_	_	_	_	_	_	_	_	_	_	_	_	_	_	_	_	_
30S-20S	_	_	_	_	_	_	_	_	_	_	_	_	_	_	_	_	_	_
40S-30S	_	_	_	_	_	_	_	_	_	_	_	_	_	_	_	_	_	_
50S-40S	_	_	_	_	_	_	_	_	_	_	_	_	_	_	_	_	_	_
60S-50S	_	_	_	_	_	_	_	_	_	_	_	_	_	_	_	_	_	_
70S-60S	_	_	_	_	_	_	_	_	_	_	_	_	_	_	_	_	_	_
80S-70S	_	_	_	_	_	_	_	_	_	_	_	_	_	_	_	_	_	_
90S-80S	_	_	_	_	_	_	_	_	_	_	_	_	_	_	_	_	_	_

Spatial correlation coefficients of BET tropical forest from the FREE vs. AVHRR broadleaf treecover (180W-0W)

FR4 vs BOBL	180W-170W	170W-160W	160W-150W	150W-140W	140W-130W	130W-120W	120W-110W	110W-100W	100W-90W	90W-80W	80W-70W	70W-60W	60W-50W	50W-40W	40W-30W	30W-20W	20W-10W	10W-0W
80N-90N	–	–	–	–	–	–	–	–	–	–	–	–	–	–	–	–	–	–
70N-80N	–	–	–	–	–	–	–	–	–	–	–	–	–	–	–	–	–	–
60N-70N	–	–	–	–	–	–	–	–	–	–	–	–	–	–	–	–	–	–
50N-60N	–	–	–	–	–	–	–	–	–	–	–	–	–	–	–	–	–	–
40N-50N	–	–	–	–	–	–	–	–	–	–	–	–	–	–	–	–	–	–
30N-40N	–	–	–	–	–	–	–	–	–	–	–	–	–	–	–	–	–	–
20N-30N	–	–	–	–	–	–	–	–	–	–	–	–	–	–	–	–	–	–
10N-20N	–	–	–	–	–	–	–	–	–	-0.14	–	–	–	–	–	–	–	–
0N-10N	–	–	–	–	–	–	–	–	–	-1.00	0.75	0.46	-0.54	–	–	–	–	-0.51
10S-0S	–	–	–	–	–	–	–	–	–	–	0.87	0.14	0.33	0.65	–	–	–	–
20S-10S	–	–	–	–	–	–	–	–	–	–	1.00	-0.15	0.42	–	-1.00	–	–	–
30S-20S	–	–	–	–	–	–	–	–	–	–	–	–	–	–	–	–	–	–
40S-30S	–	–	–	–	–	–	–	–	–	–	–	–	–	–	–	–	–	–
50S-40S	–	–	–	–	–	–	–	–	–	–	–	–	–	–	–	–	–	–
60S-50S	–	–	–	–	–	–	–	–	–	–	–	–	–	–	–	–	–	–
70S-60S	–	–	–	–	–	–	–	–	–	–	–	–	–	–	–	–	–	–
80S-70S	–	–	–	–	–	–	–	–	–	–	–	–	–	–	–	–	–	–
90S-80S	–	–	–	–	–	–	–	–	–	–	–	–	–	–	–	–	–	–

Spatial correlation coefficients of BET tropical forest from the FREE vs. AVHRR broadleaf treecover (0E-180E)

FR4 vs BOBL	0E-10E	10E-20E	20E-30E	30E-40E	40E-50E	50E-60E	60E-70E	70E-80E	80E-90E	90E-100E	100E-110E	110E-120E	120E-130E	130E-140E	140E-150E	150E-160E	160E-170E	170E-180E
80N-90N	–	–	–	–	–	–	–	–	–	–	–	–	–	–	–	–	–	–
70N-80N	–	–	–	–	–	–	–	–	–	–	–	–	–	–	–	–	–	–
60N-70N	–	–	–	–	–	–	–	–	–	–	–	–	–	–	–	–	–	–
50N-60N	–	–	–	–	–	–	–	–	–	–	–	–	–	–	–	–	–	–
40N-50N	–	–	–	–	–	–	–	–	–	–	–	–	–	–	–	–	–	–
30N-40N	–	–	–	–	–	–	–	–	–	–	–	–	–	–	–	–	–	–
20N-30N	–	–	–	–	–	–	–	–	–	–	–	–	–	–	–	–	–	–
10N-20N	–	–	–	–	–	–	–	–	–	–	0.71	–	1.00	–	–	–	–	–
0N-10N	0.13	0.07	–	–	–	–	–	–	–	1.00	0.60	0.92	–	–	–	–	–	–
10S-0S	–	0.76	–	–	–	–	–	–	–	–	0.68	0.56	-1.00	0.89	0.93	–	–	–
20S-10S	–	–	–	–	–	–	–	–	–	–	–	–	–	–	–	–	–	–
30S-20S	–	–	–	–	–	–	–	–	–	–	–	–	–	–	–	–	–	–
40S-30S	–	–	–	–	–	–	–	–	–	–	–	–	–	–	–	–	–	–
50S-40S	–	–	–	–	–	–	–	–	–	–	–	–	–	–	–	–	–	–
60S-50S	–	–	–	–	–	–	–	–	–	–	–	–	–	–	–	–	–	–
70S-60S	–	–	–	–	–	–	–	–	–	–	–	–	–	–	–	–	–	–
80S-70S	–	–	–	–	–	–	–	–	–	–	–	–	–	–	–	–	–	–
90S-80S	–	–	–	–	–	–	–	–	–	–	–	–	–	–	–	–	–	–

Difference of spatial correlation between BET tropical (SEED) vs. AVHRR broadleaf and BET tropical (FREE) vs. AVHRR broadleaf (180W-0W). Stronger correlations by the SEED are highlighted in yellow and less stronger correlation by the SEED in pink.

DIFF	180W-170W	170W-160W	160W-150W	150W-140W	140W-130W	130W-120W	120W-110W	110W-100W	100W-90W	90W-80W	80W-70W	70W-60W	60W-50W	50W-40W	40W-30W	30W-20W	20W-10W	10W-0W
80N-90N	–	–	–	–	–	–	–	–	–	–	–	–	–	–	–	–	–	–
70N-80N	–	–	–	–	–	–	–	–	–	–	–	–	–	–	–	–	–	–
60N-70N	–	–	–	–	–	–	–	–	–	–	–	–	–	–	–	–	–	–
50N-60N	–	–	–	–	–	–	–	–	–	–	–	–	–	–	–	–	–	–
40N-50N	–	–	–	–	–	–	–	–	–	–	–	–	–	–	–	–	–	–
30N-40N	–	–	–	–	–	–	–	–	–	–	–	–	–	–	–	–	–	–
20N-30N	–	–	–	–	–	–	–	–	–	–	–	–	–	–	–	–	–	–
10N-20N	–	–	–	–	–	–	–	–	–	-0.07	–	–	–	–	–	–	–	–
0N-10N	–	–	–	–	–	–	–	–	–	–	–	–	–	–	–	–	–	-0.17
10S-0S	–	–	–	–	–	–	–	–	–	–	–	**0.09**	–	**0.01**	–	–	–	–
20S-10S	–	–	–	–	–	–	–	–	–	–	–	–	-0.22	–	**1.00**	–	–	–
30S-20S	–	–	–	–	–	–	–	–	–	–	–	–	–	–	–	–	–	–
40S-30S	–	–	–	–	–	–	–	–	–	–	–	–	–	–	–	–	–	–
50S-40S	–	–	–	–	–	–	–	–	–	–	–	–	–	–	–	–	–	–
60S-50S	–	–	–	–	–	–	–	–	–	–	–	–	–	–	–	–	–	–
70S-60S	–	–	–	–	–	–	–	–	–	–	–	–	–	–	–	–	–	–
80S-70S	–	–	–	–	–	–	–	–	–	–	–	–	–	–	–	–	–	–
90S-80S	–	–	–	–	–	–	–	–	–	–	–	–	–	–	–	–	–	–

Difference of spatial correlation between BET tropical (SEED) vs. AVHRR broadleaf and BET tropical (FREE) vs. AVHRR broadleaf (0E-180E). Stronger correlations by the SEED are highlighted in yellow and less stronger correlation by the SEED in pink.

DIFF	0E-10E	10E-20E	20E-30E	30E-40E	40E-50E	50E-60E	60E-70E	70E-80E	80E-90E	90E-100E	100E-110E	110E-120E	120E-130E	130E-140E	140E-150E	150E-160E	160E-170E	170E-180E
80N-90N	–	–	–	–	–	–	–	–	–	–	–	–	–	–	–	–	–	–
70N-80N	–	–	–	–	–	–	–	–	–	–	–	–	–	–	–	–	–	–
60N-70N	–	–	–	–	–	–	–	–	–	–	–	–	–	–	–	–	–	–
50N-60N	–	–	–	–	–	–	–	–	–	–	–	–	–	–	–	–	–	–
40N-50N	–	–	–	–	–	–	–	–	–	–	–	–	–	–	–	–	–	–
30N-40N	–	–	–	–	–	–	–	–	–	–	–	–	–	–	–	–	–	–
20N-30N	–	–	–	–	–	–	–	–	–	–	–	–	–	–	–	–	–	–
10N-20N	–	–	–	–	–	–	–	–	–	–	-0.07	–	-1.00	–	–	–	–	–
0N-10N	**0.10**	–	–	–	–	–	–	–	–	-1.00	**0.40**	**0.08**	–	–	–	–	–	–
10S-0S	–	**0.24**	–	–	–	–	–	–	–	–	-0.07	–	–	-0.02	–	–	–	–
20S-10S	–	–	–	–	–	–	–	–	–	–	–	–	–	–	–	–	–	–
30S-20S	–	–	–	–	–	–	–	–	–	–	–	–	–	–	–	–	–	–
40S-30S	–	–	–	–	–	–	–	–	–	–	–	–	–	–	–	–	–	–
50S-40S	–	–	–	–	–	–	–	–	–	–	–	–	–	–	–	–	–	–
60S-50S	–	–	–	–	–	–	–	–	–	–	–	–	–	–	–	–	–	–
70S-60S	–	–	–	–	–	–	–	–	–	–	–	–	–	–	–	–	–	–
80S-70S	–	–	–	–	–	–	–	–	–	–	–	–	–	–	–	–	–	–
90S-80S	–	–	–	–	–	–	–	–	–	–	–	–	–	–	–	–	–	–

Spatial correlation coefficients of BET temperate forest from the SEED vs. AVHRR broadleaf treecover (180W-0W)

SD5 vs. BOBL	180W-170W	170W-160W	160W-150W	150W-140W	140W-130W	130W-120W	120W-110W	110W-100W	100W-90W	90W-80W	80W-70W	70W-60W	60W-50W	50W-40W	40W-30W	30W-20W	20W-10W	10W-0W
80N-90N	–	–	–	–	–	–	–	–	–	–	–	–	–	–	–	–	–	–
70N-80N	–	–	–	–	–	–	–	–	–	–	–	–	–	–	–	–	–	–
60N-70N	–	–	–	–	–	–	–	–	–	–	–	–	–	–	–	–	–	–
50N-60N	–	–	–	–	–	–	–	–	–	–	–	–	–	–	–	–	–	-1.00
40N-50N	–	–	–	–	–	–	–	–	–	–	–	–	–	–	–	–	–	-0.91
30N-40N	–	–	–	–	–	–	–	–	0.00	-0.28	–	–	–	–	–	–	–	1.00
20N-30N	–	–	–	–	–	–	–	–	–	–	–	–	–	–	–	–	–	–
10N-20N	–	–	–	–	–	–	–	–	0.18	–	–	–	–	–	–	–	–	–
0N-10N	–	–	–	–	–	–	–	–	–	–	–	–	–	–	–	–	–	–
10S-0S	–	–	–	–	–	–	–	–	–	–	0.97	–	–	–	–	–	–	–
20S-10S	–	–	–	–	–	–	–	–	–	–	-0.12	0.58	–	1.00	–	–	–	–
30S-20S	–	–	–	–	–	–	–	–	–	–	–	0.62	0.34	0.41	–	–	–	–
40S-30S	–	–	–	–	–	–	–	–	–	–	1.00	0.74	-0.37	–	–	–	–	–
50S-40S	–	–	–	–	–	–	–	–	–	–	–	–	–	–	–	–	–	–
60S-50S	–	–	–	–	–	–	–	–	–	–	–	–	–	–	–	–	–	–
70S-60S	–	–	–	–	–	–	–	–	–	–	–	–	–	–	–	–	–	–
80S-70S	–	–	–	–	–	–	–	–	–	–	–	–	–	–	–	–	–	–
90S-80S	–	–	–	–	–	–	–	–	–	–	–	–	–	–	–	–	–	–

Spatial correlation coefficients of BET temperate forest from the SEED vs. AVHRR broadleaf treecover (0E-180E)

SD5 vs. BOBL	0E-10E	10E-20E	20E-30E	30E-40E	40E-50E	50E-60E	60E-70E	70E-80E	80E-90E	90E-100E	100E-110E	110E-120E	120E-130E	130E-140E	140E-150E	150E-160E	160E-170E	170E-180E
80N-90N	–	–	–	–	–	–	–	–	–	–	–	–	–	–	–	–	–	–
70N-80N	–	–	–	–	–	–	–	–	–	–	–	–	–	–	–	–	–	–
60N-70N	–	–	–	–	–	–	–	–	–	–	–	–	–	–	–	–	–	–
50N-60N	–	–	–	–	–	–	–	–	–	–	–	–	–	–	–	–	–	–
40N-50N	–	–	–	–	–	–	–	–	–	–	–	–	–	–	–	–	–	–
30N-40N	–	–	–	–	–	–	–	1.00	–	–	–	–	–	–	–	–	–	–
20N-30N	–	–	–	–	–	–	–	–	0.85	-0.33	0.13	0.72	–	–	–	–	–	–
10N-20N	–	–	–	–	–	–	–	–	–	–	-1.00	–	–	–	–	–	–	–
0N-10N	–	–	–	-0.65	–	–	–	–	–	–	–	–	–	–	–	–	–	–
10S-0S	–	–	–	0.16	–	–	–	–	–	–	–	–	–	–	–	–	–	–
20S-10S	–	0.96	-0.73	-0.18	-0.07	–	–	–	–	–	–	–	–	–	–	–	–	–
30S-20S	–	–	–	–	1.00	–	–	–	–	–	–	–	–	–	–	–	–	–
40S-30S	–	–	–	–	–	–	–	–	–	–	–	–	–	–	-0.46	–	–	–
50S-40S	–	–	–	–	–	–	–	–	–	–	–	–	–	–	–	–	–	1.00
60S-50S	–	–	–	–	–	–	–	–	–	–	–	–	–	–	–	–	–	–
70S-60S	–	–	–	–	–	–	–	–	–	–	–	–	–	–	–	–	–	–
80S-70S	–	–	–	–	–	–	–	–	–	–	–	–	–	–	–	–	–	–
90S-80S	–	–	–	–	–	–	–	–	–	–	–	–	–	–	–	–	–	–

Spatial correlation coefficients of BET temperate forest from the FREE vs. AVHRR broadleaf treecover (180W-0W)

FR5 vs BOBL	180W-170W	170W-160W	160W-150W	150W-140W	140W-130W	130W-120W	120W-110W	110W-100W	100W-90W	90W-80W	80W-70W	70W-60W	60W-50W	50W-40W	40W-30W	30W-20W	20W-10W	10W-0W
80N-90N	–	–	–	–	–	–	–	–	–	–	–	–	–	–	–	–	–	–
70N-80N	–	–	–	–	–	–	–	–	–	–	–	–	–	–	–	–	–	–
60N-70N	–	–	–	–	–	–	–	–	–	–	–	–	–	–	–	–	–	–
50N-60N	–	–	–	–	–	–	–	–	–	–	–	–	–	–	–	–	–	-1.00
40N-50N	–	–	–	–	–	–	–	–	–	–	–	–	–	–	–	–	–	-0.91
30N-40N	–	–	–	–	–	–	–	–	0.05	-0.36	–	–	–	–	–	–	–	–
20N-30N	–	–	–	–	–	–	–	1.00	–	–	–	–	–	–	–	–	–	–
10N-20N	–	–	–	–	–	–	–	–	0.19	–	–	–	–	–	–	–	–	–
0N-10N	–	–	–	–	–	–	–	–	–	–	–	–	–	–	–	–	–	–
10S-0S	–	–	–	–	–	–	–	–	–	–	0.98	–	–	–	–	–	–	–
20S-10S	–	–	–	–	–	–	–	–	–	–	-0.18	0.60	–	1.00	–	–	–	–
30S-20S	–	–	–	–	–	–	–	–	–	–	–	0.62	0.34	0.41	–	–	–	–
40S-30S	–	–	–	–	–	–	–	–	–	–	0.49	0.74	-0.38	–	–	–	–	–
50S-40S	–	–	–	–	–	–	–	–	–	–	–	–	–	–	–	–	–	–
60S-50S	–	–	–	–	–	–	–	–	–	–	–	–	–	–	–	–	–	–
70S-60S	–	–	–	–	–	–	–	–	–	–	–	–	–	–	–	–	–	–
80S-70S	–	–	–	–	–	–	–	–	–	–	–	–	–	–	–	–	–	–
90S-80S	–	–	–	–	–	–	–	–	–	–	–	–	–	–	–	–	–	–

Spatial correlation coefficients of BET temperate forest from the FREE vs. AVHRR broadleaf treecover (0E-180E)

FR5 vs BOBL	0E-10E	10E-20E	20E-30E	30E-40E	40E-50E	50E-60E	60E-70E	70E-80E	80E-90E	90E-100E	100E-110E	110E-120E	120E-130E	130E-140E	140E-150E	150E-160E	160E-170E	170E-180E
80N-90N	–	–	–	–	–	–	–	–	–	–	–	–	–	–	–	–	–	–
70N-80N	–	–	–	–	–	–	–	–	–	–	–	–	–	–	–	–	–	–
60N-70N	–	–	–	–	–	–	–	–	–	–	–	–	–	–	–	–	–	–
50N-60N	–	–	–	–	–	–	–	–	–	–	–	–	–	–	–	–	–	–
40N-50N	–	–	–	–	–	–	–	–	–	–	–	–	–	–	–	–	–	–
30N-40N	–	–	-1.00	–	–	–	–	1.00	–	–	–	–	–	–	–	–	–	–
20N-30N	–	–	–	–	–	–	–	–	0.90	-0.38	0.13	0.72	–	–	–	–	–	–
10N-20N	–	–	–	–	–	–	–	–	–	–	-1.00	–	–	–	–	–	–	–
0N-10N	–	–	–	-0.98	–	–	–	–	–	–	–	–	–	–	–	–	–	–
10S-0S	–	–	–	0.53	–	–	–	–	–	–	–	–	–	–	–	–	–	–
20S-10S	–	-0.12	-0.73	-0.17	-0.07	–	–	–	–	–	–	–	–	–	–	–	–	–
30S-20S	–	–	–	1.00	1.00	–	–	–	–	–	–	–	–	–	–	–	–	–
40S-30S	–	–	–	–	–	–	–	–	–	–	–	–	–	–	-0.43	-1.00	–	–
50S-40S	–	–	–	–	–	–	–	–	–	–	–	–	–	–	–	–	–	1.00
60S-50S	–	–	–	–	–	–	–	–	–	–	–	–	–	–	–	–	–	–
70S-60S	–	–	–	–	–	–	–	–	–	–	–	–	–	–	–	–	–	–
80S-70S	–	–	–	–	–	–	–	–	–	–	–	–	–	–	–	–	–	–
90S-80S	–	–	–	–	–	–	–	–	–	–	–	–	–	–	–	–	–	–

Difference of spatial correlation between BET temperate (SEED) vs. AVHRR broadleaf and BET temperate (FREE) vs. AVHRR broadleaf (180W-0W). Stronger correlations by the SEED are highlighted in yellow and less stronger correlation by the SEED in pink.

DIFF	180W-170W	170W-160W	160W-150W	150W-140W	140W-130W	130W-120W	120W-110W	110W-100W	100W-90W	90W-80W	80W-70W	70W-60W	60W-50W	50W-40W	40W-30W	30W-20W	20W-10W	10W-0W
80N-90N	_	_	_	_	_	_	_	_	_	_	_	_	_	_	_	_	_	_
70N-80N	_	_	_	_	_	_	_	_	_	_	_	_	_	_	_	_	_	_
60N-70N	_	_	_	_	_	_	_	_	_	_	_	_	_	_	_	_	_	_
50N-60N	_	_	_	_	_	_	_	_	_	_	_	_	_	_	_	_	_	_
40N-50N	_	_	_	_	_	_	_	_	_	_	_	_	_	_	_	_	_	_
30N-40N	_	_	_	_	_	_	_	_	-0.06	**0.08**	_	_	_	_	_	_	_	**1.00**
20N-30N	_	_	_	_	_	_	_	-1.00	_	_	_	_	_	_	_	_	_	_
10N-20N	_	_	_	_	_	_	_	_	_	_	_	_	_	_	_	_	_	_
0N-10N	_	_	_	_	_	_	_	_	_	_	_	_	_	_	_	_	_	_
10S-0S	_	_	_	_	_	_	_	_	_	_	-0.01	_	_	_	_	_	_	_
20S-10S	_	_	_	_	_	_	_	_	_	_	**0.06**	-0.02	_	_	_	_	_	_
30S-20S	_	_	_	_	_	_	_	_	_	_	_	**0.01**	_	_	_	_	_	_
40S-30S	_	_	_	_	_	_	_	_	_	_	**0.51**	_	**0.01**	_	_	_	_	_
50S-40S	_	_	_	_	_	_	_	_	_	_	_	_	_	_	_	_	_	_
60S-50S	_	_	_	_	_	_	_	_	_	_	_	_	_	_	_	_	_	_
70S-60S	_	_	_	_	_	_	_	_	_	_	_	_	_	_	_	_	_	_
80S-70S	_	_	_	_	_	_	_	_	_	_	_	_	_	_	_	_	_	_
90S-80S	_	_	_	_	_	_	_	_	_	_	_	_	_	_	_	_	_	_

Difference of spatial correlation between BET temperate (SEED) vs. AVHRR broadleaf and BET temperate (FREE) vs. AVHRR broadleaf (0E-180E). Stronger correlations by the SEED are highlighted in yellow and less stronger correlation by the SEED in pink.

DIFF	0E-10E	10E-20E	20E-30E	30E-40E	40E-50E	50E-60E	60E-70E	70E-80E	80E-90E	90E-100E	100E-110E	110E-120E	120E-130E	130E-140E	140E-150E	150E-160E	160E-170E	170E-180E
80N-90N	_	_	_	_	_	_	_	_	_	_	_	_	_	_	_	_	_	_
70N-80N	_	_	_	_	_	_	_	_	_	_	_	_	_	_	_	_	_	_
60N-70N	_	_	_	_	_	_	_	_	_	_	_	_	_	_	_	_	_	_
50N-60N	_	_	_	_	_	_	_	_	_	_	_	_	_	_	_	_	_	_
40N-50N	_	_	_	_	_	_	_	_	_	_	_	_	_	_	_	_	_	_
30N-40N	_	_	**1.00**	_	_	_	_	_	_	_	_	_	_	_	_	_	_	_
20N-30N	_	_	_	_	_	_	_	_	-0.05	**0.05**	**0.01**	_	_	_	_	_	_	_
10N-20N	_	_	_	_	_	_	_	_	_	_	_	_	_	_	_	_	_	_
0N-10N	_	_	_	**0.33**	_	_	_	_	_	_	_	_	_	_	_	_	_	_
10S-0S	_	_	_	-0.37	_	_	_	_	_	_	_	_	_	_	_	_	_	_
20S-10S	_	**1.08**	_	-0.01	_	_	_	_	_	_	_	_	_	_	_	_	_	_
30S-20S	_	_	_	-1.00	_	_	_	_	_	_	_	_	_	_	_	_	_	_
40S-30S	_	_	_	_	_	_	_	_	_	_	_	_	_	_	-0.03	**1.00**	_	_
50S-40S	_	_	_	_	_	_	_	_	_	_	_	_	_	_	_	_	_	_
60S-50S	_	_	_	_	_	_	_	_	_	_	_	_	_	_	_	_	_	_
70S-60S	_	_	_	_	_	_	_	_	_	_	_	_	_	_	_	_	_	_
80S-70S	_	_	_	_	_	_	_	_	_	_	_	_	_	_	_	_	_	_
90S-80S	_	_	_	_	_	_	_	_	_	_	_	_	_	_	_	_	_	_

Spatial correlation coefficients of BDT tropical forest from the SEED vs. AVHRR broadleaf treecover (180W-0W)

SD6 vs. BOBL	180W-170W	170W-160W	160W-150W	150W-140W	140W-130W	130W-120W	120W-110W	110W-100W	100W-90W	90W-80W	80W-70W	70W-60W	60W-50W	50W-40W	40W-30W	30W-20W	20W-10W	10W-0W
80N-90N	–	–	–	–	–	–	–	–	–	–	–	–	–	–	–	–	–	–
70N-80N	–	–	–	–	–	–	–	–	–	–	–	–	–	–	–	–	–	–
60N-70N	–	–	–	–	–	–	–	–	–	–	–	–	–	–	–	–	–	–
50N-60N	–	–	–	–	–	–	–	–	–	–	–	–	–	–	–	–	–	–
40N-50N	–	–	–	–	–	–	–	–	–	–	–	–	–	–	–	–	–	–
30N-40N	–	–	–	–	–	–	–	–	–	–	–	–	–	–	–	–	–	–
20N-30N	–	–	–	–	–	–	–	–	-1.00	–	–	–	–	–	–	–	–	–
10N-20N	–	–	–	–	–	–	–	1.00	0.18	0.75	1.00	–	–	–	–	–	–	–
0N-10N	–	–	–	–	–	–	–	–	–	–	0.33	0.16	0.56	–	–	–	0.51	0.32
10S-0S	–	–	–	–	–	–	–	–	–	–	-0.70	-0.20	-0.55	-0.20	–	–	–	–
20S-10S	–	–	–	–	–	–	–	–	–	–	–	0.24	0.45	0.08	–	–	–	–
30S-20S	–	–	–	–	–	–	–	–	–	–	–	–	-0.47	-0.67	–	–	–	–
40S-30S	–	–	–	–	–	–	–	–	–	–	–	–	–	–	–	–	–	–
50S-40S	–	–	–	–	–	–	–	–	–	–	–	–	–	–	–	–	–	–
60S-50S	–	–	–	–	–	–	–	–	–	–	–	–	–	–	–	–	–	–
70S-60S	–	–	–	–	–	–	–	–	–	–	–	–	–	–	–	–	–	–
80S-70S	–	–	–	–	–	–	–	–	–	–	–	–	–	–	–	–	–	–
90S-80S	–	–	–	–	–	–	–	–	–	–	–	–	–	–	–	–	–	–

Spatial correlation coefficients of BDT tropical forest from the SEED vs. AVHRR broadleaf treecover (0E-180E)

SD6 vs. BOBL	0E-10E	10E-20E	20E-30E	30E-40E	40E-50E	50E-60E	60E-70E	70E-80E	80E-90E	90E-100E	100E-110E	110E-120E	120E-130E	130E-140E	140E-150E	150E-160E	160E-170E	170E-180E
80N-90N	_	_	_	_	_	_	_	_	_	_	_	_	_	_	_	_	_	_
70N-80N	_	_	_	_	_	_	_	_	_	_	_	_	_	_	_	_	_	_
60N-70N	_	_	_	_	_	_	_	_	_	_	_	_	_	_	_	_	_	_
50N-60N	_	_	_	_	_	_	_	_	_	_	_	_	_	_	_	_	_	_
40N-50N	_	_	_	_	_	_	_	_	_	_	_	_	_	_	_	_	_	_
30N-40N	_	_	_	_	_	_	_	_	_	_	_	_	_	_	_	_	_	_
20N-30N	_	_	_	_	_	_	_	0.52	0.07	0.05	_	_	_	_	_	_	_	_
10N-20N	_	_	_	1.00	_	_	_	0.69	-1.00	0.83	-0.23	_	-0.53	_	_	_	_	_
0N-10N	-0.14	-0.17	0.37	-0.65	_	_	_	_	_	_	0.77	0.84	_	_	_	_	_	_
10S-0S	_	-0.19	0.13	-0.38	_	_	_	_	_	_	0.19	0.69	1.00	-0.95	-0.80	_	_	_
20S-10S	_	_	_	-0.98	-0.23	_	_	_	_	_	_	_	_	_	_	_	_	_
30S-20S	_	_	_	_	1.00	_	_	_	_	_	_	_	_	_	_	_	_	_
40S-30S	_	_	_	_	_	_	_	_	_	_	_	_	_	_	_	_	_	_
50S-40S	_	_	_	_	_	_	_	_	_	_	_	_	_	_	_	_	_	_
60S-50S	_	_	_	_	_	_	_	_	_	_	_	_	_	_	_	_	_	_
70S-60S	_	_	_	_	_	_	_	_	_	_	_	_	_	_	_	_	_	_
80S-70S	_	_	_	_	_	_	_	_	_	_	_	_	_	_	_	_	_	_
90S-80S	_	_	_	_	_	_	_	_	_	_	_	_	_	_	_	_	_	_

Spatial correlation coefficients of BDT tropical forest from the FREE vs. AVHRR broadleaf treecover (180W-0W)

FR6 vs BOBL	180W-170W	170W-160W	160W-150W	150W-140W	140W-130W	130W-120W	120W-110W	110W-100W	100W-90W	90W-80W	80W-70W	70W-60W	60W-50W	50W-40W	40W-30W	30W-20W	20W-10W	10W-0W
80N-90N	–	–	–	–	–	–	–	–	–	–	–	–	–	–	–	–	–	–
70N-80N	–	–	–	–	–	–	–	–	–	–	–	–	–	–	–	–	–	–
60N-70N	–	–	–	–	–	–	–	–	–	–	–	–	–	–	–	–	–	–
50N-60N	–	–	–	–	–	–	–	–	–	–	–	–	–	–	–	–	–	–
40N-50N	–	–	–	–	–	–	–	–	–	–	–	–	–	–	–	–	–	–
30N-40N	–	–	–	–	–	–	–	–	–	–	–	–	–	–	–	–	–	–
20N-30N	–	–	–	–	–	–	–	–	1.00	1.00	–	–	–	–	–	–	–	–
10N-20N	–	–	–	–	–	–	–	1.00	0.17	0.75	1.00	–	–	–	–	–	–	–
0N-10N	–	–	–	–	–	–	–	–	–	–	0.33	0.04	0.56	–	–	–	0.51	0.52
10S-0S	–	–	–	–	–	–	–	–	–	–	-0.72	-0.26	-0.55	-0.20	–	–	–	–
20S-10S	–	–	–	–	–	–	–	–	–	–	–	0.24	0.43	0.06	–	–	–	–
30S-20S	–	–	–	–	–	–	–	–	–	–	–	–	-0.47	-0.67	–	–	–	–
40S-30S	–	–	–	–	–	–	–	–	–	–	–	–	–	–	–	–	–	–
50S-40S	–	–	–	–	–	–	–	–	–	–	–	–	–	–	–	–	–	–
60S-50S	–	–	–	–	–	–	–	–	–	–	–	–	–	–	–	–	–	–
70S-60S	–	–	–	–	–	–	–	–	–	–	–	–	–	–	–	–	–	–
80S-70S	–	–	–	–	–	–	–	–	–	–	–	–	–	–	–	–	–	–
90S-80S	–	–	–	–	–	–	–	–	–	–	–	–	–	–	–	–	–	–

Spatial correlation coefficients of BDT tropical forest from the FREE vs. AVHRR broadleaf treecover (0E-180E)

FR6 vs BOBL	0E-10E	10E-20E	20E-30E	30E-40E	40E-50E	50E-60E	60E-70E	70E-80E	80E-90E	90E-100E	100E-110E	110E-120E	120E-130E	130E-140E	140E-150E	150E-160E	160E-170E	170E-180E
80N-90N	_	_	_	_	_	_	_	_	_	_	_	_	_	_	_	_	_	_
70N-80N	_	_	_	_	_	_	_	_	_	_	_	_	_	_	_	_	_	_
60N-70N	_	_	_	_	_	_	_	_	_	_	_	_	_	_	_	_	_	_
50N-60N	_	_	_	_	_	_	_	_	_	_	_	_	_	_	_	_	_	_
40N-50N	_	_	_	_	_	_	_	_	_	_	_	_	_	_	_	_	_	_
30N-40N	_	_	_	_	_	_	_	_	_	_	_	_	_	_	_	_	_	_
20N-30N	_	_	_	_	_	_	_	0.56	0.03	-0.48	_	_	_	_	_	_	_	_
10N-20N	_	_	_	_	_	_	_	0.66	-1.00	0.83	-0.09	_	0.53	_	_	_	_	_
0N-10N	0.04	-0.06	0.37	-0.65	_	_	_	_	_	_	0.78	0.87	_	_	_	_	_	_
10S-0S	_	0.17	0.04	-0.38	_	_	_	_	_	_	0.52	0.72	1.00	-1.00	-0.82	_	_	_
20S-10S	_	_	_	-0.98	-0.23	_	_	_	_	_	_	_	_	_	_	_	_	_
30S-20S	_	_	_	_	1.00	_	_	_	_	_	_	_	_	_	_	_	_	_
40S-30S	_	_	_	_	_	_	_	_	_	_	_	_	_	_	_	_	_	_
50S-40S	_	_	_	_	_	_	_	_	_	_	_	_	_	_	_	_	_	_
60S-50S	_	_	_	_	_	_	_	_	_	_	_	_	_	_	_	_	_	_
70S-60S	_	_	_	_	_	_	_	_	_	_	_	_	_	_	_	_	_	_
80S-70S	_	_	_	_	_	_	_	_	_	_	_	_	_	_	_	_	_	_
90S-80S	_	_	_	_	_	_	_	_	_	_	_	_	_	_	_	_	_	_

Difference of spatial correlation between BDT tropical (SEED) vs. AVHRR broadleaf and BDT tropical (FREE) vs. AVHRR broadleaf (180W-0W). Stronger correlations by the SEED are highlighted in yellow and less stronger correlation by the SEED in pink.

DIFF	180W-170W	170W-160W	160W-150W	150W-140W	140W-130W	130W-120W	120W-110W	110W-100W	100W-90W	90W-80W	80W-70W	70W-60W	60W-50W	50W-40W	40W-30W	30W-20W	20W-10W	10W-0W
80N-90N	–	–	–	–	–	–	–	–	–	–	–	–	–	–	–	–	–	–
70N-80N	–	–	–	–	–	–	–	–	–	–	–	–	–	–	–	–	–	–
60N-70N	–	–	–	–	–	–	–	–	–	–	–	–	–	–	–	–	–	–
50N-60N	–	–	–	–	–	–	–	–	–	–	–	–	–	–	–	–	–	–
40N-50N	–	–	–	–	–	–	–	–	–	–	–	–	–	–	–	–	–	–
30N-40N	–	–	–	–	–	–	–	–	–	–	–	–	–	–	–	–	–	–
20N-30N	–	–	–	–	–	–	–	–	-2.00	-1.00	–	–	–	–	–	–	–	–
10N-20N	–	–	–	–	–	–	–	–	**0.01**	-0.01	–	–	–	–	–	–	–	–
0N-10N	–	–	–	–	–	–	–	–	–	–	–	**0.12**	–	–	–	–	–	-0.19
10S-0S	–	–	–	–	–	–	–	–	–	–	**0.02**	**0.06**	–	–	–	–	–	–
20S-10S	–	–	–	–	–	–	–	–	–	–	–	–	**0.01**	**0.02**	–	–	–	–
30S-20S	–	–	–	–	–	–	–	–	–	–	–	–	–	–	–	–	–	–
40S-30S	–	–	–	–	–	–	–	–	–	–	–	–	–	–	–	–	–	–
50S-40S	–	–	–	–	–	–	–	–	–	–	–	–	–	–	–	–	–	–
60S-50S	–	–	–	–	–	–	–	–	–	–	–	–	–	–	–	–	–	–
70S-60S	–	–	–	–	–	–	–	–	–	–	–	–	–	–	–	–	–	–
80S-70S	–	–	–	–	–	–	–	–	–	–	–	–	–	–	–	–	–	–
90S-80S	–	–	–	–	–	–	–	–	–	–	–	–	–	–	–	–	–	–

Difference of spatial correlation between BDT tropical (SEED) vs. AVHRR broadleaf and BDT tropical (FREE) vs. AVHRR broadleaf (0E-180E). Stronger correlations by the SEED are highlighted in yellow and less stronger correlation by the SEED in pink.

DIFF	0E-10E	10E-20E	20E-30E	30E-40E	40E-50E	50E-60E	60E-70E	70E-80E	80E-90E	90E-100E	100E-110E	110E-120E	120E-130E	130E-140E	140E-150E	150E-160E	160E-170E	170E-180E
80N-90N	_	_	_	_	_	_	_	_	_	_	_	_	_	_	_	_	_	_
70N-80N	_	_	_	_	_	_	_	_	_	_	_	_	_	_	_	_	_	_
60N-70N	_	_	_	_	_	_	_	_	_	_	_	_	_	_	_	_	_	_
50N-60N	_	_	_	_	_	_	_	_	_	_	_	_	_	_	_	_	_	_
40N-50N	_	_	_	_	_	_	_	_	_	_	_	_	_	_	_	_	_	_
30N-40N	_	_	_	_	_	_	_	_	_	_	_	_	_	_	_	_	_	_
20N-30N	_	_	_	_	_	_	_	-0.05	0.03	0.53	_	_	_	_	_	_	_	_
10N-20N	_	_	_	1.00	_	_	_	0.02	_	_	-0.14	_	-1.06	_	_	_	_	_
0N-10N	-0.18	-0.11	_	_	_	_	_	_	_	_	-0.01	-0.03	_	_	_	_	_	_
10S-0S	_	-0.36	0.09	_	_	_	_	_	_	_	-0.33	-0.03	_	0.05	0.02	_	_	_
20S-10S	_	_	_	_	_	_	_	_	_	_	_	_	_	_	_	_	_	_
30S-20S	_	_	_	_	_	_	_	_	_	_	_	_	_	_	_	_	_	_
40S-30S	_	_	_	_	_	_	_	_	_	_	_	_	_	_	_	_	_	_
50S-40S	_	_	_	_	_	_	_	_	_	_	_	_	_	_	_	_	_	_
60S-50S	_	_	_	_	_	_	_	_	_	_	_	_	_	_	_	_	_	_
70S-60S	_	_	_	_	_	_	_	_	_	_	_	_	_	_	_	_	_	_
80S-70S	_	_	_	_	_	_	_	_	_	_	_	_	_	_	_	_	_	_
90S-80S	_	_	_	_	_	_	_	_	_	_	_	_	_	_	_	_	_	_

Spatial correlation coefficients of BDT temperate forest from the SEED vs. AVHRR broadleaf treecover (180W-0W)

SD7 vs. BOBL	180W-170W	170W-160W	160W-150W	150W-140W	140W-130W	130W-120W	120W-110W	110W-100W	100W-90W	90W-80W	80W-70W	70W-60W	60W-50W	50W-40W	40W-30W	30W-20W	20W-10W	10W-0W
80N-90N	–	–	–	–	–	–	–	–	–	–	–	–	–	–	–	–	–	–
70N-80N	–	–	–	–	–	–	–	–	–	–	–	–	–	–	–	–	–	–
60N-70N	–	–	–	–	–	–	–	–	–	–	–	–	–	–	–	–	–	–
50N-60N	–	–	–	–	–	–	–	–	–	–	–	–	–	–	–	–	–	-0.57
40N-50N	–	–	–	–	–	-0.10	–	–	-0.23	0.43	0.62	0.75	–	–	–	–	–	0.16
30N-40N	–	–	–	–	–	–	–	–	0.47	0.80	0.28	–	–	–	–	–	–	–
20N-30N	–	–	–	–	–	–	–	–	–	–	–	–	–	–	–	–	–	–
10N-20N	–	–	–	–	–	–	–	–	–	–	–	–	–	–	–	–	–	–
0N-10N	–	–	–	–	–	–	–	–	–	–	–	–	–	–	–	–	–	–
10S-0S	–	–	–	–	–	–	–	–	–	–	–	–	–	–	–	–	–	–
20S-10S	–	–	–	–	–	–	–	–	–	–	–	–	–	–	–	–	–	–
30S-20S	–	–	–	–	–	–	–	–	–	–	–	–	–	–	–	–	–	–
40S-30S	–	–	–	–	–	–	–	–	–	–	–	1.00	-0.26	–	–	–	–	–
50S-40S	–	–	–	–	–	–	–	–	–	–	0.73	–	–	–	–	–	–	–
60S-50S	–	–	–	–	–	–	–	–	–	–	-1.00	–	–	–	–	–	–	–
70S-60S	–	–	–	–	–	–	–	–	–	–	–	–	–	–	–	–	–	–
80S-70S	–	–	–	–	–	–	–	–	–	–	–	–	–	–	–	–	–	–
90S-80S	–	–	–	–	–	–	–	–	–	–	–	–	–	–	–	–	–	–

Spatial correlation coefficients of BDT temperate forest from the SEED vs. AVHRR broadleaf treecover (0E-180E)

SD7 vs. BOBL	0E-10E	10E-20E	20E-30E	30E-40E	40E-50E	50E-60E	60E-70E	70E-80E	80E-90E	90E-100E	100E-110E	110E-120E	120E-130E	130E-140E	140E-150E	150E-160E	160E-170E	170E-180E
80N-90N	–	–	–	–	–	–	–	–	–	–	–	–	–	–	–	–	–	–
70N-80N	–	–	–	–	–	–	–	–	–	–	–	–	–	–	–	–	–	–
60N-70N	–	–	–	-0.07	–	–	–	–	–	–	–	–	–	–	–	–	–	–
50N-60N	-0.15	0.38	-0.17	-0.54	0.08	1.00	–	–	–	–	–	–	–	–	–	–	–	–
40N-50N	0.31	0.46	0.34	-0.78	-0.25	–	–	–	–	–	–	–	-0.14	0.72	0.82	–	–	–
30N-40N	–	–	–	–	–	–	–	0.10	–	–	0.16	0.19	0.99	1.00	–	–	–	–
20N-30N	–	–	–	–	–	–	–	–	0.95	0.14	-0.08	0.23	–	–	–	–	–	–
10N-20N	–	–	–	–	–	–	–	–	–	–	–	–	–	–	–	–	–	–
0N-10N	–	–	–	–	–	–	–	–	–	–	–	–	–	–	–	–	–	–
10S-0S	–	–	–	–	–	–	–	–	–	–	–	–	–	–	–	–	–	–
20S-10S	–	–	–	–	–	–	–	–	–	–	–	–	–	–	–	–	–	–
30S-20S	–	–	–	–	–	–	–	–	–	–	–	–	–	–	–	–	–	–
40S-30S	–	–	–	–	–	–	–	–	–	–	–	–	–	–	–	–	–	–
50S-40S	–	–	–	–	–	–	–	–	–	–	–	–	–	–	–	–	1.00	–
60S-50S	–	–	–	–	–	–	–	–	–	–	–	–	–	–	–	–	–	–
70S-60S	–	–	–	–	–	–	–	–	–	–	–	–	–	–	–	–	–	–
80S-70S	–	–	–	–	–	–	–	–	–	–	–	–	–	–	–	–	–	–
90S-80S	–	–	–	–	–	–	–	–	–	–	–	–	–	–	–	–	–	–

Spatial correlation coefficients of BDT temperate forest from the FREE vs. AVHRR broadleaf treecover (180W-0W)

FR7 vs BOBL	180W-170W	170W-160W	160W-150W	150W-140W	140W-130W	130W-120W	120W-110W	110W-100W	100W-90W	90W-80W	80W-70W	70W-60W	60W-50W	50W-40W	40W-30W	30W-20W	20W-10W	10W-0W
80N-90N	–	–	–	–	–	–	–	–	–	–	–	–	–	–	–	–	–	–
70N-80N	–	–	–	–	–	–	–	–	–	–	–	–	–	–	–	–	–	–
60N-70N	–	–	–	–	–	–	–	–	–	–	–	–	–	–	–	–	–	–
50N-60N	–	–	–	–	–	–	–	–	–	–	–	–	–	–	–	–	–	-0.57
40N-50N	–	–	–	–	–	-0.22	–	–	-0.06	0.43	0.63	0.75	–	–	–	–	–	0.16
30N-40N	–	–	–	–	–	–	–	–	0.44	0.79	0.45	–	–	–	–	–	–	–
20N-30N	–	–	–	–	–	–	–	–	–	–	–	–	–	–	–	–	–	–
10N-20N	–	–	–	–	–	–	–	–	–	–	–	–	–	–	–	–	–	–
0N-10N	–	–	–	–	–	–	–	–	–	–	–	–	–	–	–	–	–	–
10S-0S	–	–	–	–	–	–	–	–	–	–	–	–	–	–	–	–	–	–
20S-10S	–	–	–	–	–	–	–	–	–	–	–	–	–	–	–	–	–	–
30S-20S	–	–	–	–	–	–	–	–	–	–	–	–	–	–	–	–	–	–
40S-30S	–	–	–	–	–	–	–	–	–	–	–	1.00	-0.26	–	–	–	–	–
50S-40S	–	–	–	–	–	–	–	–	–	–	0.73	–	–	–	–	–	–	–
60S-50S	–	–	–	–	–	–	–	–	–	–	-1.00	–	–	–	–	–	–	–
70S-60S	–	–	–	–	–	–	–	–	–	–	–	–	–	–	–	–	–	–
80S-70S	–	–	–	–	–	–	–	–	–	–	–	–	–	–	–	–	–	–
90S-80S	–	–	–	–	–	–	–	–	–	–	–	–	–	–	–	–	–	–

Spatial correlation coefficients of BDT temperate forest from the FREE vs. AVHRR broadleaf treecover (0E-180E)

FR7 vs BOBL	0E-10E	10E-20E	20E-30E	30E-40E	40E-50E	50E-60E	60E-70E	70E-80E	80E-90E	90E-100E	100E-110E	110E-120E	120E-130E	130E-140E	140E-150E	150E-160E	160E-170E	170E-180E
80N-90N	–	–	–	–	–	–	–	–	–	–	–	–	–	–	–	–	–	–
70N-80N	–	–	–	–	–	–	–	–	–	–	–	–	–	–	–	–	–	–
60N-70N	–	–	–	-0.07	–	–	–	–	–	–	–	–	–	–	–	–	–	–
50N-60N	-0.14	0.39	-0.16	-0.54	0.07	0.65	–	–	–	–	–	–	–	–	–	–	–	–
40N-50N	0.31	0.46	0.34	-0.78	-0.16	–	–	–	–	–	–	–	-0.18	0.85	0.82	–	–	–
30N-40N	–	–	–	–	–	–	–	0.10	–	–	-0.24	0.19	0.99	1.00	–	–	–	–
20N-30N	–	–	–	–	–	–	–	–	0.88	0.14	-0.08	0.22	–	–	–	–	–	–
10N-20N	–	–	–	–	–	–	–	–	–	–	–	–	–	–	–	–	–	–
0N-10N	–	–	–	–	–	–	–	–	–	–	–	–	–	–	–	–	–	–
10S-0S	–	–	–	–	–	–	–	–	–	–	–	–	–	–	–	–	–	–
20S-10S	–	–	–	–	–	–	–	–	–	–	–	–	–	–	–	–	–	–
30S-20S	–	–	–	–	–	–	–	–	–	–	–	–	–	–	–	–	–	–
40S-30S	–	–	–	–	–	–	–	–	–	–	–	–	–	–	–	–	–	–
50S-40S	–	–	–	–	–	–	–	–	–	–	–	–	–	–	–	–	1.00	–
60S-50S	–	–	–	–	–	–	–	–	–	–	–	–	–	–	–	–	–	–
70S-60S	–	–	–	–	–	–	–	–	–	–	–	–	–	–	–	–	–	–
80S-70S	–	–	–	–	–	–	–	–	–	–	–	–	–	–	–	–	–	–
90S-80S	–	–	–	–	–	–	–	–	–	–	–	–	–	–	–	–	–	–

Difference of spatial correlation between BDT temperate (SEED) vs. AVHRR broadleaf and BDT temperate (FREE) vs. AVHRR broadleaf (180W-0W). Stronger correlations by the SEED are highlighted in yellow and less stronger correlation by the SEED in pink.

DIFF	180W-170W	170W-160W	160W-150W	150W-140W	140W-130W	130W-120W	120W-110W	110W-100W	100W-90W	90W-80W	80W-70W	70W-60W	60W-50W	50W-40W	40W-30W	30W-20W	20W-10W	10W-0W
80N-90N	_	_	_	_	_	_	_	_	_	_	_	_	_	_	_	_	_	_
70N-80N	_	_	_	_	_	_	_	_	_	_	_	_	_	_	_	_	_	_
60N-70N	_	_	_	_	_	_	_	_	_	_	_	_	_	_	_	_	_	_
50N-60N	_	_	_	_	_	_	_	_	_	_	_	_	_	_	_	_	_	_
40N-50N	_	_	_	_	_	**0.12**	_	_	-0.18	_	_	_	_	_	_	_	_	_
30N-40N	_	_	_	_	_	_	_	_	**0.04**	**0.01**	-0.17	_	_	_	_	_	_	_
20N-30N	_	_	_	_	_	_	_	_	_	_	_	_	_	_	_	_	_	_
10N-20N	_	_	_	_	_	_	_	_	_	_	_	_	_	_	_	_	_	_
0N-10N	_	_	_	_	_	_	_	_	_	_	_	_	_	_	_	_	_	_
10S-0S	_	_	_	_	_	_	_	_	_	_	_	_	_	_	_	_	_	_
20S-10S	_	_	_	_	_	_	_	_	_	_	_	_	_	_	_	_	_	_
30S-20S	_	_	_	_	_	_	_	_	_	_	_	_	_	_	_	_	_	_
40S-30S	_	_	_	_	_	_	_	_	_	_	_	_	_	_	_	_	_	_
50S-40S	_	_	_	_	_	_	_	_	_	_	_	_	_	_	_	_	_	_
60S-50S	_	_	_	_	_	_	_	_	_	_	_	_	_	_	_	_	_	_
70S-60S	_	_	_	_	_	_	_	_	_	_	_	_	_	_	_	_	_	_
80S-70S	_	_	_	_	_	_	_	_	_	_	_	_	_	_	_	_	_	_
90S-80S	_	_	_	_	_	_	_	_	_	_	_	_	_	_	_	_	_	_

Difference of spatial correlation between BDT temperate (SEED) vs. AVHRR broadleaf and BDT temperate (FREE) vs. AVHRR broadleaf (0E-180E). Stronger correlations by the SEED are highlighted in yellow and less stronger correlation by the SEED in pink.

DIFF	0E-10E	10E-20E	20E-30E	30E-40E	40E-50E	50E-60E	60E-70E	70E-80E	80E-90E	90E-100E	100E-110E	110E-120E	120E-130E	130E-140E	140E-150E	150E-160E	160E-170E	170E-180E
80N-90N	_	_	_	_	_	_	_	_	_	_	_	_	_	_	_	_	_	_
70N-80N	_	_	_	_	_	_	_	_	_	_	_	_	_	_	_	_	_	_
60N-70N	_	_	_	_	_	_	_	_	_	_	_	_	_	_	_	_	_	_
50N-60N	-0.01	-0.01	-0.01	_	**0.01**	**0.35**	_	_	_	_	_	_	_	_	_	_	_	_
40N-50N	_	_	_	-0.01	-0.09	_	_	_	_	_	_	_	**0.04**	-0.14	_	_	_	_
30N-40N	_	_	_	_	_	_	_	_	_	_	**0.40**	_	_	_	_	_	_	_
20N-30N	_	_	_	_	_	_	_	_	**0.06**	_	_	**0.01**	_	_	_	_	_	_
10N-20N	_	_	_	_	_	_	_	_	_	_	_	_	_	_	_	_	_	_
0N-10N	_	_	_	_	_	_	_	_	_	_	_	_	_	_	_	_	_	_
10S-0S	_	_	_	_	_	_	_	_	_	_	_	_	_	_	_	_	_	_
20S-10S	_	_	_	_	_	_	_	_	_	_	_	_	_	_	_	_	_	_
30S-20S	_	_	_	_	_	_	_	_	_	_	_	_	_	_	_	_	_	_
40S-30S	_	_	_	_	_	_	_	_	_	_	_	_	_	_	_	_	_	_
50S-40S	_	_	_	_	_	_	_	_	_	_	_	_	_	_	_	_	_	_
60S-50S	_	_	_	_	_	_	_	_	_	_	_	_	_	_	_	_	_	_
70S-60S	_	_	_	_	_	_	_	_	_	_	_	_	_	_	_	_	_	_
80S-70S	_	_	_	_	_	_	_	_	_	_	_	_	_	_	_	_	_	_
90S-80S	_	_	_	_	_	_	_	_	_	_	_	_	_	_	_	_	_	_

Spatial correlation coefficients of BDT boreal forest from the SEED vs. AVHRR broadleaf treecover (180W-0W)

SD8 vs. BOBL	180W-170W	170W-160W	160W-150W	150W-140W	140W-130W	130W-120W	120W-110W	110W-100W	100W-90W	90W-80W	80W-70W	70W-60W	60W-50W	50W-40W	40W-30W	30W-20W	20W-10W	10W-0W
80N-90N	–	–	–	–	–	–	–	–	–	–	–	–	–	–	–	–	–	–
70N-80N	–	–	–	–	–	–	–	–	–	–	–	–	–	–	–	–	–	–
60N-70N	–	–	–	–	–	–	–	–	–	–	–	–	–	–	–	–	–	–
50N-60N	–	–	–	–	–	–	-0.67	-0.19	-0.78	–	1.00	–	–	–	–	–	–	–
40N-50N	–	–	–	–	–	1.00	–	–	-0.35	-0.69	-0.70	0.29	–	–	–	–	–	–
30N-40N	–	–	–	–	–	–	–	–	–	–	–	–	–	–	–	–	–	–
20N-30N	–	–	–	–	–	–	–	–	–	–	–	–	–	–	–	–	–	–
10N-20N	–	–	–	–	–	–	–	–	–	–	–	–	–	–	–	–	–	–
0N-10N	–	–	–	–	–	–	–	–	–	–	–	–	–	–	–	–	–	–
10S-0S	–	–	–	–	–	–	–	–	–	–	–	–	–	–	–	–	–	–
20S-10S	–	–	–	–	–	–	–	–	–	–	–	–	–	–	–	–	–	–
30S-20S	–	–	–	–	–	–	–	–	–	–	–	–	–	–	–	–	–	–
40S-30S	–	–	–	–	–	–	–	–	–	–	–	–	–	–	–	–	–	–
50S-40S	–	–	–	–	–	–	–	–	–	–	–	–	–	–	–	–	–	–
60S-50S	–	–	–	–	–	–	–	–	–	–	–	–	–	–	–	–	–	–
70S-60S	–	–	–	–	–	–	–	–	–	–	–	–	–	–	–	–	–	–
80S-70S	–	–	–	–	–	–	–	–	–	–	–	–	–	–	–	–	–	–
90S-80S	–	–	–	–	–	–	–	–	–	–	–	–	–	–	–	–	–	–

Spatial correlation coefficients of BDT boreal forest from the SEED vs. AVHRR broadleaf treecover (0E-180E)

SD8 vs. BOBL	0E-10E	10E-20E	20E-30E	30E-40E	40E-50E	50E-60E	60E-70E	70E-80E	80E-90E	90E-100E	100E-110E	110E-120E	120E-130E	130E-140E	140E-150E	150E-160E	160E-170E	170E-180E
80N-90N	_	_	_	_	_	_	_	_	_	_	_	_	_	_	_	_	_	_
70N-80N	_	_	_	_	_	_	_	_	_	_	_	_	_	_	_	_	_	_
60N-70N	_	_	-0.08	_	_	1.00	-1.00	_	_	_	_	_	_	1.00	_	_	_	_
50N-60N	_	0.21	-0.46	0.41	_	1.00	_	_	0.59	-1.00	0.17	_	0.31	0.59	_	_	_	_
40N-50N	_	0.31	0.02	_	0.41	_	_	_	_	_	_	_	0.46	0.89	_	_	_	_
30N-40N	_	_	_	_	_	_	_	1.00	_	_	-0.87	_	_	_	_	_	_	_
20N-30N	_	_	_	_	_	_	_	_	_	-1.00	_	_	_	_	_	_	_	_
10N-20N	_	_	_	_	_	_	_	_	_	_	_	_	_	_	_	_	_	_
0N-10N	_	_	_	_	_	_	_	_	_	_	_	_	_	_	_	_	_	_
10S-0S	_	_	_	_	_	_	_	_	_	_	_	_	_	_	_	_	_	_
20S-10S	_	_	_	_	_	_	_	_	_	_	_	_	_	_	_	_	_	_
30S-20S	_	_	_	_	_	_	_	_	_	_	_	_	_	_	_	_	_	_
40S-30S	_	_	_	_	_	_	_	_	_	_	_	_	_	_	_	_	_	_
50S-40S	_	_	_	_	_	_	_	_	_	_	_	_	_	_	_	_	_	_
60S-50S	_	_	_	_	_	_	_	_	_	_	_	_	_	_	_	_	_	_
70S-60S	_	_	_	_	_	_	_	_	_	_	_	_	_	_	_	_	_	_
80S-70S	_	_	_	_	_	_	_	_	_	_	_	_	_	_	_	_	_	_
90S-80S	_	_	_	_	_	_	_	_	_	_	_	_	_	_	_	_	_	_

Spatial correlation coefficients of BDT boreal forest from the FREE vs. AVHRR broadleaf treecover (180W-0W)

FR8 vs BOBL	180W-170W	170W-160W	160W-150W	150W-140W	140W-130W	130W-120W	120W-110W	110W-100W	100W-90W	90W-80W	80W-70W	70W-60W	60W-50W	50W-40W	40W-30W	30W-20W	20W-10W	10W-0W
80N-90N	_	_	_	_	_	_	_	_	_	_	_	_	_	_	_	_	_	_
70N-80N	_	_	_	_	_	_	_	_	_	_	_	_	_	_	_	_	_	_
60N-70N	_	_	_	_	_	_	_	_	_	_	_	_	_	_	_	_	_	_
50N-60N	_	_	_	_	_	_	-0.67	-0.21	-0.78	_	1.00	_	_	_	_	_	_	_
40N-50N	_	_	_	_	_	1.00	_	_	-0.34	-0.69	-0.70	0.31	_	_	_	_	_	_
30N-40N	_	_	_	_	_	_	_	_	_	_	_	_	_	_	_	_	_	_
20N-30N	_	_	_	_	_	_	_	_	_	_	_	_	_	_	_	_	_	_
10N-20N	_	_	_	_	_	_	_	_	_	_	_	_	_	_	_	_	_	_
0N-10N	_	_	_	_	_	_	_	_	_	_	_	_	_	_	_	_	_	_
10S-0S	_	_	_	_	_	_	_	_	_	_	_	_	_	_	_	_	_	_
20S-10S	_	_	_	_	_	_	_	_	_	_	_	_	_	_	_	_	_	_
30S-20S	_	_	_	_	_	_	_	_	_	_	_	_	_	_	_	_	_	_
40S-30S	_	_	_	_	_	_	_	_	_	_	_	_	_	_	_	_	_	_
50S-40S	_	_	_	_	_	_	_	_	_	_	_	_	_	_	_	_	_	_
60S-50S	_	_	_	_	_	_	_	_	_	_	_	_	_	_	_	_	_	_
70S-60S	_	_	_	_	_	_	_	_	_	_	_	_	_	_	_	_	_	_
80S-70S	_	_	_	_	_	_	_	_	_	_	_	_	_	_	_	_	_	_
90S-80S	_	_	_	_	_	_	_	_	_	_	_	_	_	_	_	_	_	_

Spatial correlation coefficients of BDT boreal forest from the FREE vs. AVHRR broadleaf treecover (0E-180E)

FR8 vs BOBL	0E-10E	10E-20E	20E-30E	30E-40E	40E-50E	50E-60E	60E-70E	70E-80E	80E-90E	90E-100E	100E-110E	110E-120E	120E-130E	130E-140E	140E-150E	150E-160E	160E-170E	170E-180E
80N-90N	_	_	_	_	_	_	_	_	_	_	_	_	_	_	_	_	_	_
70N-80N	_	_	_	_	_	_	_	_	_	_	_	_	_	_	_	_	_	_
60N-70N	_	_	-0.08	_	_	1.00	-1.00	_	_	_	_	_	_	1.00	_	_	_	_
50N-60N	_	0.25	-0.46	0.41	_	1.00	_	_	0.59	0.26	0.38	_	0.05	0.59	_	_	_	_
40N-50N	_	0.31	0.02	_	0.41	_	_	_	_	_	_	_	0.46	0.75	_	_	_	_
30N-40N	_	_	_	_	_	_	_	1.00	_	_	-0.87	_	_	_	_	_	_	_
20N-30N	_	_	_	_	_	_	_	_	_	-1.00	_	_	_	_	_	_	_	_
10N-20N	_	_	_	_	_	_	_	_	_	_	_	_	_	_	_	_	_	_
0N-10N	_	_	_	_	_	_	_	_	_	_	_	_	_	_	_	_	_	_
10S-0S	_	_	_	_	_	_	_	_	_	_	_	_	_	_	_	_	_	_
20S-10S	_	_	_	_	_	_	_	_	_	_	_	_	_	_	_	_	_	_
30S-20S	_	_	_	_	_	_	_	_	_	_	_	_	_	_	_	_	_	_
40S-30S	_	_	_	_	_	_	_	_	_	_	_	_	_	_	_	_	_	_
50S-40S	_	_	_	_	_	_	_	_	_	_	_	_	_	_	_	_	_	_
60S-50S	_	_	_	_	_	_	_	_	_	_	_	_	_	_	_	_	_	_
70S-60S	_	_	_	_	_	_	_	_	_	_	_	_	_	_	_	_	_	_
80S-70S	_	_	_	_	_	_	_	_	_	_	_	_	_	_	_	_	_	_
90S-80S	_	_	_	_	_	_	_	_	_	_	_	_	_	_	_	_	_	_

Difference of spatial correlation between BDT boreal (SEED) vs. AVHRR broadleaf and BDT boreal (FREE) vs. AVHRR broadleaf (180W-0W). Stronger correlations by the SEED are highlighted in yellow and less stronger correlation by the SEED in pink.

DIFF	180W-170W	170W-160W	160W-150W	150W-140W	140W-130W	130W-120W	120W-110W	110W-100W	100W-90W	90W-80W	80W-70W	70W-60W	60W-50W	50W-40W	40W-30W	30W-20W	20W-10W	10W-0W
80N-90N	_	_	_	_	_	_	_	_	_	_	_	_	_	_	_	_	_	_
70N-80N	_	_	_	_	_	_	_	_	_	_	_	_	_	_	_	_	_	_
60N-70N	_	_	_	_	_	_	_	_	_	_	_	_	_	_	_	_	_	_
50N-60N	_	_	_	_	_	_	**1.35**	**0.41**	**1.57**	_	_	_	_	_	_	_	_	_
40N-50N	_	_	_	_	_	_	_	_	**0.68**	**1.38**	**1.40**	-0.02	_	_	_	_	_	_
30N-40N	_	_	_	_	_	_	_	_	_	_	_	_	_	_	_	_	_	_
20N-30N	_	_	_	_	_	_	_	_	_	_	_	_	_	_	_	_	_	_
10N-20N	_	_	_	_	_	_	_	_	_	_	_	_	_	_	_	_	_	_
0N-10N	_	_	_	_	_	_	_	_	_	_	_	_	_	_	_	_	_	_
10S-0S	_	_	_	_	_	_	_	_	_	_	_	_	_	_	_	_	_	_
20S-10S	_	_	_	_	_	_	_	_	_	_	_	_	_	_	_	_	_	_
30S-20S	_	_	_	_	_	_	_	_	_	_	_	_	_	_	_	_	_	_
40S-30S	_	_	_	_	_	_	_	_	_	_	_	_	_	_	_	_	_	_
50S-40S	_	_	_	_	_	_	_	_	_	_	_	_	_	_	_	_	_	_
60S-50S	_	_	_	_	_	_	_	_	_	_	_	_	_	_	_	_	_	_
70S-60S	_	_	_	_	_	_	_	_	_	_	_	_	_	_	_	_	_	_
80S-70S	_	_	_	_	_	_	_	_	_	_	_	_	_	_	_	_	_	_
90S-80S	_	_	_	_	_	_	_	_	_	_	_	_	_	_	_	_	_	_

Difference of spatial correlation between BDT boreal (SEED) vs. AVHRR broadleaf and BDT boreal (FREE) vs. AVHRR broadleaf (0E-180E). Stronger correlations by the SEED are highlighted in yellow and less stronger correlation by the SEED in pink.

DIFF	0E-10E	10E-20E	20E-30E	30E-40E	40E-50E	50E-60E	60E-70E	70E-80E	80E-90E	90E-100E	100E-110E	110E-120E	120E-130E	130E-140E	140E-150E	150E-160E	160E-170E	170E-180E
80N-90N	_	_	_	_	_	_	_	_	_	_	_	_	_	_	_	_	_	_
70N-80N	_	_	_	_	_	_	_	_	_	_	_	_	_	_	_	_	_	_
60N-70N	_	_	0.15	_	_	_	2.00	_	_	_	_	_	_	_	_	_	_	_
50N-60N	_	-0.03	0.93	_	_	_	_	_	_	0.74	-0.22	_	0.27	_	_	_	_	_
40N-50N	_	_	_	_	_	_	_	_	_	_	_	_	_	0.14	_	_	_	_
30N-40N	_	_	_	_	_	_	_	_	_	_	1.74	_	_	_	_	_	_	_
20N-30N	_	_	_	_	_	_	_	_	_	2.00	_	_	_	_	_	_	_	_
10N-20N	_	_	_	_	_	_	_	_	_	_	_	_	_	_	_	_	_	_
0N-10N	_	_	_	_	_	_	_	_	_	_	_	_	_	_	_	_	_	_
10S-0S	_	_	_	_	_	_	_	_	_	_	_	_	_	_	_	_	_	_
20S-10S	_	_	_	_	_	_	_	_	_	_	_	_	_	_	_	_	_	_
30S-20S	_	_	_	_	_	_	_	_	_	_	_	_	_	_	_	_	_	_
40S-30S	_	_	_	_	_	_	_	_	_	_	_	_	_	_	_	_	_	_
50S-40S	_	_	_	_	_	_	_	_	_	_	_	_	_	_	_	_	_	_
60S-50S	_	_	_	_	_	_	_	_	_	_	_	_	_	_	_	_	_	_
70S-60S	_	_	_	_	_	_	_	_	_	_	_	_	_	_	_	_	_	_
80S-70S	_	_	_	_	_	_	_	_	_	_	_	_	_	_	_	_	_	_
90S-80S	_	_	_	_	_	_	_	_	_	_	_	_	_	_	_	_	_	_

All maps are difference maps of occupied area (%) by each PFT of SEED-FREE at 2100.

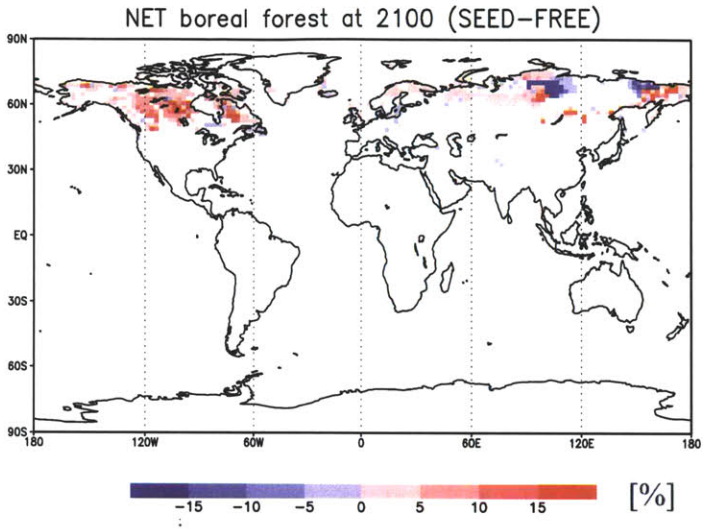

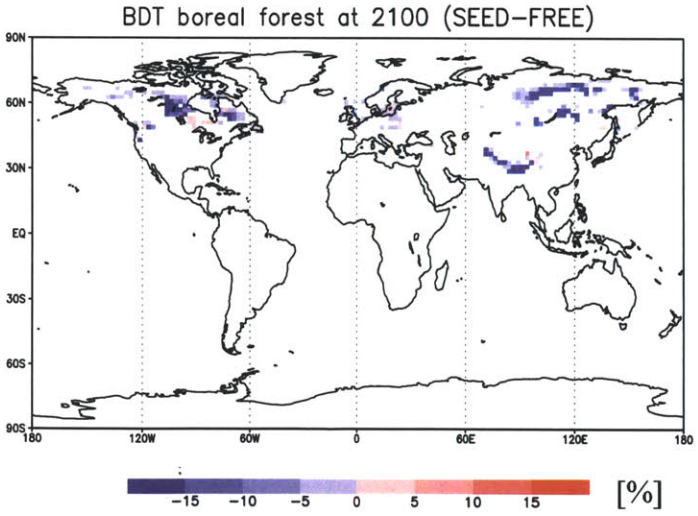

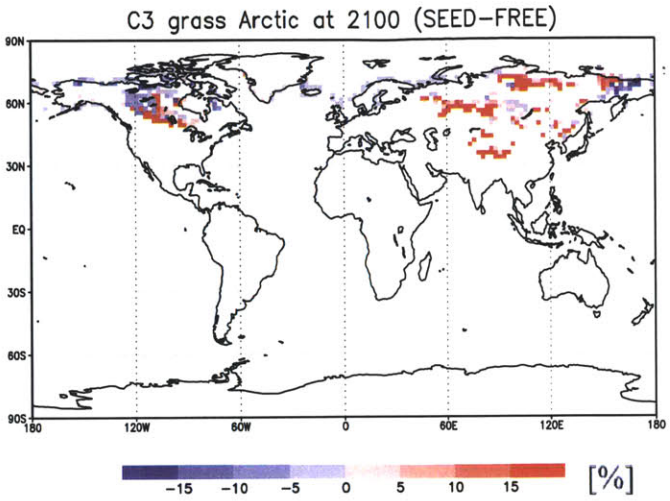
C3 grass Arctic at 2100 (SEED–FREE)
90N
60N
30N
EQ
30S
60S
90S
180
120W
60W
0
60E
120E
180
−15 −10 −5 0 5 10 15
[%]

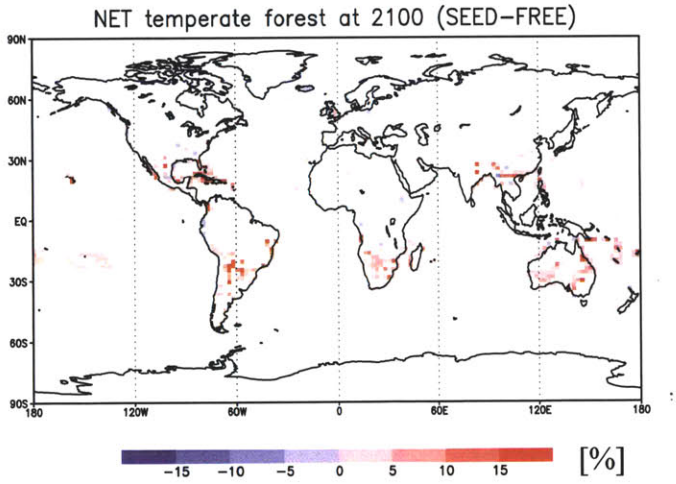
NET temperate forest at 2100 (SEED–FREE)
90N
60N
30N
EQ
30S
60S
90S
180
120W
60W
0
60E
120E
180
−15 −10 −5 0 5 10 15
[%]

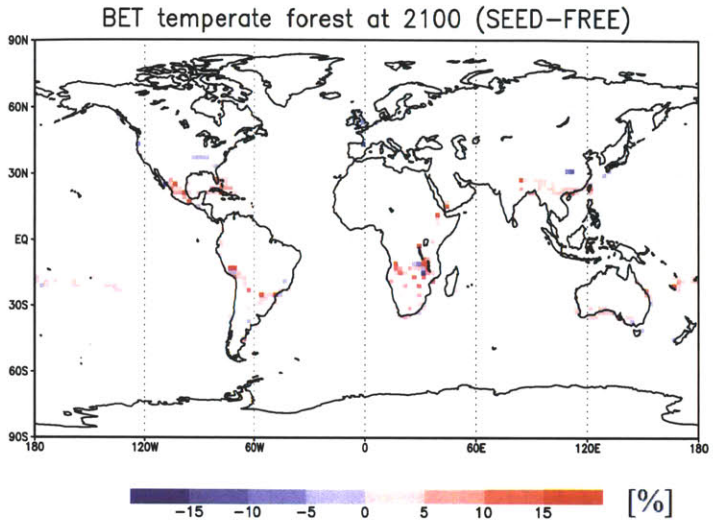
BET temperate forest at 2100 (SEED–FREE)
90N
60N
30N
EQ
30S
60S
90S
180
120W
60W
0
60E
120E
180
−15 −10 −5 0 5 10 15
[%]

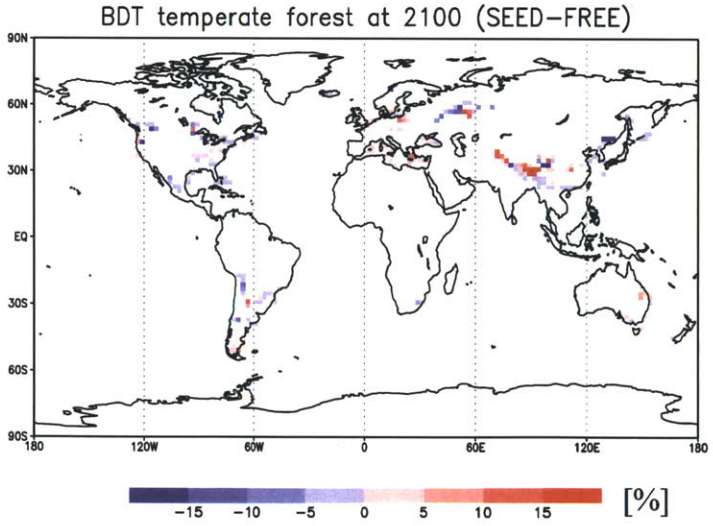
BDT temperate forest at 2100 (SEED–FREE)
90N
60N
30N
EQ
30S
60S
90S
180
120W
60W
0
60E
120E
180
−15 −10 −5 0 5 10 15
[%]

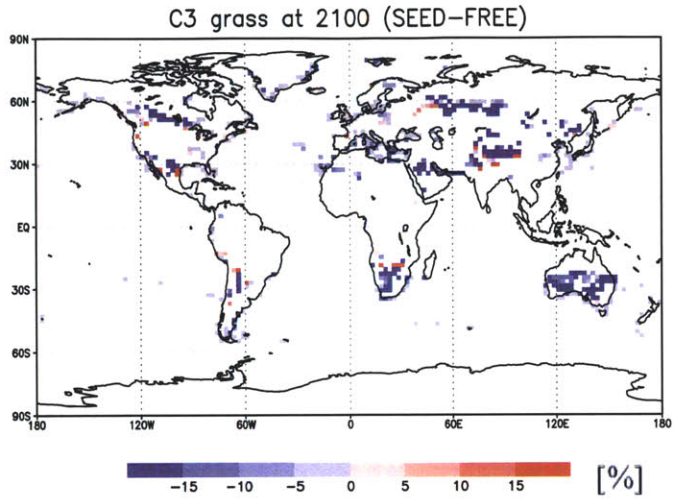
C3 grass at 2100 (SEED–FREE)
90N
60N
30N
EQ
30S
60S
90S
180
120W
60W
0
60E
120E
180
−15 −10 −5 0 5 10 15
[%]

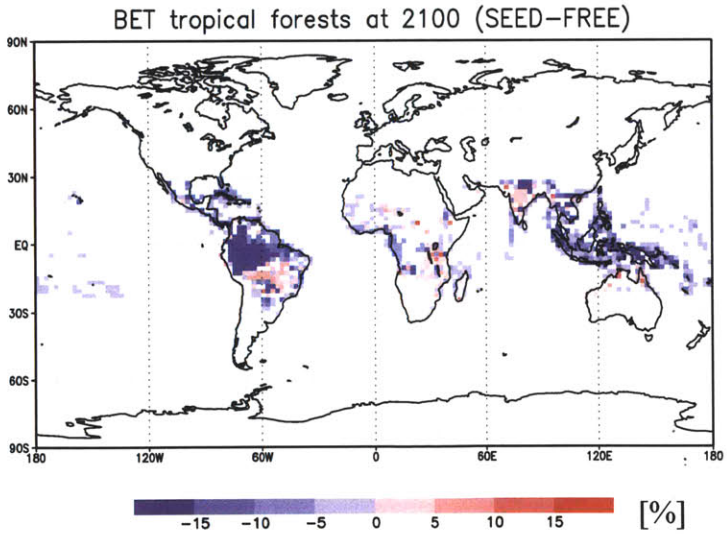
BET tropical forests at 2100 (SEED–FREE)
90N
60N
30N
EQ
30S
60S
90S
180
120W
60W
0
60E
120E
180
−15 −10 −5 0 5 10 15
[%]

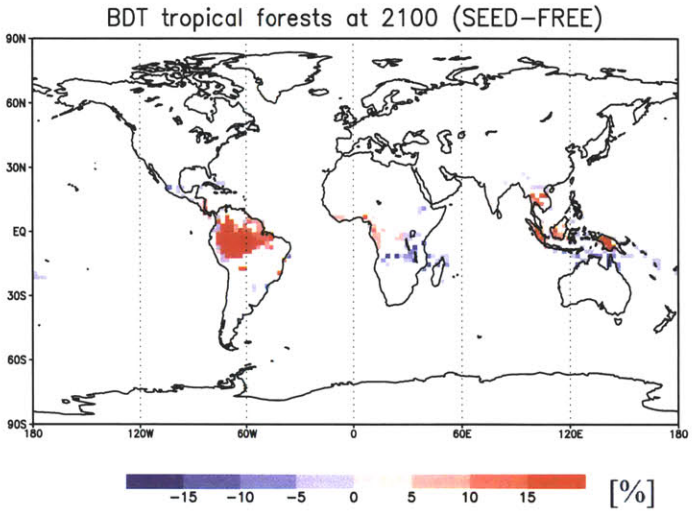
BDT tropical forests at 2100 (SEED–FREE)
90N
60N
30N
EQ
30S
60S
90S
180
120W
60W
0
60E
120E
180
−15 −10 −5 0 5 10 15
[%]

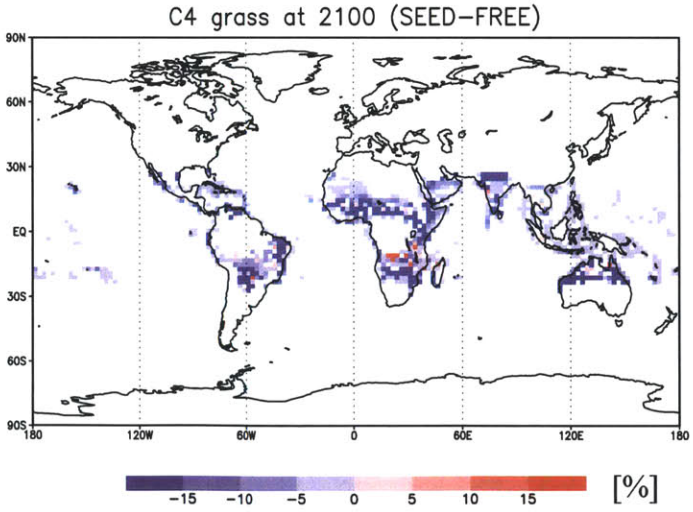
C4 grass at 2100 (SEED–FREE)
90N
60N
30N
EQ
30S
60S
90S
180
120W
60W
0
60E
120E
180
−15 −10 −5 0 5 10 15
[%]